THE REGULATION OF CHLOROPHYLL LEVELS IN MATURING KIWIFRUIT

A thesis submitted in partial fulfilment of the requirements for the

Degree of Doctor of Philosophy in Biotechnology

by Sarah M. Pilkington

University of Canterbury

2012

ACKNOWLEDGEMENTS

First and foremost, this thesis would not have been possible without my supervisors: Professor Paula Jameson (University of Canterbury), Associate Professor Andrew Allan (University of Auckland, Plant & Food Research) and Dr. Mirco Montefiori (Plant & Food Research).

Paula's unwavering eye for detail, passion for cytokinins, and care for the well-being of her students has made the path to my completed thesis a comparatively easy one. Paula led the School of Biological Sciences through an unthinkable natural disaster during my final year, and my thoughts have often been in Christchurch with UC staff and fellow PhD students.

Andy and I have laughed our way through my PhD, but without his clear sense of direction this thesis could have been swamped in the huge intriguing area that is kiwifruit ripening. His guidance, incredible knowledge of plant physiology and transcriptional control, and possibly most importantly, his sense of humour, will be missed.

I am indebted to Mirco, from teaching me science in 'Itanglish' to always being open to discussion. His interaction with so many people involved with kiwifruit in both New Zealand and Italy, from Zespri to orchardists, gives him an admirable knowledge of kiwifruit growth characteristics and an overall hands-on perspective.

I would like to thank the Tertiary Education Commission for an Enterprise Scholarship, and Zespri for their support.

Thank you to my team of experts, Neil Emery at Trent University, Canada, Janine Cooney and Dave Greenwood for help with cytokinin measurements. There are so many people to thank at Plant & Food Research, the Intragenics and Transformation team, Tim Holmes for help with photography, Monica Dragulescu for taking care of plants in the glasshouse, the Te Puke Orchard Management team, and the mappers Mark McNeilage and Paul Datson. I would also like to thank the University of Auckland Plant Development team, Jo Putterill and Karine David, for taking me under their wing. I would like to thank the top dogs,

Andrew Granger, Ian Ferguson and Roger Hellens for their work ensuring the existence of cool Breeding and Genomics projects and asking challenging questions.

I would also like to thank Geeta Chhiba for being absolutely invaluable and having an interest in people far beyond the call of duty. Thanks heaps to Andrew Dare and Rebecca Kirk, you both know lots and care lots. I would also like to thank the rest of the core members of the CHIPs (**c**olour and **h**ealth **i**n **p**lant**s**) team, Cyril Brendolise, Richard Espley, Charles Ampomah-Dwamena, Kui Lin-Wang, and Marcela Martinez-Sanchez, interested, interesting and knowledgeable scientists William Laing, Roy Storey, Sol Green and Niels Nieuwenhuizen, and fellow students, especially Jovyn Ng, Blue Plunkett and Christina Fullerton.

So, we're finally here Georgina Rae!! Thanks for being the other "glimmer twin" and also for keeping me somewhat sane through the hard bits, I'm hoping I can do the same in return.

And finally, as always, thank you so so much to Mum, Dad, Andrew, Rachael and Sam, for everything.

ABSTRACT

The chlorophyll degradation pathway is central to a number of plant processes including senescence and fruit ripening. However, the regulation of the chlorophyll degradation pathway enzymes is not well understood. The aim of this thesis was to elucidate the genetic mechanisms that control changes in pigment composition leading to fruit flesh yellowing in kiwifruit. *Actinidia deliciosa* and *A. chinensis* fruit, which are green and yellow, respectively, provide an opportunity to study the regulation of chlorophyll levels.

The expression of genes that code for enzymes of the chlorophyll and cytokinin metabolic pathways was measured using qRT-PCR. Candidates for chlorophyll degradation regulatory points were then characterised for functionality by transient transformation in *N. benthamiana*. The endogenous cytokinin levels were measured in kiwifruit and transient activation assays were carried out with the promoters of key candidate genes.

Overall, expression of the chlorophyll degradation genes was elevated in yellow fruit and expression of biosynthetic genes was higher in green fruit. The chlorophyll degradation-associated protein, *STAY-GREEN2* (*SGR2)*, was more highly expressed in yellow fruit, and transient over-expression of *SGR* was sufficient to drive chlorophyll degradation. Expression of isopentenyl transferase (*IPT)*, the rate-limiting step for cytokinin biosynthesis, showed an increase towards maturity in green fruit, but not in yellow fruit. However, both fruit had similar high levels of cytokinin nucleotides and free bases. A gene coding for *O*-glucosylation was also highly expressed in green fruit. Green fruit contained higher levels of cytokinin *O*-glucosides and ribosides towards maturity, suggesting differences in cytokinin signalling, which could lead to regulation of chlorophyll levels *via* activation of the *SGR* promoter by transcription factors.

It is likely that the chlorophyll degradation pathway and cytokinin metabolism are linked. The differential expression of cytokinin response regulators could lead to differential regulation of cytokinin levels in the fruit of the two species, and possibly differential regulation of the chlorophyll degradation pathway. Progress towards elucidation of the control of chlorophyll levels provides knowledge of this key process in kiwifruit and potentially gene-based markers for breeding new kiwifruit cultivars.

TABLE OF CONTENTS

LIST OF FIGURES

LIST OF TABLES

ABBREVIATIONS

°C	degrees Celsius
µFd	microfarad
µg	microgram
µl	microlitre
ACD	accelerated cell death
ADP	adenosine triphosphate
AHKs	*Arabidopsis* histidine kinases
AHPs	*Arabidopsis* histidine phosphotransfer proteins
ALA	5-aminolevulinic acid
ARRs	*Arabidopsis* response regulators
ATP	adenosine triphosphate
BGLU	β-glucosidase
bHLH	basic helix-loop-helix
BLAST	basic local alignment search tool
bp	base pair
CAO	chlorophyll *a* oxygenase
CBR	chlorophyll *b* reductase
cDNA	complementary deoxyribonucleic acid
CK	*A. chinensis*
CKX (or CKO)	cytokinin oxidase
cl	capsicum stay-green
CLH	chlorophyllase
CLS	chlorophyll synthase
cm	centimetre
COL	*CONSTANS*-like transcription factor
CRE	cytokinin receptor
CRF	cytokinin response factor
C_t	crossing threshold
CTAB	cetyltrimethylammonium bromide
cZ or cisZ, cisZNT, cisZR, cisZROG	*cis*-zeatin, -nucleotide, -riboside, -riboside-*O*-glucoside
d_1d_2	soybean stay-green
DA	*A. deliciosa*
DAFB	days after full bloom
DNA	deoxyribonucleic acid

DW	dry weight
DZ, DZNT, DZR, DZROG, DZOG, DZ9G	dihydro-zeatin, - nucleotide, -riboside, -riboside-*O*-glucoside, -*O*-glucoside, -9-glucoside
EA	*A. eriantha*
EDTA	ethylene diamine tetra-acetic acid
EST	expressed sequence tag
FLU	fluorescence protein
FW	fresh weight
g	gram
g	gravitational acceleration
gf	tomato green flesh stay-green
GFP	green fluorescent protein
GGPP	geranyl geranyl pyrophosphate
GLUTR	glutamyl tRNA reductase
h	hours
HCl	hydrochloric acid
I	Mendel's green cotyledon
iP, iPNT, iPR	N6-(Δ2-isopentenyl)-adenine, -nucleotide, -riboside
IPT	isopentenyl transferase
iPTP	isopentenyladenosine-5'-monophosphate
kb	kilobase
kgF	kilogram force
kV	kilovolt
l	litre
LB	Luria Bertani
LCY-β	lycopene beta cyclase
LCY-ε	lycopene epsilon cyclase
LHCB	light-harvesting chlorophyll *a*/*b* binding complex
LiCl	lithium chloride
LUC	firefly luciferase
M	molar
MADS	*MCM1 Agamous Deficiens SRF* transcription factor
MCS	metal chelating substance
MEP	methylerythritol phosphate
mg	milligram

MgCl	magnesium chloride
min	minutes
mm	millimetre
mM	millimolar
mRNA	messenger ribonucleic acid
ms	millisecond
MYB	myleoblastosis virus transcription factor family
NaOH	sodium hydroxide
nan	citrus stay-green
NCCs	non-fluorescent chlorophyll catabolites
ng	nanogram
NOL	NYC-one like
NYC1	non-yellow colouring
OD_{600}	optical density at a wavelength of 600 nanometres
PAM	pulse amplitude modulation
PAO	pheophorbide *a* oxygenase
PBS	phosphate buffered saline
PCR	polymerase chain reaction
pFCC	fluorescent chlorophyll catabolite
pmol	picomole
PPH	pheophorbide pheophytin hydrolase
ppm	parts per million
Proto	protoporphyrin IX
PSD	phytoene desaturase
PSII	photosystem II
PSY	phytoene synthase
PVP	polyvinylpyrollidone
qRT-PCR	quantitative real time polymerase chain reaction
RBCS	small subunit of ribulose-1,5-bisphosphate carboxylase
RCC	red chlorophyll catabolite
RCCR	red chlorophyll catabolite reductase
REN	Renilla luciferase
RNA	ribonucleic acid
RNAi	ribonucleic acid interference
rpm	revolutions per minute
RuBisCo	ribulose-1,5-bisphosphate carboxylase

SAG	senescence associated genes
SE	standard error
sec	seconds
SGR	stay-green
SNP	single nucleotide polymorphism
TF(s)	transcription factor(s)
Tris	tris (hydroxymethyl) aminomethane
tRNA	transfer ribonucleic acid
tZ, tZNT, tZR, tZROG, tZOG, tZ9G	*trans*-zeatin, -nucleotide, -riboside, -riboside-*O*-glucoside, - *O*-glucoside, -9-glucoside
tZOG	*trans*-*O*-glucosylzeatin
tZROG	*trans*-zeatin riboside-*O*-glucoside
v/v	volume per volume
w/v	weight per volume
ZDS	zeta-carotene desaturase
ZOG	zeatin *O*-glucosyltransferase

1. INTRODUCTION

The degradation of chlorophyll is a fundamental process that is of central importance to plant performance, yield, development, and response to both the biotic and abiotic environment. Although extensive research has been carried out on the biochemistry and molecular biology of chlorophyll metabolism, less is known about the regulation of this process. In fruit and vegetables, chlorophyll is typically high in young tissue and is degraded during maturation. The chlorophyll degradation seen in yellow fleshed kiwifruit (*Actinidia chinensis*) does not occur in the green flesh of *A. deliciosa* kiwifruit, which remains green upon maturation. These fruit, therefore, provide an ideal model system for the study of chlorophyll degradation and its control.

1.1 Background

Actinidia species are perennial, deciduous, dioecious, woody vines which produce fruit that vary in many attributes, such as size, shape, hairiness of the skin, taste and colour between species (Ferguson 1990). *A. deliciosa* was first introduced to New Zealand from China in 1904 (Ferguson and Bollard, 1990). According to Ferguson and Bollard (1990), all commercial planting of kiwifruit in New Zealand and throughout the world can be traced to this one introduction of seed. The green-fleshed *A. deliciosa*, formally known as Chinese gooseberry in New Zealand, is an oval-shaped fruit with a brown, hairy skin. The fruit develop following pollination of female flowers with pollen from male flowers (Hopping 1990). Following commercial cultivation in the 1930s, export to the United States began in 1959 (Ferguson and Huang 2007). The success of the New Zealand kiwifruit industry led to the import of *A. chinensis* seed in 1977 and the domestication of the yellow-fleshed kiwifruit species, and the first Hort16A fruit in 1990 (Ferguson and Huang 2007).

Vines flower after three years of growth, with mature fruit eventually abscising from the vine after around 250 days after full bloom (DAFB) (Beever and Hopkirk 1990). Colour change in *A. chinensis* fruit occurs at around 120 DAFB, and harvest maturity is at around 180 DAFB for *A. chinensis* and 150 DAFB for *A. deliciosa* (Beever and Hopkirk 1990). As kiwifruit ripen, starch levels decrease, soluble sugars increase, fruit weight increases, and

firmness begins to decrease (Reid *et al.* 1982). Fruit is harvested at a stage called physiological maturity, when the fruit are still firm but can be removed from the plant and will continue to ripen. The fruit are normally cool-stored to reduce the rate of ripening and therefore to achieve optimum eating quality following export (Beever and Hopkirk 1990). In the 2010/2011 financial year, Zespri global kiwifruit sales were worth over $1.5 billion, with green kiwifruit having an orchard gate return (OGR) of $32,234 per hectare and yellow fruit having an OGR of $83,785 per hectare (Zespri Annual Report 2010/2011, http://www.zespri.com).

The regulation of changes in pigment composition that lead to flesh yellowing in some kiwifruit species, and not others, has not previously been studied. Elucidation of the genetic mechanisms governing this process is essential for developing an understanding of chlorophyll degradation in kiwifruit and may provide knowledge of de-greening in other plants. Furthermore, de-greening of commercial yellow cultivars is sometimes incomplete, resulting in poor perceived quality. Also, New Zealand's reputation as a quality exporter is dependent quality traits such as the extremes of green and yellow flesh colour (Ferguson and Huang 2007). Gaining more understanding of chlorophyll degradation is important for the development of kiwifruit with desirable traits such as flesh appearance and greater health benefits, leading to superior product competitiveness for New Zealand kiwifruit in global markets.

1.2 Kiwifruit pigments

Actinidia species and cultivars can have flesh colours ranging from the commercially grown green-fleshed 'Hayward' (*A. deliciosa* (A. Chev) C. F. Liang *et* A. R. Ferguson) and yellow fleshed Hort16A 'Kiwigold' (*A. chinensis* Planch.), to naturally occurring orange, red and purple cultivars (Figure 1.1). Flesh colour is dependent on levels of the pigments chlorophyll, anthocyanin and carotenoids in the inner and outer pericarp tissues.

Most fleshy fruit are only green during the early stages of development, undergoing dramatic changes in chemical composition and ultrastructure during maturation and ripening stages (Montefiori *et al.* 2009). The conversion of chloroplasts into chromoplasts and the concomitant loss of chlorophyll is often accompanied by accumulation of

carotenoids and is associated with tissue softening and the changes in carbohydrate and organic acid metabolism (Montefiori *et al.* 2009).

The immature fruit of both *A. deliciosa* and *A. chinensis* are green (McGhie and Ainge 2002). Chlorophyll is degraded in the fruit of *A. chinensis* to colourless catabolites upon fruit ripening, leaving the yellow pigment of the carotenoids visible. The characteristic yellow flesh of *A. chinensis* is due to the synthesis of carotenoid pigment during maturation (McGhie and Ainge 2002; Ampomah-Dwamena *et al.* 2009). Generally, carotenoid levels in both *A. deliciosa* and *A. chinensis* are stable, staying around 2 µg/g FW (Montefiori *et al.* 2009). The chlorophyll degradation process, seen in yellow kiwifruit, does not occur in the green flesh of *A. deliciosa* kiwifruit, which remains green even after maturation. These two kiwifruit cultivars demonstrate that chlorophyll breakdown is a separate process from ripening, and provide an ideal model for studying the genetic and biochemical processes involved in chlorophyll degradation.

Figure 1.1. Variation in kiwifruit colour. The natural variation in colour due to differences in chlorophyll degradation between *A. arguta* (A), *A. chinensis* (C), *A. deliciosa* (D), *A. eriantha* (E) and *A. polygama* (P) (Crowhurst *et al.* 2008).

1.3 Chlorophyll biosynthetic pathway

Chlorophyll biosynthesis can be divided into three stages; the formation of 5-aminolevulinic acid (ALA), the formation of protoporphyrin IX, and the formation of chlorophyll (Figure 1.2) (Eckhardt *et al.* 2004). The formation of ALA is catalysed by the enzyme glutamyl tRNA reductase (GLUTR), the key enzyme for metabolic and environmental control, and is thus the rate controlling point of the pathway (Eckhardt *et al.* 2004). When etiolated seedlings are exposed to light, *GLUTR* mRNA levels and ALA synthesis rise in parallel (Ujwal *et al.* 2002). Current findings indicate that GLUTR activity is regulated by both heme and the FLU protein, first isolated from the *Arabidopsis* mutant *fluorescence (flu)* (Meskauskiene *et al.* 2001). The mechanism(s) regulating ALA synthesis and total chlorophyll levels remain elusive. Eight ALA molecules are condensed to uroporphyrinogen III, which is then oxidatively converted to protoporphyrinogen in three steps (Eckhardt *et al.* 2004). Initially the enzymes of the chlorophyll biosynthetic pathway were thought to localise to the envelope and stroma of the chloroplast, but GFP tracking experiments show that the later enzymes of the pathway are associated with the chloroplast envelope and thylakoid membrane (Tottey *et al.* 2003; Yamasato *et al.* 2005). Most of the genes of the chlorophyll biosynthetic enzymes show a development-dependent expression profile (Eckhardt *et al.* 2004).

1.4 Photosynthesis-associated proteins

Ribulose-1,5-bisphoshate carboxylase/oxygenase (RuBisCO) is responsible for fixing carbon dioxide for photosynthesis. The small subunits of RuBisCO are likely to have a structural function, assembling and concentrating the large subunits (Andersson and Backlund 2008). A large amount is known about the molecular biology of the small subunit, where the *RBCS* genes were among the first plant genes to be cloned, sequenced and studied (Spreitzer 2003). Thus these genes are commonly used as molecular markers for photosynthesis.

Another molecule which is integral for photosynthesis, the light-harvesting chlorophyll *a*/*b* binding (LHCB) complex of photosystem (PS) II, is located in the thylakoid membrane

where it binds chlorophyll and the whole complex collects energy from sunlight and transfers excitation energy to the PSII reaction centre (Żelisko *et al.* 2005). The functional unit is a trimer, representing various permutations of LHCB1-3 apoproteins (Żelisko *et al.* 2005). In *Arabidopsis*, there are five copies of *LHCB1*, three of *LHCB2*, and one of *LHCB3* (Żelisko *et al.* 2005). The complex binds chlorophyll *a*, chlorophyll *b*, and carotenoids in the thylakoid membrane (Kusaba *et al.* 2007). The degradation of this complex is therefore tightly regulated during senescence to prevent photochemical damage to the reaction centre (Żelisko *et al.* 2005).

1.5 Chlorophyll degradation pathway

Chlorophyll is the green pigment responsible for harvesting light during photosynthesis and is contained in the thylakoid membranes of chloroplasts, along with associated photosynthetic proteins. This pigment is degraded during leaf senescence and fruit ripening (Harpaz-Saad *et al.* 2007). Because chlorophyll synthesis and degradation occur during the development of the plant, the pathways must be tightly regulated to prevent the accumulation of harmful intermediates that damage plant tissue (Harpaz-Saad *et al.* 2007). This process also allows the recycling of nitrogen contained in the chlorophyll molecules (Robson *et al.* 2004). The basic chlorophyll degradation pathway is outlined in Figure 1.2 and 1.3, where chlorophyll *b* is degraded to fluorescent chlorophyll catabolite (pFCC), with these steps common to all plants (Alos *et al.* 2008).

The degradation of chlorophyll to the colourless pFCC metabolite involves four enzymes (Hörtensteiner 2006). Chlorophyll is initially dephytylated to chlorophyllide by the enzyme chlorophyllase (CLH) and, subsequently, a metal chelating substance removes Mg (Hörtensteiner 2006). The product, pheophorbide *a*, is then converted to pFCC in a two-step reaction by pheophorbide *a* oxygenase (PAO) and red chlorophyll catabolite reductase (RCCR) (Hörtensteiner 2006). pFCC undergoes several modifications before catabolites are finally stored in the vacuole as non-fluorescent chlorophyll catabolites (NCCs) (Hörtensteiner 2006). Chlorophyll breakdown is tightly connected with the dismantling of pigment-protein complexes and the degradation of chlorophyll binding proteins such as the LHCB complex of PSII (Hörtensteiner 2006).

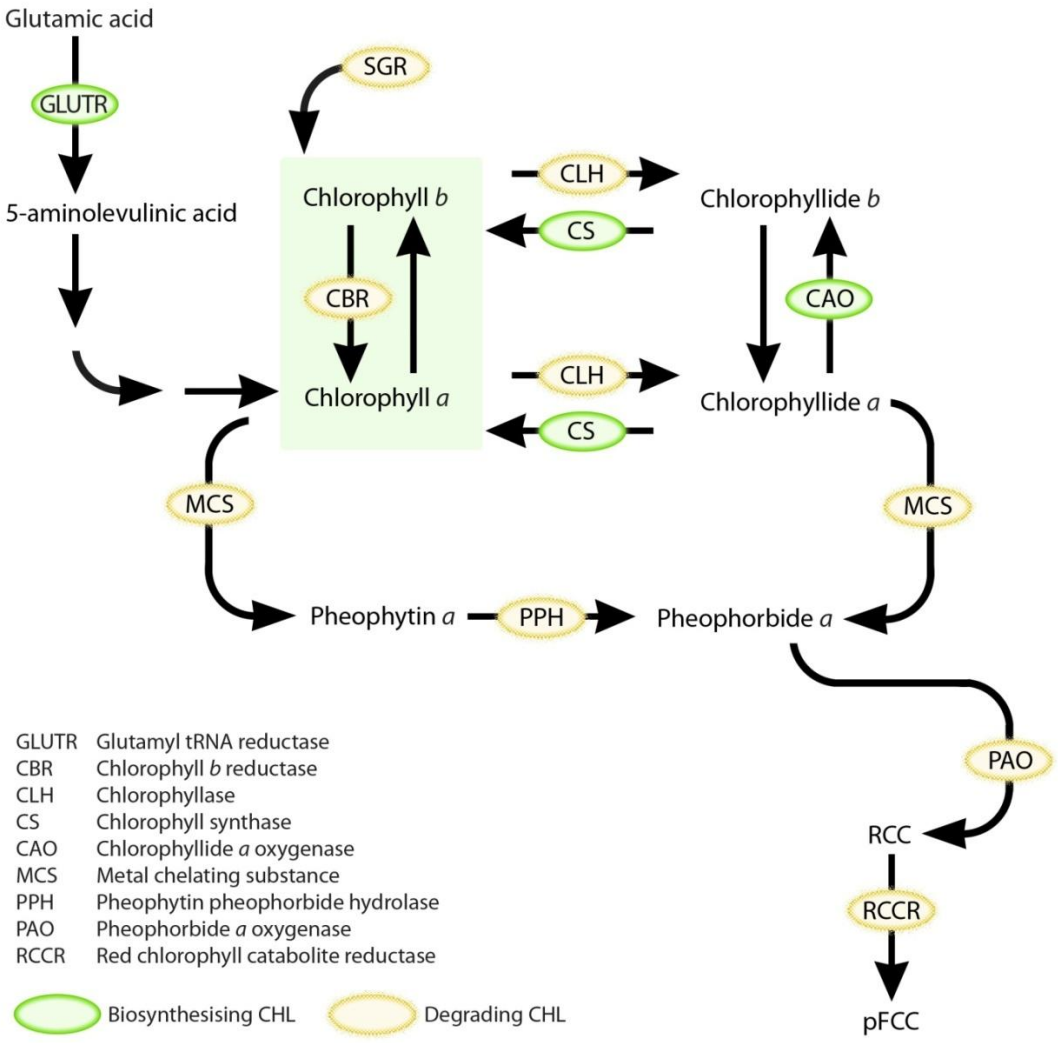

Figure 1.2. The biosynthesis and catabolism of chlorophyll. In the chlorophyll biosynthetic pathway, ALA is formed by GLUTR. Eight ALA molecules are then condensed to uroporphyrinogen III. This molecule is then converted to protochlorophyllide *a* in three steps. Chlorophyll then cycles between *a* and *b* forms, using the enzymes chlorophyll *b* reductase and chlorophyll *a* oxygenase. In the chlorophyll catabolic pathway, chlorophyll *b* is converted to chlorophyll *a* by chlorophyll *b* reductase. Chlorophyll *a* is converted to chlorophyllide *a* by chlorophyllase, and is subsequently converted to pheophorbide *a* by a metal chelating substance. The resulting pheophorbide *a* is then converted to red chlorophyll catabolite (RCC) by PAO, which is located in the chloroplast envelope. RCC is then converted to pFCC by RCCR. Several branching pathways and chlorophyll biosynthetic enzymes have been omitted for simplicity. Adapted from Eckhardt *et al.* (2004) and Schelbert *et al.* (2009).

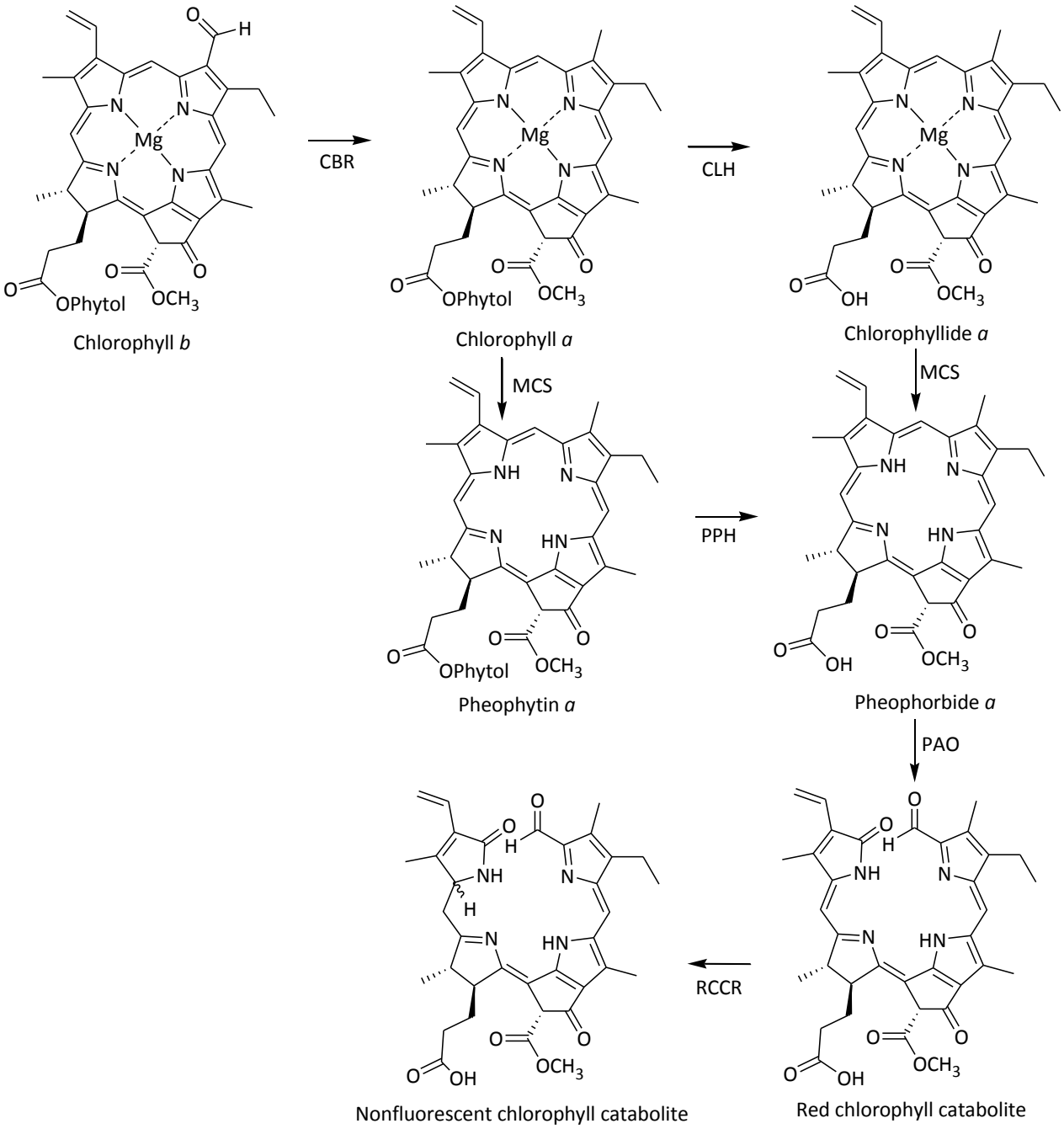

Figure 1.3 The pathway of chlorophyll breakdown in higher plants. The chemical structures of chlorophyll and chlorophyll catabolites are shown. Adapted from Hörtensteiner (2009).

1.6 Chlorophyll *b* reductase

The interconversion between chlorophyll *b* and chlorophyll *a* is important for adjusting the chlorophyll *a/b* ratio in response to any change in physiological and environmental conditions such as lack of light (Rüdiger 2002; Kusaba *et al.* 2007). This interconversion is catalysed by the enzyme chlorophyll *b* reductase (CBR) (Figure 1.2). Mutants showing delayed leaf yellowing are known as stay-green mutants, and are further discussed in Section 1.12. Previous experiments involving the stay-green mutation have determined that degradation of the light-harvesting complex depends on the conversion of chlorophyll *b* to chlorophyll *a* (Tanaka and Tanaka 2006). The stay-green genes *NON-YELLOW COLORING* (*NYC1*) and *NYC-ONE LIKE* (*NOL1*) of *Arabidopsis* are thought to encode chlorophyll *b* reductases, where the mutants are characterised by retention of the LHCB proteins, in contrast with the wild-type (Kusaba *et al.* 2007; Hörtensteiner 2009; Sato *et al.* 2009). The retention of the LHCB proteins during senescence also prevents degradation of the thylakoid grana structure, as the LHCB proteins are known to stabilise the grana by intermolecular forces (Sato *et al.* 2009). NYC1 and NOL differ only in the presence and absence of a transmembrane domain, respectively, and the expression of both genes is upregulated during senescence in rice (Sato *et al.* 2009).

1.7 Chlorophyllase

The conversion of chlorophyll *a* to chlorophyllide *a* and phytol is catalysed by the CLH enzyme. These enzymes were originally purified from *Citris sinensis* (orange) and *Chenopodium album* (white goosefoot), with subsequent isolation of the corresponding cDNA (Barry 2009). Subsequently, two genes were identified from *Arabidopsis* and designated *AtCLH1* and *AtCLH2* (Barry 2009). The majority of non-fluorescent chlorophyll catabolites are derived from chlorophyll *a*, as shown by structural analysis, which suggests that the conversion of chlorophyll *b* to chlorophyll *a* is the initial step for chlorophyll degradation (Barry 2009). Gene expression analysis has revealed that *CLH* genes can be induced by ethylene and methyl-jasmonate, which are known to stimulate chlorophyll breakdown (Tsuchiya *et al.* 1999; Barry 2009).

In higher plants, *CLH* genes encode soluble proteins that are predicted to localise in the cytoplasm, vacuole or chloroplast stroma (Park *et al.* 2007). However, there is also evidence that chlorophyllase is post-translationally processed at the *N*-terminus, yielding a mature catalytically active enzyme (Barry 2009). Cloning *CLH* genes revealed highly soluble proteins as deduced from the amino acid composition, raising questions as to the suggested localisation of chlorophyllase at the inner envelope of chloroplasts (Hörtensteiner 2006). Subcellular fractionation experiments show that chlorophyllase activity is present in the inner envelope membrane of chloroplasts (Park *et al.* 2007). However, the initial substrate, chlorophyll, is tightly bound to the LHCBI and II complexes in association with photosystem I and II, respectively (Park *et al.* 2007). Other cloned CLHs were proposed to locate outside of the plastid, based on sequence information, which implied the possible existence of additional chlorophyll breakdown pathways outside the chloroplast (Takamiya *et al.* 2000; Hörtensteiner 2006). Spatial separation between the CLH enzyme and its chlorophyll substrate was used to explain the latency of CLH in green leaves and has raised the hypothesis that there is an unidentified chlorophyll carrier in the chloroplast stroma that shuttles between the thylakoid and inner envelope membranes for chlorophyll transport (Park *et al.* 2007).

Recent investigations indicate that the two CLHs present in *Arabidopsis* are not essential for chlorophyll breakdown during leaf senescence, despite exhibiting CLH activity *in vitro* (Schenk *et al.* 2007; Hörtensteiner 2009). This questioned the relevance of CLH *in vivo*, and so it was concluded that the genuine chlorophyllase of *Arabidopsis* may not have yet been isolated (Schenk *et al.* 2007; Hörtensteiner 2009). Conversely, *Citrus* CLH was shown to localise to the chloroplast and to be active in chlorophyll breakdown during fruit ripening (Harpaz-Saad *et al.* 2007; Hörtensteiner 2009). Together, these investigations favour the existence of exclusively plastid-localised pathways of chlorophyll breakdown leading to the formation of pFCC (Hörtensteiner 2009).

1.8 Pheophytin pheophorbide hydrolase (PPH)

Recently, another enzyme of the chlorophyll degradation pathway has been identified that is responsible for dephytylation of the chlorophyll molecule, called PPH (Schelbert *et al.* 2009). PPH is an α/β hydrolase which is localised in the chloroplast and regulated during

senescence. *Arabidopsis* T-DNA insertion mutants have a stay-green phenotype (Schelbert *et al.* 2009). Rice *PPH* orthologue, *nyc3*, mutants were also reported to have a stay-green phenotype (Morita *et al.* 2009). A recent experiment in broccoli showed that PPH was responsible for senescence-induced chlorophyll dephytylation, compared with CLH, which did not show an expression pattern typical of genes related to senescence (Büchert *et al.* 2011).

1.9 Pheophorbide *a* oxygenase (PAO)

The chlorophyll degradation step catalysed by PAO is a critical step for opening of the tetrapyrrole ring of pheophorbide *a* by adding two oxygen atoms to yield RCC (Hörtensteiner 2006). This step is responsible for the loss of green colour associated with chlorophyll and the formation of colourless catabolites (Barry 2009). *PAO* gene expression is known to be highly correlated with the onset of senescence, whereas the expression of RCCR is known to be constitutive (Barry 2009). PAO is discussed further in Section 1.12.

1.10 Red chlorophyll catabolite reductase (RCCR)

RCCR works with PAO to site-specifically reduce RCC to pFCC (Hörtensteiner 2009). The colourless catabolites are then transported to the vacuole for disposal, as shown in experiments using radiolabelled NCCs in barley (Hinder *et al.* 1996). Defects in the PAO and RCCR steps were originally identified in the *accelerated cell death* (*acd*) mutants *acd1* and *acd2*, respectively (Hörtensteiner 2009). The *RCCR* gene is expressed in most tissues (including roots) and is constitutively active throughout leaf development, including senescence (Chung *et al.* 2006). In addition, RCCR protein levels do not change during senescence or pathogen attack, suggesting it is not the regulated control step in chlorophyll degradation (Chung *et al.* 2006).

1.11 Carotenoids

Carotenoids are yellow, orange or red pigments synthesised in plastids, mainly chloroplasts and chromoplasts, by nuclear encoded enzymes (Tanaka *et al.* 2008). These pigments are responsible for the yellow flesh colour of the yellow-fleshed *A. chinensis*, but are also present in high concentrations in the green flesh of *A. deliciosa* (McGhie and Ainge 2002). Plant carotenoids are 40 carbon isoprenoids containing up to 15 conjugated double bonds (Hirschberg 2001). In chloroplasts, carotenoids are associated with reaction centres and antenna complexes, reacting with and quenching triplet excited states in chlorophyll molecules, singlet oxygen, and superoxide radicals (Cunningham and Gantt 1998; Hirschberg 2001). These functions are essential for photosynthetic organisms, where an inability to form carotenoids is eventually lethal (Cunningham and Gantt 1998; Hirschberg 2001). Carotenoids also perform important roles harvesting light for photosynthesis, as precursors for the biosynthesis of the plant hormone abscisic acid, and pigments in flowers and fruit to attract pollinators and animals for seed dispersal (Cunningham and Gantt 1998; Hirschberg 2001). They are also precursors of vitamin A in human and animal diets, which may reduce the progression of diseases such as age-related macular degeneration and certain types of cancers and cardiovascular diseases. Thus fruit that accumulate high levels of carotenoids can potentially provide a rich source of these compounds (Cunningham and Gantt 1998).

The core enzymes of the carotenoid biosynthetic pathway are shown in Figure 1.4. The first committed step is the condensation of two molecules of geranyl geranyl pyrophosphate (GGPP) to form phytoene, which is catalysed by the enzyme phytoene synthase (PSY) (Cunningham and Gantt 1998). The colourless phytoene is subsequently desaturated to give zeta-carotene and lycopene. In plants, two enzymes are required for the desaturation of phytoene, phytoene desaturase (PDS) and zeta-carotene desaturase (ZDS) (Bartley *et al.* 1999). The carotenoid pathway branches at the cyclisation of lycopene. The formation of alpha-carotene requires the addition of an epsilon ring to one end of the linear lycopene molecule (yielding delta-carotene) by the enzyme lycopene epsilon cyclase (LCY-ε), followed by the activity of lycopene beta-cyclase (LCY-β), which adds a beta ring to the other end of the chain (Tanaka *et al.* 2008). In contrast, two beta rings are added to the linear lycopene molecule by the lycopene beta-cyclase enzyme (LCY-β) to form

beta-carotene (Tanaka *et al.* 2008). The flux through the branches is thus dependent on the relative activities of the cyclases involved. Previous research has shown that the major carotenoids that accumulate in kiwifruit are beta-carotene and lutein (Montefiori *et al.* 2005; Ampomah-Dwamena *et al.* 2009).

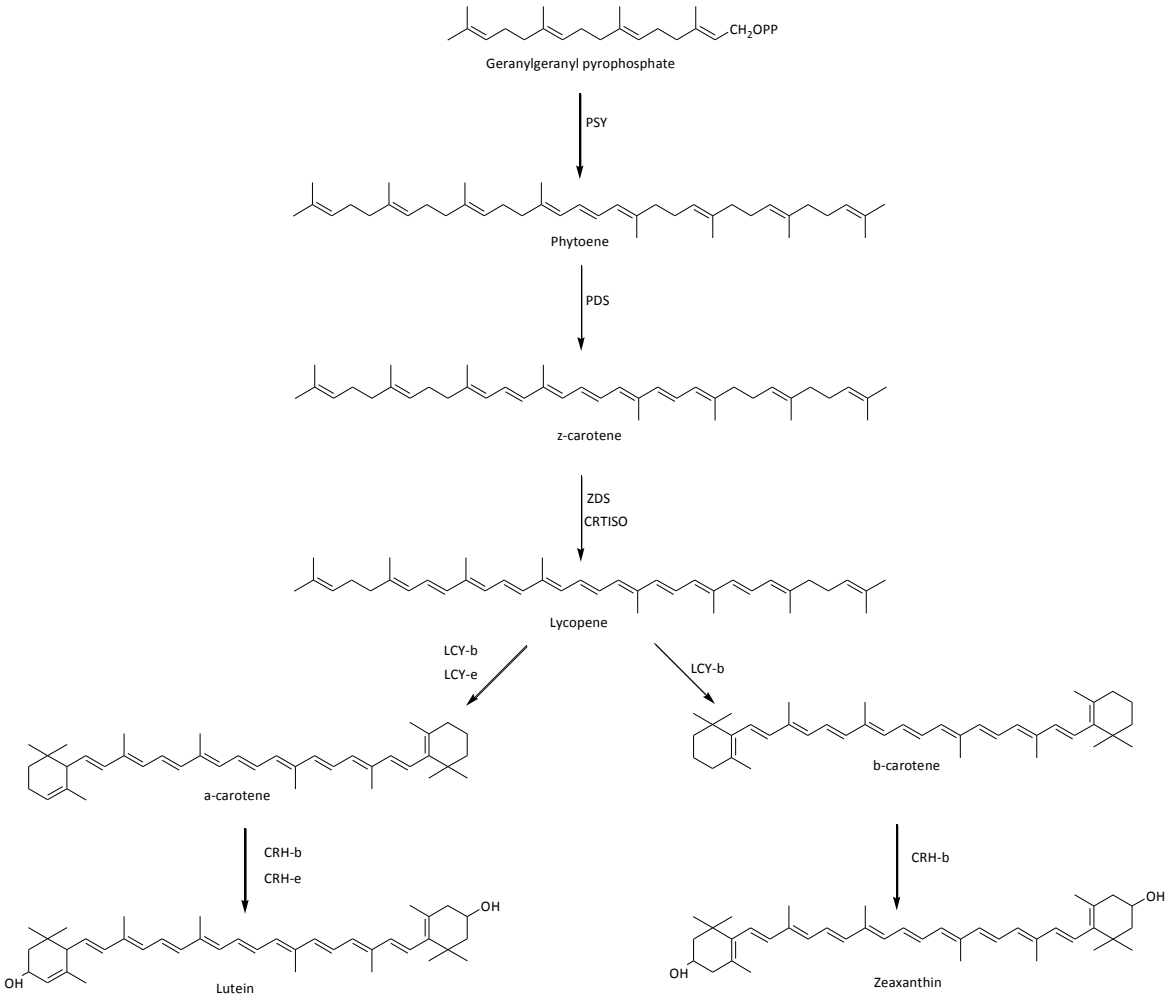

Figure 1.4. The carotenoid biosynthetic pathway. The conversion of geranylgeranyl pyrophosphate to phytoene is catalysed by the enzyme phytoene synthase (PSY). Phytoene is then converted to ζ-carotene by phytoene desaturase (PDS). Lycopene is then synthesised by the enzymes zeta-carotene desaturase and carotenoid isomerise. Two branching pathways then produce lutein and zeaxanthin. Adapted from Ampomah-Dwamena *et al.* (2009).

PDS is a potential rate-limiting enzyme in carotenoid synthesis. The RNAi silencing of this enzyme causes albinism in *Nicotiana tabacum*, suggesting that the exact matching of pigments and proteins is important for energy absorption and transfer in photosynthesis

and mismatching of them causes PSII malfunction (Wang *et al.* 2009). However, in kiwifruit, LCY-β was found to be a key regulated step (Ampomah-Dwamena *et al.* 2009).

In chloroplasts, carotenoids are located in photosynthetic membranes and integrated with chlorophyll binding proteins to form pigment-protein complexes. In chromoplasts, carotenoids are associated with polar lipids and carotenoid-associated proteins to form carotenoid-lipoprotein sequestering substructures, in order to effectively sequester and retain a large quantity of carotenoids (Lu and Li 2008). Fibrillin is a carotenoid-associated protein, comprising up to 80% of the total chromoplastic protein in capsicum fruit (Lu and Li 2008). Expression of the genes encoding these carotenoid-associated proteins is correlated with chromoplast development and carotenoid accumulation (Lu and Li 2008).

1.12 The stay-green mutants

Mutants that disrupt chlorophyll degradation, resulting in greenness of senescing leaves and cotyledons leading to stay-green phenotypes, have proven to be useful tools for identifying the underlying genes that contribute to chlorophyll degradation (Armstead *et al.* 2007; Barry 2009). Five different types of mutants (A-E) have been identified, leading to a retention of the chlorophyll (Thomas and Howarth 2000). These are classified according to the progress of senescence and loss of chlorophyll progresses. Type A stay-green plants show a delayed induction of senescence (Park *et al.* 2007). Type B stay-green plants show a normal induction of senescence, but senescence proceeds more slowly. Type D stay-green are green due to freezing or boiling, but are dead, and Type E stay-green plants are green due to higher initial levels of chlorophyll, as senescence initiation and progression is normal (Thomas and Howarth 2000). In contrast, Type C stay-green mutants arise from specific defects in the chlorophyll degradation pathway, as they undergo senescence at a normal rate, including a decline in photosynthetic capacity, but maintain chlorophyll concentrations (Barry 2009).

Type C mutants have been reported in a number of species, including soybean (d_1d_2), tomato (*gf*), rice (*sgr*), citrus (*nan*) and pepper (*cl*) (Park *et al.* 2007). It has been proposed that the genes identified in Type C stay-green mutants may encode the regulatory proteins triggering chlorophyll catabolism rather than a chlorophyll catabolic enzyme (Park *et al.*

2007). However, the absence of known domains following sequence analysis makes it difficult to propose a function for the SGR protein (Aubry *et al.* 2008).

The isolation of *SGR* homologues in different plant species has enabled testing of the hypothesis that the genetic control of stay-green in ripe fruit is similar to that in senescent leaves (Borovsky and Paran 2008). Reduced activity of PAO and the accumulation of pheophorbide *a* in several *sgr* mutants has led to the hypothesis that SGR is a modulator of PAO, where PAO may be part of the protein complex that mediates the degradation of the thylakoid membranes (Borovsky and Paran 2008). However, the recent finding that rice SGR is necessary for the degradation of the LHCB in the thylakoid membranes has led to an alternative hypothesis in which SGR-mediated degradation of the complex gives the catabolic enzymes access to the chlorophyll molecule, a hypothesis which is supported by LCHBII retention in several *sgr* mutants during leaf senescence and fruit ripening (Borovsky and Paran 2008) and outlined in Figure 1.5.

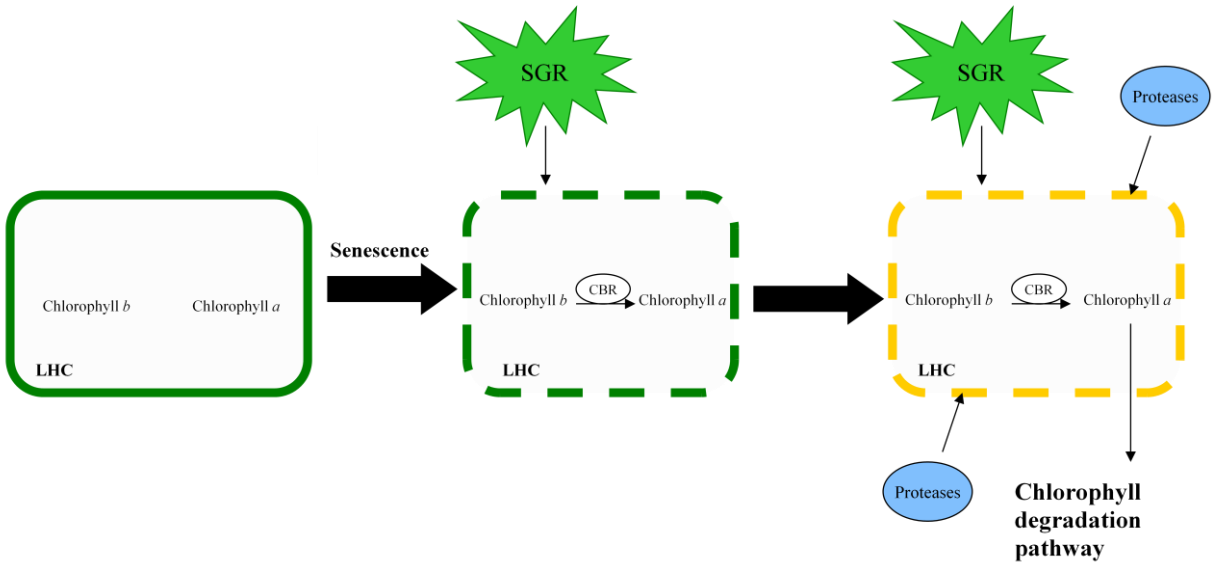

Figure 1.5. Proposed model for the role of the SGR protein. Upon initiation of senescence, the SGR protein has a role in the disassembly of the LHC, which allows proteases to degrade the complex. Chlorophyll *a* is then free to enter the chlorophyll degradation pathway. Adapted from Hörtensteiner (2009).

Fruit of the green flesh (*gf*) mutant of tomato ripen to a muddy brown colour, due to the accumulation of lycopene, coupled with a lack of chlorophyll degradation (Barry *et al.* 2008). This lack of chlorophyll degradation in *gf* is not restricted to fruit; there is retention

of chlorophyll, the thylakoid grana, LHCB and RBCS in both the fruit and leaves of the mutant (Barry *et al.* 2008). These phenomena appear to be a result of inhibition of chlorophyll degradation as opposed to a general inhibition of senescence, because senescence-associated marker genes appear to display normal expression patterns (Barry *et al.* 2008). This *gf* stay-green gene maps to chromosome 8 of tomato, which is homologous to the position of the chlorophyll retainer *cl* mutation on chromosome 1 of capsicum (Barry *et al.* 2008). It has recently been proposed that the two different mutants be referred to as *sgr* (Hörtensteiner 2009). Cotyledon colour (yellow *versus* green) in pea is regulated by Mendel's *I* locus, with the *i* mutant retaining not only greenness of the cotyledon during seed maturation, but also greenness of leaves during senescence, suggesting that this mutant is a stay-green mutant (Sato *et al.* 2007). A linkage between the *I* locus and the pea homologue of *SGR* has been shown, and previous work on Mendel's pea mutant determined the action of sgr to be independent and upstream of PAO (Armstead *et al.* 2007; Sato *et al.* 2007; Aubry *et al.* 2008).

1.13 Cytokinins

Cytokinins are a group of plant hormones produced from isoprenoid side chains derived from the methylerythritol phosphate (MEP) pathway. Cytokinins are involved in such diverse processes as the release of apical dominance, shoot meristem function, nutritional signalling and delay of senescence (Jameson 2003). Cytokinins have been implicated in the delay of senescence from the time of their first discovery, where cytokinins applied to senescing leaves led to re-greening (Richmond and Lang 1957). They are known to control the activity of genes for light-harvesting chlorophyll-binding proteins (Kulaeva *et al.* 1996). They are also known to promote the reversal of senescence by stimulating the expression of genes for the re-differentiation of senescent plastids (gerontoplasts) into chloroplasts (Robson *et al.* 2004). Similarly, cytokinin was shown to stimulate chloroplast-encoded transcription in detached barley leaves (Zubo *et al.* 2008). The cytokinin biosynthetic capacity of tobacco leaves has also been found to be reduced at the onset and during leaf senescence, although some senescing leaves have also been found to contain high levels of cytokinin *O*-glucosides, products of the cytokinin metabolic pathway (Jameson 2003).

Two biosynthetic pathways for cytokinins have been proposed; the tRNA pathway and the ADP/ATP pathway. The ADP/ATP pathway is proposed to be the major pathway, and is shown in Figure 1.6. The first step of the pathway is catalysed by the cytokinin synthase adenylate isopentenyltransferase (IPT), and is believed to be the key step of the cytokinin biosynthetic pathway, as the expression of the *IPT* gene leads to increased levels of cytokinin through the synthesis of the first committed precursor (Robson *et al.* 2004). Nine *IPT* genes have been identified in *Arabidopsis* (Kakimoto 2001; Takei *et al*. 2001). Similarly, there are eight IPT genes in rice (Sakamoto *et al.* 2006). Delayed senescence has been achieved by linking the promoters of the senescence associated genes (SAG) such as *SAG12* to the *IPT* gene in tobacco and maize (Gan and Amasino 1995; Robson *et al.* 2004).

Following the formation of *trans*-zeatin (tZ), cytokinins can be stored or inactivated (Figure 1.6 and 1.7). Cytokinin oxidases/dehydrogenases, known as CKO or CKX, inactivate *trans*-zeatin through conversion to adenine. The preferred substrates of CKX are the free bases and corresponding ribosides (Jones and Schreiber 1997). Like the *IPT* genes, the *CKX* genes also exist as a multi-gene family (Schmülling *et al.* 2003). *O*-glucosyltransferases can also convert *trans*-zeatin to *O*-glucosylzeatin (tZOG), which is resistant to oxidation by cytokinin oxidases, and is regarded as a storage form of cytokinin (Mok *et al.* 2000). The zeatin *O*-glucosyltransferase gene *ZOG1* was first isolated from *Phaseolus* (bean), and homologues have since been found in other species such as soybean and maize (Mok and Mok 2001). β-glucosidases can then reactivate tZOG back to tZ.

Other common natural isoprenoid cytokinin free bases include N^6-(Δ^2-isopentenyl)-adenine (iP), dihydro-zeatin (DZ) and *cis*-zeatin (cZ), which all have corresponding nucleotides, ribosides and glucosides (Figure 1.7). The diversity of cytokinin structures allows versatility of cytokinin functions (Mok and Mok 2001). Cytokinin activity in any particular organ is regulated through processes including *de novo* synthesis, activation, conjugation, and degradation (Kudo *et al.* 2010), as well as the differential activity of different gene family members.

The *cis*-forms of cytokinins associated with some tRNA moieties, are derived from the mevalonate (MVP) pathway. This pathway utilises IPT2 and 9 from *Arabidopsis*

(Miyawaki *et al.* 2006). As noted below, the *cis*-forms are not strongly perceived by the cytokinin receptors.

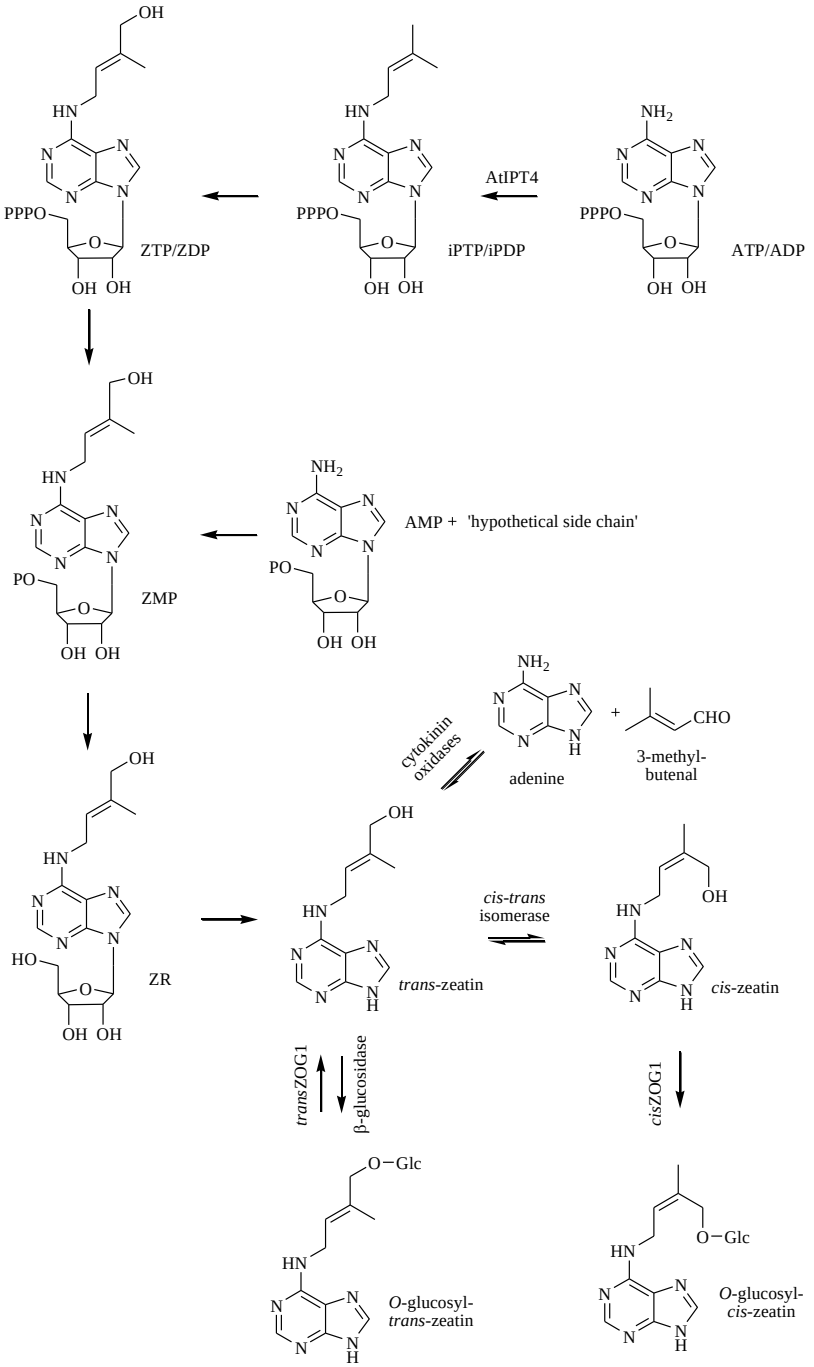

Figure 1.6. The cytokinin biosynthetic/metabolic pathway. The chemical structures of cytokinins through biosynthesis of zeatin and subsequent metabolism in *Arabidopsis*. Adapted from Haberer and Kieber (2002). Abbreviations are as follows: *Arabidopsis thaliana* isopentenyl transferase (AtIPT), isopentenyladenosine-5'-monophosphate (iPTP), zeatin riboside-5'-triphosphate (ZTP), zeatin riboside (ZR) and zeatin *O*-glucosyltransferase (ZOG).

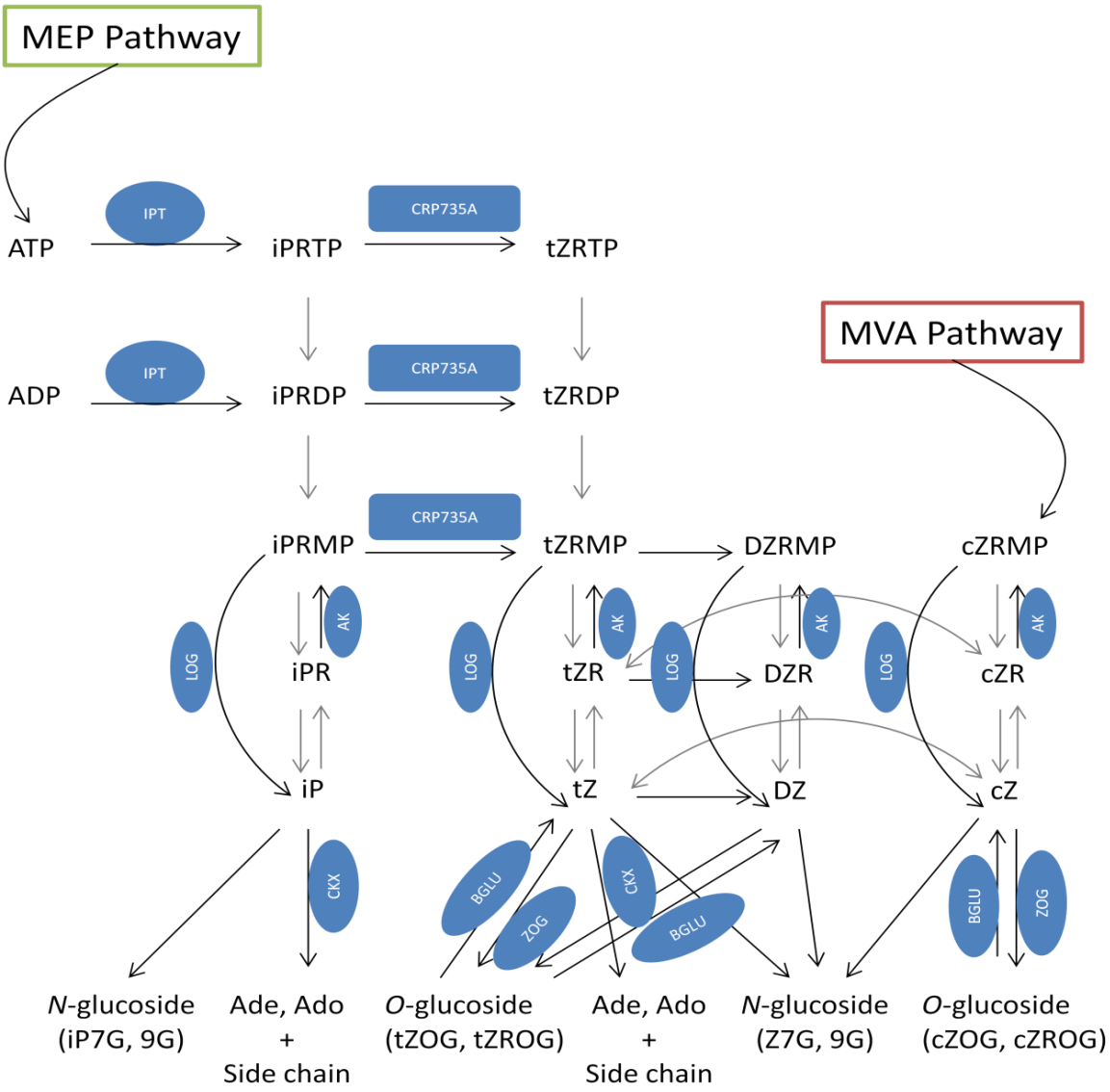

Figure 1.7. The cytokinin metabolic pathway. Current model of isoprenoid cytokinin (CK) biosynthesis pathways in *Arabidopsis*. The ADP/ATP pathway is proposed to be the major pathway, beginning with isoprenoid side chain substrates derived from the methylerythritol phosphate (MEP) pathway. IPTs utilise ATP or ADP to form iPRTP and iPRDP, respectively. Adenosine kinase (AK) phosphorylates iPR contributing to the metabolic pool of cytokinin nucleotides. The cytokinin nucleotides are converted into the corresponding tZ-nucleotides by CYP735A. iP, tZ, and the free bases can be catabolised by CKX to adenine (Ade) or adenosine (Ado). tZ can be reversibly converted to the tZOG by ZOG and BGLU. LOG has recently been identified which directly catalyses nucleotides to free bases. The *cis*-forms of cytokinins are derived from the mevalonate (MVP) pathway. Grey arrows indicate yet unidentified enzymes. Adapted from Sakakibara (2006) and Kamada-Nobusada and Sakakibara (2009).

1.14 Cytokinin signalling

Cytokinins play central roles in regulating plant growth and development through a two-component signal transduction system (Heyl and Schmülling 2003). A membrane-bound receptor kinase autophosphorylates a conserved histidine residue, and the phosphate is then transferred to a conserved asparagine residue within the receiver domain of a response regulator, originally named *Arabidopsis* response regulators (ARRs) (Figure 1.8). There are three cytokinin receptor kinases in *Arabidopsis*, AHK2, AHK3 and CRE1/AHK4 (Wulfetange *et al.* 2011). Substrate specificity studies reviewed in Shi and Rashotte (2012), showed that AHK2 has a cytokinin binding affinity of iP > tZ > iPR > tZR > DZ, and is expressed in *Arabidopsis* leaves, roots and flowers, AHK3 has a cytokinin binding affinity of tZ > tZR > DZ > iP > cZ, and is expressed in *Arabidopsis* leaves, stems, roots and flowers, and AHK4 has a cytokinin binding affinity of tZ > iP > tZR > iPR, and is mostly expressed in *Arabidopsis* roots. However, the receptors and their tissue expression patterns are not as well characterised in other species, and the receptors have not yet been extensively studied in fruit tissue.

The Type-B ARRs, which are transcription factors, then activate the expression of their target genes to mediate cytokinin-regulated growth and developmental processes (Argyros *et al.* 2008). Target genes of the ARRs have been postulated to include the cytokinin response factor genes (CRFs), which are closely related to the AP2/ethylene response factor gene family and may regulate downstream targets of the cytokinin response pathway (Rashotte *et al.* 2006; Werner and Schmülling 2009). Type-A ARRs act as part of a feedback control loop to regulate cytokinin signalling (To and Kieber 2008). Emerging evidence indicates that complex transcriptional cascades play an important role in the response to cytokinin, including changes in the expression of the components of the cytokinin signalling, biosynthetic and metabolic pathways, as well as the induction of various transcription factors (Argueso *et al.* 2010). Deciphering the mechanisms by which cytokinins regulate such diverse responses remains a key area of research.

Whole plant response to cytokinin is further regulated by translocation, where cytokinin ribosides are considered the major translocation form of cytokinin (Sakakibara 2006). High levels of tZ-type cytokinins in xylem and iP-type cytokinins in phloem, suggests that

cytokinins relay long distance signals with different biological messages mediated by variations in cytokinin side-chain structure (Sakakibara 2006; Hirose *et al.* 2008). The compartmentalisation of tZ- and iP-type cytokinins indicates that there is a selective transport system, and recent studies in *Arabidopsis* have suggested that equilibrative nucleoside transporters may have a role in the transport of ribosides and a purine permease family subset may have a role in the transport of free bases (Hirose *et al.* 2008). However, there is currently little evidence as to which form of cytokinin is transported across membranes and there is no evidence currently as to whether cytokinin detected in maturing kiwifruit is derived from external sources, or whether it is compartmentalised within the fruit.

The role of cytokinin is specific to different tissue types, including an important role in development in roots and shoots, and retention of chlorophyll in senescing leaves (Werner and Schmülling 2009). This is achieved in part by differential expression of gene family members encoding enzymes involved in cytokinin biosynthesis and homeostasis (Vyroubalová *et al.* 2009; O'Keefe *et al.* 2011). Cytokinin has been implicated in early growth and rapid cell division in fruit such as orange (Bohner and Bangerth 1988), tomato (Hernandez Minana *et al.* 1989) and apple and plum (Letham 1963). Previous experiments in *A. deliciosa* fruit have shown that the peak concentration of cytokinin coincides with early growth and rapid cell division soon after anthesis (Lewis *et al.* 1996b). However, there was also an increase in cytokinins in *A. deliciosa* observed at harvest, suggesting a role for cytokinin in the regulation of senescence or seed germination (Lewis *et al.* 1996b). These cytokinins included Z, ZR, Z9G, ZOG, iP, iPA, iP9G, ZNT and iPNT (Lewis *et al.* 1996b). The significance of changes in cytokinin content was also investigated using the application of the synthetic cytokinin *N*-(2-chloro-4-pyridyl)-*N*'-phenylurea (CPPU) (Lewis *et al.* 1996a). The application of CPPU increased fruit size attributed to increased cell division and cell size, and reduced endogenous cytokinin levels (Lewis *et al.* 1996a). CPPU treatment early in fruit development has also been reported to result in higher chlorophyll content in the outer pericarp of both *A. chinensis* and *A. deliciosa* fruit (Iwahori *et al.* 1988; Antognozzi *et al.* 1996). Cytokinin could therefore play a central role in fruit development and possibly the retention of chlorophyll in *A. deliciosa*.

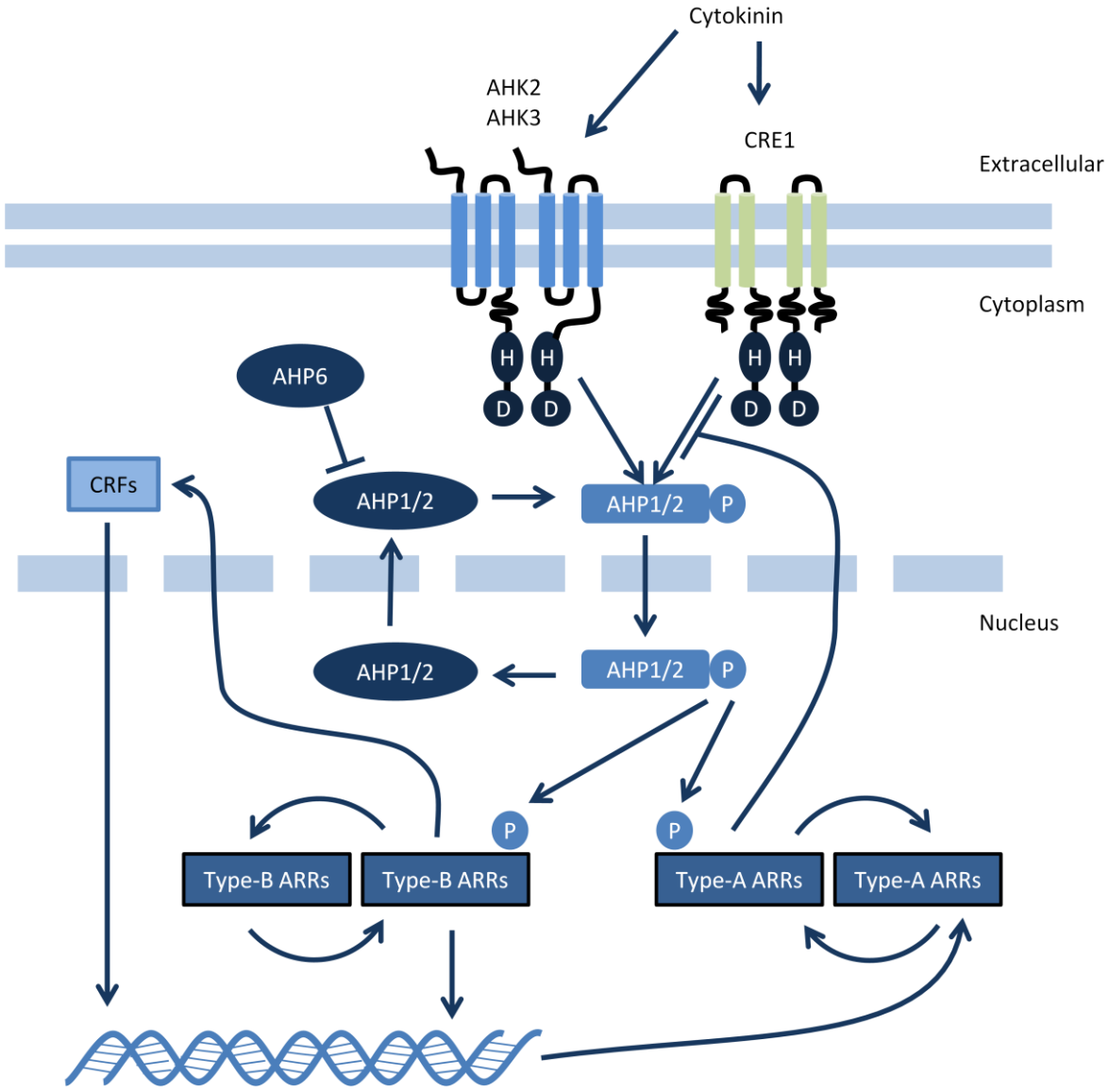

Figure 1.8. The cytokinin signalling pathway. A two-component signalling cascade is initiated by the binding of active cytokinin to histidine kinase receptors (AHKs). The phosphoryl group is transferred *via* the Asp-residue of the receptor receiver domain (green) to a conserved His of the histidine phosphotransfer proteins (AHPs). AHP6 inhibits the phosphoryl transfer, presumably by interacting with activated receptors and/or response regulators. AHP proteins relay the signal to Type-B or Type- A ARRs. Type-B ARRs are transcription factors regulating expression of their target genes including CRFs and the Type-A ARRs. One function of the Type-A ARRs is to repress signalling in a negative feedback loop. Adapted from Werner and Schmülling (2009).

1.15 Aims and Objectives

Chlorophyll degradation is a key physiological process in the plant life cycle. Stay-green mutants provide a useful tool for the study of the chlorophyll degradation pathway and the existence of a non-yellowing species of kiwifruit provides an excellent opportunity to further understand this pathway. Elucidation of the genetic regulatory mechanisms governing this process is essential for developing an understanding of chlorophyll degradation both in kiwifruit and in other plants. Furthermore, de-greening of commercial yellow cultivars is sometimes incomplete.

The principal aim of this project was to identify candidate genes for the control of chlorophyll degradation in kiwifruit. Included in this was a secondary aim to investigate whether the observed cytokinin accumulation in maturing *A. deliciosa* kiwifruit was associated with the delayed chlorophyll degradation. The research presented in this thesis involved a comparative biochemical and molecular analysis of green and yellow fleshed fruit and functional analysis of candidate genes using the kiwifruit germplasm resources available at Plant & Food Research. This knowledge will be transferred into the Plant & Food Research kiwifruit breeding programme for mapping candidate genes and in marker assisted breeding in an effort to accelerate the breeding programme.

2. MATERIALS AND METHODS

2.1 Bioinformatic Analysis

Actinidia ESTs with homology to *Arabidopsis* (or other species) proteins of interest were mined by BLAST match from the Plant & Food Research EST database.

2.1.1 Sequence analysis

DNA sequences from the Plant & Food Research *Actinidia* and *Malus* sequence databases and sequence products were analysed by Vector NTI version 9.0.0 (Invitrogen, USA) or Geneious version 5.4 (https://www.geneious.com). DNA sequence contigs were edited and compiled using Vector NTI version 9.0.0 ContigExpress and predicted protein sequences were aligned using Vector NTI version 9.0.0 AlignX.

2.1.2 Phylogenetic analysis

Phylogenetic and molecular evolutionary studies were carried out using MEGA 4 (Tamura *et al.* 2007). Bootstrap values from 100 bootstraps were included when greater than 50%.

2.2 Oligonucleotides

Oligonucleotide primers were designed to sense (F) or antisense (R) strands of DNA and were commercially synthesised (Invitrogen, New Zealand). Sequences of primers used in general cloning experiments are provided in Table 2.1. Gene-specific primers were designed for each gene to meet the MIQE guidelines (Bustin *et al.* 2009) using Primer3 (Rozen and Skaletsky (1998), code available at http://www-genome.wi.mit.edu/genome_software/other/primer3.html.) and Vector NTI version 9.0.0 (http://www.invitrogen.com).

Table 2.1. Primer sequences for PCR experiments. Primer name, EST number from the Plant & Food Research EST database, Gene name and Primer Sequence (5′ to 3′) are provided. All primers were designed to stringent criteria set out in the MIQE guidelines (Bustin *et al.* 2009).

Primer Name	EST Number	Gene Name	Primer Sequence 5′ to 3′	PCR Type
SP-003	81005	*SGR2*	GCAAAATTCTTTGGGTCAAAGTGCA	Promoter gene walk
SP-004	81005	*SGR2*	TGATCCATTGATCCATTGCCACAT	Promoter gene walk
SP-005	81005	*SGR2*	AGGGCTTAGCACTTGGCAATTTGTC	Promoter gene walk
SP-006	81005	*SGR2*	CAAAGAGGAAGATATAAATGACAATTTAGGTC	Promoter sequence
SP-067	81005	*SGR2*	CACCATTGGGGATGGGTACTCTGA	Whole gene sequence
SP-068	282554	*SGR1*	CACCAGATGGGTACTTTGACTGCTCC	Whole gene sequence
SP-069	282554	*SGR1*	ATAGTTAATCATAGAGTCTC	Whole gene sequence
SP-070	282554	*SGR1*	CAATCAAGTGTCTCGGTAGCAT	Whole gene sequence
SP-097	225823	*PPH1*	CACCCTGCTACAAGTCCAGTTATGTT	Whole gene sequence
SP-098	225823	*PPH1*	TGTTCACGCTTTTCATGGTTTA	Whole gene sequence
SP-099	276534	*RCCR*	CACCTGCGGATTCTTCAGCTATGTTT	Whole gene sequence
SP-100	276534	*RCCR*	AATACCAAGGTGTCATAACAGG	Whole gene sequence
SP-101	280505	*CBR1*	CACCCGAGTCTGTGGATATGACTATC	Whole gene sequence
SP-102	280505	*CBR1*	TTTTCCAGTCATTCCTATTTGC	Whole gene sequence
SP-103	175358	*CBR2*	CACCCTCGCAGAAGAAGATGGTGATA	Whole gene sequence
SP-104	175358	*CBR2*	TCTCATCAATCTTCACGCAGGT	Whole gene sequence
SP-105	75131	*CLH1*	CACCCGCTTGATCCGATTATCCAT	Whole gene sequence
SP-106	270679	*CLH2*	CACCCTGTGCTCATGTTTTGTCATGG	Whole gene sequence
SP-107	239173	*PAO1*	CACCGCTGAATCAATGGCTTTACTAC	Whole gene sequence
SP-108	239173	*PAO1*	TGTTAATCAATATCGGCATGTA	Whole gene sequence
SP-109	101510	*PAO2*	CACCAGCTGAATGAATGGCTTTGTTA	Whole gene sequence
SP-110	101510	*PAO2*	ATCCATATCACCCATTTTTGAT	Whole gene sequence
SP-115	325149	*ARR2*	CACCTTTTTGGTTATGGCTGCTCT	Whole gene sequence
SP-116	325149	*ARR2*	ACGTCGTGAGCCTATTCAGA	Whole gene sequence
SP-117	325148	*ARR6*	CACCTCTGAATAGGCTCACGACGT	Whole gene sequence
SP-118	325148	*ARR6*	AGAGAGTGGGTCAATCAACA	Whole gene sequence
SP-119	324616	*ARR9*	CACCTTGAGTTGGAGCAATGGGAT	Whole gene sequence
SP-120	324616	*ARR9*	TCTTGCATGAACCAACACTA	Whole gene sequence
SP-121	326078	*ARR11*	CACCATCCTTCTGTCGCTTCCATG	Whole gene sequence
SP-122	326078	*ARR11*	CCCACAGATCAATCAGACAA	Whole gene sequence
SP-123	325072	*ARR12A*	CACCCTGCTGGGAAAATGACTATT	Whole gene sequence
SP-124	325072	*ARR12A*	CAAGTGAGCGAAAATCATAT	Whole gene sequence
SP-125	325073	*ARR12B*	CACCCTCCAAAGATGACTATGGTG	Whole gene sequence
SP-126	325073	*ARR12B*	AGTCATTAGCACGATCCAAA	Whole gene sequence
SP-127	324617	*ARR17*	CACCAATCTCATGGATTCTGCTTC	Whole gene sequence
SP-128	324617	*ARR17*	TTAGTTTCTCTCAAGCCATC	Whole gene sequence
SP-129	311927	*RBCS*	CGCTGGGCCGAAAGGTCGAC	Promoter sequence
SP-132	239173	*PAO1*	GCCCACAACAACTTGGTCTT	Promoter sequence
SP-135	325149	*ARR2*	CACCAAATCAGGGCAACAAAATCG	Whole gene sequence
SP-136	325149	*ARR2*	ATGAGCAAAAGGTCCCACAG	Whole gene sequence
SP-137	325148	*ARR6*	CACCACTCCGGCGAGATTTGGTA	Whole gene sequence
SP-138	325148	*ARR6*	GATAGGCGCAAGGAATGGTA	Whole gene sequence
SP-139	324616	*ARR9*	CACCGGTTGATTTTGGCATTGGAT	Whole gene sequence
SP-140	326078	*ARR11*	CACCCGATCCTTCTGTCGCTTCC	Whole gene sequence
SP-148	280505	*CBR1*	CACCATTGTTGCTTCTCGCAGTCC	Whole gene sequence
SP-149	175358	*CBR2*	CACCGAGAGAAGCCTCGCAGAAGA	Whole gene sequence
SP-150	175358	*CBR2*	TGAAAATAAAACGTTAAATGGACAA	Whole gene sequence
SP-059	282554	*SGR1*	CACCGAGAGAAAGAAAGAGATGGGTACT	Whole gene sequence
SP-060	282554	*SGR1*	CCTACACAAACACTTATACGCACA	Whole gene sequence
SP-061	81005	*SGR2*	CCTGTAGTGAGTGTGTGATGTTGC	Whole gene sequence
SP-062	81005	*SGR2*	CCTCTAGCAACAACTCTAACCACA	Whole gene sequence
SP-073	270679	*CLH2*	CTGTGCTCATGTTTTGTCATGG	Whole gene sequence
SP-074	270679	*CLH2*	CCCGTGACATTAGGCTTCAA	Whole gene sequence
SP-075	75131	*CLH1*	GAGAGATGGCACAAGTAGTAGC	Whole gene sequence
SP-076	75131	*CLH1*	CGAAGCCTAAATGTCACAGG	Whole gene sequence
SP-154	280505	*NYC*	TTGCCTCGAATCTCAATCCT	Whole gene sequence
SP-155	280505	*NYC*	TGCATATATTTCGGGGGACT	Whole gene sequence
SP-156	175358	*NOL*	TCCATTTCCATCAGTCTCTCC	Whole gene sequence
SP-157	175358	*NOL*	CGATTCCTCCTAGCACCAAA	Whole gene sequence
SP-112	308872	*IPT*	GAAACGGACCCCGCCTCAGC	Whole gene sequence
SP-113	308872	*IPT*	GCGGTCGCGCATTGGGATTT	Whole gene sequence
SP-114	308872	*IPT-*	GCCCAACCCCGAAAGGTCGT	Whole gene sequence
SP-114	308872	*IPT-*	GCCCAACCCCGAAAGGTCGT	Whole gene sequence

2.3 End point PCR

General PCR was performed using 25 µl reactions in a MasterCycler Gradient (Eppendorf, Germany), with the following conditions for Platinum Taq (Invitrogen, USA):

Step 1	Initial denaturation	94 °C, 5 min
Step 2	Denaturation	94 °C, 30 sec
Step 3	Annealing	60 °C, 30 sec
Step 4	Elongation	72 °C, 1 min/kb
Repeat steps 2 – 4 for 35 cycles		
Step 5	Final elongation	72 °C, 5 min

2.4 Full length gene PCR

Full length gene PCR was performed using 25 µl reactions in a MasterCycler Gradient (Eppendorf, Germany), with the following conditions for Platinum Taq *pfx* (Invitrogen, USA):

Step 1	Initial denaturation	94 °C, 5 min
Step 2	Denaturation	94 °C, 15 sec
Step 3	Annealing	55 °C, 30 sec
Step 4	Elongation	68 °C, 1 min/kb
Repeat steps 2 – 4 for 35 cycles		
Step 5	Final elongation	68 °C, 5 min

2.5 Preparation of plasmid DNA

Plasmid DNA was purified from 3 ml overnight LB cultures of *E. coli* using the Invitrogen Miniprep kit (Invitrogen, USA), according to the manufacturer's instructions. Typically, the concentration of recovered DNA was estimated at 200 ng/µl. For all generic sub-cloning of PCR products for sequencing and downstream applications, the pGEM-T Easy

vector (Promega, USA) was used and ligations were carried out according to the manufacturer's instructions with the following modifications. pGEM-T Easy vector (0.5 µl), T4 DNA ligase (1 µl) and PCR product (3.5 µl) was added to 5 µl 2x rapid ligation buffer, mixed by pipetting, and incubated overnight at 4 °C.

Genomic DNA was isolated from kiwifruit leaves using the DNeasy Plant Mini Kit (Qiagen, Germany), according to the manufacturer's instructions, where a 50 µl final elution volume was used to maximise DNA concentration. Plant & Food Research TF library clones of EST-derived constructs, including most of the transcription factors used in the transient assay screen (unless described otherwise), were cloned by the Plant & Food Research Intragenics and transformation team (A. Gleave). ARRs and chlorophyll degradation pathway genes were obtained as plasmid DNA from the Plant & Food Research Intragenics and transformation team (A. Gleave) and cloned into *pHEX2S*, as described below. All vectors for plant transformation were sequenced to confirm authenticity.

2.5.1 Cloning of chlorophyll degradation pathway genes and ARR transcription factors

Full length PCR products were synthesised using whole gene sequence primers (Table 2.1) and blunt-end Platinum Taq *pfx* (Invitrogen, USA) polymerase, and ligated into the pENTR™/D-TOPO® vector using a Zero Blunt® TOPO® PCR cloning kit according to manufacturer's instructions (Invitrogen, USA) with the following modifications. Four µl PCR product, 1 µl salt solution, and 1 µl pENTR™/D-TOPO® vector were mixed by pipetting and incubated at room temperature for 1 h. Following sequencing to confirm identity and correct orientation of insert DNA, Gateway® LR Clonase™ II Enzyme Mix was used according to manufacturers' instructions (Invitrogen, USA) to move the gene of interest to *pHEX2S*.

2.5.2 Isolation of the *AcSGR* upstream promoter region by genome walking

Upstream DNA, immediately adjacent to the start codon (ATG) of *AcSGR*, was isolated from kiwifruit genomic DNA by PCR genome walking based on the GenomeWalker™ kit

(BD Biosciences Clontech, USA) protocol, with the following method. Genomic DNA was isolated as described above. Seven libraries were constructed from high quality gDNA preparations by digestion with seven restriction enzymes (*Dra*I, *Ecl*13611, *Eco*RV, *Apa*I, *Sca*I, *Ssp*I and *Stu*I), leaving blunt ends, to which the GenomeWalker™ adaptor was ligated. Nested primers to the coding region of *AcSGR* were designed (Table 2.1) and used in conjunction with adaptor primers for primary and secondary PCR, following the manufacturer's method for GenomeWalker™. A second genome walk was performed, with nested primers based on the sequence from the first walk The PCR products were cloned using the pGEM-T easy cloning vector as described above, and the sequences aligned using Vector NTI version 9.0 (Invitrogen, USA). This resulted in approximately 1 kb of confirmed upstream sequence from the transcription start site. The plasmid DNA was then digested, and the gene of interest ligated into *pGREEN 0800-LUC* (Hellens *et al.* 2005) using a rapid ligation kit (Roche, Germany). The *AcRBCS* and *AcPAO* promoters were isolated by designing PCR primers for the 1 kb region immediately upstream of the ATG from a draft genome scaffold alignment which had recently become available from the Plant & Food Research *Actinidia* genome sequencing project.

2.6 Manipulation of bacteria

Growth media were sterilised by autoclaving at 120 °C for 20 min. If necessary the pH was adjusted using NaOH or HCl. Selection antibiotics were added as required.

2.6.1 Transformation of *E. coli* (DH5α)

Competent *E. coli* DH5α (sub-cloning efficiency 1 x 10^6) were transformed by the freeze-thaw method. A 5 µl aliquot of plasmid DNA or ligation reaction mixture was added to 25 µl thawed cells in a 1.5 ml Eppendorf and gently mixed. The cells were incubated on ice for 15 min before heat shock at 42 °C for 40 sec in a water bath. The cells were then cooled on ice for 2 min. 450 µl of Luria-Bertani (LB) broth (1% (w/v) bactotryptone, 0.5% (w/v) yeast extract, 1% (w/v) NaCl, pH 7.0.) was added to each tube and incubated for an hour and a half at 37 °C, with shaking at 250 rpm. Aliquots of 30 µl were spread onto LB agar plates containing the appropriate antibiotic, either Ampicillin (100 mg/ml),

Kanamycin (50 mg/ml) or Spectinomycin (100 mg/ml). The plates were incubated at 37 °C overnight.

2.6.2 Transformation of *Agrobacterium* GV3101

Agrobacterium tumefaciens GV3101 (MP90) was transformed by electroporation with *pHEX2S* containing ESTs of interest or *pGREENII 0800-LUC* containing promoters of interest (Hellens *et al.* 2005). Competent cells (50 µl aliquots) were thawed on ice and plasmid DNA (50-200 ng in 1 µl water) was added, gently mixed, and pipetted into a pre-chilled electroporation cuvette (0.2 cm gap, Bio-Rad Laboratories, USA). The cuvette was placed in a GenePulser (Bio-Rad Laboratories, USA) and electroporation was carried out at a voltage of 2.5 kV (capacitance 25 µFd, resistance: 400 Ω) with a typical pulse time of 7-9 ms. The cells were recovered by addition of 1 ml LB, transferred to 1.5 ml tubes and incubated at room temperature, with shaking (60 rpm) for 2 h. Aliquots of 10 µl were spread onto separate LB plates (LB broth containing 1.5% (w/v) bactoagar) containing the appropriate antibiotics, either Kanamycin (50 mg/ml)/Rifampicin (25 mg/ml)/Gentinomycin (10 mg/ml) or Spectinomycin (50 mg/ml)/Rifampicin (25 mg/ml)/Gentinomycin (10 mg/ml). Plates were grown at 30 °C for 48 h.

2.7 DNA sequencing

DNA sequencing was carried out by the Allan Wilson Centre Genome sequencing service (AWCGS), at Massey University, Palmerston North, using capillary separation on an ABI3730 Genetic Analyser (Applied Biosystems, USA).

2.8 Collection of kiwifruit tissue and measurement of fruit characteristics

At each sampling time, ten fruit were collected at random from one vine from each cultivar (*A. deliciosa* (A. Chev) C. F. Liang *et* A. R. Ferguson) cv. 'Hayward' and *A. chinensis* Planch. cv. 'Hort16A') grown under normal commercial management at the Plant & Food Research Orchard, Te Puke, New Zealand. Fruit from an *A. chinensis* x *A. deliciosa* cross,

an *A. eriantha* x *A. chinensis* cross, and an *A. chinensis* mapping population grown in the same orchard were also sampled. Sampling dates for each cultivar are given as days after full bloom (90% flowers open), (DAFB).

Each fruit was measured for the fruit characteristics of colour, firmness, soluble sugars, dry matter and weight. The outer pericarp tissues of the same fruit were cut from the skin and locules, to ensure that only the outer pericarp tissue was harvested, and snap frozen in liquid nitrogen and stored at -80 °C. The outer pericarp tissue of ten fruit was pooled for each sampling point, and a second year of fruit was collected as a biological replicate.

2.8.1 Kiwifruit flesh colour measurements

Flesh colour was measured with a MINOLTA CR-300 chromameter (Osaka, Japan) in L*c*h* mode, calibrated on a white tile using D65 light. Measurements were routinely carried out after a 2 mm thick slice of skin and outer pericarp had first been removed from one face of the fruit.

2.8.2 Kiwifruit firmness measurements

A slice of skin was removed from the fruit prior to conducting the puncture test, which involved driving a 2.5 mm diameter flat-tipped probe into the flesh at a speed of 4 mm/s using a Fruit Texture Analyser and the Fruit Analyst Interface version 2005.2.0.8 (GÜSS, South Africa). One measurement was taken per fruit and recorded as kgF.

2.8.3 Kiwifruit soluble sugars measurements

Soluble solids concentration was determined by squeezing a drop of juice from each end of the fruit onto a hand-held refractometer (model N-20E, Atago, Tokyo). Measurements were recorded as °Brix.

2.8.4 Chlorophyll measurements

Chlorophyll was extracted and measured in 80% (v/v) acetone in 2.5 mM phosphate buffer pH 7.5 for determination of chlorophyll concentrations and chlorophyll *a/b* ratio using the methods and extinction coefficients of Porra *et al.* (1989). Chlorophyll concentration in µg/ml was calculated as follows:

Chlorophyll $a = 12.25\ A^{663.6} - 2.55\ A^{646.6}$
Chlorophyll $b = 20.31\ A^{646.6} - 4.91\ A^{663.6}$
Chlorophylls $a + b = 17.76\ A^{646.6} + 7.34\ A^{663.6}$
Concentration was then converted to µg/g FW.

2.9 RNA extraction from kiwifruit tissue

For each sample, 15 ml RNA extraction buffer (2% (w/v) CTAB (hexadecyltrimethylammonium bromide), 2% (w/v) PVP (polyvinylpyrrolidinone), 100 mM Tris-HCl (pH 8.0), 25 mM EDTA, 2.0 M NaC1, 0.5 g/L spermidine with 2% (v/v) 2-mercaptoethanol added prior to use) was pre-heated to 65 ºC. Fruit tissue (2 g) was ground in liquid nitrogen and added to the extraction buffer. An equal volume of chloroform/isoamyl alcohol was added, thoroughly mixed by inversion, and the homogenate was centrifuged for 10 min at 1,700 x *g* at room temperature to separate the phases. The top aqueous phase was then re-treated with an equal volume of chloroform/isoamyl alcohol and centrifuged for 10 min at 10,000 rpm at room temperature to separate the phases. The aqueous phase was then removed. LiCl was added to a final concentration of 2 M and the sample was stored at 4 ºC overnight. The sample was centrifuged at 4 ºC for 20 min at 1,700 x *g* to pellet the RNA and the supernatant was removed. The pellet was disolved in 500 µl SSTE (1M NaCl, 0.5% (v/v) SDS, 10 mM Tris-HCl pH 8.0, 1 mM EDTA pH 8.0) and transferred to a clean microcentrifuge tube. An equal volume of chloroform/isoamyl alcohol was added and the phases were separated by centrifugation at 18,000 x *g* at 4 ºC. The aqueous phase was removed, two volumes of EtOH added, and the sample was stored at -80 ºC for 30 min to precipitate the RNA. The sample was centrifuged at 18,000 x *g* for 20 min at 4 ºC to pellet the RNA and the supernatant discarded. The pellet was then dried and re-suspended in 150 µl water. RNA

integrity and concentration were assessed by gel electrophoresis (Figure 2.1) and quantified using a NanoDrop® ND-1000 UV-Vis Spectrophotometer (NanoDrop Technologies, USA).

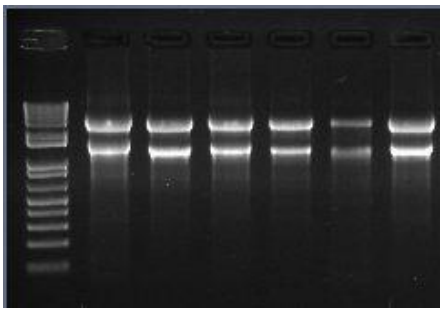

Figure 2.1. Representative RNA gel electrophoresis results. Representative gel electrophoresis results for *A. deliciosa* RNA samples. A 1 kb plus DNA ladder (Invitrogen, New Zealand) is shown in lane one. Samples in lanes two to seven show two clear bands of 28S and 18S RNA with little smearing, indicating good RNA quality for subsequent cDNA synthesis.

2.10 cDNA synthesis

RNA samples were treated with DNase (Ambion, Applied Biosciences, USA), according to the manufacturer's instructions and concentrations were determined using a NanoDrop® ND-1000 UV-Vis Spectrophotometer (NanoDrop Technologies, USA). The concentration of RNA used for each cDNA synthesis was kept constant at 1 μg for each sample. Reactions were performed using a Transcriptor First Strand cDNA Synthesis kit (Roche, Germany), according to the manufacturer's instructions and the supplied oligo(dT) primers.

2.11 Quantitative real-time PCR (qRT-PCR)

Kiwifruit were sampled as described in Section 2.8. Tissue from 10 fruit from each cultivar was pooled and RNA was isolated from kiwifruit samples using the pinetree method, previously described by Chang *et al.* (1993). Following DNase treatment, first-strand

cDNA synthesis was carried out. Genes encoding enzymes and regulators of the chlorophyll biosynthetic and degradation pathways were identified by homology in the Plant & Food Research expressed sequence tag (EST) database (Crowhurst *et al.* 2008). Gene-specific primers, as given in Table 2.2, were designed for each gene to meet the MIQE guidelines (Bustin *et al.* 2009) using Primer3 (Rozen and Skaletsky (1998), code available at http://www-genome.wi.mit.edu/genome_software/other/primer3.html.) and Vector NTI version 9.0.0 (http://www.invitrogen.com), allowing the qRT-PCR reactions to be carried out according to the manufacturer's instructions (Roche Diagnostics, Germany).

qRT-PCR steps consisted of pre-incubation at 95 °C for 5 min followed by 45 temperature cycles (95 °C (30 sec), 60 °C (30 sec) and 72 °C (30 sec)), with a final extension at 72 °C for 5 min, using the LightCycler 480 (Roche LightCycler 1.5; Roche Diagnostics). All reactions were performed using the LightCycler FastStart SYBR Green Master Mix (Roche Diagnostics) according to the procedure described by the manufacturer. Reactions were performed in triplicate using 2 µl Master Mix, 0.5 µM each primer, 1 µl diluted cDNA and nuclease-free water (Roche Diagnostics) to a final volume of 5 µl. A negative control was included in each run consisting of 2 µl Master Mix, 0.5 µM each primer and nuclease-free water (Roche Diagnostics) to a final volume of 5 µl. Fluorescence was measured at the end of each annealing step at 60 °C, and amplification was followed by a melting curve analysis with continual fluorescence data acquisition during the 65 – 95 °C melt, an example of this is given for *AdPP2A* in Figure 2.2.

The raw data were analysed with the LightCycler 480 software, version 4, and expression was rationalised to three reference genes, *A. deliciosa ACTIN*, *PP2A* and *EF1α*, to minimize variation in cDNA template levels. Reference genes were selected for their consistent transcript level throughout fruit tissues (crossing threshold (Ct) values changing by < 2 cycles) determined by qRT-PCR. For each gene, a standard curve was generated using a cDNA serial dilution, and the resulting PCR efficiency calculations (ranging between 1.5 and 2.3) were imported into target/reference expression ratio data analysis. An example of the standard curve for *AdPP2A* is shown in Figure 2.3. The target/reference ratio of a target gene was calculated on the reaction efficiency and the crossing point deviation of the target gene and reference gene. To ensure that the transcripts of single genes had been amplified, qRT-PCR amplicons were sequenced and confirmed as the expected DNA sequences. Melting curve analysis was also performed on qRT-PCR

samples using the LightCycler 480 software, version 4, to ensure that primers produced one PCR product. Error bars shown in qRT-PCR data are technical replicates, representing the means ± SE of four replicate qRT-PCR reactions.

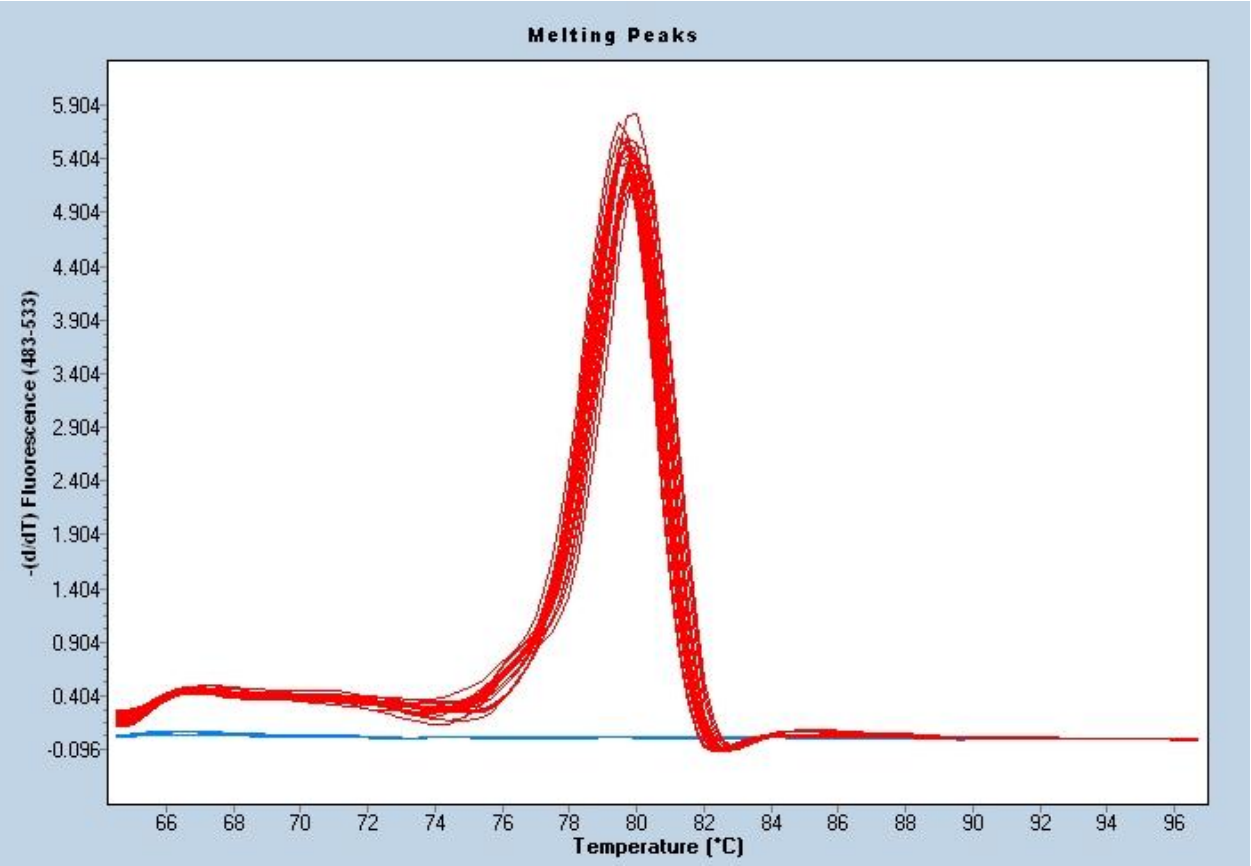

Figure 2.2. A representative melt curve analysis for *AdPP2A*. All qRT-PCR experiments were followed by a melt curve analysis to check for the amplification of a single product (red). No-template control samples were included (blue). This graph shows a uniform melt of 79 °C, confirming specific amplification. Data was analysed with the LightCycler 480 software, version 4 (Roche, Germany).

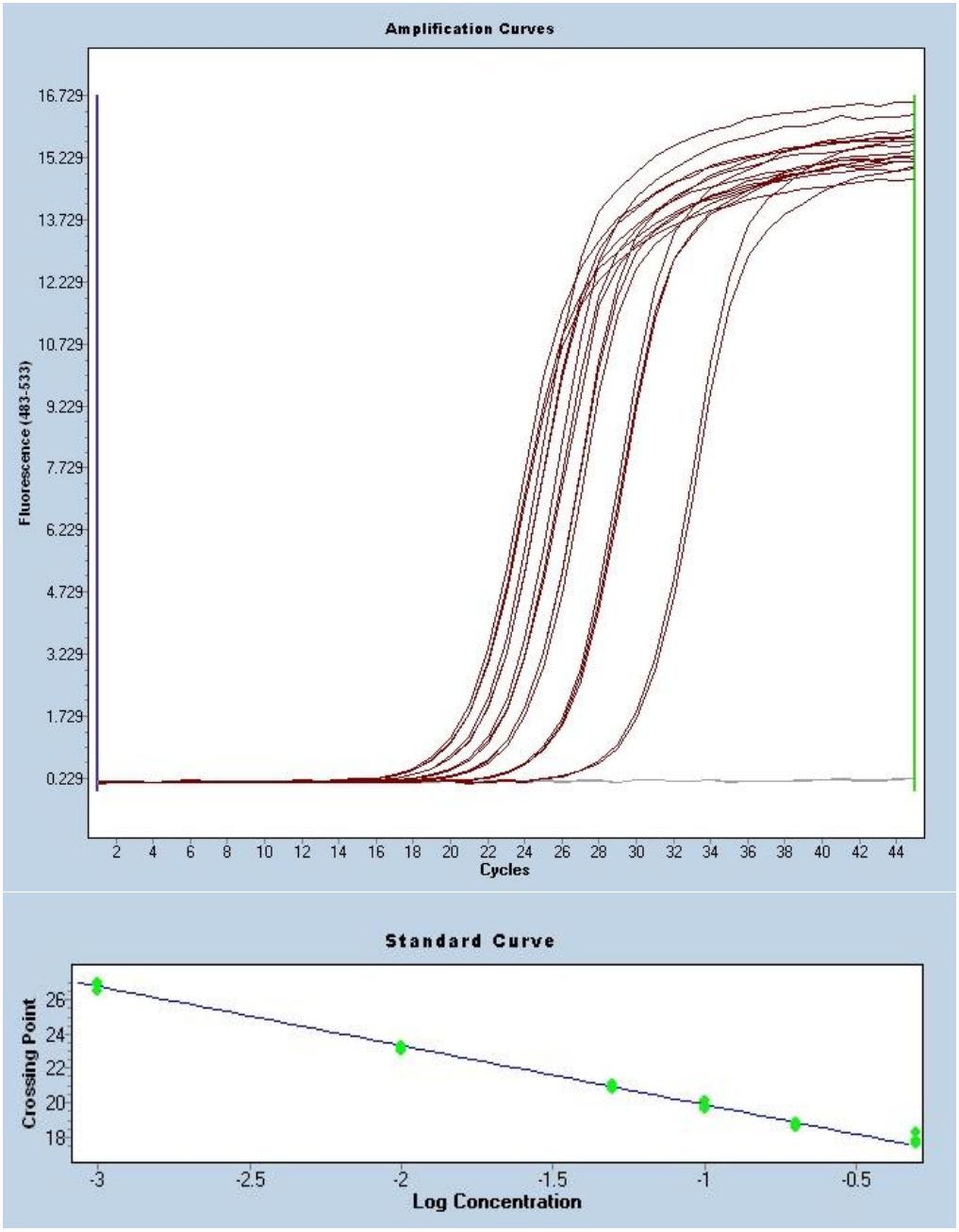

Figure 2.3. Serial dilutions of cDNA template used to generate a standard curve representing primer efficiency. A representative sample for *AdPP2A* shows a dilution series of 0.5, 0.2, 0.1, 0.05, 0.01 and 0.001. Efficient amplification of the template is seen at all dilutions over 45 cycles. Raw data was used to construct a curve representing the efficiency of the primer pair to amplify the target DNA. The resulting efficiency of this sample is 1.950 with an error of 0.0635. Data was analysed with the LightCycler 480 software, version 4 (Roche, Germany).

Table 2.2. Primer sequences for qRT-PCR experiments. Primer name, EST number from the Plant & Food Research EST database, Gene name and Primer Sequence (5′ to 3′) are provided. All primers were designed to stringent criteria set out in the MIQE guidelines (Bustin *et al.* 2009).

Primer Name	EST Number	Gene	Primer Sequence 5′ to 3′
Actin	-	-	TGCATGAGCGATCAAGTTTCAAG
Actin	-	-	TGTCCCATGTCTGGTTGATGACT
CHP	-	-	TGGGTCCAAGAAAGACGAGCC
CHP	-	-	GCCCTTCCTCTTCACCATCAAA
EF1	-	-	GCACTGTCATTGATGCTCCT
EF1	-	-	CCAGCTTCAAAACCACCAGT
PP2A	-	-	GCAGCACATAATTCCACAGG
PP2A	-	-	TTTCTGAGCCCATAACAGGAG
SP-007	225823	*PPH1*	TTGCGGGGGTTCCAAATGAA
SP-008	225823	*PPH1*	TGCCATACCACGAACCAGGACATT
SP-009	285383	*PPH2*	GGTCTTGGATTGGGACTCATTTTGC
SP-010	258383	*PPH2*	CCAAGGGAATCTCGGACAAGATAAA
SP-011	276534	*RCCR1*	TGTTTGATTGGAACGACGAAGAGCTT
SP-012	276534	*RCCR1*	CAGCAGGCTTAGCATTTCGAGATT
SP-013	280505	*CBR1*	GACCCTTATTGCAGTTCAGTGAT
SP-014	280505	*CBR1*	AGACCGCACTTTGTTGACCCATAGA
SP-015	175358	*CBR2*	CCATTTCCATCTGTCTCTCCTCTTT
SP-016	175358	*CBR2*	CATGGGTTCTCTGCTCGAAGAA
SP-017	302876	*CLS1*	AGAGACTGACGCTAACGAAG
SP-018	302876	*CLS1*	TCCATATATCCGTCTCTTGC
SP-019	307269	*PAPF*	GCCAAACCCATCAAAGAAGA
SP-020	307269	*PAPF*	ATTGGCTGCTTCAAGTTTGC
SP-021	322001	*GTR1*	CTCGTCTTCTCCGAGCCTCT
SP-022	322001	*GTR1*	TCAACAGGTGCAGTGTGGAT
SP-023	258653	*GTR2*	GGTTATTGGAGCAGGCAAGA
SP-024	258653	*GTR2*	CGGATGGCAGCTACTCTCTC
SP-025	260884	*CAO*	AGCAGGATGGAATGATCTGG
SP-026	260884	*CAO*	CGGAAGCTCCATGACAATCT
SP-027	311927	*RUB*	CTCCTCCTCTGCGGTTACCT
SP-028	311927	*RUB*	CCAGAGCTACGAGAGCCACT
SP-029	305437	*LHCB1*	GGATTCGGCAAGAAGAAAGC
SP-030	305437	*LHCB1*	TAATCGCCCACCAGACTACC
SP-031	48185	*LHCB2*	TGGATTTGGCAAGAAGAAGG
SP-032	48185	*LHCB2*	AATCGCCTACCAGACTACCG
SP-033	319319	*CAB1*	CTGTCAGGACCGTACCACTTGG
SP-034	319319	*CAB1*	AAGCCCGTCGCTCTCTTCTC
SP-035	311138	*CAB2*	CTGTCAGGACCGTACCACTTGG
SP-036	311138	*CAB2*	AAGCCCGTCGCTCTCTTCTC
SP-037	308872	*IPT8*	GCCACTGCTGCAACAAATTA
SP-038	308872	*IPT8*	CCCATAATCACCACGACCTT
SP-039	157269	*IPT3*	AAAGGCTCATCAGACGTTCG
SP-040	157269	*IPT3*	GAGCCTGGGAGAATGACATC

Primer Name	EST Number	Gene	Primer Sequence 5′ to 3′
SP-041	42116	*CKX5*	CCGGTTCTCTATTGCCTTGA
SP-042	42116	*CKX5*	CTGGAACCTCAGGTCTTTGC
SP-043	99598	*ZOG*	ACACCCCTCAAAGACGTGAG
SP-044	99598	*ZOG*	GTCTGTGGTTCGGAGAAAGC
SP-045	104489	*BGLU40*	CACCCAAAACTCAGCCTCTC
SP-046	104489	*BGLU40*	ACCGCCACATGACCAAGTA
SP-047	301111	*BGLU1*	GGAAAAGAAGGTCCCCATTG
SP-048	301111	*BGLU1*	TCTAGCCGTACCGTCTCTGG
SP-049	274589	*BGLU2*	ACGGTACGGCTAGACACTGG
SP-050	274589	*BGLU2*	AATGAAGACGTCCCAGATGC
SP-051	313626	*SAG12*	TCGCTGTTGTTGGTATTGGA
SP-052	313626	*SAG12*	AGATTGCCATGATTGACGTG
SP-053	303872	*IPT8*	CGAACAAAAATCAGAGCTGGA
SP-054	303872	*IPT8*	CAAGAGCGAACGTCTGATGA
SP-055	75131	*CLH1*	CGCTTGATCCGATTATCCAT
Sp-056	75131	*CLH1*	CGACACCTTGCTTGCACATA
SP-057	270679	*CLH2*	CCATCTATTGCTCCAACACG
SP-058	270679	*CLH2*	AACACGAAATTGTCATCACACC
SP-071	251262	*OGLY*	AGAGAAGCCTCACGCAGTGT
SP-072	251262	*OGLY*	TGAACTCGGTGTTGACGAAG
SP-077	175358	*CBR2*	GGAATACCTTGTCCCAAGCA
SP-078	175358	*CBR2*	CCTAGCACCGAAAGCAAATC
SP-079	325149	*ARR2*	GAAGCAGGAGCCAAGTATGG
SP-080	325149	*ARR2*	GGATGACGTCGTGAGCCTAT
SP-081	1833785	*ARR4*	CCACAGCCGTCACTTTACAA
SP-082	1833785	*ARR4*	TCGATGAATTCTTGCCTTCC
SP-083	325148	*ARR6*	CCTATCCCATCGTGTTTCGT
SP-084	325148	*ARR6*	AACCCAGAAGGGTCACAATG
SP-085	324616	*ARR9*	AGGGCTTTCACCAGACAGAA
SP-086	324616	*ARR9*	TGATCTTGCATGAACCAACAC
SP-087	326078	*ARR11*	ATTCAACCATCTCCCACTGC
SP-088	326078	*ARR11*	TGGACGCTGGTTTCTCTCTT
SP-089	325072	*ARR12A*	CATCTCATGGCCCAAATCTT
SP-090	325072	*ARR12A*	TCCCCAGAGCTGATTGTTCT
SP-091	325073	*ARR12B*	AATGAAAAGTGGGGAGAGCA
SP-092	325073	*ARR12B*	TCCAAAATCCGGCTTAGTTG
SP-093	2232475	*ARR13*	GTTAACCCTGGCACGTTCAT
SP-094	2232475	*ARR13*	AAGGTTGTTTGGACCAATGC
SP-095	324617	*ARR17*	AAAGCCTCTCAAGCAAGCAG
SP-096	324617	*ARR17*	ATCAAGCAGCCTTTCTCCAA
SP-158	2279282	*IPT3*	TTCCCTTCCTGTGCTCAACT
SP-159	2279282	*IPT3*	CAAATTCGGGGACACCAATA

2.12 Statistics

Pearson's correlation analyses between hue angle colour measurements from Section 2.8.1 and RT-qPCR measurements from Section 2.11 were performed using Minitab 15 Statistical software (Minitab Inc., USA) and standard basic correlation analysis parameters.

2.13 Transient transformation of *Nicotiana benthamiana*

N. benthamiana plants were grown under glasshouse conditions in full potting mix, using natural light with daylight extension to 16 h, until at least two fully expanded leaves were available for infiltration with *Agrobacterium*. Plants were maintained in the glasshouse for the duration of the experiment.

Transient assays were carried out using the methods described previously in Hellens *et al.* (2005). *Agrobacterium* was cultured on LB agar (Invitrogen) containing selection antibiotics and incubated at 28 °C. A 10 µl loop of bacteria was re-suspended in 10 ml of infiltration buffer (10 mM $MgCl_2$, 0.5 µM acetosyringone) and incubated at room temperature with gentle shaking for 2 h. The cultures were then adjusted to an OD_{600} of 0.6 - 0.8 with additional infiltration buffer before infiltration. Each *Agrobacterium* culture was then mixed 50:50 with *Agrobacterium* transformed with *p19* to reduce silencing in the plants. Infiltrations were performed according to the methods described by Voinnet *et al.* (2003). Approximately 1 ml of infiltration buffer containing *Agrobacterium* was infiltrated at two points into a young leaf of *N. benthamiana*.

2.13.1 Photosynthetic yield of transiently transformed *N. benthamiana* leaves

Loss of fluorescence was used as a measure of chlorophyll degradation using a photosynthesis yield analyser, MINI - Pulse Amplitude Modulation (PAM) portable chlorophyll fluorometer (Heinz Walz GmbH, Germany) as described previously for barley leaves in Shabala *et al.* (2005). Leaves were dark-adjusted by covering with black polythene for 30 min. Measurement was conducted under the polythene in the dark. Chlorophyll fluorescence was

measured at 660 to 760 nm. The photosynthesis yield (overall quantum yield of photochemical energy, was expressed as: Yield (Y) = (Fm′ – F)/Fm′ = ΔF/Fm.

2.13.2 Fluorescence microscopy of transiently transformed *N. benthamiana* leaves

Fluorescence microscopy was kindly carried out on transiently transformed tobacco leaves by Richard Espley and Midori Jones at Plant & Food Research. *N. benthamiana* leaves were examined for the presence of chlorophyll using an Olympus Vanox AHT3 microscope (Olympus Optical, Tokyo, Japan) in epifluorescence mode (excitation wavelength:465–495 nm; emission: 515 nm and above). Images were recorded using a CoolSNAP (Roper Scientific Ltd., Tucson, Arizona) colour digital camera.

2.14 Dual luciferase assay of transiently transformed *N. benthamiana* leaves

N. benthamiana plants were grown and infiltrated as described in Section 2.13. Transformed *Agrobacterium* cultures containing *pGREENII 0800-LUC* reporter cassettes with candidate promoter insert, as described in Hellens *et al*. (2005), or *pHEX2S* with candidate TF insert were cultured on LB plates containing the appropriate antibiotics and incubated at 28 °C. A 10 µl loop of bacteria was re-suspended in 5 ml infiltration buffer (10 mM $MgCl_2$, 0.5 µM acetosyringone) and incubated at room temperature with gentle shaking for 2 h. The cultures were then adjusted to an OD_{600} of 0.6 - 0.8 with additional infiltration buffer before infiltration. Each *Agrobacterium* TF culture was then mixed 50:50 with *Agrobacterium* transformed with each promoter of interest. For combinatorial TF infiltrations, 100 µl promoter culture, 300 µl of each TF and *pHEX2S* up to 1 ml. Infiltrations were performed according to the methods of (Voinnet *et al.* 2003), using a 1 ml syringe with no needle. Approximately 150 µl of this *Agrobacterium* mixture was infiltrated at two points per young, fully expanded leaf of *N. benthamiana*. Two leaves were infiltrated per gene, and randomised to different plants.

Transient expression was assayed three days after inoculation. Two replicates were taken per leaf of 2 mm diameter leaf discs, which were excised from each plant using a leaf hole punch, and crushed in 50 µl phosphate buffered saline (PBS) (6.3 mM Na_2PO_4, 0.2 mM Na_2HPO_4,

0.2 mM KH_2PO_4, 2.6 mM KCl, 138 mM NaCl, pH 7.4.). Plate-based assays were conducted using a Victor Luminometer, according to the manufacturers' instructions for the dual luciferase assay, using the Dual Glow assay reagents for firefly luciferase and Renilla luciferase (REN) (Targeting Systems, USA). The fluorescence of LUC was measured relative to REN, where an increase in the LUC:REN ratio indicates an activation of the candidate promoter by candidate TFs.

2.15 Kiwifruit seedling experiments

Kiwifruit seed extraction was carried out based on in-house methods at Plant & Food Research. The skin was removed from two store-bought yellow-fleshed kiwifruit and diced. Seeds were extracted by placing the flesh in a pectinase:water solution (1:200 v/v) (Rohm Rohapect D5L) at room temperature for 24 h. The solution was then passed through a strainer and the remaining seeds were washed with water. The seeds were then soaked in 5% (v/v) hypochlorite solution for five min, and then washed with water. The clean seeds were then placed in a 9 cm Petri dish lined with filter paper (Whatman, 110 mm No.1) and dried in the laminar flow hood for around 2 h. Dry seeds were stored at 4 °C in a 15 ml Falcon tube.

2.15.1 Propagation of kiwifruit seedlings

Seeds were stratified prior to sowing. Seeds were placed in a 9 cm Petri dish lined with filter paper (Whatman, 110 mm No.1), which had been dampened with 1 ml sterile water. Petri dishes were sealed with parafilm and placed at -20 °C for 24 h. The seeds were then placed onto ½ MS media in tubs, and grown in a light and temperature controlled growth room (12 h light (50 $\mu Em^{-2}s^{-1}$), 12 h dark, 22 °C) for about 25 days, or until the seedlings had reached the four leaf stage.

2.15.2 Dark-induced seedling senescence

Seedlings for dark-induced senescence experiments were prepared as described above. Four individual seedlings were transferred singularly into tubs which were then individually

wrapped in aluminium foil. The tubs were placed in a box lined with aluminium foil. A tub was removed from the box each week to assess for dark-induced senescence, without exposing the remaining plants to the light. Control seedlings were maintained in a light and temperature controlled growth room (12 h light (50 $\mu Em^{-2}s^{-1}$), 12 h dark, 22 °C) for the duration of the experiment.

2.16 Kiwifruit transformation experiments

Stable transgenic kiwifruit lines of *A. deliciosa* and *A. chinensis* were grown from calluses transformed by *Agrobacterium* containing *pHEX4* control and *pSAK778S*:*SGR* or *pTKO2*:*SGR*, respectively, by Tianchi Wang at Plant & Food Research.

2.16.1 Dark induced senescence in leaf patches

Mature, fully expanded kiwifruit leaves from transgenic kiwifruit lines were removed from the plant and immediately cut into 1 cm^2 sections. The method for dark induced senescence experiments in leaf patches was adapted from previous methods used for rice, as described by Sato *et al.* (2009). Three leaf patches from the same leaf were used as replicates, placed in distilled water in a petri dish. Control samples were maintained in a light and temperature controlled growth room (12 h light (50 $\mu Em^{-2}s^{-1}$), 12 h dark, 22 °C) for the duration of the experiment. Dark samples were wrapped in aluminium foil and were also maintained in the temperature controlled growth room at 22 °C, and assessed in a dark room, to avoid exposing the leaf patches to light. Ethylene treated samples were incubated in 10 µl/l ethylene overnight and then treated in the same way as the control samples. Leaf patches were assessed for senescence every seven days, and photographs were taken of the leaves at 0 days and at 60 days of each treatment.

2.16.2 Infiltrating kiwifruit seedlings

Transient assays were carried out as described for *N. benthamiana* leaves in Section 2.13. Approximately 1 ml of infiltration buffer containing *Agrobacterium* was infiltrated at two points into a young leaf of *A. chinensis*.

2.16.3 Injex system for kiwifruit infiltration

Agrobacterium was cultured on LB agar containing selection antibiotics and incubated at 28 °C. A 10 µl loop of bacteria was re-suspended in 10 ml of 100 µM infection buffer (0.22% (w/v) MS + vitamin, 2% (w/v) sucrose, 0.1% (v/v) 100 µM acetosyringone, pH 6.0) to an OD_{600} of 0.6 - 0.8, and incubated at room temperature with gentle shaking for 2 h before infiltration. Approximately 1 ml of infection buffer containing *Agrobacterium* was infiltrated using an Injex30 Needle Free Injection System (Injex Pharma Ltd., Germany) into *A. eriantha* fruit in the transverse direction. Fruit were cut and photographed after 5 days.

2.17 CPPU treatment of *A. chinensis* kiwifruit

Three treatments were used, synthetic cytokinin *N*-(2-chloro-4-pyridyl)-*N*'-phenylurea (CPPU) (4×10^{-5} M) wicks, CPPU (4×10^{-5} M) dipping and control, with 20 fruit per treatment. *A. chinensis* Planch. cv. 'Hort16A') were grown under normal commercial management at the Plant & Food Research Orchard, Te Puke, New Zealand, and fruit were treated at approximately 165 DAFB. Wicking and dipping was kindly carried out by Andrew Barnett at the Plant & Food Research Orchard, Te Puke. First dye was introduced to the pedicel of the fruit using cotton wicks (several cotton threads twined together) and blue food colouring. A heavy sewing needle was used to pull the pre-wetted 15 cm wick through the centre of the pedicel. One end of the wick was immersed in solution inside a micro-centrifuge tube, while the other end was left trailing for 5 cm. The trailing end and any exposed parts of the wick were then wetted again with water, and the micro-centrifuge tube secured to the plant with a twist tie. Fruit were harvested after four weeks by S. Pilkington and measured for the fruit characteristics of colour, firmness, soluble sugars, dry matter and weight. Weight of each fruit was recorded in grams.

2.18 Liquid chromatography mass spectrometry (LC-MS/MS)

LC-MS/MS was carried out on three different machines, with the kind help of Dave Greenwood (Plant & Food Research and the University of Auckland), Janine Cooney (Plant & Food Research) and Neil Emery (Trent University, Canada). Sample extraction and purification was carried out by SMP for analysis by Dave Greenwood and Janine Cooney, as outlined as follows. Samples for analysis by Neil Emery were homogenised to a powder with liquid nitrogen in a mortar and pestle and freeze-dried. The sample extraction, purification and analysis was then carried out by Amy Galer in Neil Emery's laboratory, Trent University, Canada (see Appendix Section 9.2).

2.18.1 Sample extraction

The extraction method was employed as described previously in Hoyerová *et al.* (2006) with minor modifications. The biological samples were homogenised to a powder with liquid nitrogen in a mortar and pestle. The samples were then extracted with 1 ml of the modified Bieleski's solvent (methanol/water/formic acid: 75/20/5, v/v/v) containing the labelled internal standard (100 pmol $^{2}H_{6}Z$). The mixture was shaken with a Thermomixer comfort (Eppendorf, Germany) at 1200 rpm and 37 °C for 30 min. Vortexing was carried out at the maximum setting for 1 min. The extracts were then centrifuged at 16 000 x *g* for 3 min. The 800 µl supernatants were collected, and the residues were re-extracted with 800 µl of the modified Bieleski's solvent.

2.18.2 Column purification

The method proposed in Dobrev and Kamínek (2002) was used with minor modifications as described below. The extracted supernatants were passed through 30-mg Oasis HLB cartridges (Waters, USA) and dried in a centrifugal concentrator. The dried samples were dissolved in 1 ml of 1 M formic acid and introduced in the 30-mg Oasis MCX columns (Waters, USA) for purification. The cartridges were conditioned with 1 ml of methanol and allowed to equilibrate with 1 ml of 1 M formic acid. Each sample was loaded on a cartridge, and the cartridge was washed with 1 ml of 1 M formic acid. Fractions of ABAs, IAA, and

GAs were eluted with 1 ml of methanol. Fractions of cytokinin nucleotides were eluted with 1 ml of 0.35 M ammonium hydroxide, the cytokinin fractions were eluted with 1 ml of 0.35 M ammonium hydroxide in 60% (v/v) methanol. The obtained eluates were dried by centrifugation under vacuum. The second extracts were centrifuged at 16 000 x *g* for 3 min, and the obtained 700 µl supernatants were combined with the initial extracted volume.

3. FRUIT DEVELOPMENT AND qRT-PCR OF CANDIDATE GENES FOR THE CONTROL OF CHLOROPHYLL LEVELS

3.1 Introduction

In kiwifruit, the control of chlorophyll levels has not yet been elucidated and the transcript levels of possible candidate genes have not been measured to date, as discussed in Chapter One. In research reported in this chapter, the transcript levels of chlorophyll pathway genes were analysed to ascertain whether gene expression of chlorophyll degradation correlated with green and yellow flesh colour in kiwifruit. The relative transcript levels of genes involved with chlorophyll biosynthesis and degradation, cytokinin biosynthesis and homeostasis, and carotenoid biosynthesis were determined using qRT-PCR in tissues from several fruit development series from the Plant & Food Research germplasm collection. This germplasm included the well-characterised *A. chinensis* 'Hort16A' and *A. deliciosa* 'Hayward' cultivars, which are yellow and green at maturity, respectively. Also chosen were an *A. deliciosa* x *A. chinensis* cross, which segregates for yellow and green flesh colour, an *A. chinensis* mapping population which segregates for different degrees of yellow flesh colour, and an *A. eriantha* x *A. chinensis* cross, which segregates for yellow and green flesh colour. As *A. chinensis* and *A. deliciosa* have different full bloom dates (for the 2009 this was 28 October 2008 and 27 November 2008, respectively) and slightly different maturity rates, samples were collected as DAFB, where sampling dates were as equivalent as possible. The full bloom flower sample was collected and labelled as 0 DAFB. Some fruit measurements were not taken when fruit was too small for sampling.

3.2 Fruit development and expression of candidate genes in *A. deliciosa* and *A. chinensis*

The fruit were sampled and characterised for fruit colour, weight, firmness and soluble sugars, before gene expression analysis was carried out on candidate genes for the control of chlorophyll degradation, as described in Section 2.11.

3.2.1 Changes in selected fruit characteristics during kiwifruit development

Photographs of developing fruit of *A. deliciosa* and *A. chinensis* fruit in 2009 and 2010 are presented in Figure 3.1 and 3.2, respectively. Measurements of fruit colour, soluble sugars, weight and firmness in 2009 are shown in Figure 3.3. The difference in hue angle at maturity was the biggest difference between these two species.

Figure 3.1. *A. chinensis* and *A. deliciosa* developmental fruit series (2009). Colour change in *A. chinensis* (top) and *A. deliciosa* (bottom) at each sampling stage of fruit development in 2009. *A. chinensis* photographs were taken at 37, 83, 132, 169, 203, 233 DAFB (right to left). *A. deliciosa* photographs were taken at 46, 95, 132, 166, 196 and 237 DAFB (right to left).

Analysis of fruit flesh pigmentation of *A. chinensis* and *A. deliciosa* in the 2009 fruit series showed that the fruit of both species were green at the beginning of development (Figure 3.1) and had a similar hue angle (Figure 3.3). The hue angle of yellow fruit decreased over development, from 118° to less than 100°, which is generally a change from a green hue to a yellow hue. Conversely, in *A. deliciosa* fruit, the hue angle remained above 110° throughout fruit development. The firmness profiles were very similar for both species. *A. chinensis* fruit were a slightly lighter weight at maturity, but showed a similar rate of weight increase to *A. deliciosa* fruit. *A. chinensis* fruit were also higher in soluble sugars than *A. deliciosa* fruit, with the largest increase in soluble sugars after 170 DAFB.

Figure 3.2. *A. chinensis* and *A. deliciosa* developmental fruit series (2010). Colour change in *A. chinensis* (top) and *A. deliciosa* (bottom) at each sampling stage of fruit development in 2010. *A. chinensis* photographs were taken at 48, 92, 137, 179, 215, and 246 DAFB (right to left). *A. deliciosa* photographs were taken at 49, 94, 136, 172, 203, and 238 DAFB (right to left).

Measurements of fruit characteristics in 2010 are shown in Figure 3.4. The difference in hue angle was again the largest difference between these two species. The hue angle of yellow fruit was very similar to the pattern observed for 2009. However, for *A. deliciosa* fruit in 2010, the hue angle decreased to 108° towards the end of fruit development. This is apparent in the photos of the fruit at maturity (Figure 3.2). Despite this difference in colour, the soluble sugars, weight and firmness profiles were very similar for both species, and similar to the profiles observed for the 2009 fruit.

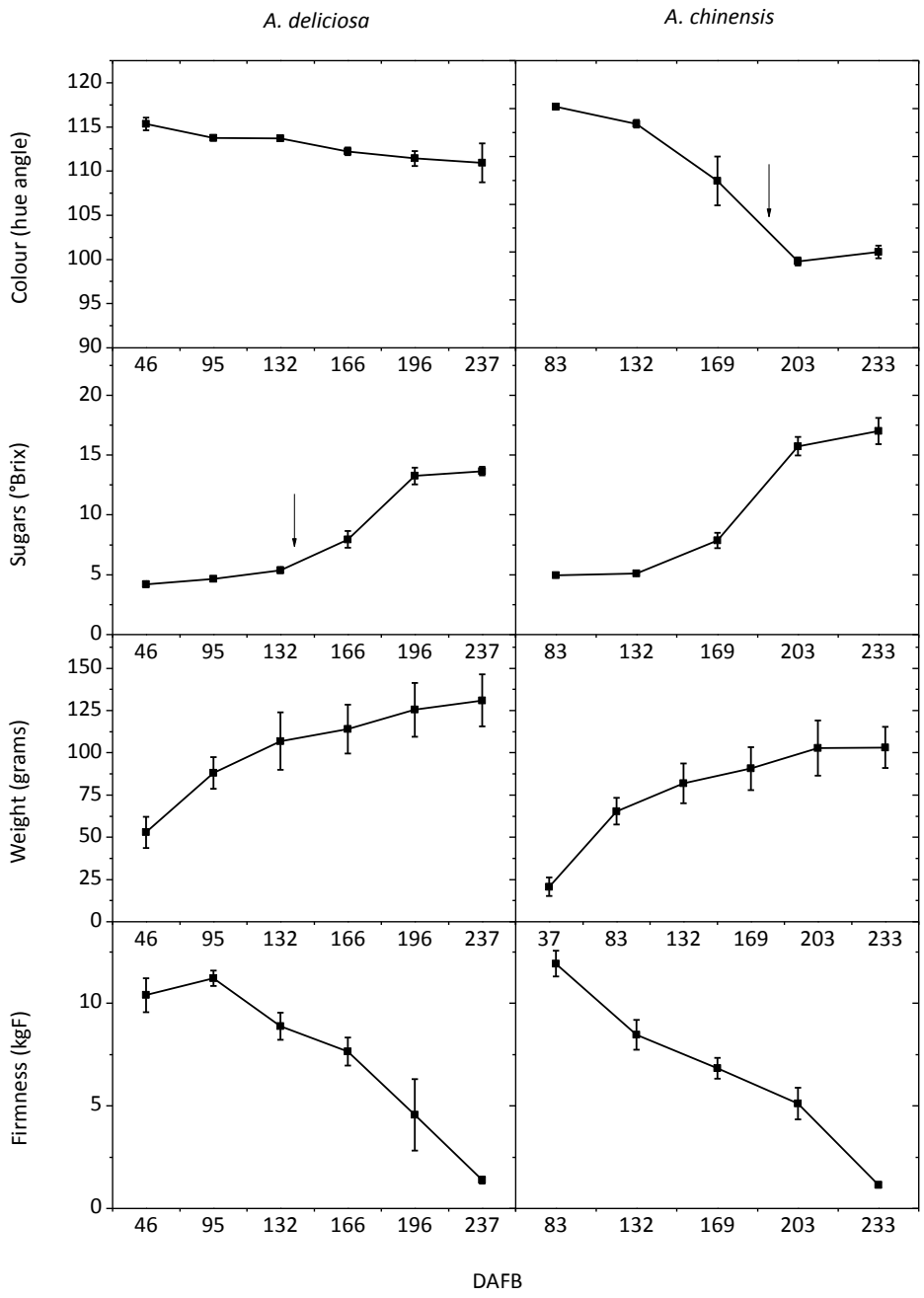

Figure 3.3. Colour, soluble sugars, weight and firmness of *A. chinensis* and *A. deliciosa* fruit over development in 2009. Colour is measured as hue angle, where a hue angle below 100° is yellow, a hue between 100° and 110° is green/yellow, and a hue above 110° is green. Soluble sugars are measured in °Brix, weight is measured in grams, and firmness is measured in kgF. Measurements are given for *A. deliciosa* (left panels) and *A. chinensis* (right panels) over fruit development (DAFB). Arrows indicate commercial harvest points as determined by maturity standards for soluble sugar levels in *A. deliciosa* and colour measurements in *A. chinensis*. Error bars indicate standard deviation (n=10).

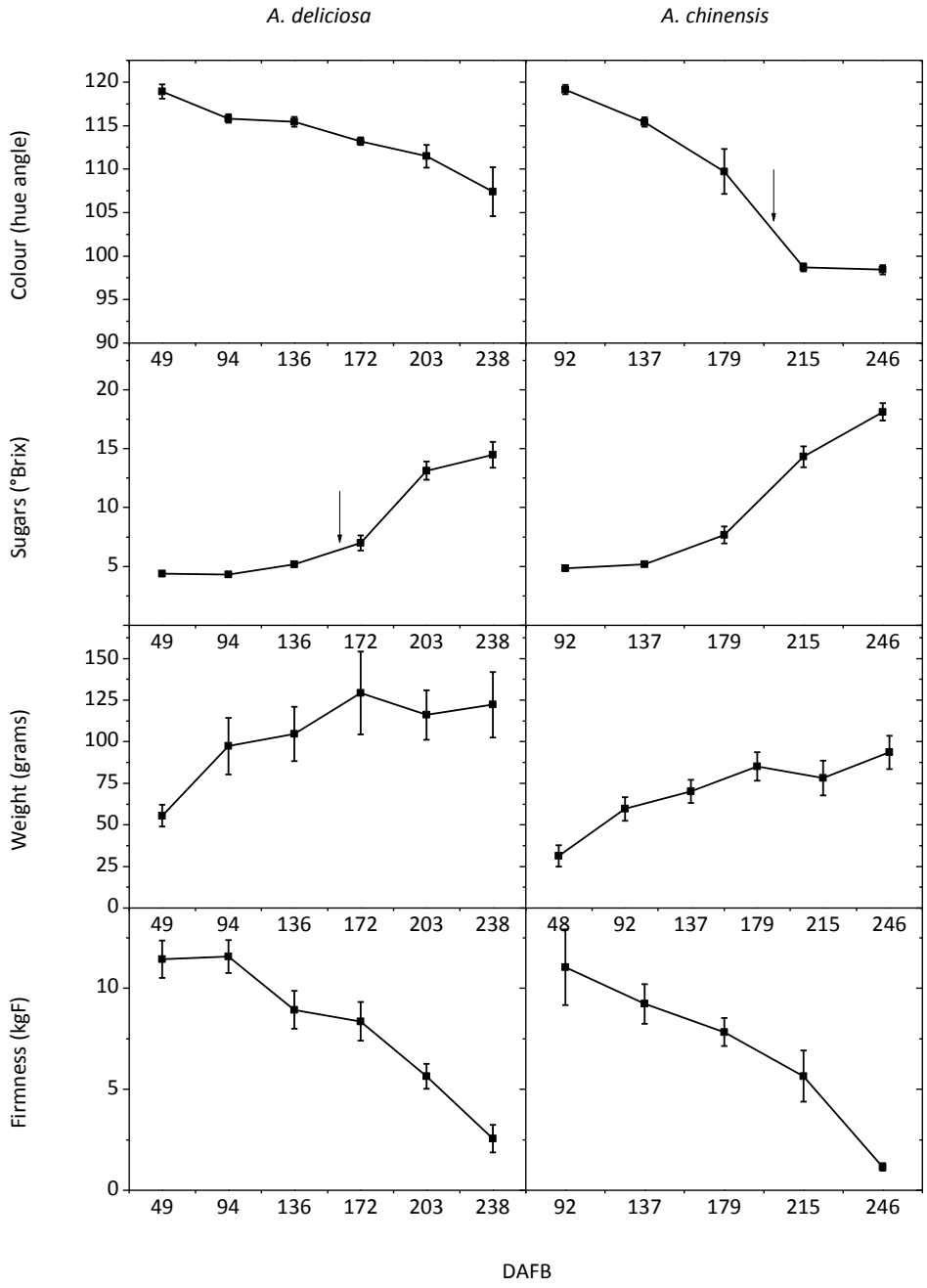

Figure 3.4. Colour, soluble sugars, weight and firmness of *A. chinensis* and *A. deliciosa* fruit over development in 2010. Colour is measured as hue angle, where a hue angle below 100° is yellow, a hue between 100° and 110° is green/yellow, and a hue above 110° is green. Soluble sugars are measured in °Brix, weight is measured in grams, and firmness is measured in kgF. Measurements are given for *A. deliciosa* (left panels) and *A. chinensis* (right panels) over fruit development (DAFB). Arrows indicate commercial harvest points as determined by maturity standards for soluble sugar levels in *A. deliciosa* and colour measurements in *A. chinensis*. Error bars indicate standard deviation (n=10).

Chlorophyll concentration was also measured in the 2010 fruit series to confirm the hue angle results (Table 3.1). The chlorophyll concentration in green fruit decreased to about 30% of the initial concentration. In contrast, in work by Montefiori *et al.* (2009) the chlorophyll concentration in green fruit fluctuated slightly but remained at more than 93% of the initial concentration throughout fruit development. This indicates the fruit had begun to de-green in 2010 compared with other years. In yellow fruit, chlorophyll was degraded to about 20% of the initial concentration during development in yellow fruit. The ratio of chlorophyll *a/b* fluctuated between 1.37 and 0.64 for *A. chinensis*, and 1.10 and 0.72 for *A. deliciosa* during fruit development. The concentration of carotenoids was not measured as it is known to be constant and similar in both fruit types across development (Montefiori *et al.* 2009).

Table 3.1. Chlorophyll concentration of *A. deliciosa* and *A. chinensis* over fruit development (DAFB). Concentrations of chlorophyll *a*, chlorophyll *b*, chlorophyll *a* and *b* and the chlorophyll *a/b* ratio are expressed in µg/g FW.

A. deliciosa	DAFB	Chlorophyll *a*	Chlorophyll *b*	*a* + *b*	*a/b*
	49	3.90	5.44	9.34	0.72
	94	4.86	5.98	10.84	0.81
	136	2.77	2.52	5.29	1.10
	172	2.33	2.30	4.63	1.01
	203	2.30	2.14	4.44	1.08
	238	1.50	1.78	3.28	0.84
A. chinensis	DAFB	Chlorophyll *a*	Chlorophyll *b*	*a* + *b*	*a/b*
	48	3.33	2.95	6.29	1.13
	92	4.04	2.95	6.99	1.37
	137	2.91	2.50	5.42	1.17
	179	1.55	1.87	3.42	0.83
	215	1.11	1.66	2.77	0.67
	246	1.04	1.63	2.67	0.64

3.2.2 Selection of gene candidates for the control of chlorophyll levels

Gene candidates were selected based on information in the literature (Chapter One), and mined into the Plant & Food Research EST database. By utilising BLAST match of published candidate genes from *Arabidopsis* or other reference species, candidates were identified for all the steps of interest of chlorophyll biosynthesis and degradation, carotenoid biosynthesis and cytokinin biosynthesis, degradation and conjugation (Table 3.2). As the *Actinidia* sequences

are from expressed sequence tags (ESTs) (Crowhurst *et al.* 2008), all the genes show some expression. Following analysis of EST frequency and source library, gene candidates were selected which were most likely to represent the genes active in fruit tissue. However, *CLH1* and *CLH2* were found only in leaf and bud libraries. Also, EST frequency counts (Table 3.2) showed that some genes were more abundant than their homologues; for example, *PAO2* is more abundant than *PAO1*, *CBR1* is more abundant than *CBR2*, and *SGR2* is more abundant than *SGR1*. *SGR3* and *SGR4* are very similar in sequence to *SGR2* but were less expressed and therefore were not used in further experiments. The recently published *PPH* genes from rice and *Arabidopsis* (Morita *et al.* 2009; Schelbert *et al.* 2009) were a good BLAST match to two kiwifruit *PPH* homologues, where *PPH1* was more abundant than *PPH2*, and one *RCCR*-like gene was found that had not been previously identified (Crowhurst *et al.* 2008).

RBCS, *LHCB1* and *LHCB2* are very abundant in kiwifruit tissue. Three genes with high homology to *GLUTR* were found, of which *GLUTR1* and *GLUTR2* were chosen for future experiments because of their high abundance. Similarly, two *CAB* genes were present in kiwifruit, where *CAB1* was chosen over *CAB2* for further experiments because of its higher abundance.

The carotenoid candidates were mined from the Plant & Food Research EST database during previous work by Ampomah-Dwamena *et al.* (2009). In this work, *PSY* was created by gene RACE. *PAPF*, or fibrillin, a carotenoid binding protein, was also included in this study.

The *IPT* family includes nine members in *Arabidopsis*. *IPT1*, *3*, *4*, *5*, *6*, *7* and *8* have the same kiwifruit EST as their best BLAST match. This EST was therefore subsequently referred to as *IPT*. *IPT2* had a different EST as its best BLAST match. However, this was not included in the qRT-PCR work as the most abundant active cytokinin is considered to be *trans*-zeatin (Haberer and Kieber 2002), whereas *IPT2* and *IPT9* are known to be involved with the production of the *cis*-type cytokinins (Miyawaki *et al.* 2006), as outlined in Chapter One. *CKX* and *ZOG* each matched one kiwifruit homologue, and *BGLU* matched two kiwifruit homologues. *BGLU44* did not produce a PCR product in initial primer tests, and thus only *BGLU42* was used for qRT-PCR studies, and renamed *BGLU*. A *SAG12* gene homologue with high abundance in *A. chinensis* young fruit was also included.

Table 3.2. Kiwifruit gene candidates for the control of chlorophyll levels. Tissue source from which the primary expressed gene was isolated is shown with expression (number of EST reads from various tissue sources), best *Arabidopsis* BLAST match and GenBank deposit number.

Gene	Gene Name	Kiwifruit Source	No. of ESTs	Reference BLAST match	GenBank Number
Chlorophyll Biosynthetic Pathway					
GTR1	Glutamyl tRNA synthase	*A. chinensis* leaves	34	AT1G58290	FG513131
GTR2	Glutamyl tRNA synthase	*A. chinensis* meristems	23	AT1G58290	FG487415
GTR3	Glutamyl tRNA synthase	*A. chinensis* meristems	4	AT1G58290	FG494770
CLS	Chlorophyll synthase	*A. chinensis* active meristems	13	AT3G51820	FG495946
CAO	Chlorophyll *a* oxygenase	*A. chinensis* young fruit	8	AT1G44446	FG508604
RBCS	Ribulose bisphosphate carboxylase small subunit	*A. chinensis* active meristems	108	AT1G67090	FG501379
LHCB1	Light harvesting chlorophyll *b* binding complex of photosystem II	*A. chinensis* active meristems	41	AT3G08940	FG498497
LHCB2	Light harvesting chlorophyll *b* binding complex of photosystem II	*A. deliciosa* developing shoot buds	61	AT2G40100	FG405725
CHP	Chloroplast precursor	*A. chinensis* young fruit	9	AT3G50820	FG527135
CAB1	Chlorophyll *a/b* binding protein	*A. eriantha* young fruit	42	AT4G10340	FG527942
CAB2	Chlorophyll *a/b* binding protein	*A. chinensis* active meristems	10	AT4G10340	FG521611
Chlorophyll Degradation Pathway					
CLH1	Chlorophyllase	*A. chinensis* meristems	16	AT1G19670	FG432265
CLH2	Chlorophyllase	*A. deliciosa* petal	11	AT1G19670	FG490037
PAO1	Pheophorbide *a* oxygenase	*A. chinensis* ripe fruit	10	AT3G44880	FG455506
PAO2	Pheophorbide *a* oxygenase	*A. chinensis* flower	49	AT3G44880	FG438539
SGR1	Stay-green	*A. polygama* petal	2	AT4G22920	FG509383
SGR2	Stay-green	*A. deliciosa* petal	14	AT4G22920	FG436032
SGR3	Stay-green	*A. deliciosa* petal	5	AT4G22920	FG453460
SGR4	Stay-green	*A. deliciosa* petal	6	AT4G22920	FG429776
RCCR	Red chlorophyll catabolite reductase	*A. eriantha* ripe fruit skin	8	AT4G37000	FG508120
CBR1	Chlorophyll *b* reductase	*A. eriantha* petal	20	AB255025	FG508817
CBR2	Chlorophyll *b* reductase	*A. arguta* petal	2	AT5G04900, AB255026	FG452828

PPH1	Pheophytin pheophorbide hydrolase	*A. eriantha* petal	8	AT1G54570	FG483222
PPH2	Pheophytin pheophorbide hydrolase	*A. polygama* petal	2	AT1G54570	FG509501
Carotenoid Biosynthetic Pathway					
PSY	Phytoene synthase	Created from RACE	-	-	-
PDS	Phytoene desaturase	*A. chinensis* meristems	73	AT4G14210	FG496959
CRTISO	Carotenoid isomerase	*A. deliciosa* petal	32	AT1G06820	FG435001
PAPF	Fibrillin	*A. chinensis* young fruit	32	AT3G26070	FG519998
Cytokinin Genes					
IPT	Isopentenyl transferase/cytokinin synthase	*A. deliciosa* ripe fruit	11	AT3G23630	FG525359
IPT2	Isopentenyl transferase/cytokinin synthase	*A. chinensis* young fruit	17	AT2G27760	FG504645
CKX	Cytokinin oxidase/dehydrogenase	*A. eriantha* young fruit	4	AT1G75450	FG422203
ZOG	Zeatin *o*-glucosidase	*A. deliciosa* ripe fruit	11	AT1G22380	Plant & Food Research EST 99598
BGLU42	β-glucosidase	*A. deliciosa* ripe fruit	32	AT5G36890	FG441373
BGLU44	β-glucosidase	*A. chinensis* young fruit	40	AT3G18080	FG519392
SAG	Senescence associated gene 12	*A. chinensis* young fruit	38	AT5G45890	FG523933

3.2.3 Expression of candidate genes for the control of chlorophyll de-greening in *A. chinensis* and *A. deliciosa*

Oligonucleotide primers were designed using the optimisation criteria and measurements of primer efficiency outlined in Chapter Two and tested by end point PCR to ensure identity with kiwifruit source sequence and identity between *A. chinensis* and *A. deliciosa*. The levels of transcripts encoding the gene candidates selected in Section 3.2.2 were compared by qRT-PCR between green *A. deliciosa* and yellow *A. chinensis* fruit from the cDNA collected from the fruit developmental series described in Chapter Two. Pearson's correlation coefficients were then calculated to test correlation between gene expression and fruit colour.

3.2.3.1 Expression of chlorophyll biosynthetic pathway and photosynthesis-associated gene candidates

The expression of genes involved with chlorophyll biosynthesis, as well as *RBCS, LHCB1*, *CAB* and *CHP*, was measured by qRT-PCR in *A. deliciosa* and *A. chinensis* in 2009 (Figure 3.5). The highest expression of all of the genes was seen at 95 DAFB in *A. deliciosa* only. The expression of the chlorophyll associated genes is co-ordinated with the expression of the chlorophyll biosynthetic genes. The expression of *GLUTR1* and *LHCB2* was also measured and showed similar patterns to their homologues (see Appendix Section 9.1). When the spike in expression at 95 DAFB is excluded, the expression of the biosynthetic-related genes is similar between species. However, this spike in expression does not appear to be erroneous, as the mean expression of the reference genes for this sample was within the two cycle range for reference genes at the other sample dates. Such an increase could be due to climatic conditions or a metabolic change at this key point where cell division stops and expansion begins.

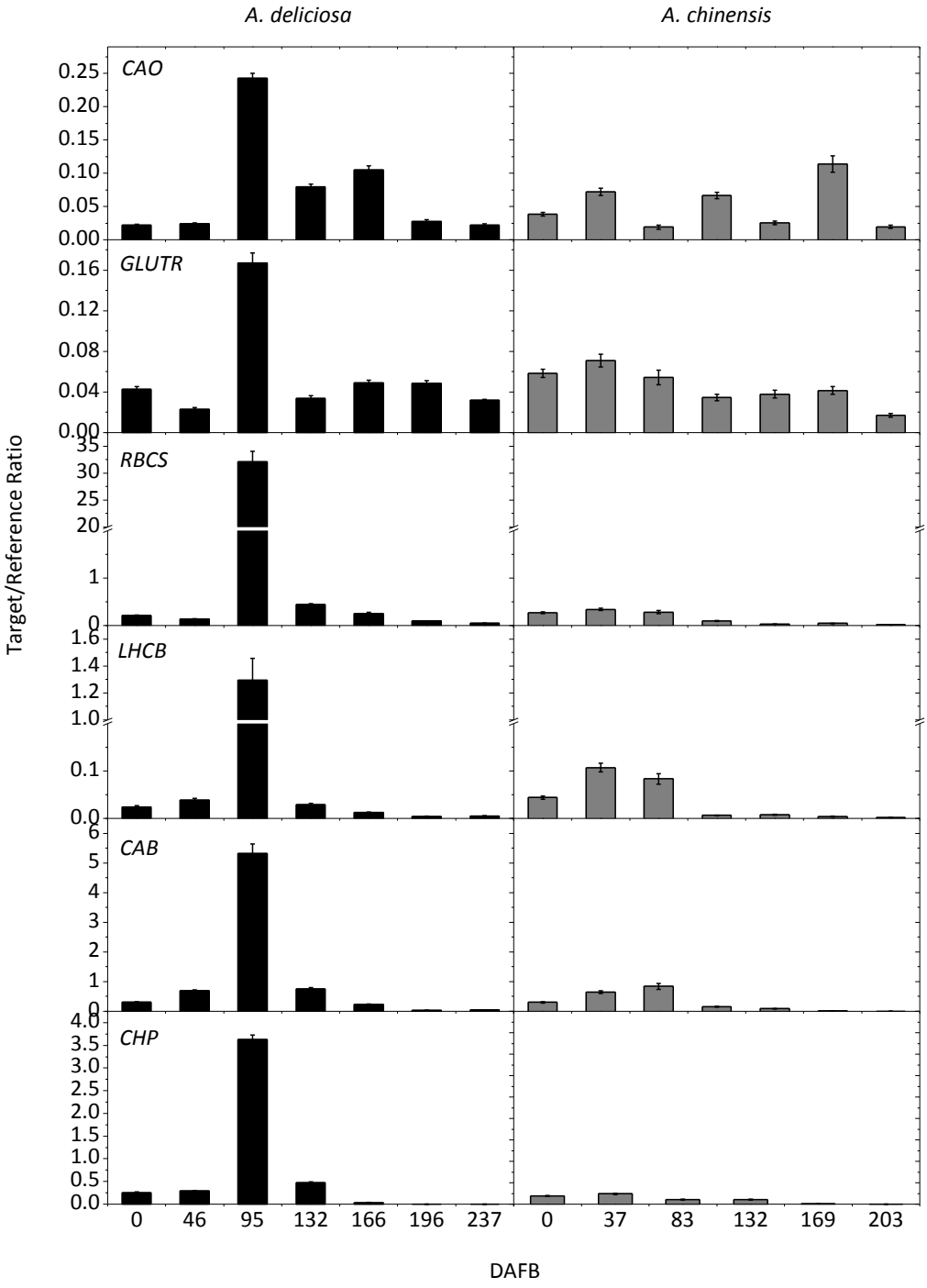

Figure 3.5. Expression of chlorophyll biosynthetic and photosynthesis-associated genes in *A. chinensis* and *A. deliciosa* fruit over development in 2009. Expression of chlorophyll biosynthetic pathway and photosynthesis-associated genes (see Table 3.2 for abbreviations) in *A. deliciosa* (left panels, black bars) and *A. chinensis* (right panels, grey bars) over fruit development (days after full bloom; DAFB), measured as a target/reference ratio. Error bars indicate standard error (n=4).

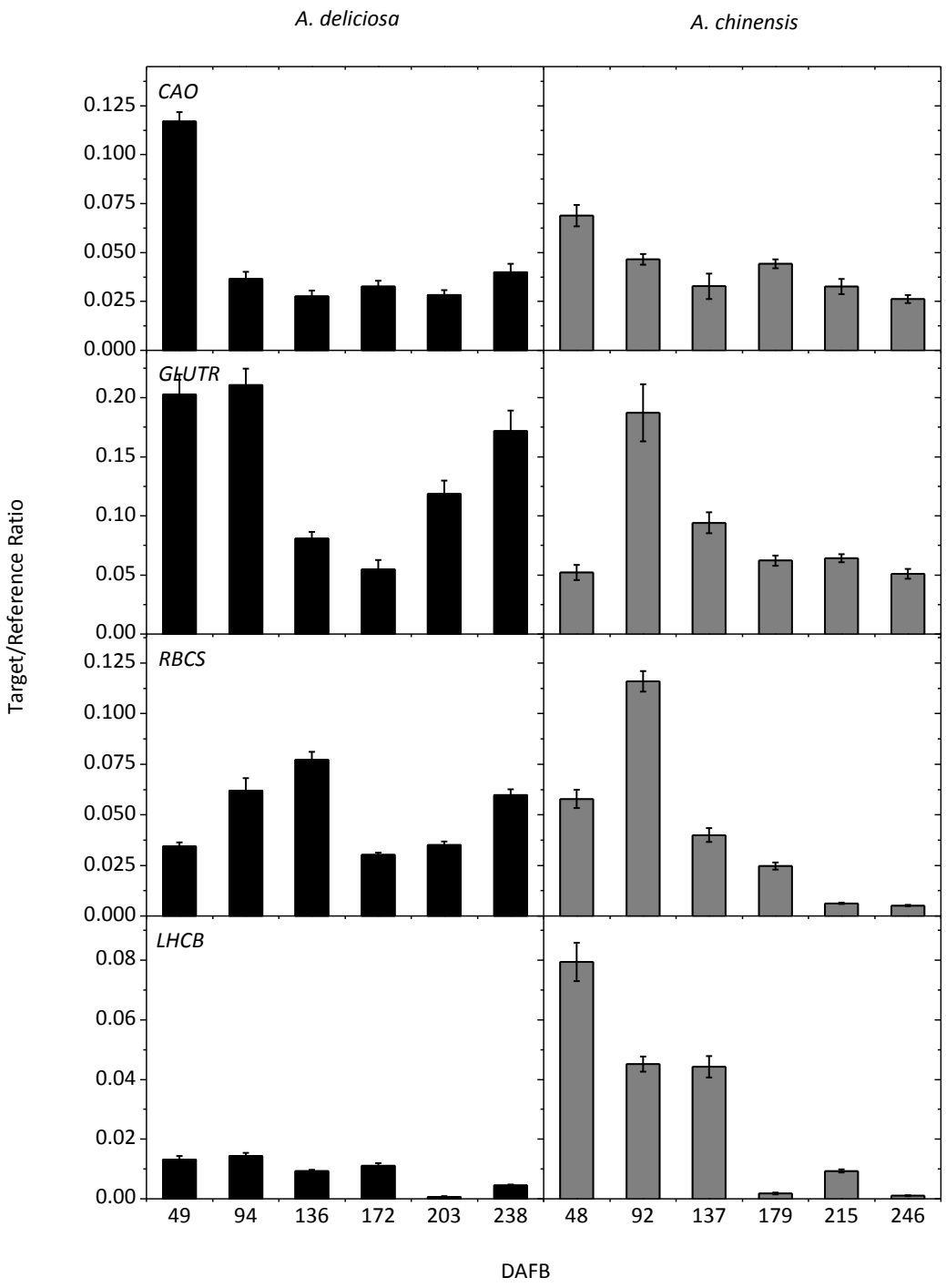

Figure 3.6. Expression of chlorophyll biosynthetic and photosynthesis-associated genes in *A. chinensis* and *A. deliciosa* fruit over development in 2010. Expression of chlorophyll biosynthetic pathway and photosynthesis-associated genes (see Table 3.2 for abbreviations) in *A. deliciosa* (left panels, black bars) and *A. chinensis* (right panels, grey bars) over fruit development (days after full bloom; DAFB), measured as a target/reference ratio. Error bars indicate standard error (n=4).

The expression of the chlorophyll biosynthesis and photosynthesis-related genes were measured by qRT-PCR in *A. chinensis* and *A. deliciosa* in a second season, 2010 (Figure 3.6). Expression patterns were similar to the expression of these genes in 2009, with the exception of the 95 DAFB sample. The spike in expression seen in 2009 was not present in the 2010 samples. Thus subtle trends in the data over development were easier to depict in the 2010 fruit samples, where maximal gene expression target/reference ratios in 2010 were similar to 2009 excluding the 95 DAFB samples.

Expression of *CAO* was higher in green fruit than in yellow fruit at most stages of fruit development. In contrast, the expression of *GLUTR1* was similar for most time points in green and yellow fruit and was relatively constant over development, except for the earliest time point in green kiwifruit. *RBCS* expression fluctuated slightly but remained high during development of green fruit, whereas its expression decreased during the development of yellow fruit. *LHCB1* was more highly expressed in *A. chinensis* at the early stages of fruit development, decreasing during fruit maturity. *CAB1* and *CHP* gene expression was not measured in the 2010 fruit series because their expression was similar to that of *RBCS* and *LHCB1* in 2009.

3.2.3.2 Expression of chlorophyll degradation pathway gene candidates

The expression of chlorophyll degradation and degradation-related genes was also measured by qRT-PCR in *A. chinensis* and *A. deliciosa* in 2009 (Figure 3.7) and 2010 (Figure 3.8). *CLH1* showed no apparent fruit expression in the later stages of fruit development when several primer pairs were used. This was consistent between fruit series in 2009 and 2010. The expression of *CBR1* was higher in 2009 than 2010, but this was due to a spike in expression at 166 DAFB. If the spike is excluded, the expression patterns are very similar. *CBR1* expression in 2010 was slightly higher in yellow fruit than in green fruit. Overall, *PAO1* expression was slightly higher in yellow fruit than in green in 2009. The expression of *PAO1* was ten-fold higher in 2009 than 2010. The expression increased in *A. chinensis* fruit over development in 2009, whereas in *A. deliciosa* fruit the *PAO1* expression remained low throughout development. *PPH* expression was similar between green and yellow fruit over fruit development, tending to increase towards fruit maturity. The target/reference ratio for *RCCR* was a maximum of 0.025 in 2009 compared with a

maximum of 0.060 in 2010. Despite this difference in maximal expression, the pattern over development was slightly higher in yellow fruit and consistent between sampling years. The expression of *PAO2* and *CBR2* were also measured and showed similar patterns to their homologues, and *CLH2* showed little expression for the majority of fruit development (see Appendix Section 9.1).

Both kiwifruit species have two expressed versions of the *SGR* gene. *SGR1* was more highly expressed in 2010 than 2009. In 2010, *SGR1* expression was similar in both fruit over development, but with a large increase in expression in green fruit at 238 DAFB. This could be related to the slight yellowing seen in *A. deliciosa* fruit at this stage of development. The expression of *SGR2* was much higher in 2009, with a maximum expression of around 0.0075 at 95 DAFB. However, if this sample is excluded as in the chlorophyll biosynthetic gene expression data, the expression of *SGR2* was slightly higher in *A. chinensis* in both years towards fruit maturity.

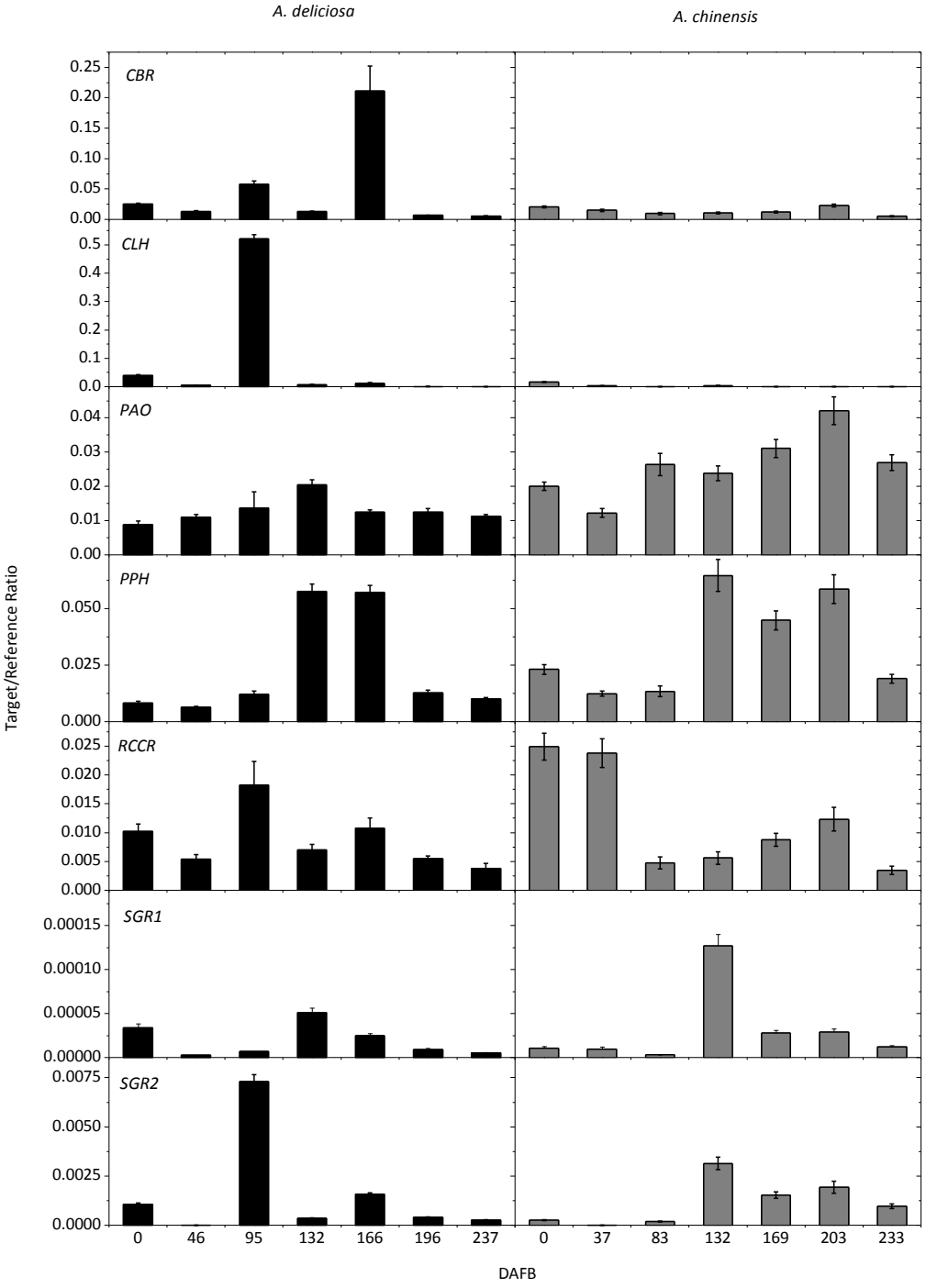

Figure 3.7. Expression of chlorophyll degradation genes in *A. chinensis* and *A. deliciosa* fruit over development in 2009. Expression of chlorophyll degradation pathway genes (see Table 3.2 for abbreviations) in *Actinidia deliciosa* (left panels, black bars) and *A. chinensis* (right panels, grey bars) over fruit development (days after full bloom; DAFB), measured as a target/reference ratio. Error bars indicate standard error (n=4).

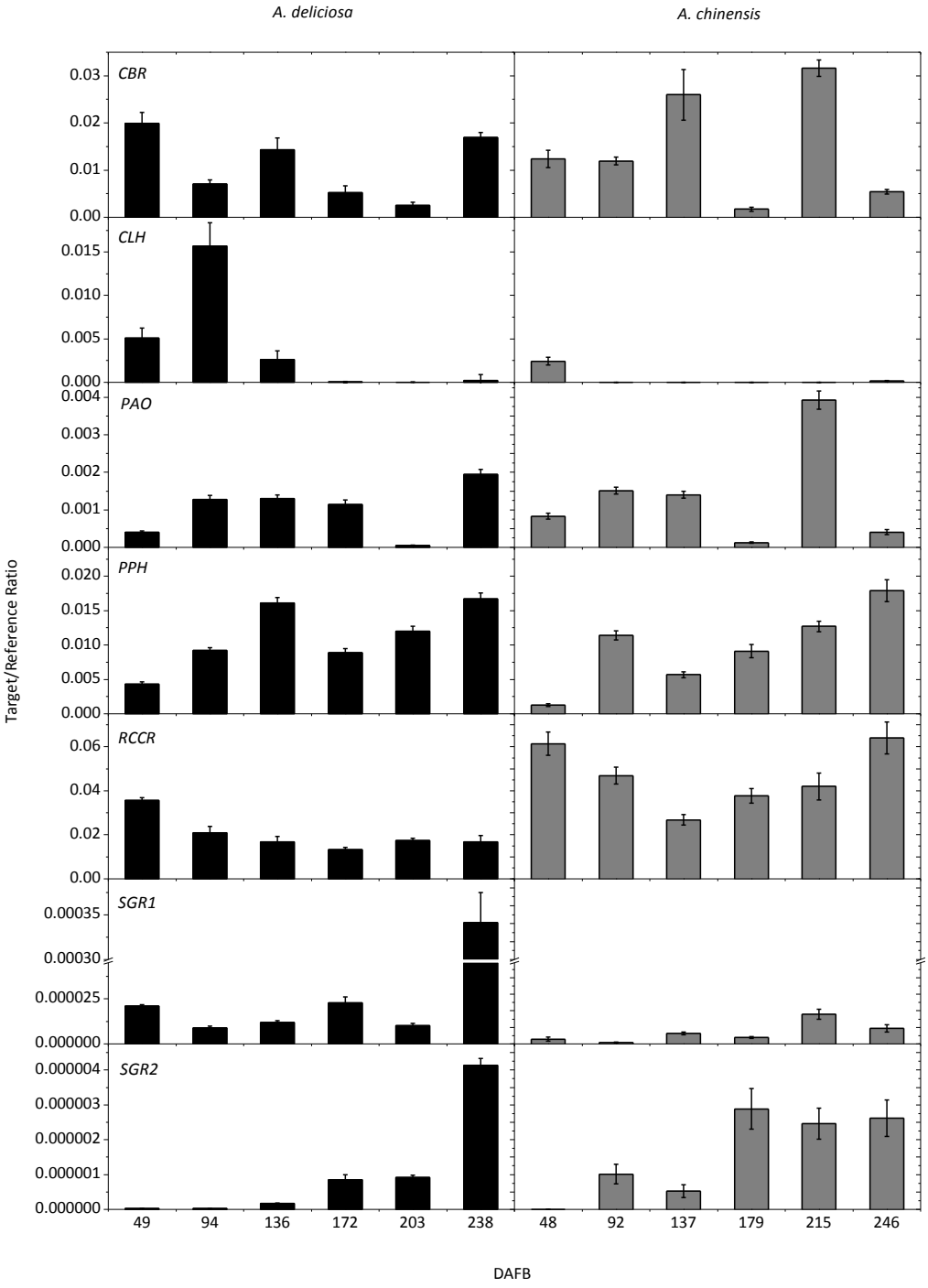

Figure 3.8. Expression of chlorophyll degradation genes in *A. chinensis* and *A. deliciosa* fruit over development in 2010. Expression of chlorophyll degradation pathway genes (see Table 3.2 for abbreviations) in *Actinidia deliciosa* (left panels, black bars) and *A. chinensis* (right panels, grey bars) over fruit development (days after full bloom; DAFB), measured as a target/reference ratio. Error bars indicate standard error (n=4).

A Pearson's correlation coefficient (r) test was carried out on qRT-PCR data to determine if there were any statistically significant correlations between gene expression and flesh colour measured by hue angle measurements for 2009 (Table 3.3) and 2010 (Table 3.4). A negative correlation indicates a decrease in hue angle, or yellowing, with an increase in gene expression and a positive correlation indicates an increase in hue angle, or greening, with an increase in gene expression.

There was a significant negative correlation between *PAO1* expression and yellow fruit colour in 2009 ($p \leq 0.01$) (Table 3.3). The other genes did not show significant correlations between expression and fruit colour. There were several significant pair-to-pair gene correlations: *PPH* and *SGR1* ($p \leq 0.01$), *CBR* and *CAO*, *GLUTR1* and *RBCS* ($p \leq 0.001$, $p \leq 0.01$ and $p \leq 0.001$, respectively), *CAO* and *GLUTR1* and *RBCS* (both $p \leq 0.001$) and *GLUTR1* and *RBCS* ($p \leq 0.001$). However, these significant correlations were not significant in the 2010 data, and could have been influenced by the large expression values for 95 DAFB, as mentioned in Section 3.2.3.1.

In 2010, there was a significant negative correlation for *SGR2* and *PPH* expression with yellow fruit colour ($p \leq 0.01$ and 0.05, respectively) and *RBCS* showed a significant positive correlation with green fruit colour ($p \leq 0.05$). *SGR1*, *PAO1*, *GLUTR* and *CAO* did not show significant correlations with fruit colour. Pair-to-pair correlation coefficients of gene expression suggest co-ordination of expression of *SGR1*, *SGR2* and *PPH*, but not the entire chlorophyll degradation pathway (Table 3.4).

Table 3.3. Pearson's correlation, r, comparing relative gene expression over fruit development to hue angle colour measurement in green and yellow kiwifruit in 2009. *indicates p≤0.05, **indicates p≤0.01 and ***indicates p≤0.001.

Pearson's correlation, r	*SGR1*	*SGR2*	*CBR1*	*PPH*	*PAO1*	*CAO*	*GLUTR*	*RBCS*
Colour	**0.041**	**-0.010**	**-0.124**	**-0.262**	**-0.716**	**0.072**	**0.301**	**0.182**
	(0.889)	**(0.975)**	**(0.830)**	**(0.410)**	**(0.009**)**	**(0.825)**	**(0.342)**	**(0.571)**
SGR1	-	-	-	-	-	-	-	-
SGR2	0.211	-	-	-	-	-	-	-
	(0.511)							
CBR1	0.436	-0.021	-	-	-	-	-	-
	(0.156)	(0.948)						
PPH	0.745	0.130	0.331	-	-	-	-	-
	(0.005**)	(0.687)	(0.293)					
PAO1	0.269	0.048	0.351	0.516	-	-	-	-
	(0.398)	(0.883)	(0.264)	(0.086)				
CAO	0.047	0.859	0.070	0.165	-0.057	-	-	-
	(0.885)	(0.000***)	(0.830)	(0.609)	(0.859)			
GLUTR	-0.213	0.797	-0.231	-0.256	-0.248	0.851	-	-
	(0.506)	(0.002**)	(0.470)	(0.421)	(0.436)	(0.000***)		
RBCS	-0.171	0.885	-0.197	-0.251	-0.214	0.849	0.933	-
	(0.595)	(0.000***)	(0.540)	(0.432)	(0.504)	(0.000***)	(0.000***)	

Table 3.4. Pearson's correlation, r, comparing relative gene expression over fruit development to hue angle colour measurement in green and yellow kiwifruit in 2010. *indicates p≤0.05, **indicates p≤0.01 and ***indicates p≤0.001.

Pearson's correlation, r	*SGR1*	*SGR2*	*CBR1*	*PPH*	*PAO1*	*CAO*	*GLUTR*	*RBCS*
Colour	**-0.213**	**-0.714**	**0.092**	**-0.637**	**-0.324**	**0.430**	**0.476**	**0.679**
	(0.506)	**(0.009**)**	**(0.775)**	**(0.026*)**	**(0.305)**	**(0.136)**	**(0.118)**	**(0.012*)**
SGR1	-	-	-	-	-	-	-	-
SGR2	0.701	-	-	-	-	-	-	-
	(0.011*)							
CBR1	-0.098	-0.161	-					
	(0.762)	(0.617)						
PPH	0.436	0.628	-0.137	-	-	-	-	-
	(0.157)	(0.029*)	(0.672)					
PAO1	0.299	0.336	0.045	0.255	-	-	-	-
	(0.345)	(0.286)	(0.890)	(0.424)				
CAO	0.287	-0.117	-0.194	-0.005	0.019	-	-	-
	(0.366)	(0.716)	(0.546)	(0.987)	(0.953)			
GLUTR	-0.043	-0.334	-0.153	-0.631	-0.241	0.400	-	-
	(0.895)	(0.273)	(0.634)	(0.028*)	(0.450)	(0.198)		
RBCS	0.144	-0.264	-0.129	-0.023	0.050	0.546	0.056	-
	(0.656)	(0.406)	(0.690)	(0.944)	(0.876)	(0.066)	(0.864)	

3.2.3.3 Expression of cytokinin and senescence associated gene candidates

The expression profiles for the cytokinin genes in 2009 are shown in Figure 3.9. The expression of *IPT*, the initial step in the cytokinin biosynthetic pathway, showed an increase towards maturity in green fruit. This was not seen in yellow fruit, where expression remained low. *BGLU* expression was highest in both fruit at the beginning of development, with very little expression towards the end of fruit development. Like *IPT*, *ZOG* showed higher expression in green fruit, increasing towards fruit maturity. The expression profiles for *CKX* and *SAG12* had a relatively similar pattern in both fruit. *CKX* expression was highest in the middle stages of fruit development.

In 2010, the expression of *IPT* had a higher target/reference ratio when compared with the 2009 data, 0.04 and 0.02, respectively, but had a similar trend, where the expression increased in green fruit towards maturity. As in the 2009 fruit series, the *BGLU* expression in 2010 was highest in both fruit at the beginning of development, with very little expression towards the end of fruit development. *ZOG* expression was also similar to 2009 with a higher maximum expression in green fruit at maturity. CKX expression was high at 46 DAFB in green fruit, but followed a similar trend as 2009 for the rest of development. *SAG12* was not measured in 2010 due to its similar expression in *A. chinensis* and *A. deliciosa* in 2009.

A Pearson's correlation coefficient (r) test was also carried out on cytokinin gene qRT-PCR data from 2009 (Table 3.5) and 2010 (Table 3.6). Despite high gene expression in green fruit compared with yellow fruit, there were no significant correlations between cytokinin biosynthetic gene expression and fruit colour in either year. However, there was a significant pair-to-pair gene positive correlation between *IPT* and *ZOG* ($p \leq 0.01$).

The pair-to-pair correlation of cytokinin genes to selected chlorophyll degradation genes is calculated in Table 3.7. The expression of *ZOG* and *PPH* was highly positively correlated, with a highly significant r value of 0.836 ($p \leq 0.001$). *CBR* expression was also significantly positively correlated with the expression of *ZOG* ($p \leq 0.05$). There was a significantly negative correlation between the expression of *PPH* and *BGLU* ($p \leq 0.01$), and the expression of *BGLU* had a significant negative correlation with the expression of

SGR1 and *SGR2* (both $p \leq 0.05$). *IPT* expression was also significantly correlated with the expression of *PAO1* ($p \leq 0.001$). This indicates that the two pathways may be co-regulated.

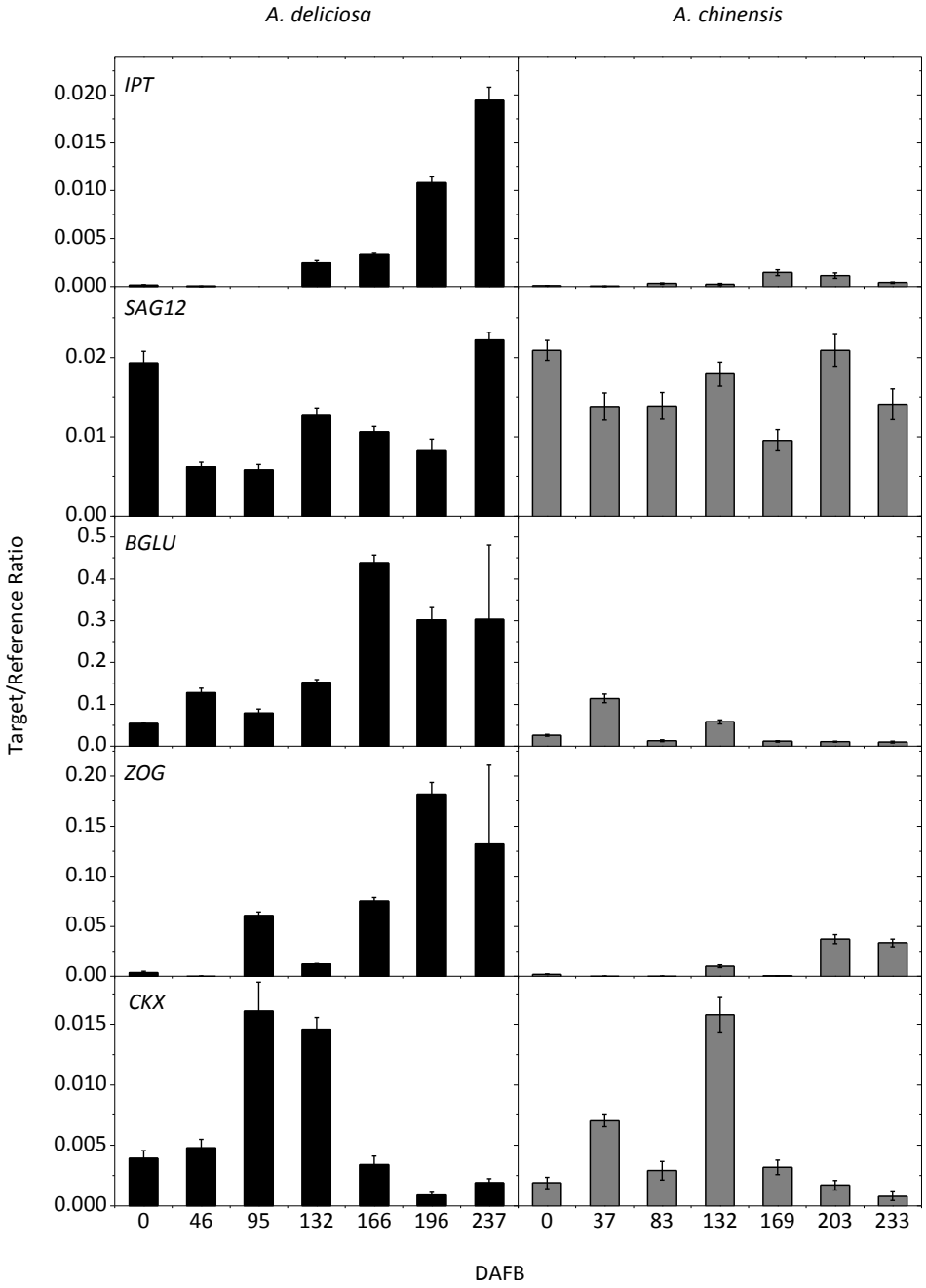

Figure 3.9. Expression of cytokinin biosynthetic genes in *A. chinensis* and *A. deliciosa* fruit over development in 2009. Expression of cytokinin biosynthetic pathway genes (see Table 3.2 for abbreviations) in *Actinidia deliciosa* (left panels, black bars) and *A. chinensis* (right panels, grey bars) over fruit development (days after full bloom; DAFB), measured as a target/reference ratio. Error bars indicate standard error (n=4).

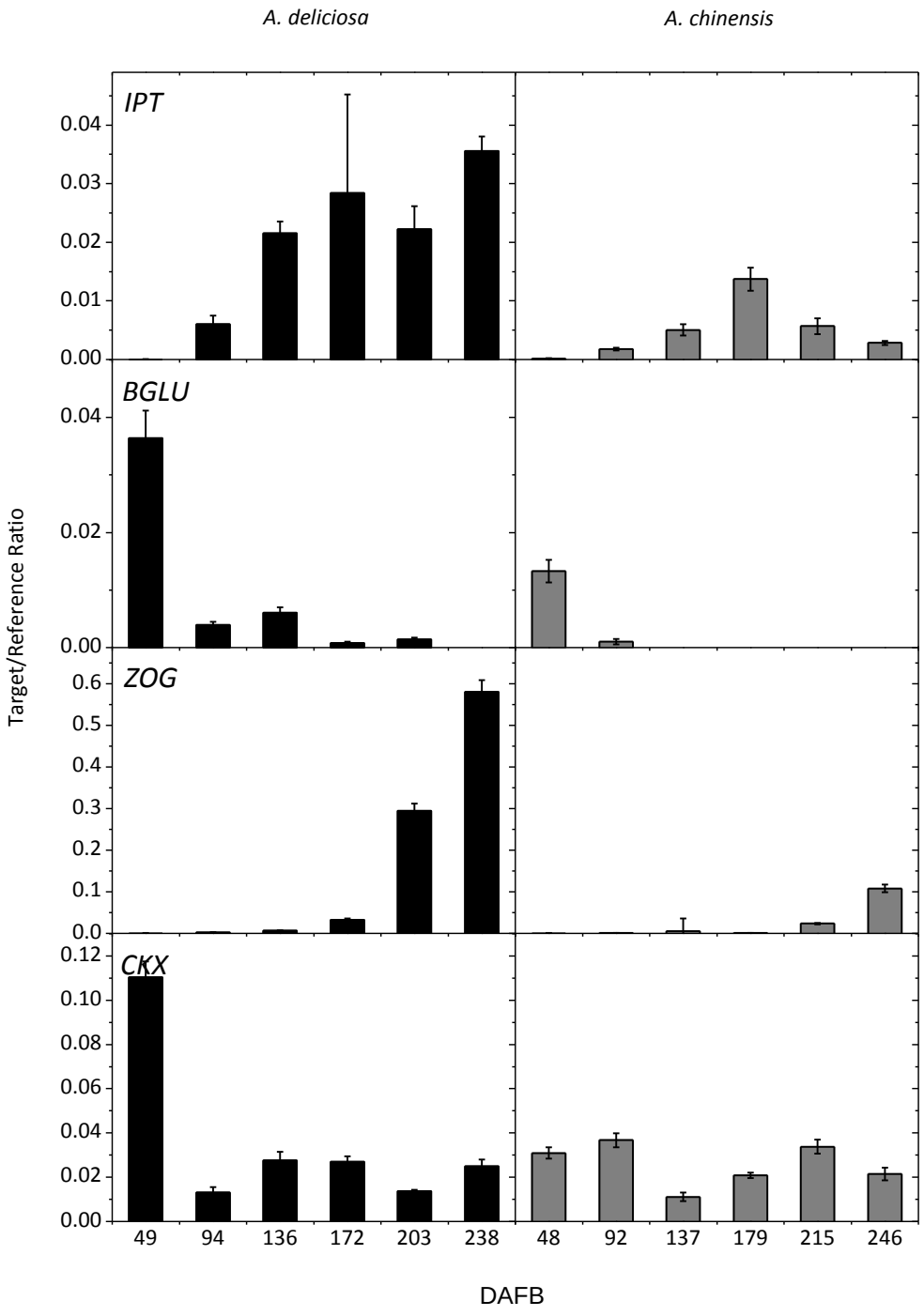

Figure 3.10. Expression of cytokinin biosynthetic genes in *A. chinensis* and *A. deliciosa* fruit over development in 2010. Expression of cytokinin biosynthetic pathway genes (see Table 3.2 for abbreviations) in *Actinidia deliciosa* (left panels, black bars) and *A. chinensis* (right panels, grey bars) over fruit development (days after full bloom; DAFB), measured as a target/reference ratio. Error bars indicate standard error (n=4).

Table 3.5. Pearson's correlation, r, comparing relative cytokinin gene expression over fruit development in 2009 to hue angle colour measurement in green and yellow kiwifruit. *indicates p≤0.05, **indicates p≤0.01 and ***indicates p≤0.001.

Pearson's correlation, r	*IPT*	*BGLU*	*ZOG*	*CKX*
Colour	**0.068**	**0.401**	**-0.000**	**0.476**
	(0.842)	**(0.221)**	**(0.999)**	**(0.138)**
IPT	-	-	-	-
BGLU	-0.280	-	-	-
	(0.405)			
ZOG	0.799	-0.261	-	-
	(0.003**)	(0.437)		
CKX	-0.351	0.152	-0.320	-
	(0.291)	(0.665)	(0.337)	

Table 3.6. Pearson's correlation, r, comparing relative cytokinin biosynthetic gene expression over fruit development in 2010 to hue angle colour measurement in green and yellow kiwifruit. *indicates p≤0.05, **indicates p≤0.01 and ***indicates p≤0.001.

Pearson's correlation, r	*IPT*	*BGLU*	*ZOG*	*CKX*
Colour	**-0.163**	**-0.267**	**-0.356**	**0.310**
	(0.612)	**(0.402)**	**(0.256)**	**(0.327)**
IPT	-	-	-	-
BGLU	-0.428	-	-	-
	(0.165)			
ZOG	0.485	-0.279	-	-
	(0.110)	(0.381)		
CKX	-0.168	0.239	0.146	-
	(0.612)	(0.454)	(0.327)	

Table 3.7. Pearson's correlation, r, comparing relative cytokinin biosynthetic gene expression over fruit development in 2010 to chlorophyll degradation gene expression in green and yellow kiwifruit. *indicates p≤0.05, **indicates p≤0.01 and ***indicates p≤0.001.

Pearson's correlation, r	*SGR1*	*SGR2*	*PPH*	*PAO1*	*CBR1*
IPT	0.146	-0.134	0.201	0.783	0.370
	(0.617)	(0.648)	(0.490)	(0.001***)	(0.192)
BGLU	-0.540	-0.658	-0.759	-0.227	-0.330
	(0.046*)	(0.010**)	(0.002**)	(0.435)	(0.250)
ZOG	0.197	0.450	0.836	-0.056	0.651
	(0.500)	(0.106)	(0.000***)	(0.848)	(0.012*)
CKX	0.432	0.117	-0.043	0.322	-0.204
	(0.123)	(0.690)	(0.884)	(0.261)	(0.483)

3.2.3.4 Expression of carotenoid biosynthetic gene candidates

The expression of the carotenoid biosynthetic genes *PSY*, *PDS*, *CRTISO*, and the carotenoid binding protein *PAPF* was measured in *A. deliciosa* and *A. chinensis* in 2009 by qRT-PCR and is presented in Figure 3.11. *PSY* expression was higher in green fruit at the beginning of development and decreased during maturity. The expression of *PDS*, *CRTISO* and *PAPF* was similar in *A. deliciosa* and *A. chinensis*, which correlates with the level of carotenoids, which is relatively constant in both species over fruit development (Montefiori *et al.* 2009). Because expression of the carotenoid genes was similar in *A. chinensis* and *A. deliciosa*, these genes are unlikely to be responsible for modulating chlorophyll degradation, and for this reason were not included in future experiments.

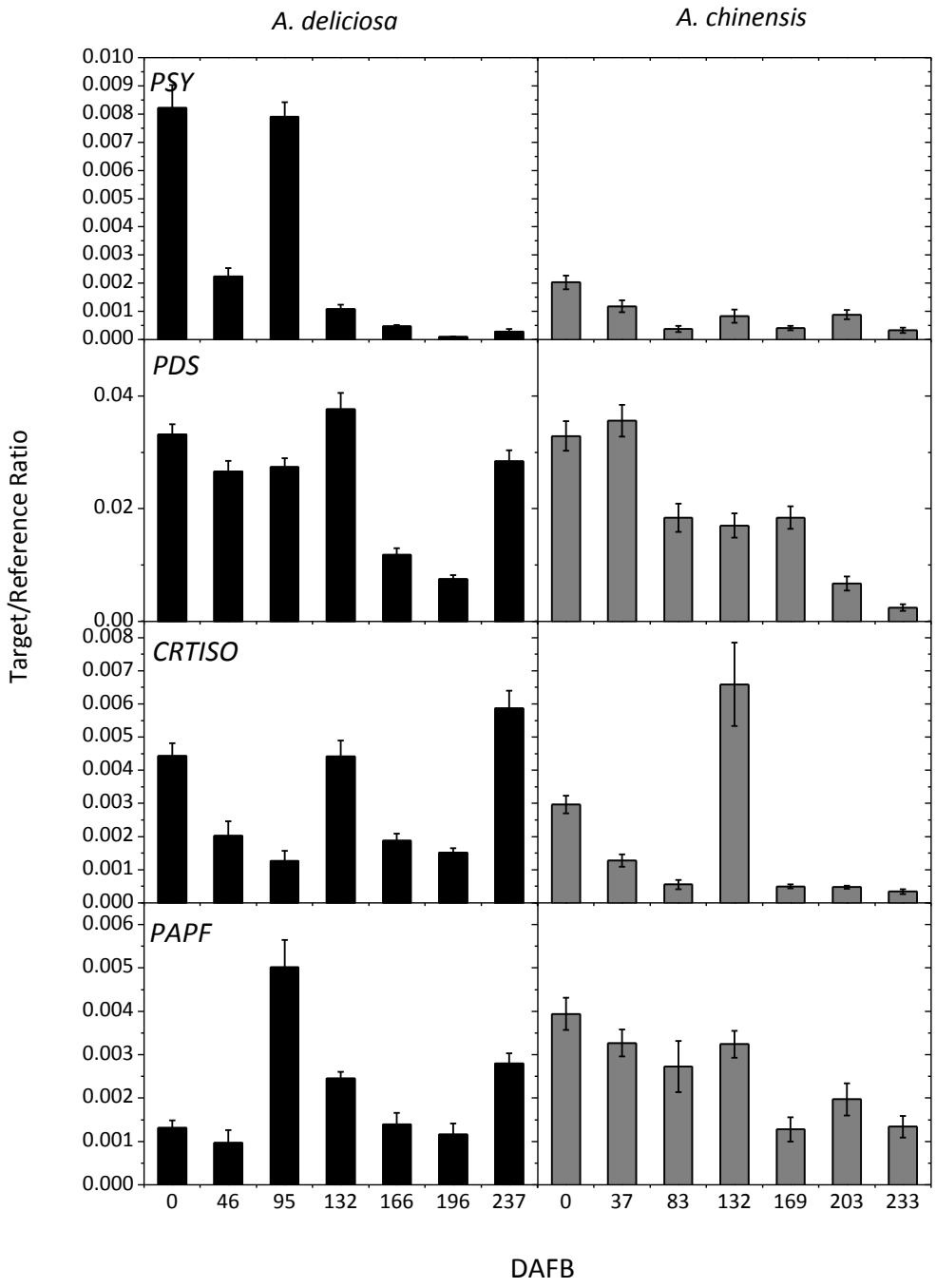

Figure 3.11. Expression of carotenoid biosynthetic genes in *A. chinensis* and *A. deliciosa* fruit over development in 2009. Expression of carotenoid biosynthetic pathway genes (see Table 3.2 for abbreviations) in *Actinidia deliciosa* (left panels, black bars) and *A. chinensis* (right panels, grey bars) over fruit development (days after full bloom; DAFB), measured as a target/reference ratio. Error bars indicate standard error (n=4).

3.3 Fruit development and expression of candidate genes in an *A. chinensis* x *A. deliciosa* cross

An inter-specific cross between *A. deliciosa* (DA) and *A. chinensis* (CK) resulted in a population with differential levels of chlorophyll degradation during fruit maturity (DA x CK) (Seal, A.G., Unpublished). Three representative vines were chosen from the population which have green, green/yellow, and yellow flesh colour. The fruit were sampled and characterised for fruit colour, weight, firmness and soluble sugars, before gene expression analysis was carried out on candidate genes for the control of chlorophyll degradation, as described previously in Chapter Two.

3.3.1 Chlorophyll degradation during kiwifruit development

Photographs of developing fruit from the three vines from the DA x CK cross, DA x CK (green), DA x CK (green/yellow) and DA x CK (yellow) in 2009 are presented in Figure 3.12. Measurements of fruit colour, soluble sugars, weight and firmness of the same fruit are shown in Figure 3.13. These results confirmed that the fruit had been correctly phenotyped, and were segregating for green and yellow flesh colour. The levels of soluble sugars, firmness and fruit weight were very similar, with DA x CK (yellow) fruit having slightly lighter weight fruit. The fruit from the DA x CK cross were between 30 and 60 grams and were smaller than *A. chinensis* and *A. deliciosa* fruit, which weighed more than 100 grams (Figure 3.3 and 3.4). The DA x CK fruit showed very similar soluble sugars and firmness curves to *A. chinensis* and *A. deliciosa*. The DA x CK (yellow) fruit had fewer sample points than DA x CK (green) and DA x CK (yellow) as there were no fruit left on the vine after 185 DAFB. The 0 DAFB sample is the flower at full bloom, and was thus included in gene expression measurements but not in measurements of fruit colour, firmness, sugars and weight.

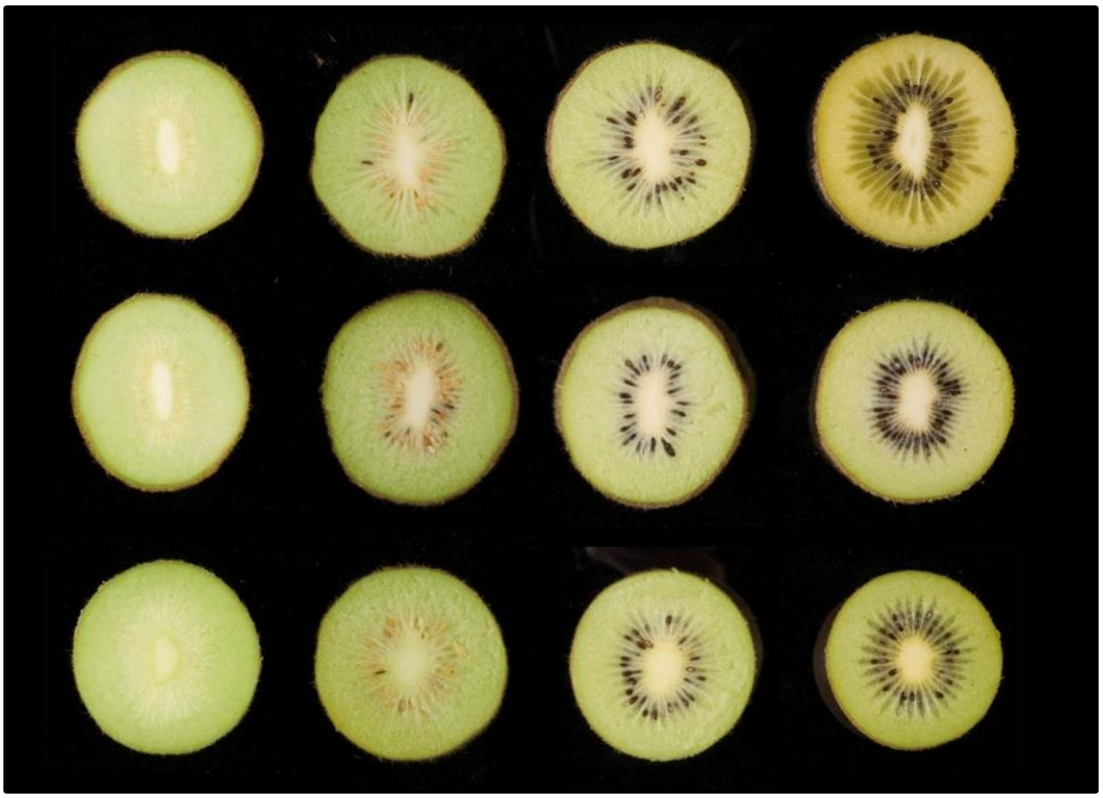

Figure 3.12. *A. chinensis* and *A. deliciosa* cross developmental fruit series photographs (2009). Colour change in DA x CK (yellow) (top) and DA x CK (green/yellow) (middle) and DA x CK (green) (bottom) at each sampling stage of fruit development in 2009. DA x CK (green/yellow) and DA x CK (green) photographs were taken at 65, 114, 151 and 215 DAFB (right to left), and DA x CK (yellow) photographs were taken at 65, 114, 151 and 185 DAFB.

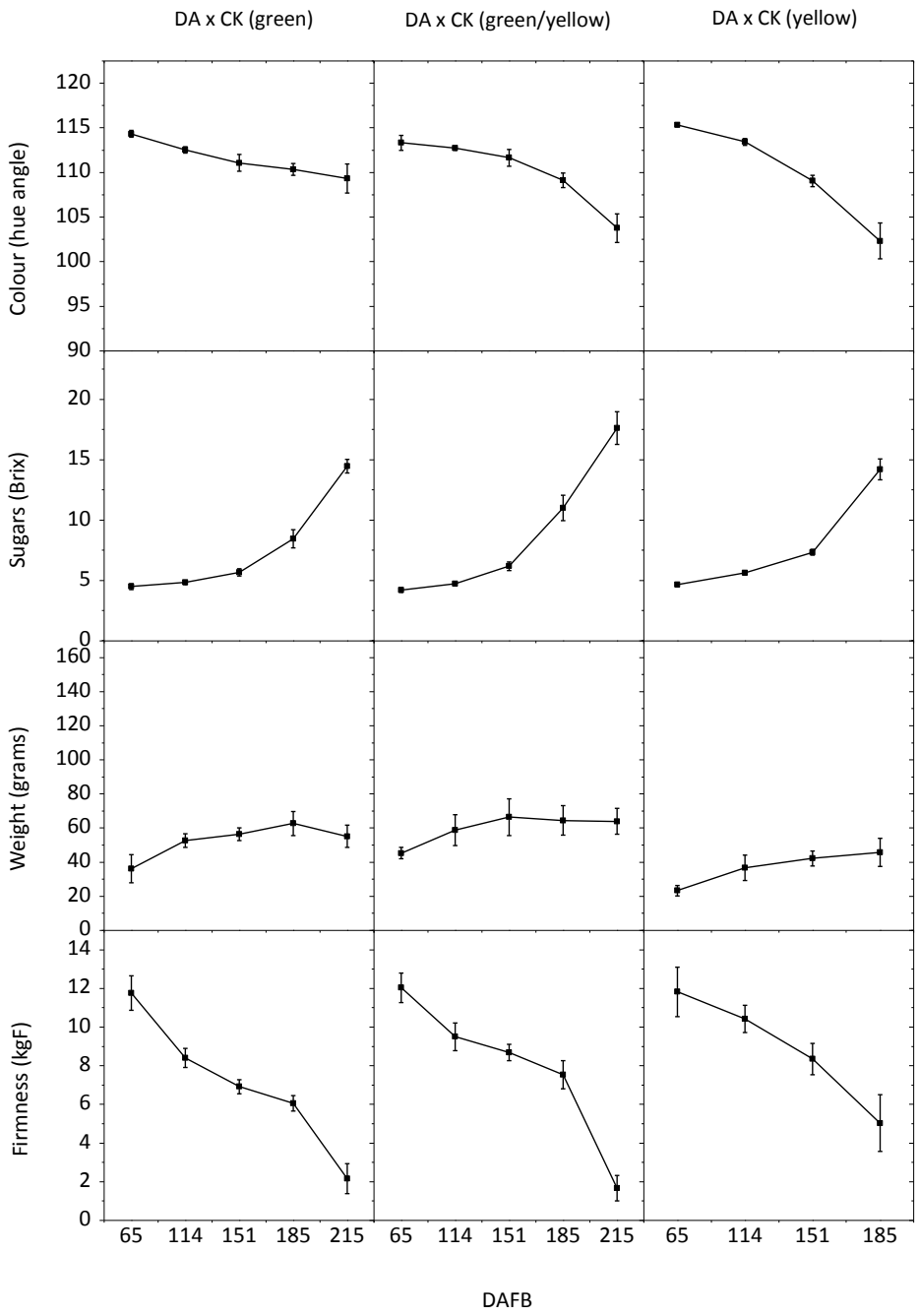

Figure 3.13. Colour, soluble sugars, weight and firmness of an *A. deliciosa* x *A. chinensis* cross over development in 2009. Colour is measured as hue angle, where a hue angle below 100° is yellow, a hue between 100° and 110° is green/yellow, and a hue above 110° is green. Soluble sugars are measured in °Brix, weight is measured in grams, and firmness is measured in kgF. Measurements are given for DA x CK (green) (left panels), DA x CK (green/yellow) (middle panels) and DA x CK (yellow) (right panels) over development (DAFB) for the 2009 fruit series. Error bars indicate standard deviation (n=10).

3.3.2 Expression of candidate genes for the control of chlorophyll de-greening in an *A. deliciosa* x *A. chinensis* cross

Primers used were the same as for the gene expression studies in *A. chinensis* and *A. deliciosa* (Section 3.2.3). The levels of transcripts encoding the gene candidates, selected in Section 3.2.2 and further continued from Section 3.2.3, were compared by qRT-PCR between DA x CK (green), DA x CK (green/yellow) and DA x CK (yellow) from the cDNA collected from the development series described in Chapter Two. Correlation coefficients were then calculated to test for correlation between gene expression and fruit colour.

3.3.2.1 Expression of chlorophyll degradation candidate genes

The expression of the chlorophyll degradation genes in the DA x CK population is shown in Figure 3.14. *SGR1* and *SGR2* had very similar expression profiles, where overall expression was highest in DA x CK (yellow), median in DA x CK (green/yellow) and lowest in DA x CK (green), which is consistent with the data for *A. chinensis* and *A. deliciosa*. The expression of *PAO2* was slightly lower in DA x CK (green). However, the expression for *PAO1* and *PAO2* was very similar in all of the fruit across development. *PPH* expression was highest at the later stages of fruit development, where the transcript levels are highest in green fruit. This upward trend across fruit development is the same as in *A. chinensis* and *A. deliciosa* in 2010, although the gene expression levels were less diverse in these three lines. The expression of *RCCR* was higher in *A. chinensis* fruit compared with *A. deliciosa*, whereas in the DA x CK population, the expression in DA x CK (green/yellow) was highest at the beginning of fruit development, and in DA x CK (green) and DA x CK (yellow) the expression was highest at the end of fruit development. This suggests that the expression of *RCCR* fluctuates, but is reasonably constitutive. *CBR* expression was similar in the three DA x CK fruit and constant over fruit development.

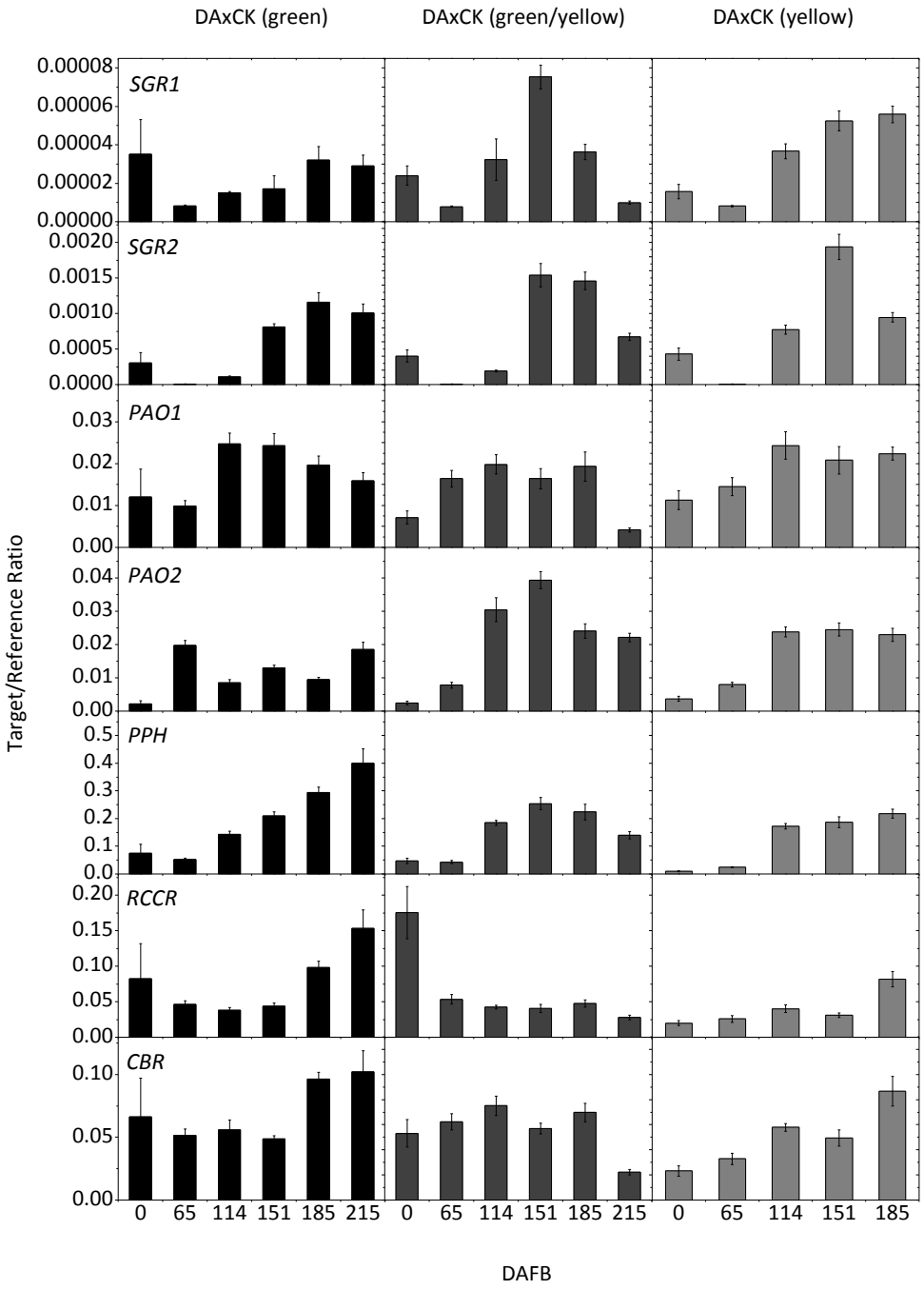

Figure 3.14. Expression of chlorophyll degradation genes in an *A. chinensis* x *A. deliciosa* cross over fruit development in 2009. Expression of chlorophyll degradation pathway genes (see Table 3.2 for abbreviations) in DA x CK (green) (left panels, black bars), DA x CK (green/yellow) (middle panels, dark grey bars) and DA x CK (yellow) (right panels, grey bars) over fruit development (days after full bloom; DAFB), measured as a target/reference ratio. Error bars indicate standard error (n=4).

A Pearson's correlation coefficient (r) test was carried out on qRT-PCR data to find statistically significant correlations between gene expression and flesh colour, measured by hue angle from Section 3.3.1, for 2009 (Table 3.8). None of the chlorophyll degradation genes were significantly correlated with flesh colour. However, there were several significant pair-to-pair correlations, where *SGR1* expression was significantly positively correlated with the expression of *SGR2*, *PAO2*, and *PPH* ($p \leq 0.001$, $p \leq 0.01$ and $p \leq 0.05$, respectively). *SGR2* expression was also significantly positively correlated with *PPH* expression ($p \leq 0.05$), *PPH* expression was significantly positively correlated with *RCCR* and *CBR* expression (both $p \leq 0.01$) and *RCCR* expression was very significantly positively correlated with *CBR* expression ($p \leq 0.001$). This suggests that the chlorophyll degradation pathway is tightly co-ordinated in the DA x CK population.

Table 3.8. Pearson's correlation, r, comparing relative chlorophyll degradation gene expression over fruit development to hue angle colour measurement in DA x CK kiwifruit. *indicates p≤0.05, **indicates p≤0.01, ***indicates p≤0.001.

Pearson's correlation, r	*SGR1*	*SGR2*	*PAO1*	*PAO2*	*PPH*	*RCCR*	*CBR*
Colour	**-0.325**	**-0.459**	**0.138**	**-0.242**	**-0.405**	**-0.249**	**-0.150**
	(0.256)	**(0.098)**	**(0.638)**	**(0.404)**	**(0.150)**	**(0.391)**	**(0.608)**
SGR1	-	-	-	-	-	-	-
SGR2	0.769	-	-	-	-	-	-
	(0.001***)						
PAO1	0.352	0.213	-	-	-	-	-
	(0.218)	(0.466)					
PAO2	0.743	0.503	-0.083	-	-	-	-
	(0.002**)	(0.067)	(0.779)				
PPH	0.551	0.656	0.279	0.322	-	-	-
	(0.041*)	(0.011*)	(0.334)	(0.261)			
RCCR	0.122	0.181	0.068	-0.128	0.731	-	-
	(0.678)	(0.535)	(0.816)	(0.662)	(0.003**)		
CBR	0.351	0.236	0.400	0.025	0.704	0.846	-
	(0.218)	(0.417)	(0.156)	(0.933)	(0.005**)	(0.000***)	

3.3.2.2 Expression of cytokinin gene candidates

The expression of the cytokinin genes in the DA x CK population is shown in Figure 3.15. The expression of *ZOG* was highest in DA x CK (green) fruit at maturity, with lower expression in DA x CK (green/yellow) and DA x CK (yellow) fruit. The expression of *IPT* was similar and constitutive across fruit development in all three fruit. In contrast, the expression of *BGLU* was highest in all fruit at the beginning of fruit development, where the highest expression was in DA x CK (yellow) fruit, with a downward trend in expression towards fruit maturity. *CKX* expression was highest in DA x CK (green/yellow) fruit at the mid stages of development, but showed a similar trend in all three fruit.

Correlation coefficients were also calculated for the cytokinin gene expression data. The expression of *BGLU* was significantly negatively correlated with fruit flesh colour ($p \leq 0.05$), and the expression of *ZOG* was significantly positively correlated with fruit flesh colour ($p \leq 0.05$). *BGLU* also had a significant negative correlation with the expression of *ZOG* ($p \leq 0.05$). Thus these results from the DA x CK population suggest these genes are good candidates for the co-ordination of cytokinin regulation or homeostasis, and therefore the control of chlorophyll degradation in kiwifruit.

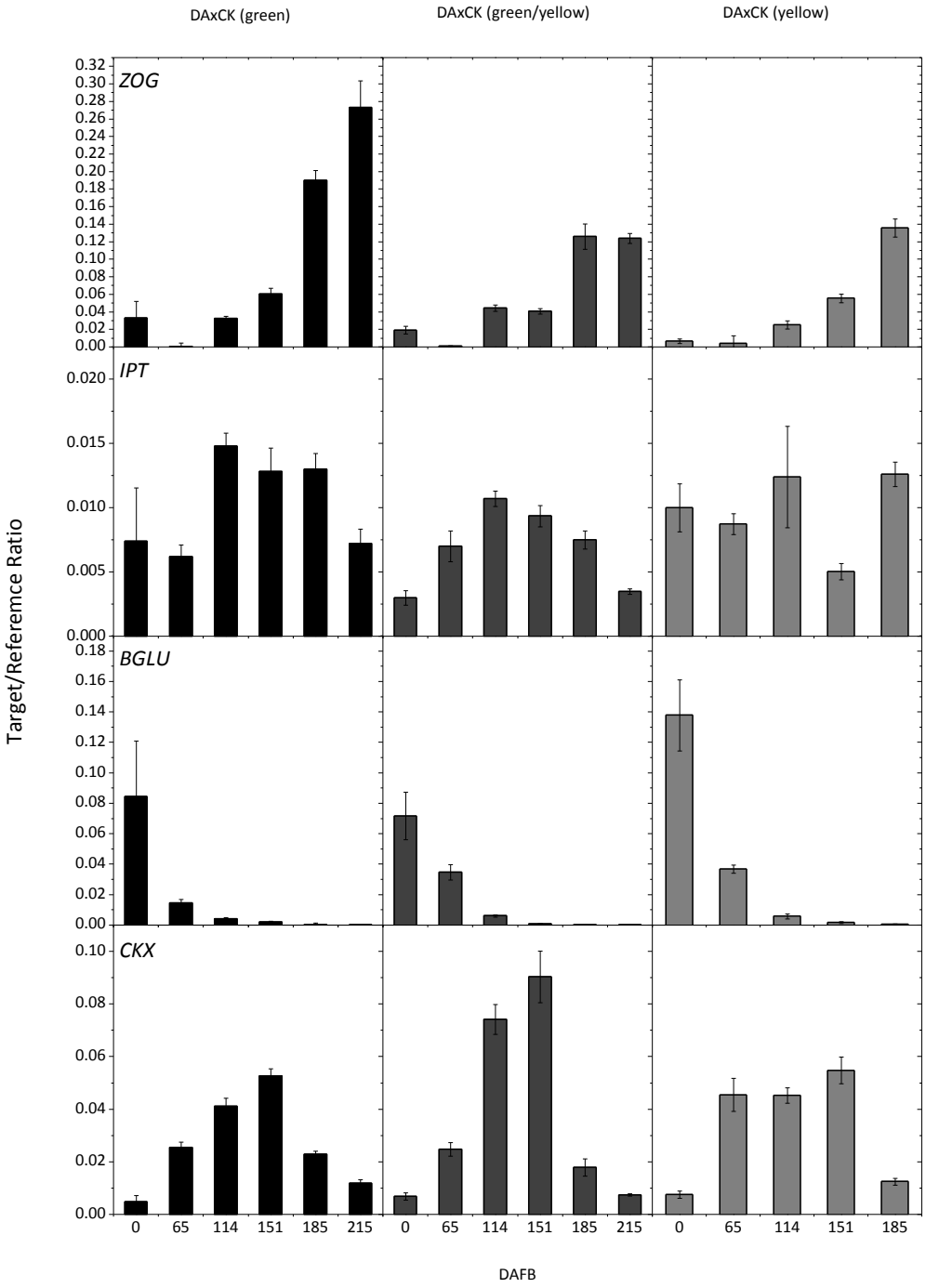

Figure 3.15. Expression of cytokinin biosynthetic genes in an *A. chinensis* x *A. deliciosa* cross over fruit development in 2009. Expression of cytokinin genes (see Table 3.2 for abbreviations) in DA x CK (green) (left panels, black bars), DA x CK (green/yellow) (middle panels, dark grey bars) and DA x CK (yellow) (right panels, grey bars) over fruit development (days after full bloom; DAFB), measured as a target/reference ratio. Error bars indicate standard error (n=4).

Table 3.9. Pearson's correlation, r, comparing relative cytokinin biosynthetic gene expression over fruit development to hue angle colour measurement in DA x CK kiwifruit. *indicates p≤0.05, **indicates p≤0.01, ***indicates p≤0.001.

Pearson's correlation, r	*IPT*	*BGLU*	*ZOG*	*CKX*
Colour	**0.161**	**0.530**	**-0.591**	**0.483**
	(0.582)	**(0.030*)**	**(0.026*)**	**(0.080)**
IPT	-	-	-	-
BGLU	-0.180	-	-	-
	(0.537)			
ZOG	-0.035	-0.565	-	-
	(0.905)	(0.035*)		
CKX	0.243	0.004	-0.526	-
	(0.402)	(0.989)	(0.053)	

3.4 Expression of candidate genes in an *A. chinensis* mapping population

An *A. chinensis* mapping population was created at Plant & Food Research for use in constructing breeding populations for mapping (Fraser *et al.* 2009). Two representative vines were chosen from the population which have differing flesh colours at maturity, in the same genetic background, as they are both *A. chinensis*. MP012 has lime-coloured flesh, and MP246 has light yellow flesh. The fruit were sampled and characterised for fruit colour, weight, firmness and soluble sugars, before gene expression analysis was carried out on candidate genes for the control of chlorophyll degradation, as described previously in Chapter Two.

3.4.1 Chlorophyll degradation during kiwifruit development

Photographs of the fruit from two vines from the *A. chinensis* mapping population MP012 (lime) and MP024 (light yellow) over development in 2009 are presented in Figure 3.16. Measurements of fruit colour, soluble sugars, weight and firmness of the same fruit are shown in Figure 3.17. These results confirmed that the fruit had been correctly phenotyped, and had lime and light yellow flesh colour, although the difference in hue angle is small. The levels of soluble sugars and firmnesses were very similar between MP012 and MP246, and had very similar soluble sugars and firmness curves to *A. chinensis* and *A. deliciosa*. Fruit from *A. chinensis* MP246 (light yellow) were lighter at maturity compared to fruit from MP 012 (lime).

Figure 3.16. *A. chinensis* mapping population developmental fruit series photographs (2010). Colour change in *A. chinensis* MP012 (top) and *A. chinensis* MP246 (bottom) at each sampling stage of development in 2009. Photographs were taken at 83, 132, 169, and 233 DAFB (right to left).

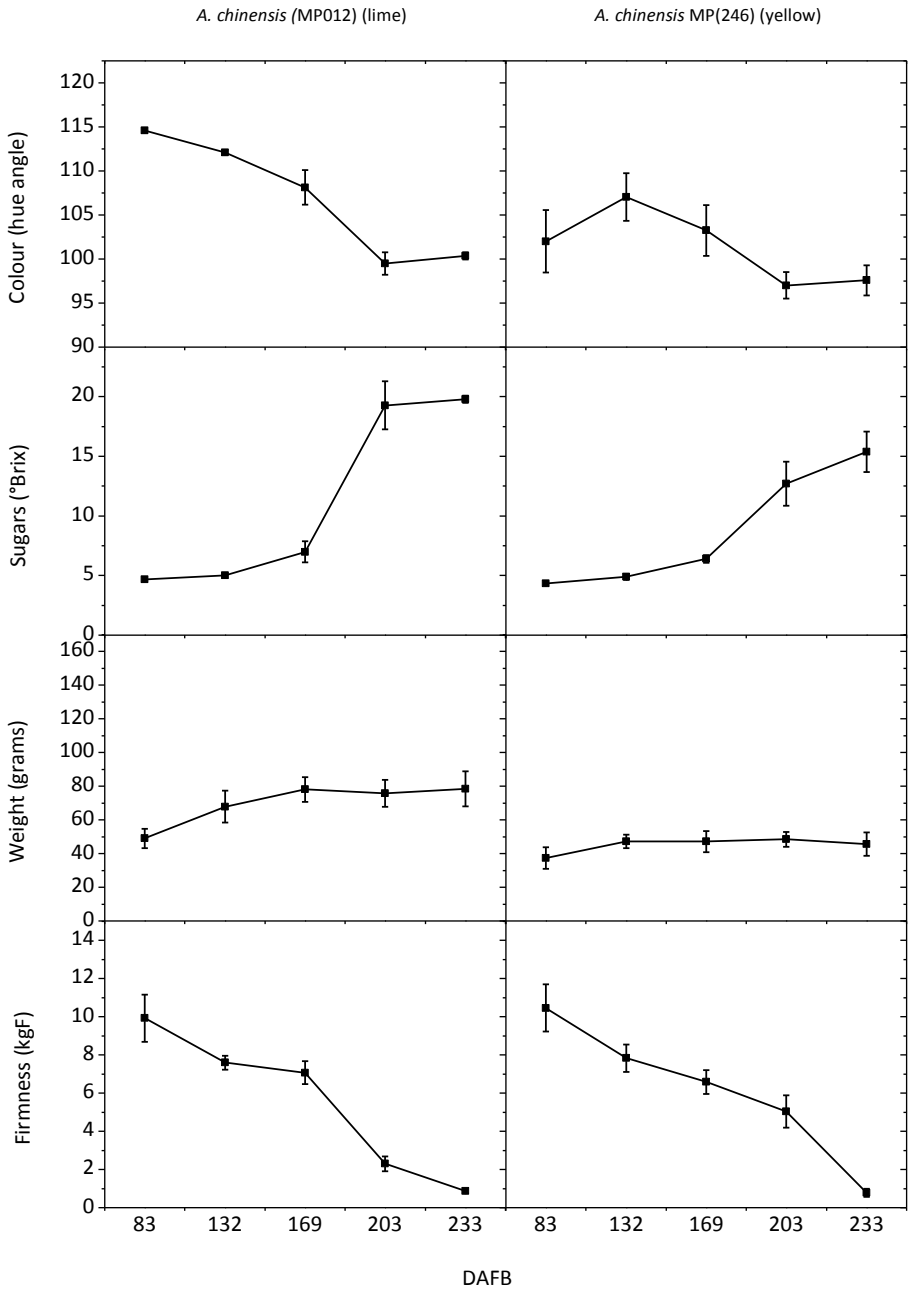

Figure 3.17. Colour, soluble sugars, weight and firmness of *A. chinensis* mapping population fruit over development in 2009. Colour is measured as hue angle, where a hue angle below 100° is yellow, a hue between 100° and 110° is green/yellow, and a hue above 110° is green. Soluble sugars are measured in °Brix, weight is measured in grams, and firmness is measured in kgF. Measurements are given for *A. chinensis* MP012 (lime) (left panels) and *A. chinensis* MP246 (light yellow) (right panels) over fruit development (DAFB) for the 2009 fruit series. Error bars indicate standard deviation (n=10).

3.4.2 Expression of candidate genes for the control of chlorophyll de-greening in the *A. chinensis* mapping population

The primers used were the same as for the previous gene expression studies (Section 3.2.3). The levels of transcripts encoding the gene candidates selected in Section 3.2.2 and further continued from Section 3.2.3 were compared by qRT-PCR between *A. chinensis* MP012 (lime) and *A. chinensis* MP246 (light yellow) from the cDNA collected from the development series described in Chapter Two.

3.4.2.1 Expression of chlorophyll degradation gene candidates

The expression of *SGR1*, *SGR2* and *PAO1* was measured by qRT-PCR in extreme individuals of the *A. chinensis* mapping populations (Figure 3.18). *SGR1* expression was similar between lime and light yellow fruit over fruit development, with the exception of the 203 DAFB in MP024, which had the highest *SGR1* expression. This trend was also seen in the expression of *SGR2*. Overall, *PAO1* expression was slightly higher in light yellow fruit than in lime fruit. The expression of *SGR1* and *SGR2* was lower in the *A. chinensis* mapping population than in *A. chinensis* and *A. deliciosa*, in comparison to the expression of *PAO1*, which was consistent with the *A. chinensis* and *A. deliciosa* 2009 series.

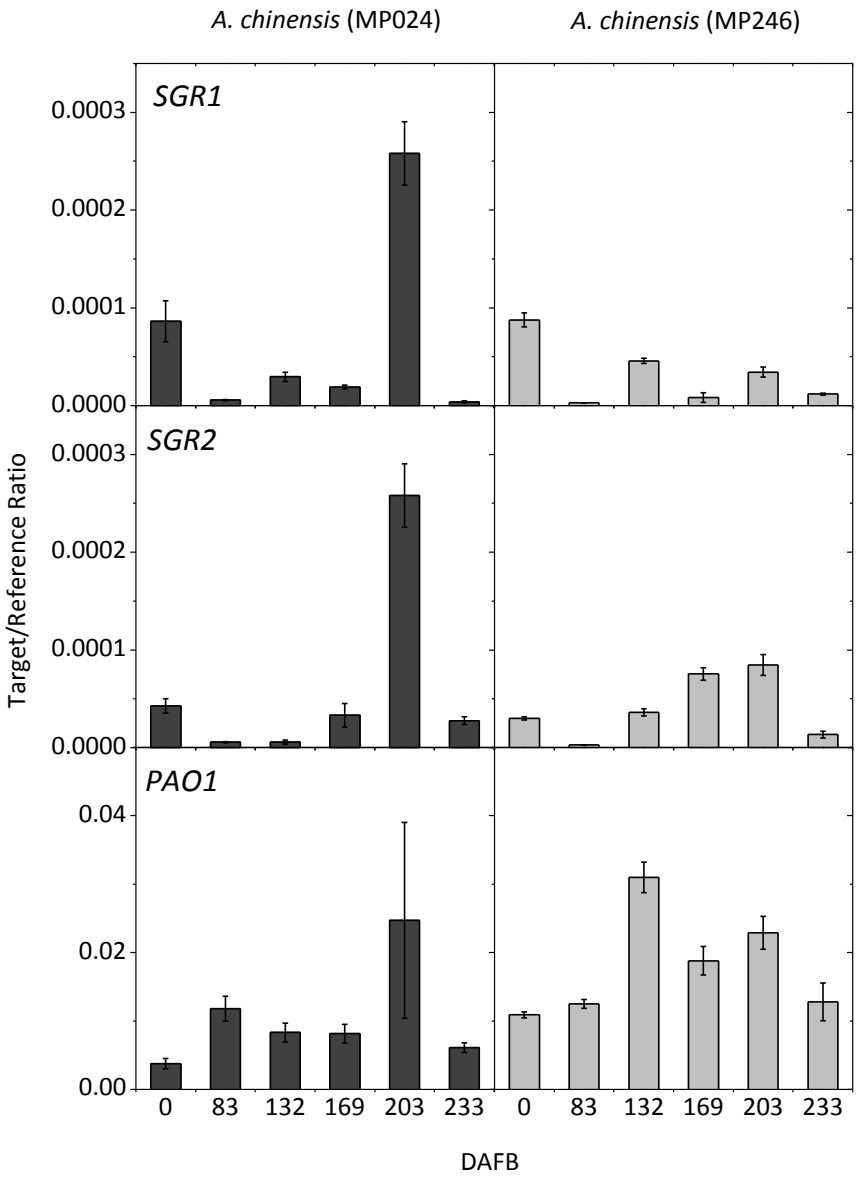

Figure 3.18. Expression of chlorophyll degradation genes in the *A. chinensis* mapping population over fruit development in 2009. Expression of chlorophyll degradation pathway genes (see Table 3.2 for abbreviations) in DA *A. chinensis* MP012 (lime) (left panels, dark grey bars), and *A. chinensis* MP246 (light yellow) (right panels, grey bars) over fruit development (days after full bloom; DAFB), measured as a target/reference ratio. Error bars indicate standard error (n=4).

3.5 Expression of candidate genes in an *A. eriantha* x *A. chinensis* cross

An inter-specific cross between *A. eriantha* (EA), another green-fleshed kiwifruit species, and *A. chinensis* (CK) resulted in a population with extremely different levels of chlorophyll degradation during fruit maturity (EA x CK) (Fraser, L. G., Unpublished). Two representative vines were chosen from the population which have bright green and bright yellow flesh colour. The fruit were sampled in 2010 and characterised for fruit colour, weight, firmness and soluble sugars, before gene expression analysis was carried out on candidate genes for the control of chlorophyll degradation, as described previously in Chapter Two.

3.5.1 Chlorophyll degradation during kiwifruit development

Photographs of the two vines from the EA x CK cross over fruit development in 2010 are presented in Figure 3.19. Measurements of the fruit characteristics colour, soluble sugars, weight and firmness of the same fruit are shown in Figure 3.20. These results confirmed that the fruit had bright green and bright yellow flesh colour. In general, the EA x CK fruit ripened very quickly, before 200 DAFB, and produced very small fruit of less than 30 grams. The EA x CK (yellow) fruit had a higher level of soluble sugars, and were not as firm at maturity as the EA x CK (green) fruit.

The RNA and resulting cDNA from the EA x CK population was of poor quality and thus the reference genes used had a very low level of expression over fruit development. It was therefore not possible to obtain meaningful gene expression results for candidate genes. However, this population has been used for further work into gene segregation in Chapter Four, due to the very significant differences in fruit flesh colour in the population.

Figure 3.19. EA x CK developmental fruit series photographs (2010). Colour change in EA x CK (green) (top) and EA x CK (yellow) (bottom) at each sampling stage of fruit development in 2010. All photographs were taken at 57, 102, 144 and 180 DAFB (right to left).

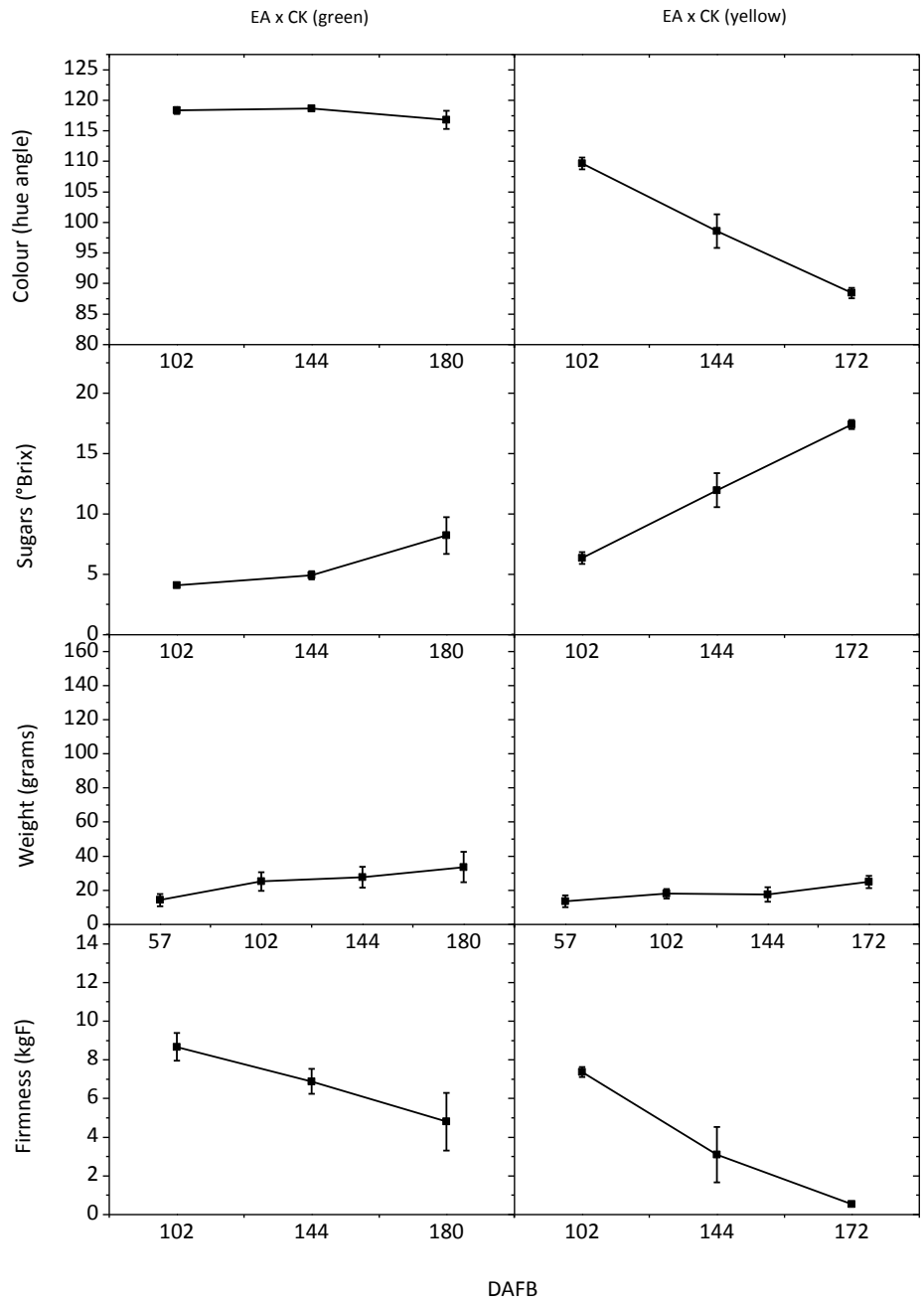

Figure 3.20. Colour, soluble sugars, weight and firmness of an *A. eriantha* x *A. chinensis* cross over development in 2010. Colour is measured as hue angle, where a hue angle below 100° is yellow, a hue between 100° and 110° is green/yellow, and a hue above 110° is green. Soluble sugars are measured in °Brix, weight is measured in grams, and firmness is measured in kgF. Measurements are given for EA x CK (green) (left panels) and EA x CK (yellow) (right panels) over fruit development (DAFB) for the 2010 fruit series. Error bars indicate standard deviation (n=10).

3.6 Discussion

A. deliciosa have, until recently, been distinguished from other fruit by their relatively high concentrations of chlorophyll in mature and ripe fruit. While new cultivars of kiwifruit, such as *A. chinensis*, de-green during fruit development, *A. deliciosa* fruit remain green until harvest at fruit physiological maturity and during extended storage (up to 20 weeks) (Ben-Arie *et al.* 1982; Harman and McDonald 1989). If left on the vine, kiwifruit will soften to the stage of eating ripeness, ripen further, and eventually abscise from the plant at an overripe stage or around 250 DAFB, at which point *A. deliciosa* fruit are still green (Warrington and Weston 1990).

In *A. deliciosa*, it is the concentration of chlorophyll which determines the flesh colour of the kiwifruit (McGhie and Ainge 2002; Montefiori *et al.* 2009). It is known that chlorophyll concentrations remain high in green kiwifruit, despite the detection of some of the catabolites of chlorophyll degradation (Montefiori *et al.* 2009). In contrast, many other immature fruits and vegetables are green and lose chlorophyll upon ripening, for example, capsicum, tomato, bananas, and oranges.

In kiwifruit the chlorophyll concentration (Table 3.1) correlates well with the hue angle of the fruit flesh (Figure 3.3 and 3.4). This flesh is unlikely to be photosynthetically active as kiwifruit have a thick brown skin shielding the flesh from light. The ratio of chlorophyll *a/b* is similar in both fruit, and lower than senescing leaves. Accelerated colour change started after approximately 130 DAFB in yellow fruit, in agreement with results obtained by Montefiori *et al*. (2009), who showed that chlorophyll concentration was higher in immature green fruit than in immature yellow fruit.

Ultrastructural studies have been performed previously on green and yellow kiwifruit fruit (Montefiori *et al.* 2009). This work showed that chromoplasts are present at maturity in yellow fruit, and fully formed chloroplasts are present at maturity in green fruit (200 DAFB). The presence of chlorophyllide *a*, pheophytin *a* and pheophorbide *a* was shown in both green and yellow fruit, indicating that chlorophyll turnover was occurring.

Chlorophyll de-greening is a co-ordinated process and appears to involve down-regulation of chlorophyll biosynthesis and up-regulation of chlorophyll degradation (Wagstaff *et al.* 2009). Consequently, in *A. deliciosa*, the overall relative rate of biosynthesis to degradation must be greater than in *A. chinensis*. The chlorophyll biosynthetic gene *GLUTR1* is expressed at similar levels in green and yellow fruit. This is the key committed step for chlorophyll biosynthesis (Eckhardt *et al.* 2004). The chlorophyll-associated genes *RBCS* and *CAO* are slightly down-regulated in yellow fruit across fruit development compared with green fruit, suggesting coordinated down-regulation of the biosynthetic pathway in yellow fruit. These results are consistent with previous observations in the literature, where *RBCS* expression decreased during leaf senescence in *Brassica napus* and *Hordeum vulgare* (Buchanan-Wollaston and Ainsworth 1997; Kleber-Janke and Krupinska 1997). The genes involved with chlorophyll biosynthesis showed a large spike in expression at 95 DAFB in 2009, which may indicate that these genes are under the control of a circadian rhythm, as seen in the expression of *CAB* in *Arabidopsis* (Millar and Kay 1996) and *LHCB* in bean (Kaldis *et al.* 2003). This result was observed despite sampling being undertaken at the same time each day to minimise possible expression fluctuations due to circadian rhythm.

The transcript levels of known steps in the chlorophyll degradation pathway were also measured. There was no expression of *CLH* during fruit maturation, which is consistent with previous work which suggests that CLH is not essential for senescence-related chlorophyll breakdown (Schenk *et al.* 2007). The chlorophyll degradation gene *PPH* was similarly expressed in green and yellow fruit, indicating that the differences in flesh colour between *A. deliciosa* and *A. chinensis* were not due to lack of *PPH* expression. According to Rodoni *et al.* (1997), the PAO enzymatic step is the critical step for loss of green colour in canola (*Brassica napus*). *PAO1* was expressed in fruit of both cultivars, but was expressed more highly and earlier in development in yellow fruit. This could indicate a possible regulatory point for chlorophyll degradation in the fruit flesh. Because *PAO1* is expressed in green kiwifruit, lack of chlorophyll degradation in green fruit is likely to be associated with altered accessibility or transport of chlorophyll components to the chloroplast envelope, or the absence of another factor required for the reaction, and thus the regulatory point should be upstream (Akhtar *et al.* 1999). The peak in expression of *SGR1* and *SGR2* seen at the end of fruit development in green fruit is likely to be related to some de-greening of the green fruit at this sampling time point in 2010. With the exception

of this last time point, *SGR2* was more highly expressed in yellow fruit, indicating another potential regulatory step of chlorophyll degradation. Expression of the chlorophyll degradation genes was slightly elevated in yellow fruit across development compared with expression in green fruit. This suggested that the genes of the chlorophyll degradation pathway and other degradation associated proteins are well regulated. If these genes encode functional proteins, then it is likely that their differential regulation causes the green and yellow flesh phenotypes.

The results of expression analysis of the same genes in DA x CK and *A. chinensis* mapping populations did not show *SGR* expression segregating with green and yellow colour. However, these results may be influenced by a number of factors including ploidy, and the subtle difference between green and yellow flesh colour in these fruit. *A. deliciosa* is hexaploid and *A. chinensis* is diploid (2n), thus the resulting DA x CK cross is tetraploid (4n). However, an *A. eriantha* (diploid) and *A. chinensis* (diploid) EA x CK cross, segregating for green and yellow colour, did not provide further insight into the control of chlorophyll degradation.

Endogenous analyses of cytokinins in developing fruit have usually shown a peak of activity co-incident with cell division in orange, tomato and apple (Letham 1963; Bohner and Bangerth 1988; Hernandez Minana *et al.* 1989). However, high levels of cytokinin were also shown in *A. deliciosa* at maturity (Lewis *et al.* 1996b).

Interestingly, the gene expression of *IPT*, the rate-limiting step in the cytokinin biosynthetic pathway, showed an increase towards maturity in green fruit, which was not seen in yellow fruit. This is consistent with whole cytokinin measurements in *A. deliciosa* fruit in previous work by Lewis *et al.* (1996b). One of the genes involved with cytokinin homeostasis, *ZOG*, showed a similar trend, with higher expression in green fruit, increasing towards fruit maturity, potentially indicating a high level of cytokinin *O*-glucosylation in green fruit. The expression profile for *CKX* had a relatively similar pattern in both fruit. Because changes in CKX activity alter the cytokinin levels in tissues, CKX enzymes are important in controlling local cytokinin levels and are considered to contribute to the regulation of cytokinin-dependent processes (Schmülling *et al.* 2003). In previous work in *N. tabacum* by Jones and Schreiber (1997) and Motyka *et al.* (2003) and in *Brassica rapa* by O'Keefe *et al.* (2011), *CKX* expression was linked to *IPT* expression.

This does not occur in *A. deliciosa*, suggesting that there could be a breakdown in homeostatic control. Despite high gene expression in green fruit compared with yellow fruit, there were no significant correlations between cytokinin biosynthetic gene expression and fruit colour in either year. However, there were significant pair-to-pair gene correlations between *IPT* and *ZOG* and *BGLU* which indicates that the pathway may be co-regulated.

The expression of the cytokinin biosynthetic genes shows some significant pair-to-pair correlations with the expression of the chlorophyll degradation genes, including *PPH* and *CBR* positively correlating with *ZOG* expression; *SGR1*, *SGR2* and *PPH* negatively correlating with *BGLU* expression; and *IPT* positively correlating with *PAO1* expression. This indicates that in addition to co-ordinative regulation of the cytokinin biosynthetic pathway alone, it may also be co-regulated with the chlorophyll degradation pathway.

There was a significant positive correlation between *ZOG* and fruit flesh colour and negative correlation between *BGLU* and fruit flesh colour in the DA x CK population. However, the expression of *BGLU* was high in the early stages of fruit development, suggesting that expression of this gene is not involved with colour change, which occurs later in development. However, these results suggest that *ZOG* is a good candidate for further investigation into the control point for chlorophyll degradation and/or co-ordination of cytokinin homeostasis and chlorophyll degradation in kiwifruit.

3.6.1 Chapter summary

The transcripts of genes from the chlorophyll biosynthetic pathway, chlorophyll degradation pathway, carotenoid biosynthetic pathway and the cytokinin biosynthetic pathway were detected in both green and yellow fruit tissue. Thus the colour difference between green and yellow fruit is not due to the loss of transcription of a step, leading to retention of chlorophyll in green fruit. The chlorophyll biosynthetic genes were excluded as candidates for the control of chlorophyll degradation in kiwifruit as their expression was slightly higher overall in green fruit. Similarly, the carotenoid biosynthetic genes were also excluded as candidates as their expression was similar in green and yellow fruit. Overall, the chlorophyll degradation gene transcripts accumulated to a higher level in yellow tissue

and cytokinin biosynthetic gene transcripts accumulated to a higher level in green tissue, and *SGR*, *PPH*, *PAO1*, *IPT*, *ZOG* and *BGLU* showed co-ordinated regulation with significant pair-to-pair correlations.

The magnitude of the differences was not as great as might have been expected from the changes in colour and chlorophyll. Consequently, other processes, for example the spatial separation of chlorophyll and the degradation machinery, or hormonal regulation, may be delaying de-greening in green fruit. Further experiments were designed to characterise the key chlorophyll degradation candidates in kiwifruit, compare the endogenous cytokinin levels in *A. deliciosa* and *A. chinensis*, and investigate the transcriptional regulation of candidates for the control of chlorophyll degradation.

4. FUNCTIONAL CHARACTERISATION OF CANDIDATE KIWIFRUIT GENES FOR THE CONTROL OF CHLOROPHYLL LEVELS

4.1 Introduction

The genes encoding chlorophyll degradation pathway enzymes are expressed in both green and yellow kiwifruit. This indicates that the colour difference between green and yellow fruit is apparently not due to the loss of transcription of an enzymatic step, and thus retention of chlorophyll in green fruit. The chlorophyll biosynthetic genes were excluded as candidates for the control of chlorophyll levels in kiwifruit as their expression was slightly higher overall in green fruit. Similarly, the carotenoid biosynthetic genes were also excluded as candidates as their expression was similar in green and yellow fruit. Overall, the chlorophyll degradation gene transcripts accumulated to a higher level in yellow tissue. In research reported in this chapter, different methods for studying the functionality of chlorophyll degradation genes were tested using transient transformation assays in tobacco and kiwifruit, the key candidate genes for chlorophyll degradation were characterised in green and yellow kiwifruit by sequencing and *in silico* analysis, and the possibility that green and yellow colour is controlled by a single gene was investigated using an *A. chinensis* x *A. eriantha* cross which segregates for green and yellow fruit flesh colour.

4.2 Transient assay of chlorophyll degradation activity in *Nicotiana benthamiana* leaves

The activity of genes involved in pigment production pathways can be visualised using transient transformation. Transient over-expression of rice *SGR* caused a visible yellowing of infiltrated leaf patches in *N. benthamiana* (Park *et al.* 2007). Transient infiltration of genes involved in the regulation of the anthocyanin biosynthetic pathway has also been previously reported, for example *MdMYB10,* an apple MYB transcription factor, where transient over-expression in *N. tabacum* leaves produced red pigmentation around the

infiltration site (Espley *et al.* 2007). *Arabidopsis* MYB10 has also been transiently over-expressed in *A. eriantha* fruit, with a visible red pigmentation around the core of the fruit

Full length coding sequences of kiwifruit *CLH1*, *CBR1*, *CBR2*, *PPH1*, *PAO1*, *RCCR*, *SGR1* and *SGR2* were cloned into plant expression vectors, as described in Chapter Two. These plasmids were transformed into *Agrobacterium tumefaciens* and syringed into expanding *N. benthamiana* leaves (Hellens *et al.* 2005). The effect of transient infiltration of selected chlorophyll degradation pathway genes is shown in Figure 4.1. Infiltration of *SGR1* and *SGR2* caused chlorophyll degradation from green to yellow in the leaves of *N. benthamiana*. Infiltration of *CLH1* and *PAO1* produced some leaf yellowing. This yellowing response was not seen upon infiltration of the other degradation pathway genes.

Yellowing was quantified using the chlorophyll fluorescence measurement technique of Pulse Amplitude Modulation (PAM) (Shabala *et al.* 2005) (Figure 4.2). Infiltration and transient expression of *PAO1* and the empty vector control did not decrease the chlorophyll fluorescence ratio of the leaves, indicating that there was no effect on chlorophyll levels upon transient infiltration. In contrast, infiltration of both *SGR1* and *SGR2* caused a large decrease in PSII quantum yield in the *SGR1* and *SGR2* patches within two days, with minimal chlorophyll fluorescence at four days after infiltration. This can be viewed using fluorescence microscopy, as shown in Figure 4.3, which shows very little chlorophyll fluorescence upon infiltration with *SGR2*.

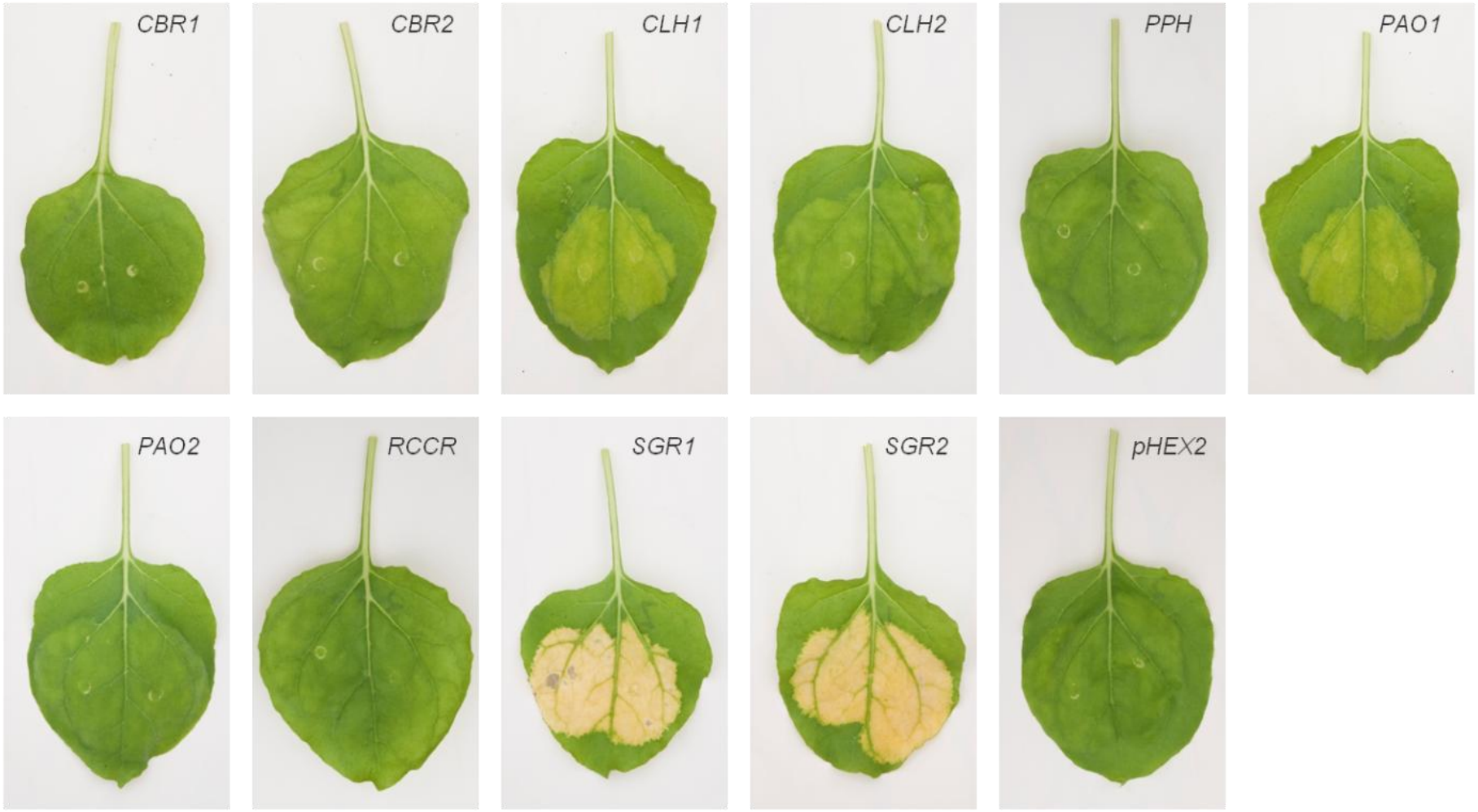

Figure 4.1. Transient assay of chlorophyll degradation genes in *N. benthamiana*. The effect of overexpression of *CBR1*, *CBR2*, *CLH1*, *CLH2*, *PPH*, *PAO1*, *PAO2*, *RCCR*, *SGR1* and *SGR2* against the *pHEX2* control can be seen visually in *N. benthamiana* leaves.

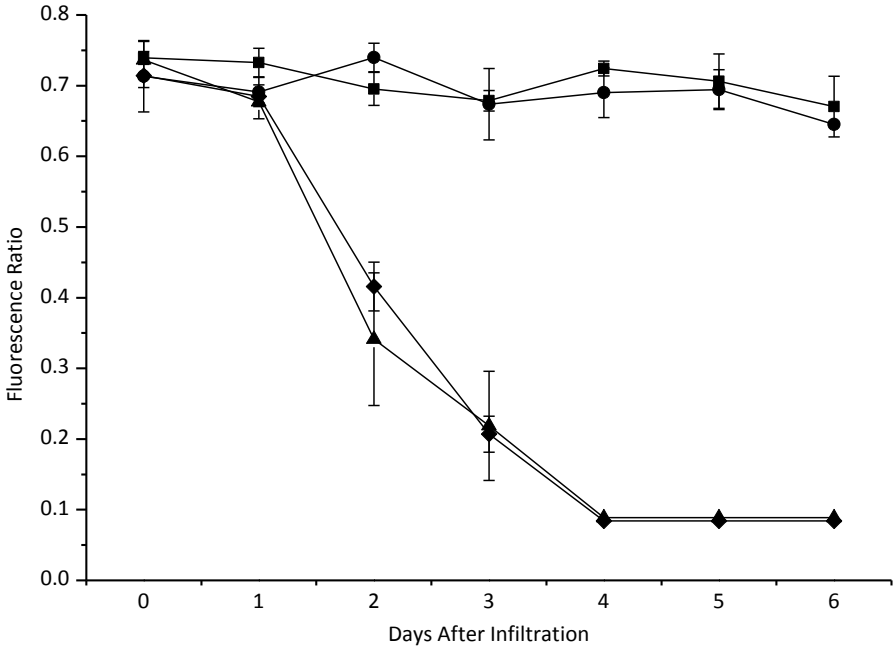

Figure 4.2. Transient assays in tobacco show different chlorophyll degradation responses.
A loss of chlorophyll fluorescence due to chlorophyll degradation using Pulse Amplitude Modulation (PAM). Genes measured were *PAO1* (square markers, ■), *SGR1* (triangle markers, ▲), *SGR2* (diamond markers, ♦) and *pHEX2* control (round markers, ●).

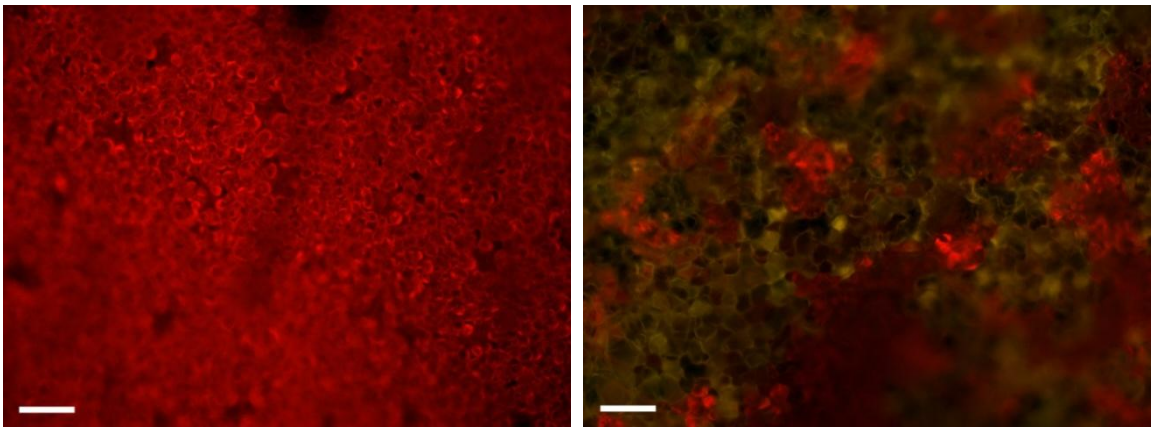

Figure 4.3. Chlorophyll fluorescence microscopy. Chlorophyll fluorescence (red) in a control leaf (left) compared with a leaf infiltrated with *SGR2* (right). Scale bar represents 100 microns. Microscopy by Frederik Polzin.

4.3 Developing alternative methods for investigating chlorophyll degradation in kiwifruit

In order to model chlorophyll degradation in kiwifruit, whole *A. chinensis* seedlings were placed in the dark to induce senescence and chlorophyll degradation (as described in Chapter Two), (Figure 4.4). The kiwifruit seedlings in the light developed normally, producing large, green leaves. The seedlings in the dark showed an elongated cotyledon and the leaves did not show any growth, but remained green. These results show that *A. chinensis* seedlings do not undergo a normal pattern of dark-induced senescence, even after 12 weeks of dark treatment.

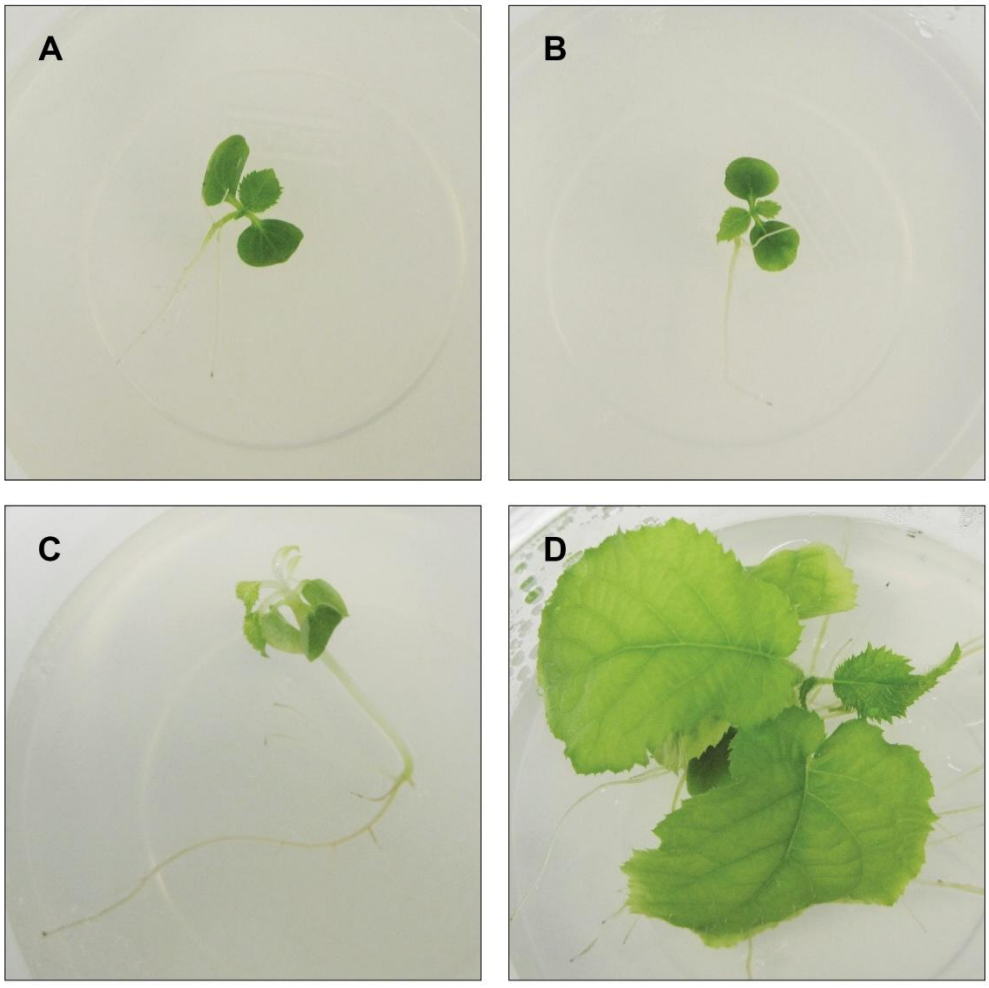

Figure 4.4. Dark-induced senescence in kiwifruit seedlings. *A. chinensis* seedlings at the four leaf stage (A and B) were placed in the dark for 12 weeks (C) or light for 12 weeks (D). Seedlings are representative of four replicates.

A leaf patch experiment was then carried out to induce senescence in detached kiwifruit leaves. The *A. chinensis* leaves were lighter green than the *A. deliciosa* leaves at the beginning of the experiment, which is typical between the two species (Figure 4.5). In addition to controls, *A. deliciosa pSAK778S:SGR* over-expression lines and *A. chinensis pTKO2:SGR* knockout lines were included. *A. chinensis* knock out plants, *A. deliciosa* over-expressing plants and both *A. chinensis* and *A. deliciosa* controls were transformed by Tianchi Wang at Plant & Food Research, as described in Chapter Two. Leaf patches were cut from mature leaves and placed in distilled water in a Petri dish, as previously described for dark-induced senescence experiments in detached leaves of rice (Sato *et al.* 2009). Photographs were taken of the leaves at 0 days and at 60 days of each treatment (Figure 4.6). Ethylene treated samples were incubated in 10 µl/l ethylene overnight and then treated in the same way as the control samples. These results showed that there was no visible de-greening at 60 days in any of the leaf patches, despite some visible cell death.

Figure 4.5. *A. chinensis* and *A. deliciosa* leaves. Mature *A. chinensis* (left) and *A. deliciosa* (right) leaves. Scale bar is in cm.

Figure 4.6. Dark-induced senescence in kiwifruit leaf patches. *A. deliciosa pHEX4* control, *A. chinensis pHEX4* control, *A. deliciosa pSAK277S:SGR* and *A. chinensis pSAK778S:SGR* leaf patches following treatment of cold, dark, ethylene or control at 0 days and at 60 days.

The ability to transiently transform kiwifruit seedlings was also explored as a possible method for investigating chlorophyll degradation in a kiwifruit system. *AcMYB10* was used for initial work as an activator of anthocyanin production. The visible results following transient infiltration of *A. chinensis* leaves are shown in Figure 4.7. A few red cells are visible around the infiltration site, but the majority of cells were not transformed.

Figure 4.7. Transient infiltration of kiwifruit seedlings. *A. chinensis* seedling leaf following infiltration with *Agrobacterium* containing *AcMYB10*. The circular infiltration site is visible, the top right corner of the site is marked with an arrow.

The Injex needle-free delivery system was also used to transiently transform *A. eriantha* fruit, where *Agrobacterium* is forced into the fruit by application of the delivery system to the skin on the transverse side of the kiwifruit. (Figure 4.8). Red anthocyanin pigmentation is visible around the core of fruit transformed with *AtMYB10*, where the anthocyanin pathway has been over-expressed. However, there was no visible chlorophyll degradation around the core of fruit transformed with *SGR*.

Figure 4.8. Transient transformation of *A. eriantha* fruit. *A. eriantha* fruit were transiently infiltrated with *Agrobacterium* containing *SGR* (left) and *AtMYB10* (right). Red pigmentation is visible around the core of fruit transformed with *AtMYB10*.

4.4 *In silico* analysis of CLH in kiwifruit

In higher plants, *CLH* genes encode soluble proteins that are predicted to localise in the cytoplasm, vacuole or chloroplast stroma (Park *et al.* 2007). Subcellular fractionation experiments show that CLH activity is present in the inner envelope membrane of chloroplasts whereas, the initial substrate, chlorophyll, is tightly bound to the LHCBI and II complexes (Park *et al.* 2007). Based on sequence information, other *CLHs*, such as *C. sinensis CLH*, were proposed to locate outside of the plastid, which implied the possible existence of additional chlorophyll breakdown pathways outside the chloroplast (Takamiya *et al.* 2000; Hörtensteiner 2006). The sequences of kiwifruit *AdCLH1* and *AcCLH2* were analysed by ChloroP (Emanuelsson *et al.* 1999), and were predicted not to have a chloroplast transit peptide sequence, indicating that they are unable to localise to the chloroplast.

The CLHs also have a conserved lipase motif containing a serine residue as the active site, which is consistent with the hydrolytic activity of CLH. Various site-directed mutagenesis experiments of *Chenopodium album CLH* have revealed that the serine residue is vital for the expression of CLH activity (Jacob-Wilk *et al.* 1999). Kiwifruit CLH analysis found that *AdCLH1* contains this serine residue in the conserved serine-lipase motif and causes some de-greening upon transient over-expression in *N. benthamiana*, whereas *AcCLH2* does not, as seen from sequence alignments and transient over-expression (Figure 4.1). Despite the differences in activity, the CLHs were not investigated further, due to their low gene expression in kiwifruit over fruit development.

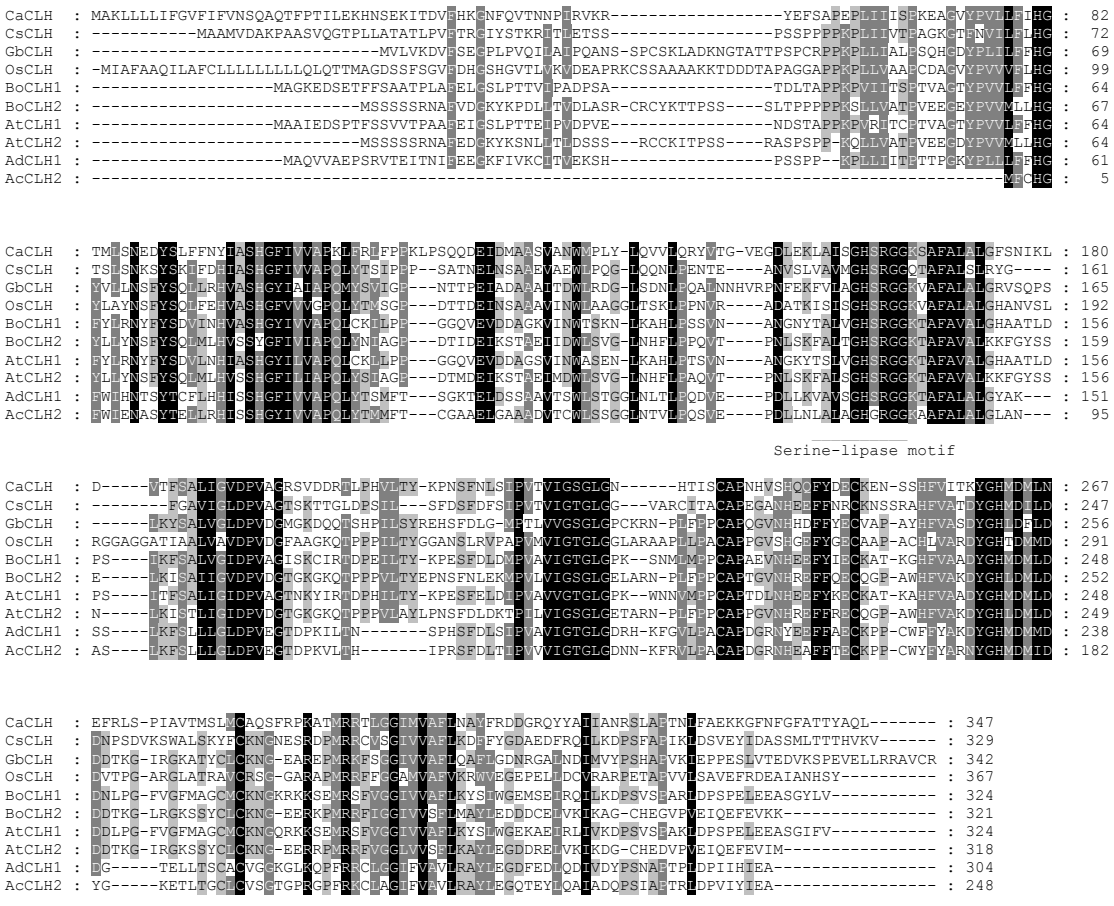

Figure 4.9. Protein sequence alignment of CLHs from kiwifruit and other species. Sequence alignment of CLH proteins. The conserved lipase motif is underlined (Jacob-Wilk *et al.* 1999). Black shading with white letters, grey shading with white letters and grey shading with black letters indicate 100%, 80% and 60% sequence identity, respectively.

4.5 Stay-green

The kiwifruit *SGR1* and *SGR2* were shown to induce chlorophyll degradation upon transient infiltration in tobacco (Figure 4.1). In several diverse species (for example pea, rice, tomato, capsicum and soybean (Guiamet *et al.* 1991; Cha *et al.* 2002; Efrati *et al.* 2005; Armstead *et al.* 2007)), mutations in the coding sequence of the SGR protein cause changes in the rate of chlorophyll breakdown. Consequently, *SGR1* and *SGR2* from *A. deliciosa* and *A. chinensis* were sequenced. The protein sequences of these genes are most similar to the SGR sequences from pea and soybean (Figure 4.10). Both *SGR1* and *SGR2* are present in green and yellow fruit. The protein sequence of *A. chinensis* SGR1 is identical to the protein sequence of *A. deliciosa* SGR1, and this is the same for SGR2. SGR1 is 67% identical to SGR2. Although there were SNP differences between clones of these genes that could affect translation, none of these resulted in an amino acid change. The full length deduced protein sequences of *A. deliciosa SGR1* and *SGR2* and *A. chinensis SGR1* and *SGR2* were aligned with SGR sequences of other plant species (Figure 4.11). The single amino acid changes in pea and capsicum SGR proteins, identified as responsible for a lack of de-greening, are marked in Figure 4.11. The kiwifruit SGR sequences do not contain any of these known *SGR* mutations (Figure 4.11). It is therefore likely that, providing the transcripts of *SGR1* and *SGR2* are converted into protein, these proteins would be functional.

A. chinensis SGR knock out plants (*pTKO2:SGR*), *A. deliciosa 35S:SGR* over-expressing plants (*pSAK778S:SGR*) and both *A. chinensis* and *A. deliciosa* controls (*pHEX4*) were transformed as described in Section 4.3. *A. deliciosa* over-expressing *SGR2* on the actinidin fruit –specific promoter were also transformed, to assess the effect of *SGR2* on fruit colour. RNA was extracted from leaves of the transgenic plants and, following cDNA synthesis, plants were characterised using *SGR2*-specific primers (Figure 4.12). All but one of the *pTKO2* knock-out plants contained knocked-down levels of *SGR2* and, likewise, all but one of the *pSAK778S* plants were over-expressing *SGR2*. Plants transformed with the actinidin promoter had not been characterised at the time of writing this thesis as they had not yet fruited. Photographs of the knockout and over-expression lines show a normal phenotype (Figure 4.13).

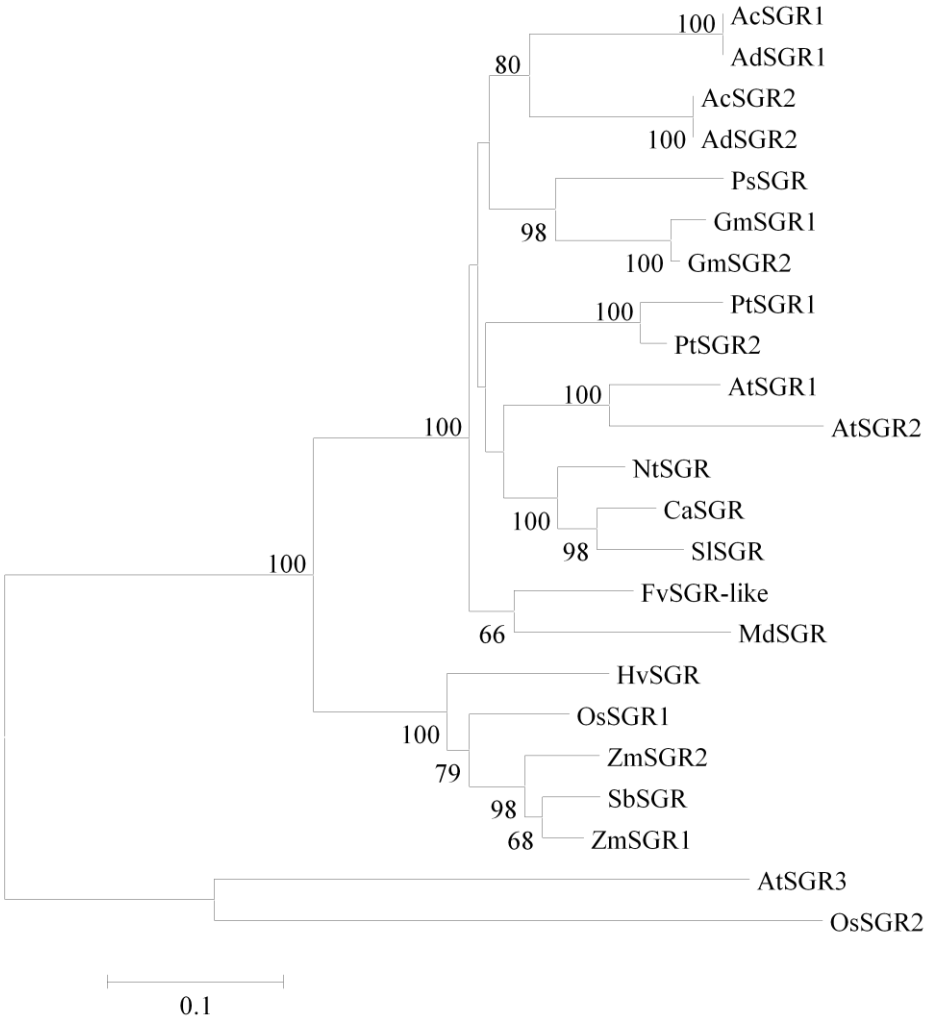

Figure 4.10. Phylogenetic tree of SGR. Updated from Hörtensteiner (2009). The unrooted phylogenetic tree of full length protein sequences aligned using Clustal W. Branch support values from 100 bootstraps are indicated when higher than 50%. GenBank protein accession numbers are as follows: *Arabidopsis thaliana* AtSGR1, AAW82962; AtSGR2, AAU05981; AtSGR3, AAM14392; *Capsicum annuum* CaSGR, ACB56586; *Frugaria vesca* FvSGR-like; *Glycine max* GmSGR1, AAW82959; GmSGR2, AAW82960; *Hordeum vulgare* HvSGR, AAW82955; *Malus domestica* MdSGR; *Nicotiana tabacum* NtSGR, ABY19382; *Oryza sativa* OsSGR1, AAW82954; OsSGR2, BAF16284; OsSGR3, CAE05787; *Pisum sativum* PsSGR, CAP04954; *Solanum lycopersicon* SlSGR, ACB56587; *Sorghum bicolor* SbSGR, AAW82958; *Zea mays* ZmSGR1, AAW82956; ZmSGR2, AAW82957. *Populus trichocarpa* protein sequences were obtained from the Joint Genome Institute (see http://jgi.doe.gov), and the protein IDs are as follows: PtSGR1, 548540; PtSGR2, 646534.

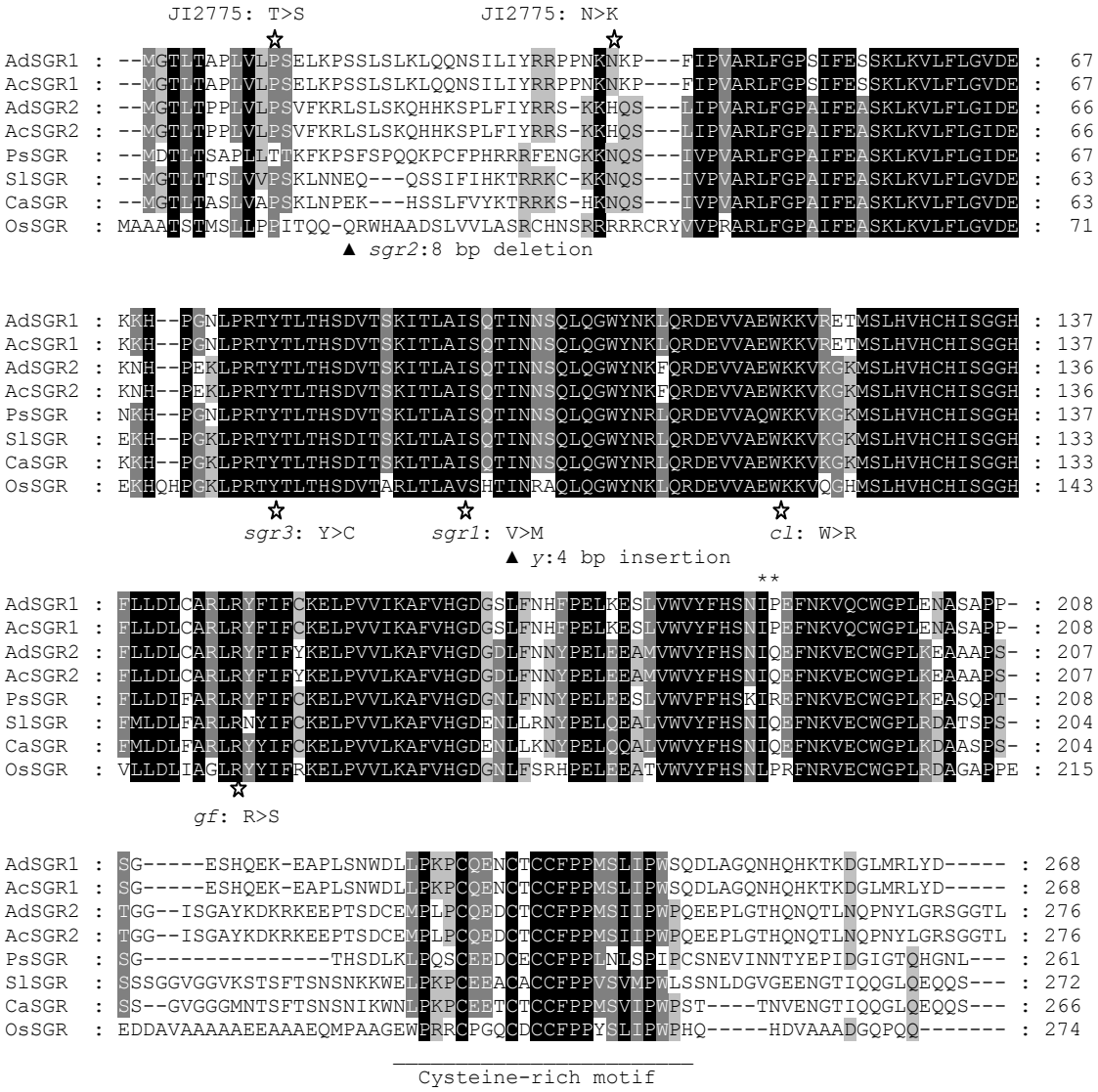

Figure 4.11. Protein sequence alignment of SGR from kiwifruit and other species. Sequence alignment of SGR proteins. Sites of mutations are marked with a star in PsSGR (JI2775), OsSGR (*sgr*), CaSGR (*cls*) and SlSGR (*gf*), respectively. In each case, the type or consequence of mutation found in different SGR mutants is indicated. The site of an amino acid insertion found to be responsible for the SGR phenotype in pea is indicated by ** (Sato *et al.* 2007). A conserved cysteine-rich motif is underlined. Black shading with white letters, grey shading with white letters and grey shading with black letters indicate 100%, 80% and 60% sequence identity, respectively.

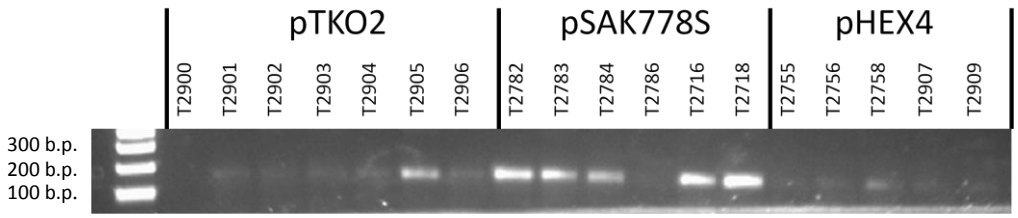

Figure 4.12. End-point PCR of SGR2 in kiwifruit transformants. End point PCR was performed to determine *SGR2* expression in *A. chinensis* knock-outs (*PTKO2*) cDNA, *A. deliciosa* over-expressors (*pSAK778S*) and *A. chinensis* and *A. deliciosa* control (*pHEX4*).

Figure 4.13. Kiwifruit *SGR* over-expression and knock-out lines. *A. deliciosa SGR* over-expression vines are visible in the middle of the picture (left) and *A. chinensis SGR* knock-out vines are visible in the middle of picture (right). Kiwifruit *AcMYB10* over-expression lines are also visible in the top right corner (right).

The rate of leaf drop was measured in kiwifruit *SGR* over-expression and knockout lines to determine whether senescence had been altered in these vines. Rate of leaf drop, as well as autumnal de-greening, should be part of the senescence process. *A. deliciosa* vines over-expressing *SGR* and *A. chinensis SGR* knockout lines did not have a different rate of leaf drop from control plants, as seen in Figure 4.14.

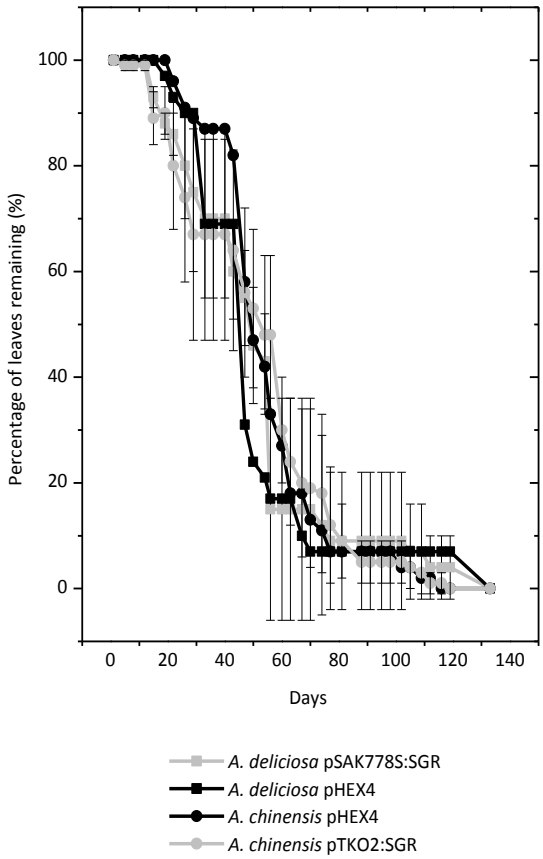

Figure 4.14. Leaf counts of kiwifruit *SGR* knockout and over-expression lines.
Leaves on kiwifruit *SGR* knockout and over-expression lines were counted during leaf senescence in the winter. The number of leaves remaining is given as a percentage of the number of mature leaves on the vine at the beginning of winter. Error bars are standard error of three replicate vines.

4.6 Investigating whether chlorophyll degradation can be controlled by a single gene

Interspecific crosses are useful in order to provide a genetic linkage to green and yellow colour phenotype in kiwifruit. In most species where a stay-green phenotype is described, the yellow phenotype is dominant (Guiamet *et al.* 1991; Cha *et al.* 2002; Efrati *et al.* 2005; Armstead *et al.* 2007). If yellow colour is dominant and a single gene in kiwifruit, it would be assumed that a green parent would be homozygous recessive for yellow colour. The yellow parent could therefore be either homozygous dominant or heterozygous.

Possible theoretical parents and resulting progeny are displayed in Figure 4.15. It would be expected that the resulting F1 population from a cross between two homozygous parents would all be yellow. Similarly, if the yellow parent was heterozygous, it would be expected that the resulting F1 population would have a 1:1 ratio of yellow to green flesh colour. If yellow colour is dominant but yellow colour is prevented by an inhibitor (I), the resulting progeny from a heterozygous cross would have a 3:13 ratio of yellow to green flesh colour. Alternatively, if yellow colour is inherited as two genes (A and B), the resulting progeny from a heterozygous cross would have a 9:7 ratio of yellow to green flesh colour.

a

	y	y
Y	Yy	Yy
Y	Yy	Yy

b

	y	y
Y	Yy	Yy
y	yy	yy

c

	CI	**Ci**	**cI**	**ci**
CI	CCII	CCIi	CcII	CcIi
Ci	CCIi	CCii	CcIi	Ccii
cI	CcII	CcIi	ccII	ccIi
ci	CcIi	Ccii	ccIi	ccii

d

	AB	**Ab**	**aB**	**ab**
AB	AABB	AABb	AaBB	AaBb
Ab	AABb	AAbb	AaBb	Aabb
aB	AaBB	AaBb	aaBB	aaBb
ab	AaBb	Aabb	aaBb	aabb

Figure 4.15. Theoretical green and yellow crosses. Resulting progeny from a cross between a homozygous dominant yellow parent and a homozygous recessive green parent (a), between a heterozygous yellow parent and a homozygous recessive green parent (b), between parents heterozygous for colour (C or c) and colour inhibited (I or i) alleles (c), and between parents heterozygous for two factors which contribute to colour together (A, a, B or b) (d). Green and yellow boxes represent the phenotype of the associated genotype.

A. eriantha (EA) and *A. chinensis* (CK) crosses were made at Plant & Food Research in 1993-1994 for a study of peelability (Seal, A. G., Personal Communication). The resulting F1 population is useful for studying segregation of green and yellow flesh colour. The parents of the cross were two female EA and 17 male CK. The resulting diploid F1 generation (EA x CK) contained 13 families, and 117 females. The hybrid vines were phenotyped for flesh colour as described in Chapter Two and colour measurements are given in Figure 4.16. Fruit photographs of the F1 generation are presented in Figure 4.17. Colour measurements gave a ratio of green:green/yellow:yellow of 44:16:2. If green/yellow fruit are classified as able to

de-green, the ratio becomes green:yellow of 44:18. This ratio is closest to a 3:1 ratio of green:yellow, which suggests that green colour is the dominant phenotype. However, with such a small sample size, it is possible that either of the ratios given in Figure 4.15 for two alleles could also be correct.

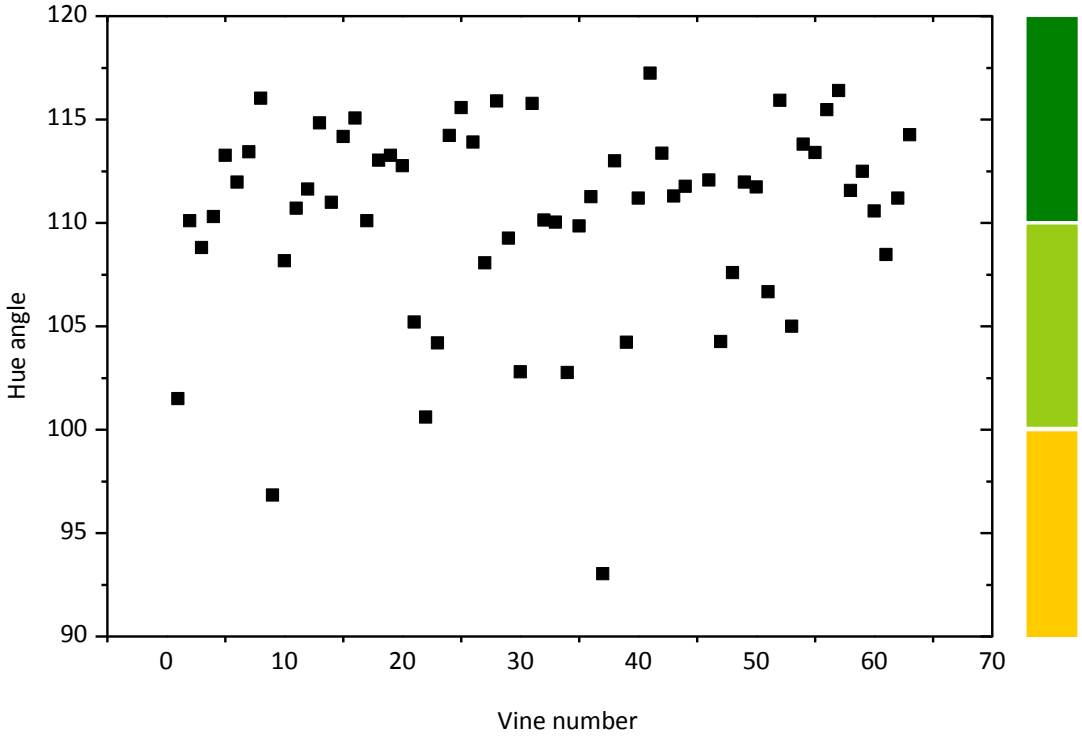

Figure 4.16. Colour distribution of individuals from an *A. eriantha* x *A. chinensis* cross. Colour is measured as hue angle, where a hue angle below 100° is yellow, a hue between 100° and 110° is green/yellow, and a hue above 110° is green. Adjacent colour bar shows fruit flesh colour at the corresponding hue angle.

Figure 4.17. Individuals from an *A. eriantha* x *A. chinensis* cross. Colour at sampling in 2011 of fruit from an *A. eriantha* x *A. chinensis* cross at around 190 DAFB.

4.7 Discussion

The ability of the kiwifruit genes involved in chlorophyll degradation to induce chlorophyll degradation upon over-expression in tobacco was measured using transient assays combined with fluorescence measurements of chlorophyll. The PAM technique, which measures PSII quantum yield, was shown to be an effective technique for measuring chlorophyll degradation during transient infiltration assays. Both *SGR1* and *SGR2* caused rapid chlorophyll degradation in *N. benthamiana* leaves upon transient infiltration. These results suggest that the over-expression of SGR alone is sufficient to drive chlorophyll degradation. These genes are expressed in both green and yellow fruit, but more *SGR2* expression was measured in yellow fruit (Figure 3.7 and 3.8).

Following completion of the experimental work, *CBR* was re-aligned using a newly available genome scaffold, and it was found that the *CBR2* gene used in the infiltration experiments was not full length, as originally thought from EST sequencing. Future work should include full-length cloning and transient infiltration of *CBR2* to test the function of this gene.

Three other methods were used in an attempt to determine the mechanism underlying the differences in chlorophyll degradation between *A. chinensis* and *A. deliciosa*: dark-induced senescence in kiwifruit seedlings, dark-induced senescence in kiwifruit leaf patches, and transient transformation of kiwifruit seedlings. Kiwifruit seedlings did not display chlorophyll degradation in the dark, which is seen in systems such as *Arabidopsis* and pea (Symons and Reid 2003). This may be due to their ability to persist on nutrient agar without light. As kiwifruit are a vine that must survive under a canopy, these species may have disassociated their dark-related senescence. Kiwifruit leaf patches also did not display a normal degradation response when subjected to darkness, cold, or ethylene. The dark-induced senescence results for the leaf patches were similar to the seedling response, which is further evidence to suggest that the chlorophyll degradation pathway is disassociated from light signals to some degree in kiwifruit leaves. Cold treatment at 4°C was tested as kiwifruit vines lose their leaves in winter. However, cold treatment was also not sufficient to drive chlorophyll degradation. This could be due to lack of a whole plant signal in response to cold. Direct infiltration of kiwifruit seedlings with candidate genes showed that

some individual cells had been transformed, as red anthocyanin pigment was produced by the over-expression of *MYB10*. However, this technique required much more method development before it could be used for the study of chlorophyll degradation. Like grapevine leaves, for which the quality of the plant material is a barrier to an efficient method for *Agrobacterium*-mediated transient expression (Santos-Rosa *et al.* 2008), kiwifruit leaves are difficult to infiltrate, which could be due to the tight composition of the apoplastic space compared with tobacco leaves.

Both *SGR1* and *SGR2* are present in green and yellow fruit. The protein sequences for SGR1 and SGR2 from *A. chinensis* are identical to the protein sequences for SGR1 and SGR2 from *A. deliciosa*, respectively. SGR1 is 67% identical to SGR2, and the kiwifruit SGR sequences are most similar to SGR sequences from pea and soybean, and do not contain any known SGR sequence mutations. Therefore it is likely that these genes produce functional SGR proteins in both *A. deliciosa* and *A. chinensis*. Taken together with the qRT-PCR results from Chapter Three, this suggests that the control point for chlorophyll degradation in kiwifruit is upstream of the SGR protein. This control point could be associated with, for example, endogenous hormone levels, expression of transcription factors, or a SNP in the *SGR* promoter which affects transcription factor binding.

In many plants where stay-green genes have been described, for example capsicum and tomato, research has involved genetic linkage of the phenotype to candidate genes (Akhtar *et al.* 1999; Efrati *et al.* 2005). Genetic analysis to test the linkage of candidate genes to the trait in kiwifruit is complicated due to variation between chromosome counts of different kiwifruit species. The two species used in this study, which are the two kiwifruit species commonly grown and consumed, differ in ploidy, where *A. deliciosa* is hexaploid and *A. chinensis* is diploid. This makes an interspecific cross difficult and the resulting inheritance pattern complicated, even in the case of a single gene. *A. eriantha* is a green-fleshed kiwifruit species which is diploid, and has been crossed with yellow *A. chinensis*. Progeny of this cross segregated for green and yellow flesh colour with the majority of progeny being green. This may indicate that the stay-green kiwifruit phenotype is not inherited as a single recessive gene, whereas in many other species the stay-green phenotype is a single recessive gene (Armstead *et al.* 2006; Sato *et al.* 2007). The small and variable number of

seedlings per family limits the value of the data, and a further study of the study of green and yellow colour inheritance patterns in kiwifruit would be valuable.

4.7.1 Chapter summary

Transient infiltration of tobacco leaves with the kiwifruit *SGR1* and *SGR2* induced rapid and significant chlorophyll degradation. A more efficient method of studying the action of these genes in kiwifruit itself was not found. The *CLH* genes in kiwifruit are present but unlikely to be involved in the delay of chlorophyll degradation in green kiwifruit. The *SGR* genes are present and identical at the protein level, so it is likely that the genes produce functional proteins in both species, and indicates that the control point for chlorophyll degradation in kiwifruit is upstream of the chlorophyll degradation pathway. A possible control point for the chlorophyll degradation pathway could be differential transcription factor binding to *SGR* gene promoters between the two species which could be caused by a SNP, or there could also be differences in hormonal regulation of the chlorophyll degradation pathway. However, the gene inheritance studies showed that the green and yellow colour phenotype in kiwifruit is unlikely to be controlled by a single gene.

5. ENDOGENOUS CYTOKININ IN KIWIFRUIT

5.1 Introduction

Cytokinin has been implicated in the delay of senescence in many previous experiments, ranging from exogenous application to over-expression of *IPT*, the first committed step for cytokinin biosynthesis. Gene expression studies in Chapter Three showed that the expression of *IPT*, the key committed step for cytokinin biosynthesis, and *ZOG*, the enzyme for glucosylating cytokinin into a storage form, was high in green kiwifruit at 196 – 237 DAFB. In contrast, there was very little expression of *ZOG* in yellow fruit. There were significant pair-to-pair gene expression correlations between enzymes involved in cytokinin metabolism and chlorophyll degradation, suggesting another possible link between cytokinin metabolism and kiwifruit chlorophyll levels. There was also a significant positive correlation between *ZOG* and fruit flesh colour in the DA x CK population, which could indicate that there may be differences in cytokinin metabolism between these two kiwifruit species.

Several experiments have tested the effect of *N*-(2-chloro-4-pyridyl)-*N*'-phenylurea (CPPU) application on kiwifruit growth (Iwahori *et al.* 1988; Patterson *et al.* 1993; Antognozzi *et al.* 1996; Lewis *et al.* 1996a) as previously described in Section 1.14. Both *A. deliciosa* and *A. chinensis* fruit have been reported to have higher chlorophyll contents in the outer pericarp when treated with CPPU early in fruit development, consistent with the known effect of cytokinins on promoting the greening of plant tissue (Iwahori *et al.* 1988; Antognozzi *et al.* 1996). If cytokinin is key to lack of de-greening in *A. deliciosa*, then the application of CPPU at later stages could lead to delay of yellowing in *A. chinensis* fruit.

Analyses of endogenous cytokinins in developing fruit, such as orange, tomato and apple, have usually shown a peak of activity co-incident with cell division (Ozga and Reinecke 2003). However, in kiwifruit, while such a peak exists, high levels of cytokinin were also shown in *A. deliciosa* at harvest maturity (Lewis *et al.* 1996b). The cytokinin concentrations in fully mature *A. deliciosa* fruit and maturing *A. chinensis* fruit have not previously been measured. Whether this peak in *A. deliciosa* cytokinin concentration is

related to the maintenance of chlorophyll levels is also currently unknown. Therefore, a comparison of the endogenous cytokinin levels between *A. deliciosa* and *A. chinensis* is important.

In research reported in this chapter, an *IPT* gene is characterised in kiwifruit, the effect of CPPU on the de-greening of *A. chinensis* fruit is reported, and cytokinin levels are reported for *A. chinensis* and *A. deliciosa* during development.

5.2 *IPT* sequencing in kiwifruit

IPT is a multigene family in *Arabidopsis* containing nine members (Kakimoto 2001; Takei *et al.* 2001). Kiwifruit *IPT* genes were identified by BLAST match, and named for their best BLAST match in *Arabidopsis* (Figure 5.1). Primers to kiwifruit *IPT* EST 308872 were designed and gene expression was measured, as shown in Figure 3.9 and 3.10.

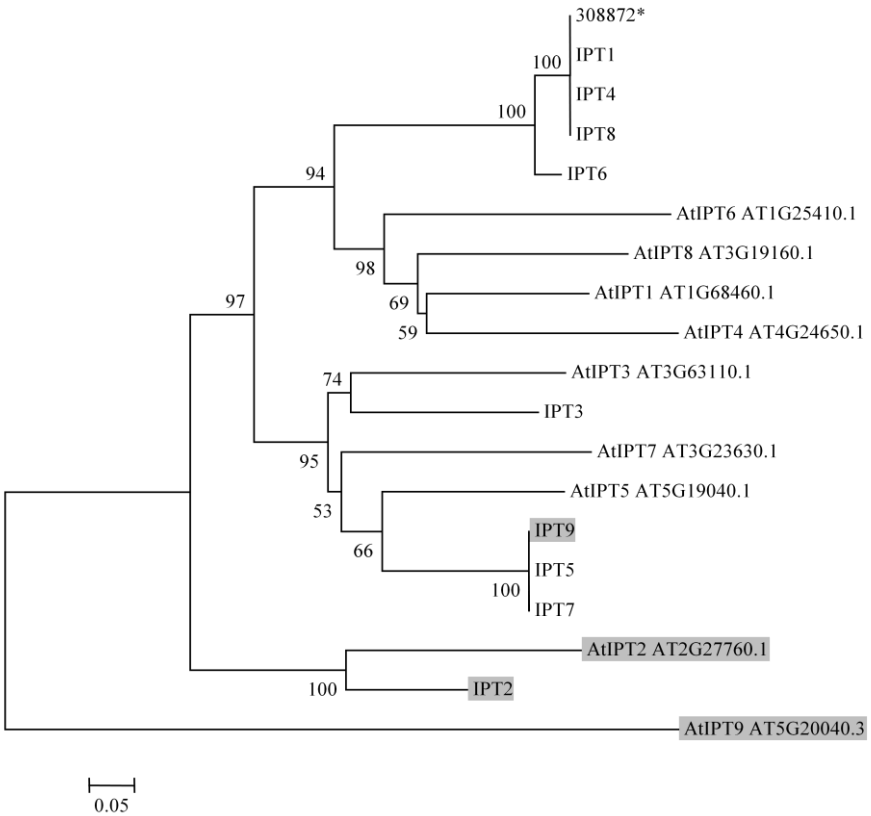

Figure 5.1. Phylogenetic tree of IPT. The unrooted phylogenetic tree of full length protein sequences from *Arabidopsis* and *A. chinensis* aligned using Clustal W. Branch support values from 100 bootstraps are indicated when higher than 50%. Shading indicates IPTs involved in *cis*-zeatin synthesis.

Following qRT-PCR analysis (Chapter Three), melt curve analysis was performed on all products of the qRT-PCR experiments, where all primer pairs, with the exception of *IPT*, produced one product. Analysis of the *IPT* qRT-PCR product showed two different melting temperatures, suggesting two products (Figure 5.2). These two products were only present in the *A. deliciosa* samples, and not the *A. chinensis* samples. This could be due to extra mutations within the product or extra gene copies in hexaploid *A. deliciosa* compared with diploid *A. chinensis*.

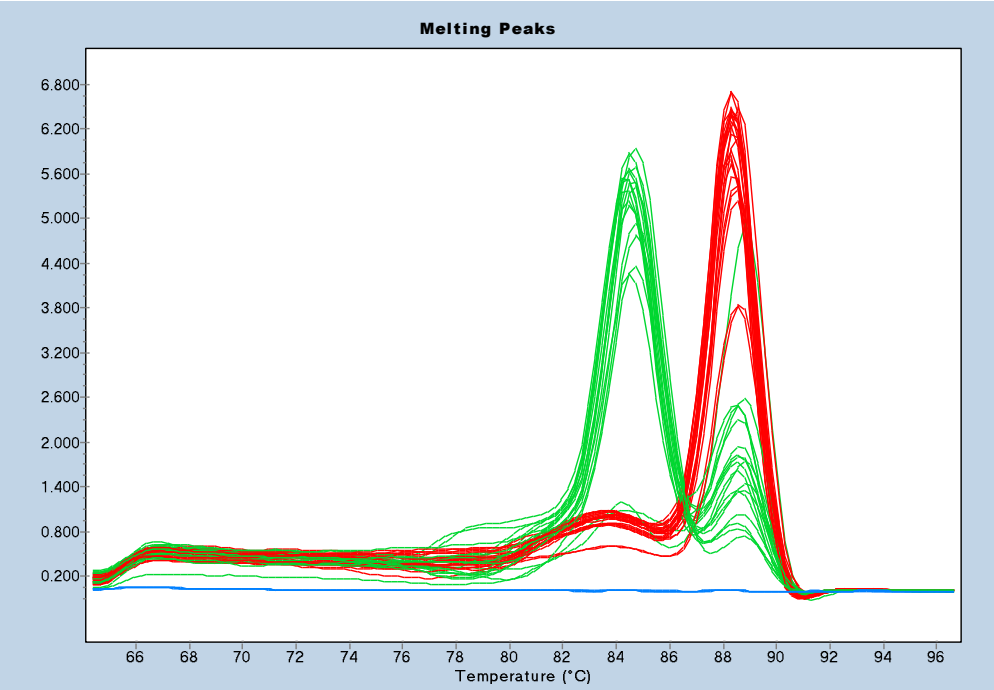

Figure 5.2. Melt curve analysis from qRT-PCR of *A. deliciosa* and *A. chinensis*. Analysis of the melting temperature of qRT-PCR products from *A. deliciosa* (green) and *A. chinensis* (red) was conducted using the LightCycler® 480 1.5.0 Software (Roche, Germany).

The qRT-PCR products from Figure 5.2 were sequenced to verify their identity as *IPT* genes (Figure 5.3). The products are similar, with the exception of a 36 base pair deletion in the one of the *IPT* products of *A. deliciosa*, designated IPTΔ. Attempts to design primers for the *IPT*- product alone were unsuccessful due to design constraints of the small variable region.

Figure 5.3. DNA sequence alignment of the qRT-PCR products from *A. deliciosa* and *A. chinensis*. The smaller qRT-PCR product (*IPTΔ*) from *A. deliciosa* was aligned with the genome scaffold BLAST match from *A. chinensis* and the *IPT* product from *A. chinensis*. Black shading with white letters and grey shading with black letters indicates 100% and 60% sequence identity, respectively.

The *IPTΔ* product was then translated into a full length protein to assess the possible effect of a 36 base pair deletion on the protein sequence (Figure 5.4). When translated into a theoretical protein, IPTΔ has a 12 amino acid deletion after amino acid 35 of the N-terminal. The deletion is not in a conserved region of the protein, as shown by lack of similarity in this region between the most similar IPTs from *Actinidia* and *Arabidopsis*.

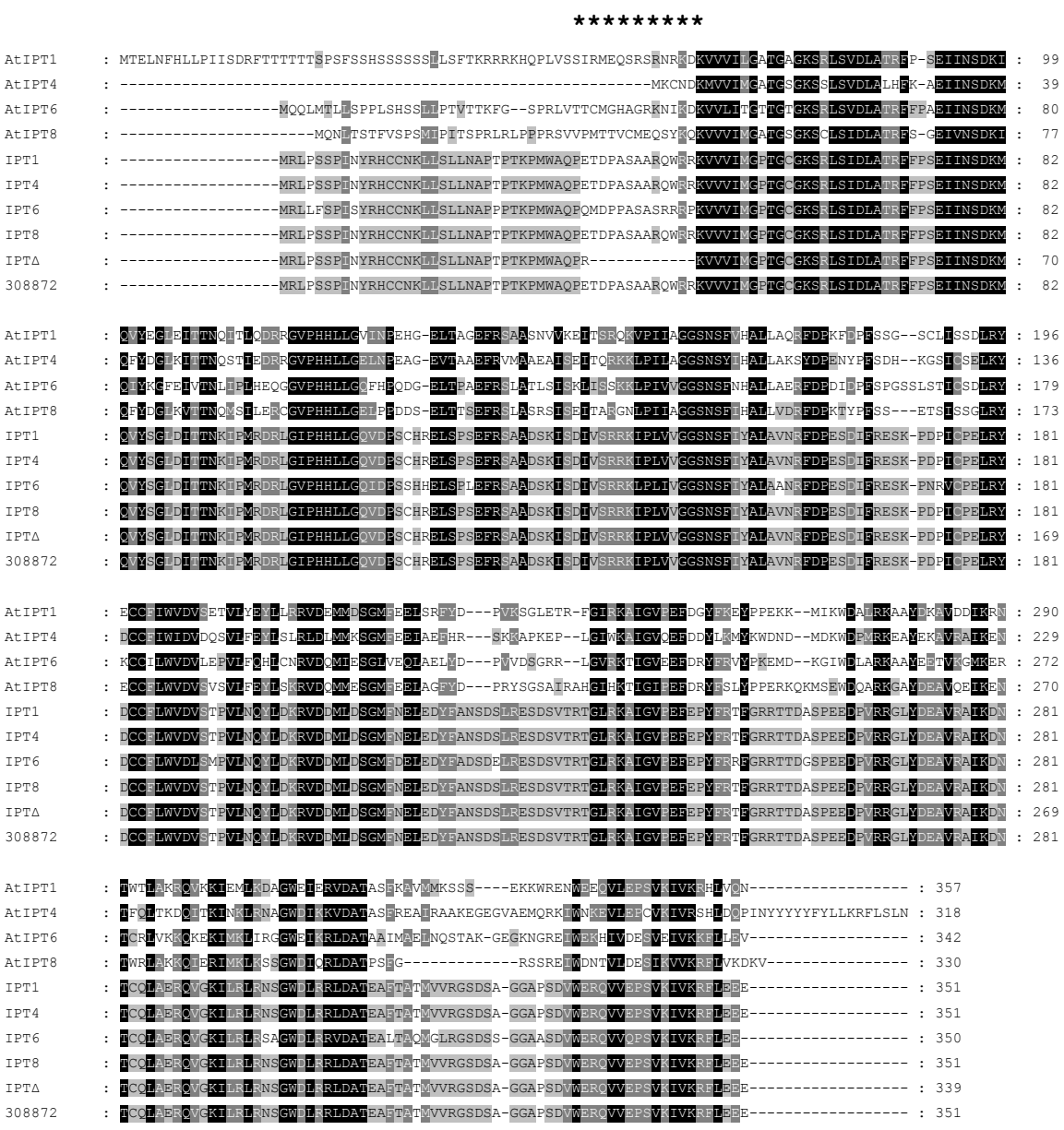

Figure 5.4. Protein sequence alignment of the theoretical IPT- protein with IPTs from *Actinidia* and *Arabidopsis*. The theoretical IPTΔ protein was aligned by Clustal W with IPT from *A. chinensis* (EST 308872) and IPTs from *Actinidia* and *Arabidopsis* (designated AtIPT). The site of an amino acid deletion in *A. deliciosa* is indicated by **. Black shading with white letters, grey shading with white letters and grey shading with black letters indicate 100%, 80% and 60% sequence identity, respectively.

5.3 Cytokinin application to *A. chinensis* fruit

The application of synthetic cytokinins has previously been reported to delay yellowing of *A. chinensis* fruit when applied at early stages of development (Iwahori *et al.* 1988). To investigate this in kiwifruit, CPPU was applied to yellow *A. chinensis* kiwifruit at 165 DAFB, during colour change (Figure 5.5). Two methods were used, dipping the fruit in CPPU, and wicking CPPU through the pedicel. Measurements of fruit weight and colour were then taken four weeks later, at 191 DAFB.

Figure 5.5. CPPU application experiment in *A. chinensis.* *A. chinensis* vines at 165 DAFB in the same block with either CPPU wicked fruit (pink), CPPU dipped fruit (blue) or control fruit (yellow) (a). Fruit were wicked through the pedicel, where CPPU was contained in an Eppendorf tube (b). Experiments using blue dye showed the translocation through the fruit vasculature *via* the wicking method (c).

Dye tracer experiments in Figure 5.5c showed that the dye was taken up into the fruit in the wicking treatment. However, these results showed that the majority of the treatment was being taken up into the inner pericarp of the fruit surrounding the core (Figure 5.5c). Measurements of the fruit characteristics are shown in Figure 5.6. There was no significant difference in weight or hue angle between the different treatments.

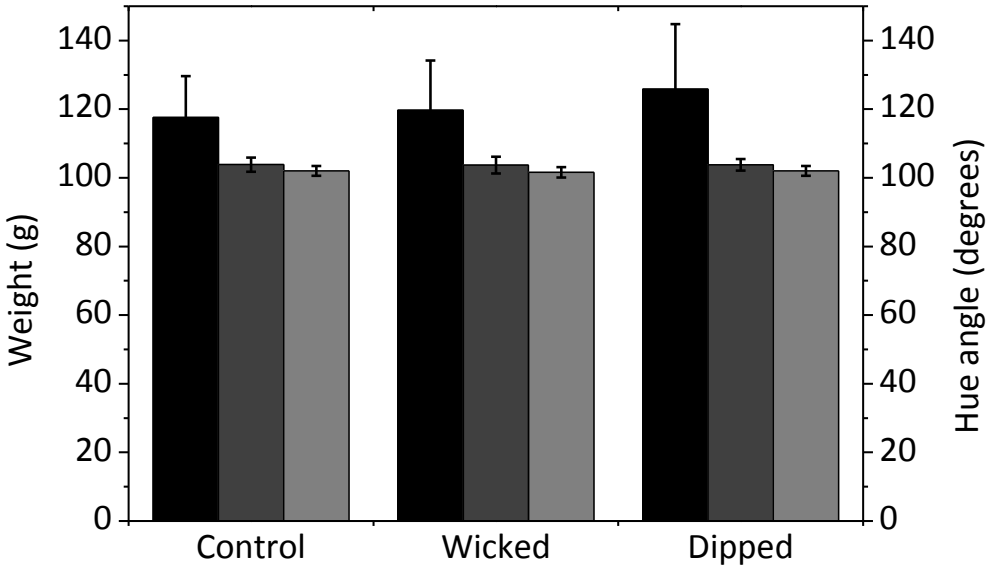

Figure 5.6. Fruit weight and hue angle of *A. chinensis* treated with CPPU. Measurements of fruit weight (black bars, left axis), hue angle at 1 mm (dark grey bars, right axis) and hue angle at 2 mm (light grey bars, right axis) for control, wicked, and dipped *A. chinensis* fruit.

5.4 Endogenous cytokinins in *A. deliciosa* and *A. chinensis*.

A comparison of the endogenous cytokinin content in the outer pericarp tissue in developing *A. chinensis* and *A. deliciosa* fruit was made. Advancement of liquid chromatography and mass spectrometry techniques has recently allowed very sensitive and accurate measurement of small quantities of compounds such as cytokinins from complex plant matrices which was previously very difficult (Novák *et al.* 2008). This technique was therefore employed to measure the endogenous cytokinin levels in *A. chinensis* and *A. deliciosa*. A known concentration of an internal standard was added to each sample during extraction. The ratio of labelled to unlabelled internal cytokinin standard was used to estimate the concentration of endogenous compound in the sample.

5.4.1 Measuring total and constituent cytokinin levels in kiwifruit using triple quadrupole HPLC-MS/MS

The endogenous cytokinins were measured in *A. deliciosa* and *A. chinensis* in both 2009 and 2010 (Figure 5.7). Extractions and preliminary measurements were performed in New Zealand by SMP, Dave Greenwood (University of Auckland, Plant & Food Research) and Janine Cooney (Plant & Food Research) (see Appendix Section 9.2). Ultimately, for a comprehensive analysis, cytokinin extraction and quantification measurements were performed at Trent University, Canada, by Neil Emery. The total cytokinin complement was very similar in green and yellow kiwifruit over both years.

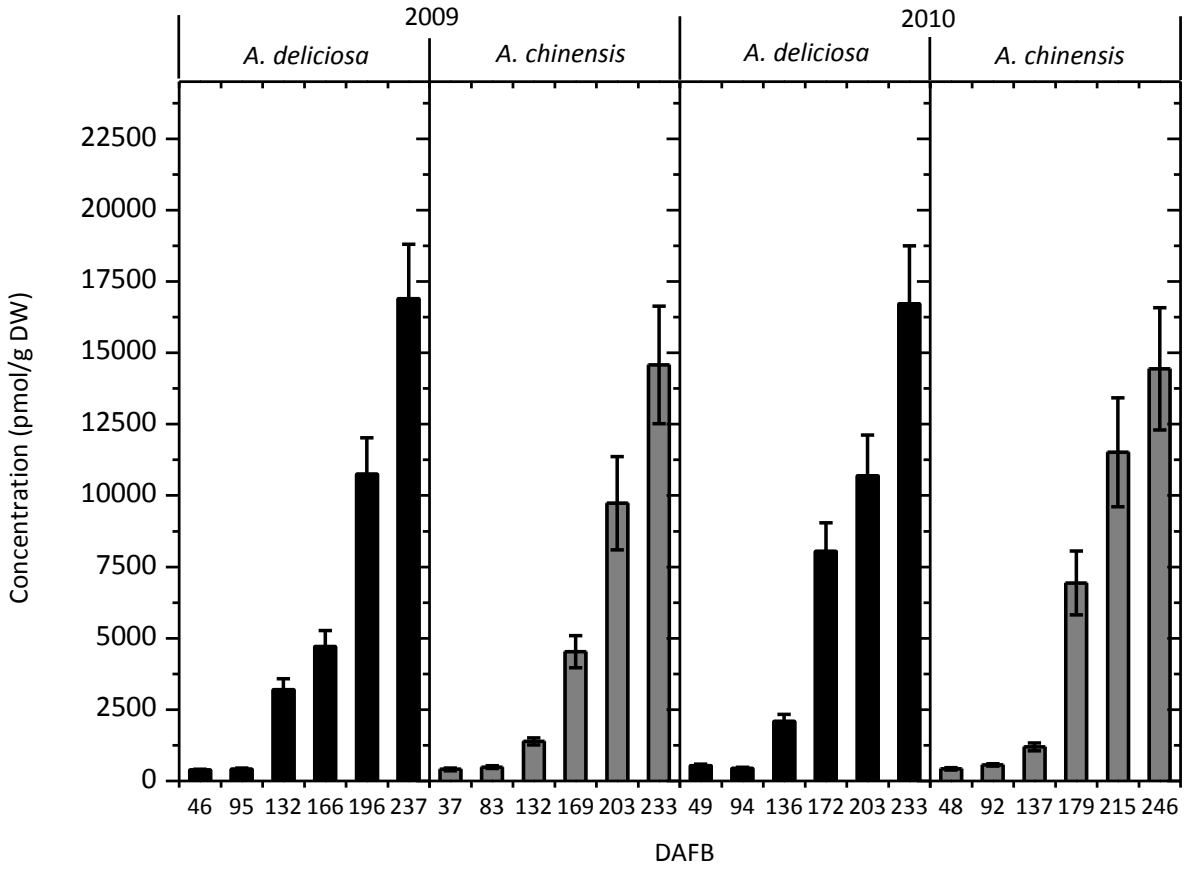

Figure 5.7. Total cytokinin concentration in *A. deliciosa* and *A. chinensis* in 2009 and 2010. *A. deliciosa* samples are shown as black bars, *A. chinensis* samples are shown as grey bars in 2009 (left) and 2010 (right). Error bars are standard error of technical replicates (n=3).

Although the total concentration of fruit cytokinin was similar between species, the nature of constituent cytokinins distinctly differed between species. The concentration of cytokinin nucleotides is presented in Figure 5.8. The nucleotide analysis did not differentiate between -triphosphates, -diphosphates and/or -monophosphates. Overall, tZNT reached the highest concentration of any of the cytokinins detected. DZNT and iPNT concentrations were also high, but at a concentration more than ten-fold lower, with very little cisZNT observed. The pattern of concentration of the free bases (Figure 5.9) is mirrored in the concentrations of the cytokinin ribosides (Figure 5.10), with the *trans*-

cytokinins at significantly greater levels than the dihydro- and the isopentenyl-cytokinins, and very low levels of the *cis*-cytokinins. tZROG and DZROG had the highest concentration of the *O*-glucoside cytokinins, reaching levels similar to those of tZ and tZR (Figure 5.11). The cytokinin 9-glucosides, tZ9G and DZ9G were only detected at low levels.

The cytokinin nucleotide, tZNT, reached very high concentrations by the end of fruit maturity in both species, at up to over 23,500 pmol/g DW (Figure 5.8). DZNT showed a similar pattern but at a ten-fold lower concentration. The concentration of iPNT increased over fruit development, up until the last two samples, where the concentration increased in green fruit and decreased in yellow fruit. This trend was more marked in 2009 than in 2010. At this fruit stage, yellow fruit had de-greened and green fruit was beginning to de-green in 2010, as measured by hue angle in Figure 3.4. In most samples, cisZNT was only present in the early stages of fruit development, with the exception of the *A. deliciosa* 233 DAFB sample.

The concentration of the free base cytokinin tZ, increased over development, and was highest in yellow fruit in 2009 at over 1000 pmol/g DW (Figure 5.9). However, the levels of tZ in green and yellow fruit were similar in 2010. DZ was detected at a low concentration, around 20 pmol/g DW. The concentration of cytokinin ribosides tZR and DZR also increased over maturity (Figure 5.10). The concentration of tZR was highest in *A. deliciosa* towards fruit maturity in 2009. However, in 2010, when the fruit were beginning to de-green, the tZR concentration was not as high. Despite this, the concentration of tZR was much higher in *A. deliciosa* fruit at 196 DAFB compared with 203 DAFB in *A. chinensis*, a significant developmental stage for colour change. This pattern was very similar for DZR, but at a much lower concentration. The level of iPR was high in yellow fruit in 2009 at 131 and 169 DAFB. However, this pattern was not seen in the same species in 2010.

DZROG and tZROG concentrations increased towards fruit maturity in *A. deliciosa* to very high levels (Figure 5.11). In contrast, *A. chinensis* fruit contained very little DZROG and tZROG. tZOG followed this same trend, but at concentrations ten-fold lower than DZROG and tZROG. tZ9G increased over fruit development in *A. chinensis* only.

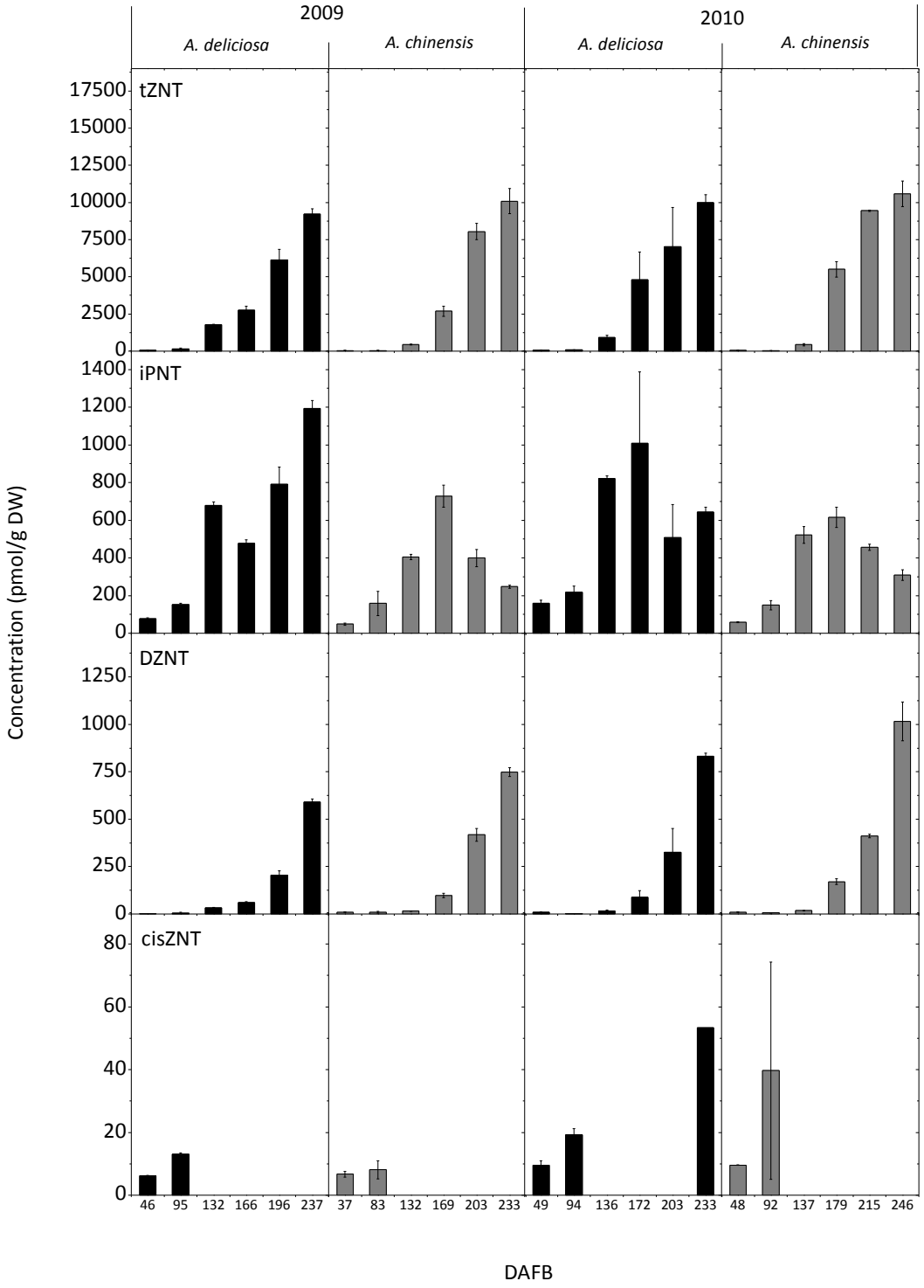

Figure 5.8. Concentration of cytokinin nucleotides in *A. deliciosa* and *A. chinensis* in 2009 and 2010. *A. deliciosa* samples are shown as black bars, *A. chinensis* samples are shown as grey bars in 2009 (left) and 2010 (right). Error bars are standard error of technical replicates (n=3).

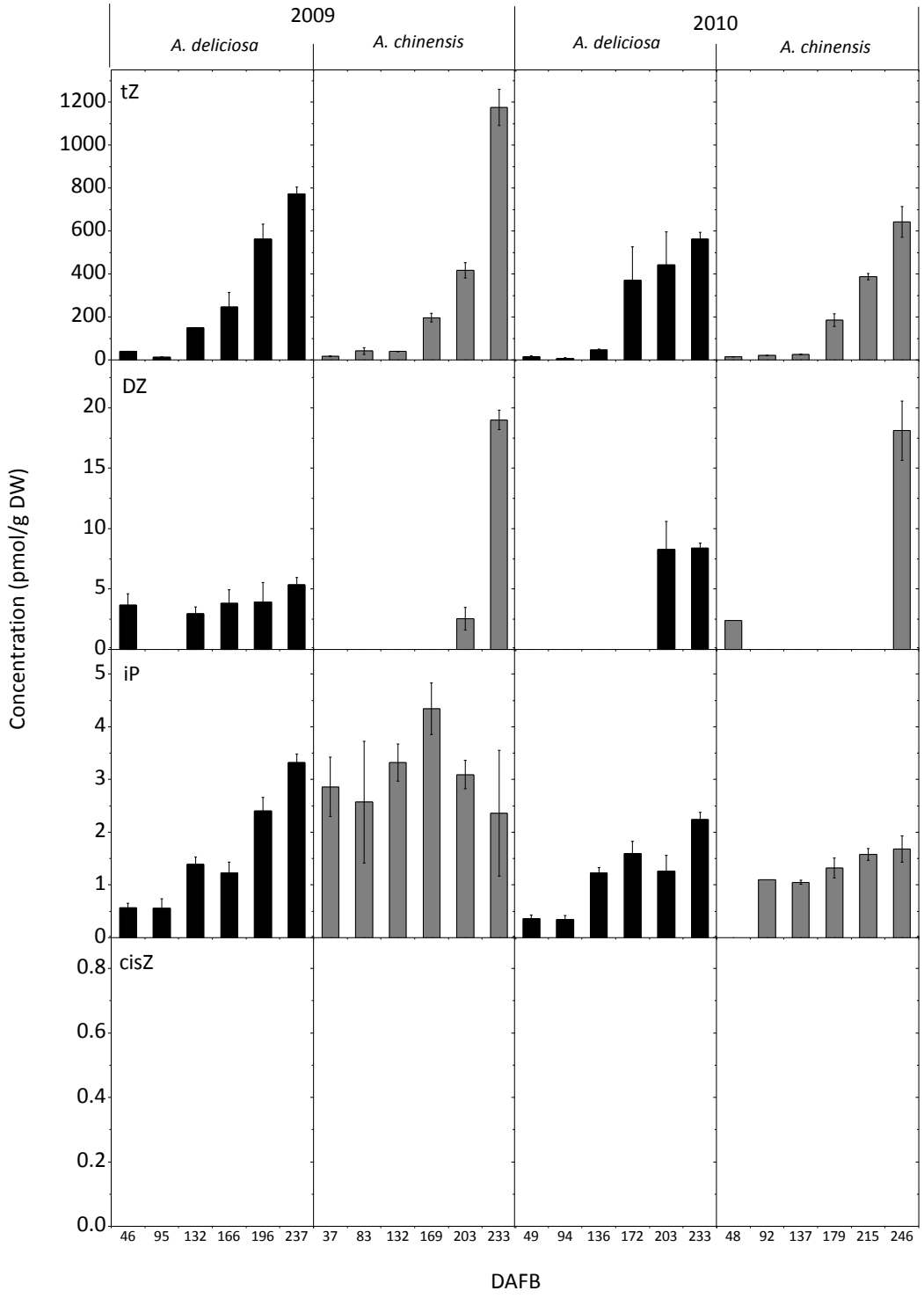

Figure 5.9. Concentration of cytokinin free bases in *A. deliciosa* and *A. chinensis* in 2009 and 2010. *A. deliciosa* samples are shown as black bars, *A. chinensis* samples are shown as grey bars in 2009 (left) and 2010 (right). Error bars are standard error of technical replicates (n=3).

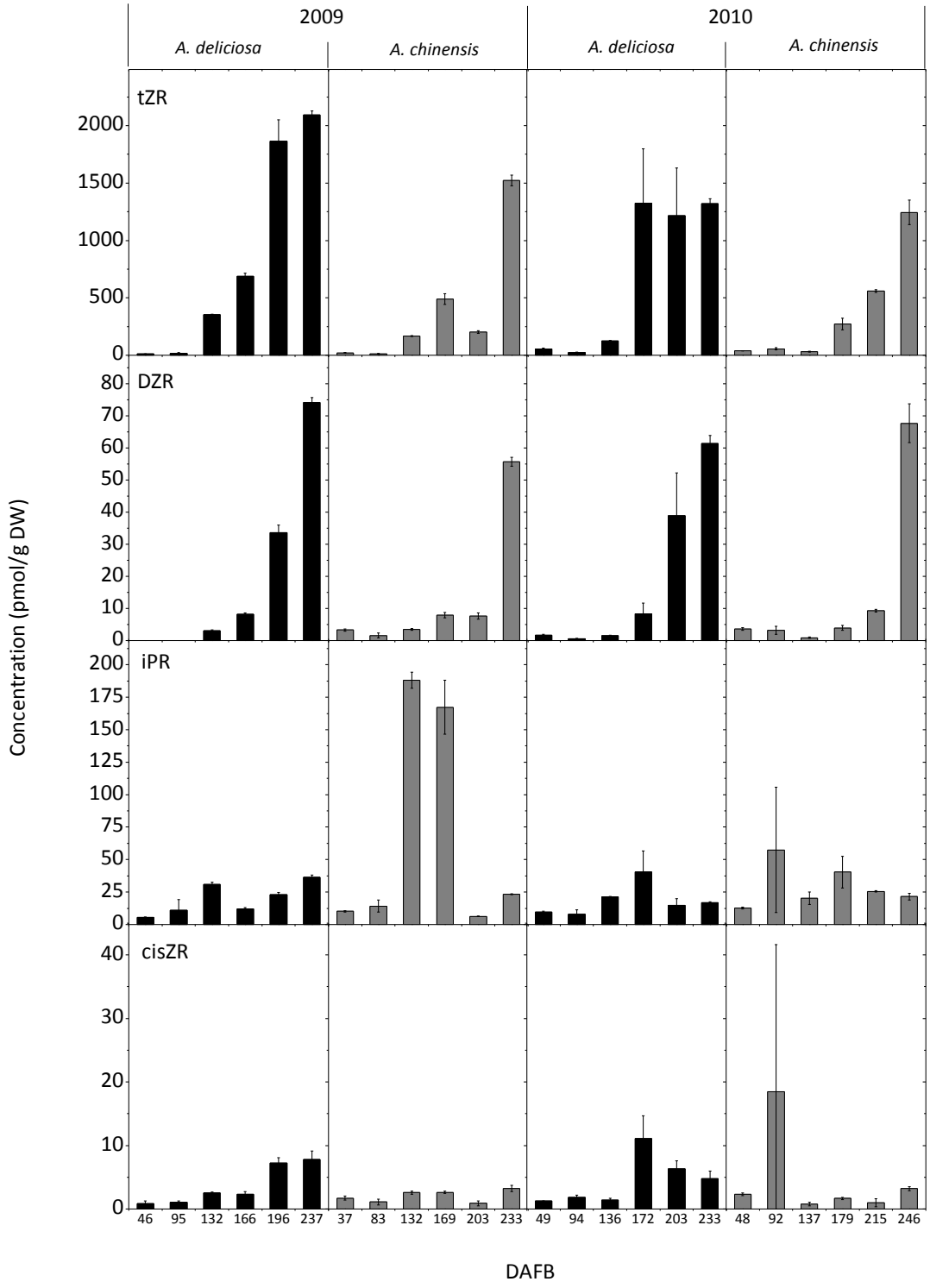

Figure 5.10. Concentration of cytokinin ribosides in *A. deliciosa* and *A. chinensis* in 2009 and 2010. *A. deliciosa* samples are shown as black bars, *A. chinensis* samples are shown as grey bars in 2009 (left) and 2010 (right). Error bars are standard error of technical replicates (n=3).

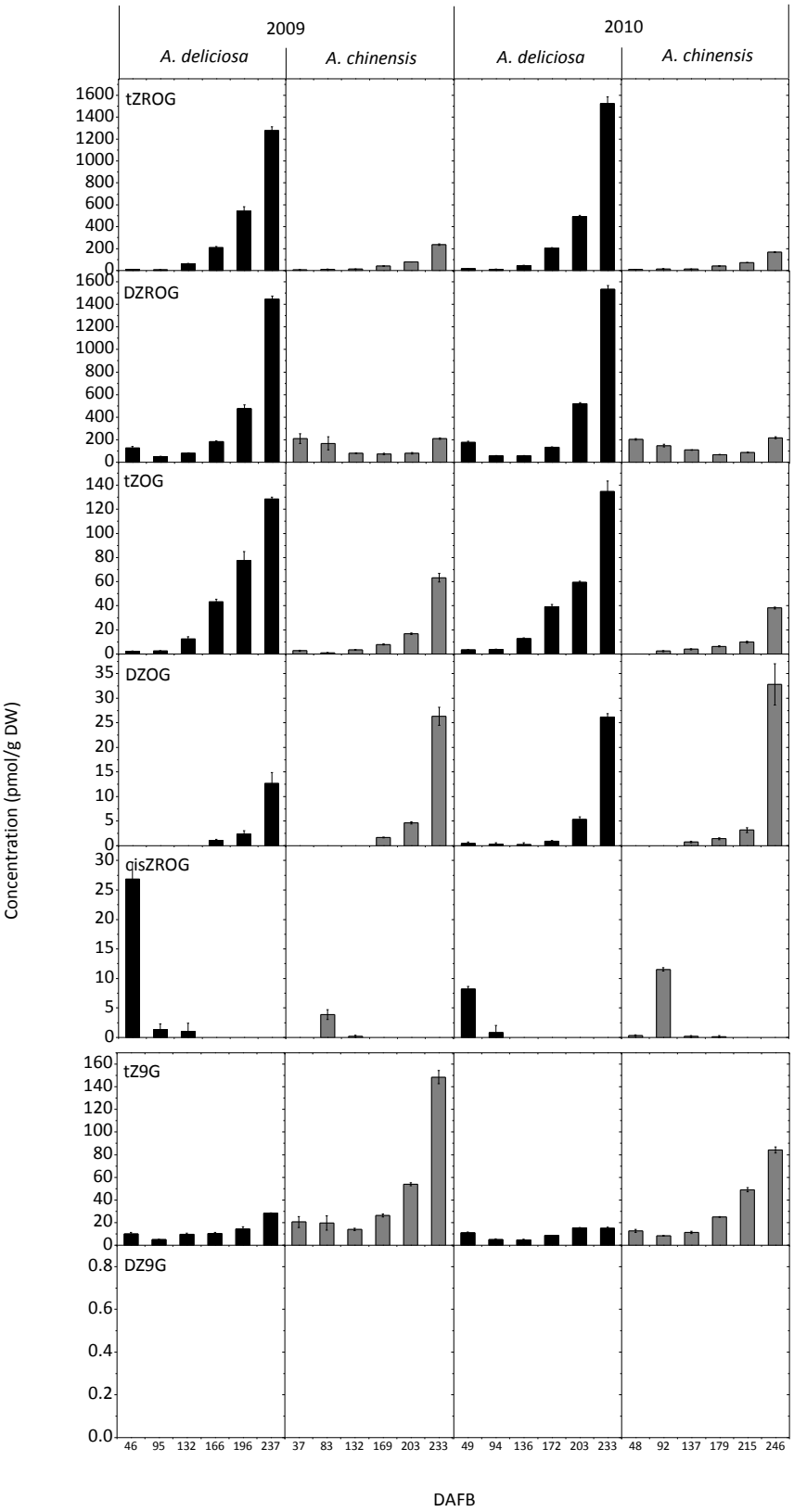

Figure 5.11. Concentration of cytokinin glucosides in *A. deliciosa* and *A. chinensis* in 2009 and 2010. *A. deliciosa* samples are shown as black bars, *A. chinensis* samples are shown as grey bars in 2009 (left) and 2010 (right). Error bars are standard error of technical replicates (n=3).

5.5 Discussion

IPT is the key committed step for plant cytokinin biosynthesis. In *A. deliciosa* fruit there were two *IPT* qRT-PCR products, with one containing a 36 base pair deletion. When translated into a theoretical protein, the resulting protein contained a deletion of 12 amino acids near the N-terminus of the protein. This deletion was not located in a conserved region of the protein, and didn't produce a frame shift. Although not in a conserved domain, the theoretical protein could be conformationally constrained by the short N-terminus. Further experiments are required to determine whether the IPTΔ protein from *A. deliciosa* is a different *IPT* gene homoeologue or a different allele, and whether the resulting protein is functional. Over-expression of *IPT* in *A. chinensis* could confirm that endogenous cytokinin is key to the delay of yellowing. However, this experimental work was not possible due to time restraints, as kiwifruit flowering occurs following a minimum of three years of growth.

CPPU has been shown to act like an active cytokinin (Takahashi *et al.* 1978), and the application of CPPU has been shown to increase kiwifruit size, despite decreasing the levels of endogenous cytokinins in a proposed feedback mechanism (Lewis *et al.* 1996a). The application of CPPU to kiwifruit has also been shown to increase the greening of outer pericarp tissue in both *A. chinensis* and *A. deliciosa* when applied at early stages of fruit development (Iwahori *et al.* 1988; Patterson *et al.* 1993). However, in the current study, the application of CPPU at 165 DAFB was found to have no effect on the colour of the fruit. This could be due to initiation of the irreversible de-greening process prior to CPPU production. Further experiments are required to ascertain the point of 'no return' for de-greening in *A. chinensis*.

Measuring cytokinin levels is difficult due to their relatively low levels among the bulk of other substances in plant extracts (Dobrev and Kamínek 2002; Novák *et al.* 2008). Because of problems with standards and quantification using the equipment available at Plant & Food Research, samples were sent to the laboratory of Professor Neil Emery at Trent University, Canada, for triple quadrupole LC-MS/MS analysis. This allowed a more thorough measurement of constituent cytokinins, and revealed interesting trends in green and yellow kiwifruit. Cytokinin activity is regulated by de novo synthesis, activation,

conjugation and degradation (Kudo *et al.* 2010). Structural variations of cytokinin side chains confer specificity of interactions with the cytokinin-receptors (Sakakibara 2006). Cytokinin has a co-ordinated function as both a long distance messenger and a local signal, although the physiological differentiation and the mechanisms of the dual signalling system have not been elucidated (Sakakibara 2006).

In general, most patterns were similar between *A. deliciosa* and *A. chinensis*, but with some differences in metabolism. The levels of cytokinin in both kiwifruit species were surprising, both in terms of the quantity and developmental pattern: for example very high levels and peaking at maturity, rather than during cell division, when compared with tomato (Bohner and Bangerth 1988). There were high levels of *IPT* expression in *A. deliciosa* compared with low expression in *A. chinensis* during fruit maturity (Figure 3.9 and 3.10). However, the concentration of cytokinin nucleotides, the product of the IPT step, was similar in both species. tZNT had the highest concentration of the cytokinin nucleotides. However, there were differences in the iPNT concentration between kiwifruit species, which increased over fruit development, until the last two samples, where the concentration increased in green fruit and decreased in yellow fruit. This trend was more marked in 2009 than in 2010, where yellow fruit had de-greened, and green fruit was beginning to de-green in 2010, as measured by hue angle in Figure 3.4. This suggests, also, that cytokinin biosynthesis may be differentially regulated in kiwifruit compared with other fruit. A possible reason for this could be that the expression of another *IPT* gene family member was responsible for the production of excess nucleotides and free bases in yellow kiwifruit.

The pattern of concentration of the free bases is mirrored in the concentrations of the cytokinin ribosides, with the *trans*-cytokinins at greater levels than the dihydro- and the isopentenyl-cytokinins. A similar pattern was seen for the cytokinin ribosides. The concentration of tZR was highest in *A. deliciosa* towards fruit maturity in 2009. However, at 215 DAFB in 2010, when the fruit were beginning to de-green, the tZR concentration was not as high. The excess tZR appears to be transformed to tZROG which was also much higher in green. One hypothesis is that *A. deliciosa* regulates cytokinin activity by *O*-glucosylation, with the very high tZR activating the glucosylation process (Figure 5.12). This is consistent with gene expression results in Figure 3.9, 3.10 and 3.15, where *ZOG* was more highly expressed in maturing green fruit.

In contrast, *A. chinensis* fruit contained very little tZROG and DZROG. Yellow kiwifruit may not have such a large requirement for *O*-glucosylation because of observed lower tZR concentrations, especially at later stages compared with green fruit. In *A. chinensis*, there may be down-regulation of cytokinin biosynthesis by lowering production of early pathway iPNT, which is consistent with lower *IPT* gene expression in yellow fruit compared with green fruit (Figure 3.9, and 3.10). Both species contained a large pool of tZNT, so a critical difference might be at adenosine kinase which phosphorylates tZR to tZNT (Moffatt *et al.* 2000). If this was occurring at a greater rate in yellow fruit (Figure 5.12), then the *O*-glucosyltransferases would only have excess tZR levels to conjugate in green kiwifruit. Over-expression of *IPT* coupled to a senescence-dependent promoter suppressed drought-induced leaf senescence, and led to increased levels of tZ, and glucosylated forms of cytokinin in tobacco (Rivero *et al.* 2007). Increased active and glucosylated cytokinin levels, with over-expression of *IPT* coupled to a senescence-associated promoter, was also seen in cassava (Zhang *et al.* 2010). However, both species had high levels of tZ, the active free base.

In addition, yellow fruit could have a feedback loop which down-regulates the fruit's own synthesis, leading to lower iPNT levels. This could lead to the high tZ levels observed in yellow fruit, due to the action of LOG, the enzyme responsible for the one-step conversion of cytokinin nucleotides to free bases. Conversely, green fruit could be unable to down-regulate synthesis, leading to the need for *O*-glucosylation. Alternatively, the loss of a cytokinin receptor could lead to the inability to sense high cytokinin levels in green fruit, leading to increased synthesis and *O*-glucosylation.

There were only trace concentrations of *cis*-cytokinins in both *A. chinensis* and *A. deliciosa*. This is consistent with previous reports of *trans*-cytokinins being the major and active form of cytokinin in eudicots (Gajdošová *et al.* 2011). The constituent cytokinins were found to be the same species observed at similar concentrations to previous work by Lewis *et al.* (1996a) in *A. deliciosa* outer pericarp tissue.

Cytokinin responses can be regulated by changes in the expression of components for the biosynthetic and metabolic pathways and components for cytokinin signalling (Argueso *et al.* 2010). Cytokinin receptor research has revealed that the three AHKs in *Arabidopsis* each have different affinities for different forms of cytokinin (Higuchi *et al.* 2004;

Nishimura *et al.* 2004; Riefler *et al.* 2006). Ligand specificity studies of the AHK3 receptor indicated an affinity for tZ > ZR > DZ > iP > cZ in *Arabidopsis*, and AHK3 is the cytokinin receptor implicated in the delay of senescence in leaves (Kim *et al.* 2006; Riefler *et al.* 2006). However, cytokinin receptors have not yet been extensively studied in fruit tissue. It is possible that there are fruit-specific cytokinin receptors that have different affinities for the different forms of cytokinin, or that there is differential expression of receptors in fruit tissue. This could be due to differential expression of these receptors in green and yellow fruit, or gene homeologues in hexaploid *A. deliciosa* compared with diploid *A. chinensis*.

Previous research has indicated that cytokinin protects the cell membranes and the photosynthetic machinery from oxidative damage during delay of senescence, by reducing levels of reactive oxidant species and enhancing the activity of antioxidant enzymes (Zavaleta-Mancera *et al.* 2007). Thus high cytokinin levels should lead to the delay of yellowing. It is possible that despite its high cytokinin levels, yellow fruit may still not have enough cytokinin to delay de-greening, compared with green fruit. Similarly, another process such as ethylene-induced ripening or signalling due to levels of hydrogen peroxide or sugars could overcome the high cytokinin levels in yellow fruit but not green fruit.

5.5.1 Chapter summary

Both green and yellow kiwifruit have unusually high levels of cytokinin towards maturity. However, there were major differences in the metabolism of cytokinin in mature fruit between *A. chinensis* and *A. deliciosa*. These differences are consistent with observations from the gene expression work in Chapter Three. Because structural variations of cytokinins affect their interaction with cytokinin receptors, cytokinin signalling will be affected. Further work is required to ascertain whether these differences in cytokinin levels can affect flesh colour.

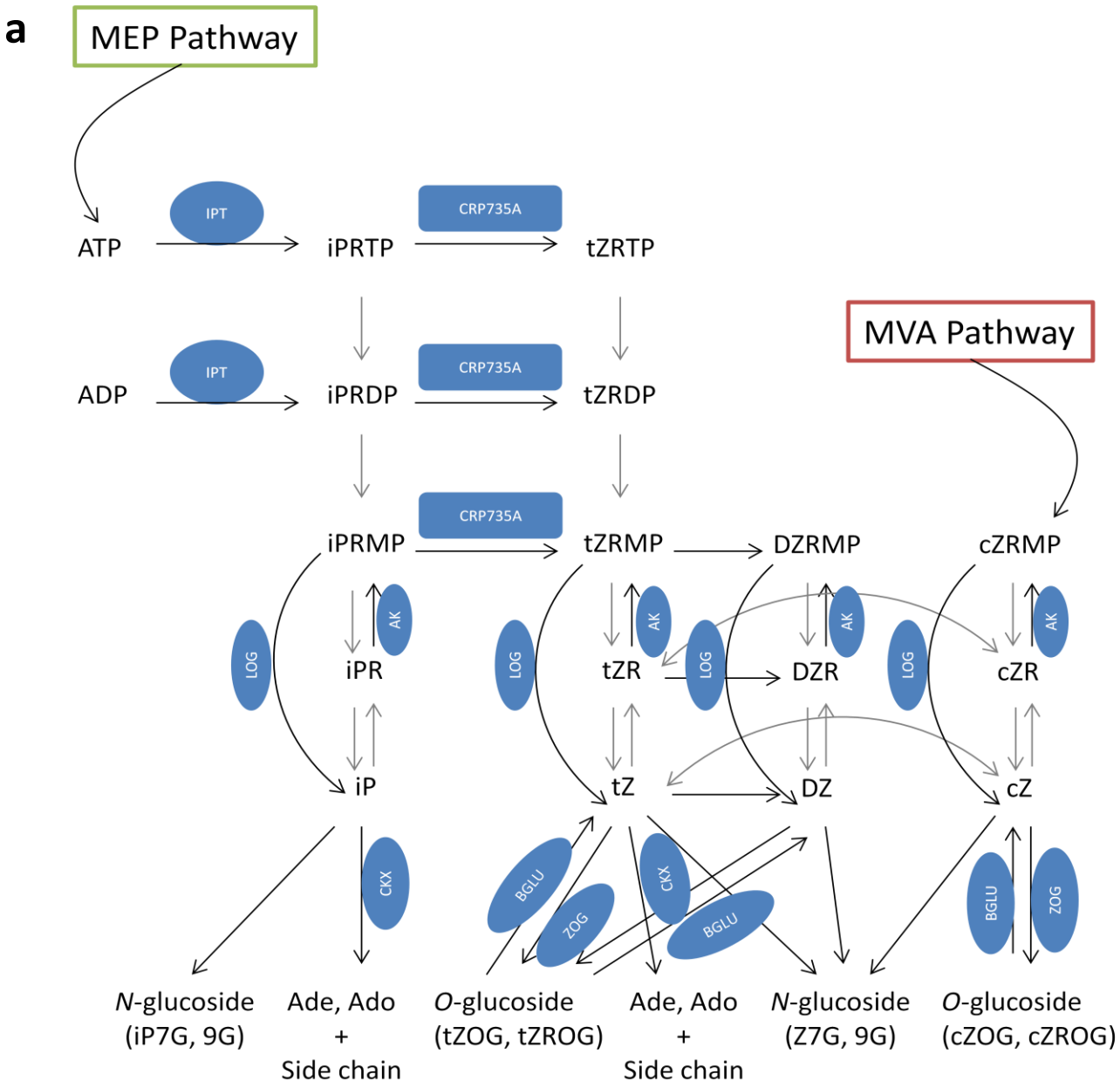

Figure 5.12. Cytokinin biosynthesis and homeostasis. The cytokinin metabolic pathway (a). iP and tZ originate from the methylerythritol phosphate (MEP) pathway, *cis*-Z originates from the mevalonate (MVA) pathway. IPTs utilise ATP or ADP to form iPRTP and iPRDP, respectively. The nucleotides are converted into tZ-nucleotides by CYP735A and iPR is phosphorylated by AK. iP, tZ, and the free bases can be catabolised by CKX to Ade or Ado. tZ can be reversibly converted to the *O*-glucoside by ZOG and BGLU. Free bases also can be converted to the *N*-glucoside by cytokinin *N*-glucosyltransferase. LOG has recently been identified which directly catalyses nucleotides to free bases. cZ and tZ can be interconverted by a yet unidentified zeatin *cis-trans* isomerase. Legend continues on next page.

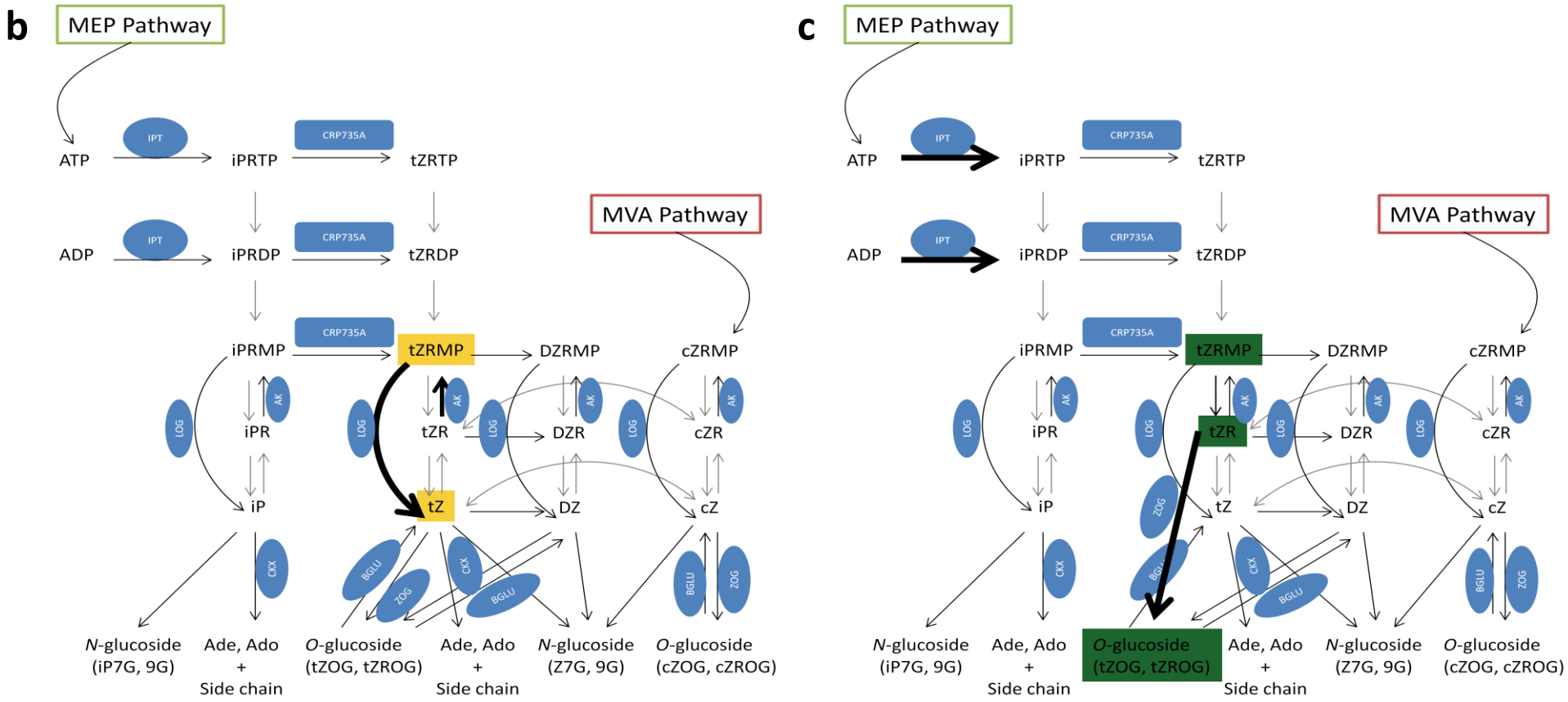

Figure 5.12. Cytokinin biosynthesis and homeostasis, continued.

A model for yellow kiwifruit (b) and green kiwifruit (c) is included. The width of the arrows indicates the strength of metabolic flow, and grey arrows show yet unidentified enzymes. Adapted from Sakakibara (2006) and Kamada-Nobusada and Sakakibara (2009).

6. FUNCTIONAL ANALYSIS OF CANDIDATE GENE PROMOTERS

6.1 Introduction

Chlorophyll degradation during fruit development is a temporally coordinated process central to fruit maturation. It is highly likely that de-greening is repressed in young fruit and then activated in mature fruit *via* a regulatory network (Balazadeh *et al.* 2008). Transcription factors have been shown to play a central role in these networks, regulating gene expression by binding *cis*-elements in the 5′ upstream regulatory regions of target genes, resulting in their activation or suppression (Balazadeh *et al.* 2008). Cytokinins may well be intrinsic to this network, involved at many levels from ligand/receptor to nuclear activation.

To investigate the link between high cytokinin levels in maturing fruit, observed in Chapter Five, and chlorophyll de-greening, transient assays were performed on two promoters from genes involved in the chlorophyll degradation pathway, *SGR* and *PAO*. The *RBCS* promoter was also included as a representative of genes required for the photosynthetic apparatus. As described in Chapter One, cytokinin is perceived *via* a phosphorelay, which leads to the activation of cytokinin response regulators, the ARRs. The Type-A ARRs have short C-terminal domains and are transcriptionally upregulated by cytokinin treatment and are negative regulators of cytokinin signalling. The Type-B ARRs contain DNA binding and transactivating domains at the C-terminus that positively regulate transcription of cytokinin-activated targets, including the Type-A *ARRs* (To and Kieber 2008). In this chapter, qRT-PCR was used to measure expression of *ARRs* in kiwifruit over fruit development. The interaction of the ARRs with three promoters cloned from *A. chinensis*, *SGR*, *PAO* and *RBCS* was assayed, along with other well-characterised transcription factors.

6.2 Selection of candidate *Arabidopsis* response regulator (ARR) genes in kiwifruit

A phylogenetic tree of kiwifruit and *Arabidopsis* ARRs is presented in Figure 6.1. Nine putative ARR proteins, translated from the Plant & Food Research EST database, showed high sequence homology to the 22 *Arabidopsis* ARRs. Kiwifruit ARR2, 11, 12a and 12b cluster in the Type-A *Arabidopsis* clade, and kiwifruit ARR6, 9 and 17 cluster in the Type-B *Arabidopsis* clade. Kiwifruit ARR4 and 13 cluster in the Type-A clade, but are not closely related.

6.3 Expression of *ARR* transcription factor genes in kiwifruit

Oligonucleotide primers were designed using the optimisation criteria and measurements of primer efficiency outlined in Chapter Two, and tested by end point PCR to ensure identity with kiwifruit source sequence and identity between *A. chinensis* and *A. deliciosa*. The levels of transcripts encoding the *ARR* genes were compared by qRT-PCR between green *A. deliciosa* and yellow *A. chinensis* fruit in cDNA from the 2010 fruit developmental series described in Chapter Two.

The expression of *ARR* genes was measured by qRT-PCR in *A. deliciosa* and *A. chinensis* in 2010 (Figure 6.2). Most of the *ARRs* had similar expression in green and yellow fruit in 2010. *ARR 6* and *9* showed higher expression in green fruit at the beginning of development, but the expression was similar in green and yellow fruit later in development. *ARR17* expression increased over fruit development in green fruit, with little expression in yellow fruit. The expression of *ARR 2, 11* and *12a* was very similar in green and yellow kiwifruit. *ARR12b* and *ARR13* had increased expression at maturity in green fruit, which was starting to de-green at this stage (see Chapter Three, Figure 3.2).

Plasmid DNA was not available for *ARR4* and *13* as they were ESTs from deep sequencing. However, full length versions of five of the remaining seven kiwifruit *ARRs* were cloned into *pHEX2S* for transient assays.

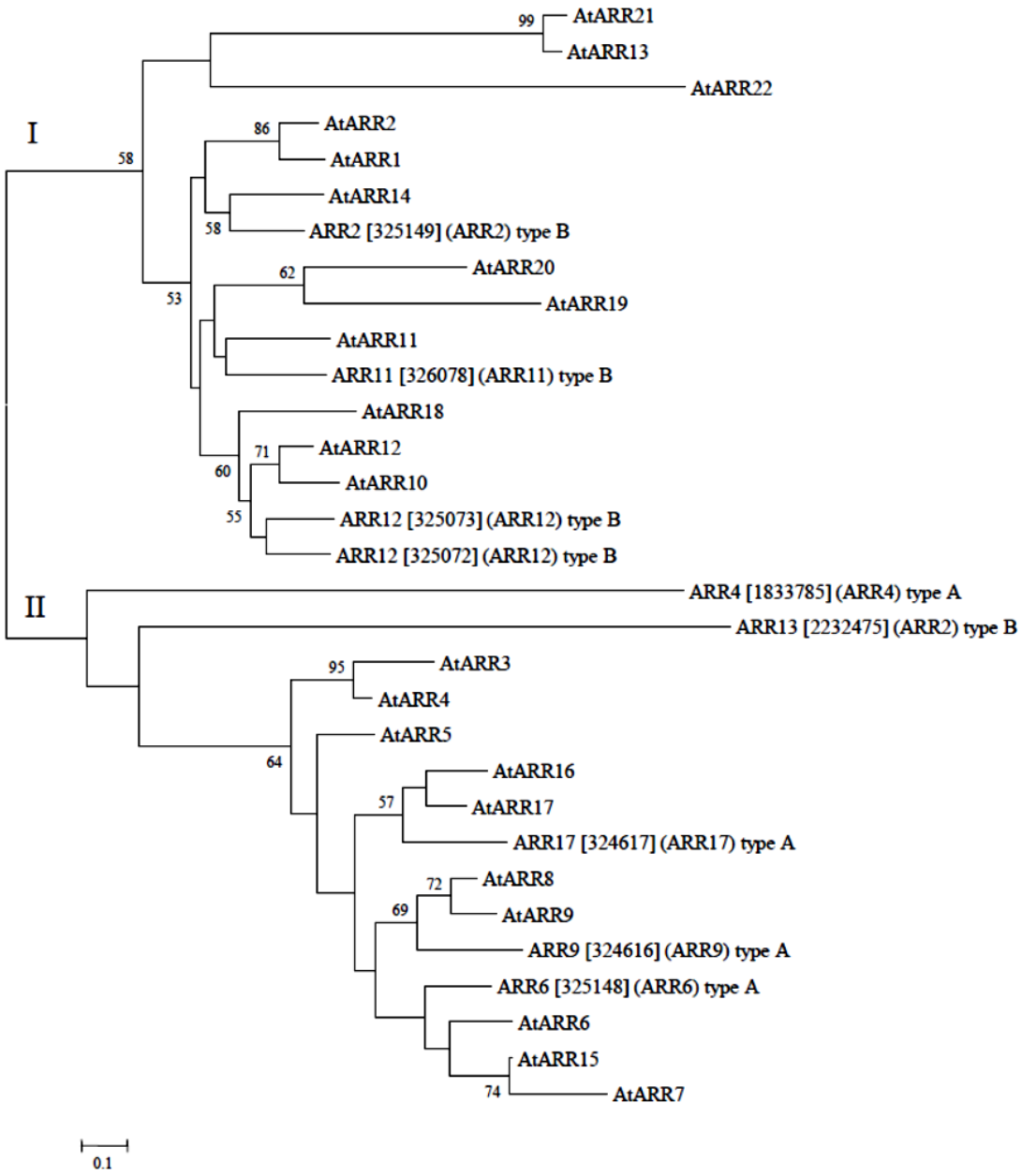

Figure 6.1. Phylogenetic tree of *Actinidia* and *Arabidopsis* ARRs. The unrooted phylogenetic tree of full length protein sequences aligned using Clustal W. Branch support values from 100 bootstraps are indicated when higher than 50%. Two clades (I and II) are distinguished. *Arabidopsis* MIPS designation numbers are as in Heyl and Schmülling (2003).

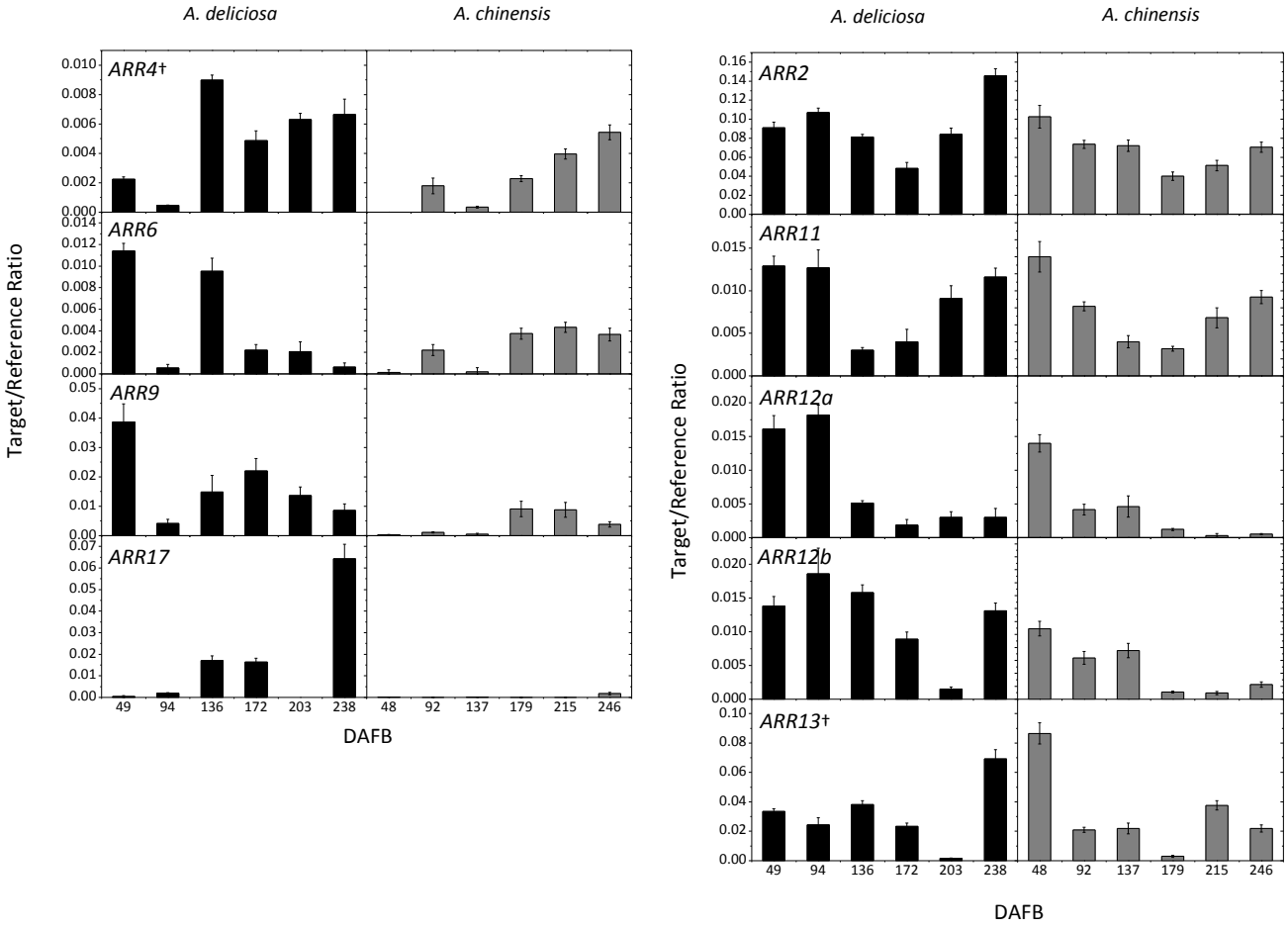

Figure 6.2. Expression of ARRs in *A. chinensis* and *A. deliciosa* fruit over development in 2010. Expression of kiwifruit Type-A (left) and Type-B (right) ARRs in *A. deliciosa* (left panels, black bars) and *A. chinensis* (right panels, grey bars) over fruit development (days after full bloom; DAFB), measured as a target/reference ratio. *ARR4* and *ARR13* are ESTs from deep sequencing (marked by †). Error bars indicate standard error (n=4).

6.4 *In silico* analysis of *cis*-acting elements

Transcription factors recognise specific *cis*-regulatory sequences that are generally located in proximity to the gene coding sequence on the region referred to as the promoter. An *in silico* analysis of the 1 kb upstream promoter region of *RBCS*, *PAO* and *SGR* was performed using the PLACE database (Plant *cis*-acting regulatory elements – http://www.dna.affrc.go.jp/PLACE/signalscan.html) (Higo *et al.* 1999). Priority was given to *cis*-acting elements having a potential association with chlorophyll, photosynthesis, or light regulation. The *SGR* promoter was isolated from a previously created gene walk library (Pilkington, 2007, Unpublished) and primers were designed for the *RBCS* and *PAO* promoters from the Plant & Food Research *Actinidia* genome database of scaffolds. Promoter sequences with annotated TF binding motifs are shown for *RBCS* (Figure 6.3), *PAO* (Figure 6.4), and *SGR* (Figure 6.5). The complete PLACE analysis is shown in Appendix 185.

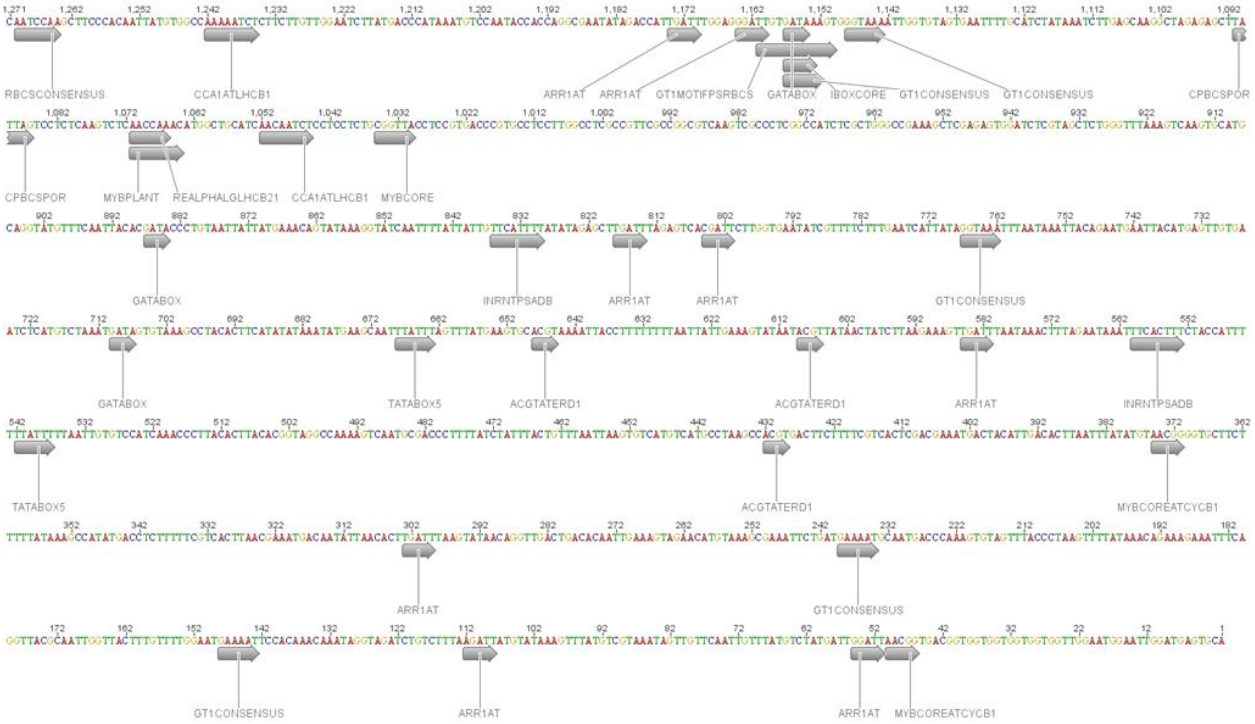

Figure 6.3. *RBCS* promoter. The 5′ upstream region of *Actinidia RBCS*. Bases are marked in the 3′ to 5′ direction with the A of the ATG as base 1. The motifs associated with light regulation are annotated using Geneious 5.4, available from http://www.geneious.com (Drummond *et al.* 2011).

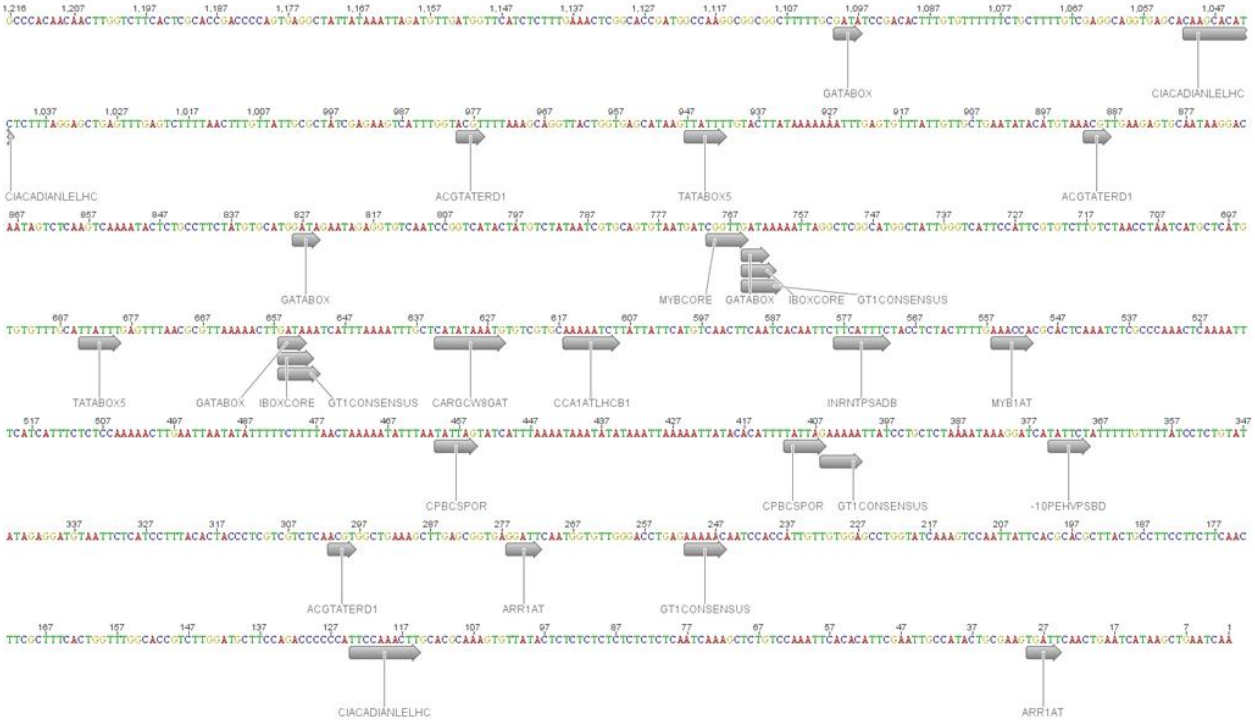

Figure 6.4. *PAO* promoter. The 5′ upstream region of *Actinidia PAO*. Bases are marked in the 3′ to 5′ direction with the A of the ATG as base 1. The motifs associated with light regulation are annotated using Geneious 5.4, available from http://www.geneious.com (Drummond *et al.* 2011).

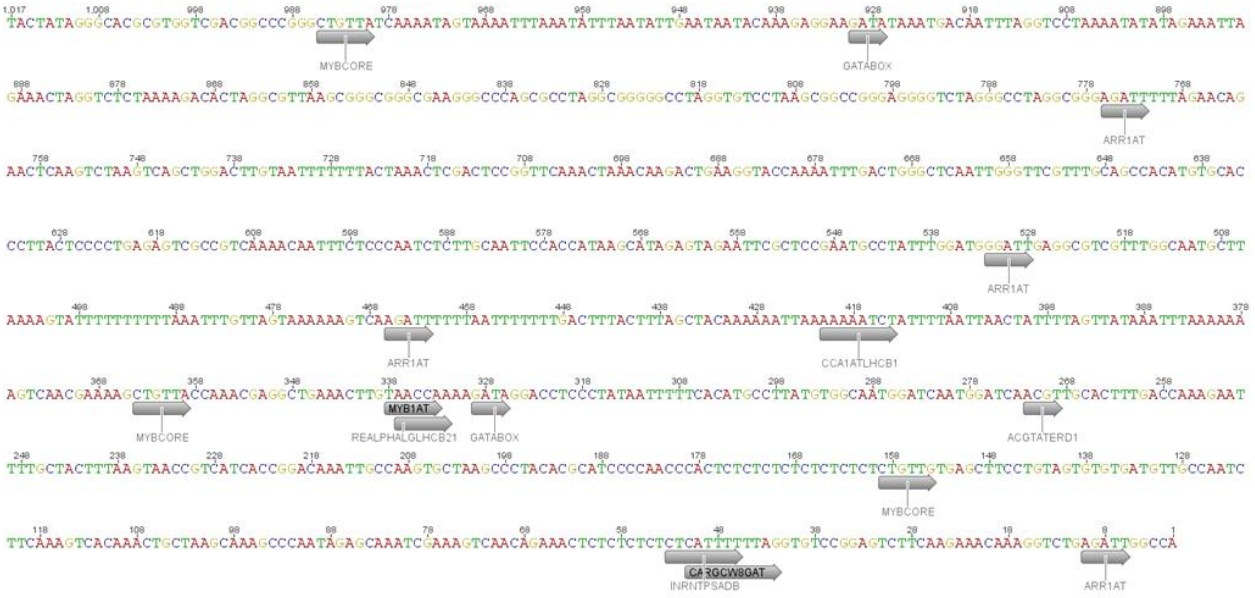

Figure 6.5. *SGR* promoter. The 5′ upstream region of *Actinidia SGR*. Bases are marked in the 3′ to 5′ direction with the A of the ATG as base 1. The motifs associated with light regulation are annotated using Geneious 5.4, available from http://www.geneious.com (Drummond *et al.* 2011).

Results from the PLACE analysis including the annotated motifs from Figures 6.3, 6.4 and 6.5 are presented in Table 6.1. A number of MYB-related elements were identified, including MYB1AT, MYBCORE, MYBCOREATCYCB1, MYBPLANT and CCA1ATLHCB1. This indicates that the MYB transcription factor family are good candidates to be used in promoter studies. A number of motifs were specific to the *RBCS* promoter, such as GT1MOTIFPSRBCS, MYBPLANT and RBCSCONSENSUS. Similarly, the motifs -10PEHVPSBD and CIRCADIANLELHC were specific to the *PAO* promoter. The SGR promoter did not contain the recognition sites of many motifs from the PLACE database, but shared some similar elements with the *RBCS* and *PAO* promoters. In all three promoters, a number of transcription factors involved with light regulation were identified.

6.5 Selection of candidate TFs

Full length clones of a number of the *ARR* genes described in Section 6.2 were obtained and cloned into *pHEX2* for transient assay experiments. Additional candidates were selected from the collection of cDNA-derived TF clones from the EST database at Plant & Food Research. In particular, COLs, MADS and MYBs with *35S* promoters were chosen from both apple (*Malus domestica*) and kiwifruit (*Actinidia sp.*) (Table 6.2). MYBs were chosen because of their over-representation in the PLACE analysis. They have also been implicated in control of fruit colour and cytokinin regulation (Allan *et al.* 2008; Guo and Gan 2011). COLs were chosen for their role in temporal and light regulation (Suarez-Lopez *et al.* 2001) and MADS were chosen as they have previously been implicated in the control of fruit development (Becker and Theißen 2003; Seymour *et al.* 2008).

Table 6.1. Analysis of promoter regions for *cis*-acting element sites. Sequences were analysed using the PLACE database. The elements, recognition sites, TF family, promoter (number of sites), and literature reference are given. Degenerate sequence codes are N = G, A, T or C, R = G or A, W = A or T, Y = T or C, K = G or T, and M = A or C.

Site name	Recognition site	TF family	Promoter	Reference
-10PEHVPSBD	TATTCT	-	*PAO* (1)	(Thum *et al.* 2001)
ACGTATERD1	ACGT	-	*RBCS* (3) *PAO* (1) *SGR* (1)	(Simpson *et al.* 2003)
ARR1AT	NGATT	ARR	*RBCS* (9) *PAO* (2) *SGR* (4)	(Sakai *et al.* 2000) (Ross *et al.* 2004)
CARGCW8GAT	CWWWWWWWWG	MADS	*PAO* (1) *SGR* (1)	(Tang and Perry 2003; Folter and Angenent 2006)
CCA1ATLHCB1	AAMAATCT	MYB-Related	*RBCS* (2) *PAO*(1) *SGR* (1)	(Wang *et al.* 1997)
CIACADIANLELHC	CAANNNNATC	-	*PAO* (2)	(Piechulla *et al.* 1998)
CPBCSPOR	TATTAG	-	*RBCS* (1) *PAO* (2)	(Fusada *et al.* 2005)
GATABOX	GATA	C2C2-GATA	*RBCS* (3) *PAO* (4) *SGR* (2)	(Lam and Chua 1989; Gilmartin *et al.* 1990; Teakle *et al.* 2002; Reyes *et al.* 2004; Rubio-Somoza *et al.* 2006)
GT1MOTIFPSRBCS	KWGTGRWAAWRW	Trihelix	*RBCS* (1)	(Gilmartin *et al.* 1990; Villain *et al.* 1996; Zhou 1999)
IBOXCORE	GATAA	-	*RBCS* (1) *PAO* (2)	(Terzaghi and Cashmore 1995)
INRNTPSADB	YTCANTYY	-	*RBCS* (2) *PAO* (1) *SGR* (1)	(Nakamura *et al.* 2002)
MYB1AT	WAACCA	MYB	*PAO* (1) *SGR* (1)	(Abe *et al.* 2003)
MYBCORE	CNGTTR	MYB	*RBCS* (1) *PAO* (1) *SGR* (3)	(Lüscher and Eisenman 1990) (Urao *et al.* 1993)
MYBCOREATCYCB1	AACGG	MYB	*RBCS* (2)	(Planchais *et al.* 2002)
MYBPLANT	MACCWAMC	MYB	*RBCS* (1)	(Tamagnone *et al.* 1998)
RBCSCONSENSUS	AATCCAA	-	*RBCS* (1)	(Manzara and Gruissem 1988)
REALPHALGLHCB21	AACCAA	-	*RBCS* (1) *SGR* (1)	(Degenhardt and Tobin 1996)
TATABOX5	TTATTT	-	*RBCS* (2) *PAO* (2)	(Tjaden *et al.* 1995)

Table 6.2. Candidate transcription factors. Candidates were selected from the TF collection at Plant & Food Research. EST number, source organism and TF family are described. The TF family includes the species name where annotated in the database.

EST Number	Source Organism	TF Family
COLs		
165042	apple	*MdCOL8*
63907	apple	*MdCOL15*
230102	apple	*MdCOL11*
184121	apple	*MdCOL9*
266796	apple	*MdCOL12*
266925	apple	*MdCOL16*
280937	apple	*MdCOL13*
163999	apple	*MdCOL7*
135922	apple	*MdCOL3*
4149	apple	*MdCOL14*
186469	apple	*MdCOL10*
152694	apple	*MdCOL5*
158833	apple	*MdCOL1*
175322	kiwifruit	*AaCOL1*
268989	kiwifruit	*AcCOL4*
58691	kiwi	*AdCOL8*
27026	kiwi	*AeCOL5*
186787	kiwi	*AcCOL2*
300246	kiwi	*AcCOL6*
195415	kiwi	*AdCOL3*
140144	apple	*MdCOL4*
MADS/TCP		
229693	apple	*MdMADS17*
135738	apple	*MdMADS19*
12966	apple	*MdMADS2*
315840	apple	*MADS*
44986	apple	*TCP4*
127967	apple	*MdMADS18*
14362	apple	*MdMADS91*
217009	apple	*TCP2*
126829	apple	*MdMADS21*
218692	apple	*MADS/AGL6*
264354	apple	*MdMADS23*
264261	apple	*MADS/AGL*
15992	apple	*MADS15*
132385	apple	*MdMADS14*
13196	apple	*MADS/AGL*
185746	apple	*TCP4*
141100	apple	*TCP4*
15077	apple	*MADS/AGL1*
262928	apple	*MdMADS221*
322003	kiwi	*AcMADS10/AcAP1*
191712	kiwi	*AcMADS3/AcAP3*
11569	apple	*MdMADS24/AcSEP4*
140045	apple	*MdCNR*
ARRs		
325149	kiwifruit	*ARR2*
325148	kiwifruit	*ARR6*
324616	kiwifruit	*ARR9*
326078	kiwifruit	*ARR11*
325072	kiwifruit	*ARR12a*
325073	kiwifruit	*ARR12b*
324617	kiwifruit	*ARR17*

EST Number	Source Organism	TF Family
MYB		
260530	kiwifruit	*AcMYBR3*
68260	apple	*MdMYB111*
115016	kiwifruit	*AdMYB8*
281053	kiwifruit	*AdMYB7*
319286	kiwifruit	*AcMYB10*
206670	kiwifruit	*AdMYBR2*
RE17	apple	*MdMYB10*
153949	apple	*MdMYB15*
271656	apple	*MdMYB16*
254072	apple	*MdMYB17*
34436	kiwifruit	*AdMYB10*
260695	kiwifruit	*AcMYB7*
68074	apple	*MdMYB7*
71019	apple	*MdMYB11*
267148	apple	*MdMYB25*
40976	kiwifruit	*AdMYB4*
13436	malus	*MdMYB22*
12615	malus	*MdMYB14*
57783	malus	*MdMYB6*
66649	malus	*MdMYB8*
41717	kiwifruit	*AeMYB22*
48125	kiwifruit	*AdMYB15*
34763	kiwifruit	*AdMYB11*
57543	apple	*MdMYB13*
71567	kiwifruit	*AdMYB6*
110004	apple	*MdMYB24*
71990	kiwifruit	*AdMYB4*
137954	apple	*MdMYB21*
92351	apple	*MdMYB4*
76973	kiwifruit	*AdMYB1*
130813	apple	*MdMYB19*
73067	kiwifruit	*AdMYB16*
114155	kiwifruit	*AdMYB2*
72716	apple	*MdMYB3*
114610	kiwifruit	*AdMYB14*
276085	kiwifruit	*AeMYB15*
173934	kiwifruit	*AaMYB19*
141599	apple	*MdMYB91*
203252	kiwifruit	*AdMYB5*
164933	apple	*MdMYB47*
168019	kiwifruit	*AeMYB14*
148384	apple	*MdMYB23*
268488	apple	*MdMYB88*
173531	apple	*MdMYB18*
180628	apple	*MdMYB5*
248326	apple	*MdMYB12*
281990	kiwifruit	*AcMYB1*
247911	kiwifruit	*AdMYB13*
285181	kiwifruit	*AcMYB3*
142992	apple	*MdMYB20*
141378	apple	*MdMYB92*
4038	apple	*MdMYB93*
69355	apple	*MdMYB2*

6.6 Dual luciferase transient assay screen for interacting transcription factors

The dual luciferase system has been shown to provide a rapid method of transient gene expression analysis (Hellens *et al.* 2005). Trans-activation of the luciferase gene was measured as a ratio of *35S:Renilla* after transient transformation in *N. benthamiana*. A transcription factor introduced to the plant cell by one *Agrobacterium* population can bind recognition sites in a target promoter introduced into the same plant cell from another *Agrobacterium* population, which promotes the expression of *LUC*, relative to *35S:Renilla*. A more detailed methodology is outlined in Section 2.14. The interaction of three promoters, *SGR2*, *PAO1* and *RBCS* with COLs, MYBS, MADS, and ARRs was investigated in order to elucidate possible relationships between the promoters and these cofactors.

The results from the transcription factor assays were first graphed by promoter to allow the overall patterns to be visualised. There was very little activation of the *RBCS* promoter (Figure 6.6) or the *PAO* promoter (Figure 6.7), above baseline without additional *Agrobacterium*, with any of the transcription factors. The largest activation of the *RBCS* was seen by the TFs *ARR17* (325017), *MdCOL8* (165042), *MdCOL1* (158833), and *MdMYB91* (141599). The largest activation of the *PAO* promoter was seen by the TFs *MdMYB88* (268488), *MdMADS19* (135738) and *ARR17* (324617). However, this activation was not as high as the activation of the *SGR* promoter (Figure 6.8). Ratios of LUC to REN were generally 0.01-0.05 for *RBCS*, 0.02-0.1 for *PAO*, and 0.1-0.9 for the *SGR* promoter. The results were then graphed by transcription factor family, to allow more subtle interactions to be seen.

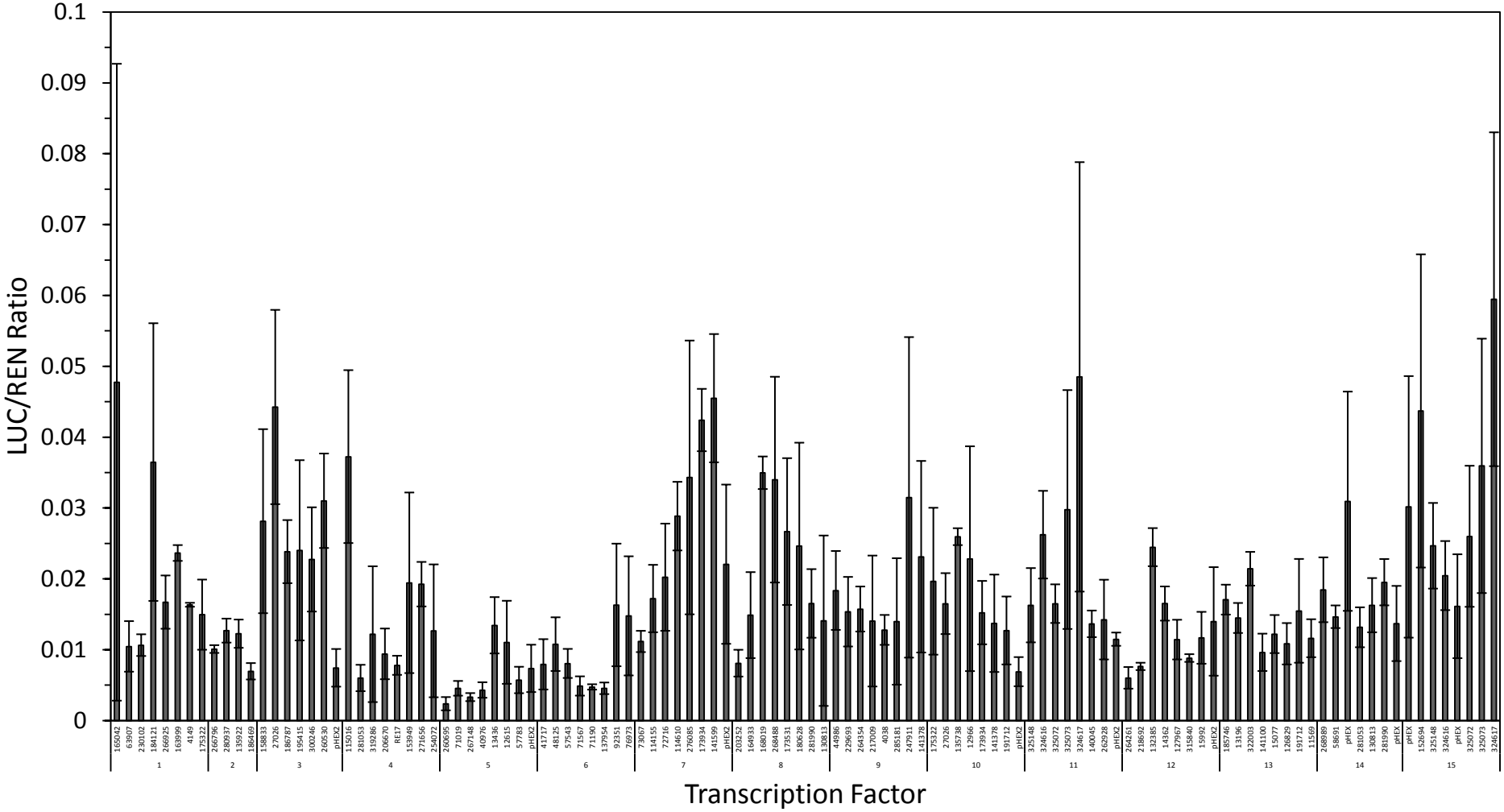

Figure 6.6. Interaction of the *RBCS* promoter and selected transcription factors in transient tobacco transformation assays. Luminescence measurements are expressed as a ratio of luciferase to renilla (LUC/REN ratio) for the *RBCS* promoter and selected transcription factors. The transcription factors are described by their EST number from the Plant & Food Research EST collection (see Table 6.2), and grouped by the plate on which they were assayed with the relevant *pHEX2* control sample. Error is standard error (n=4).

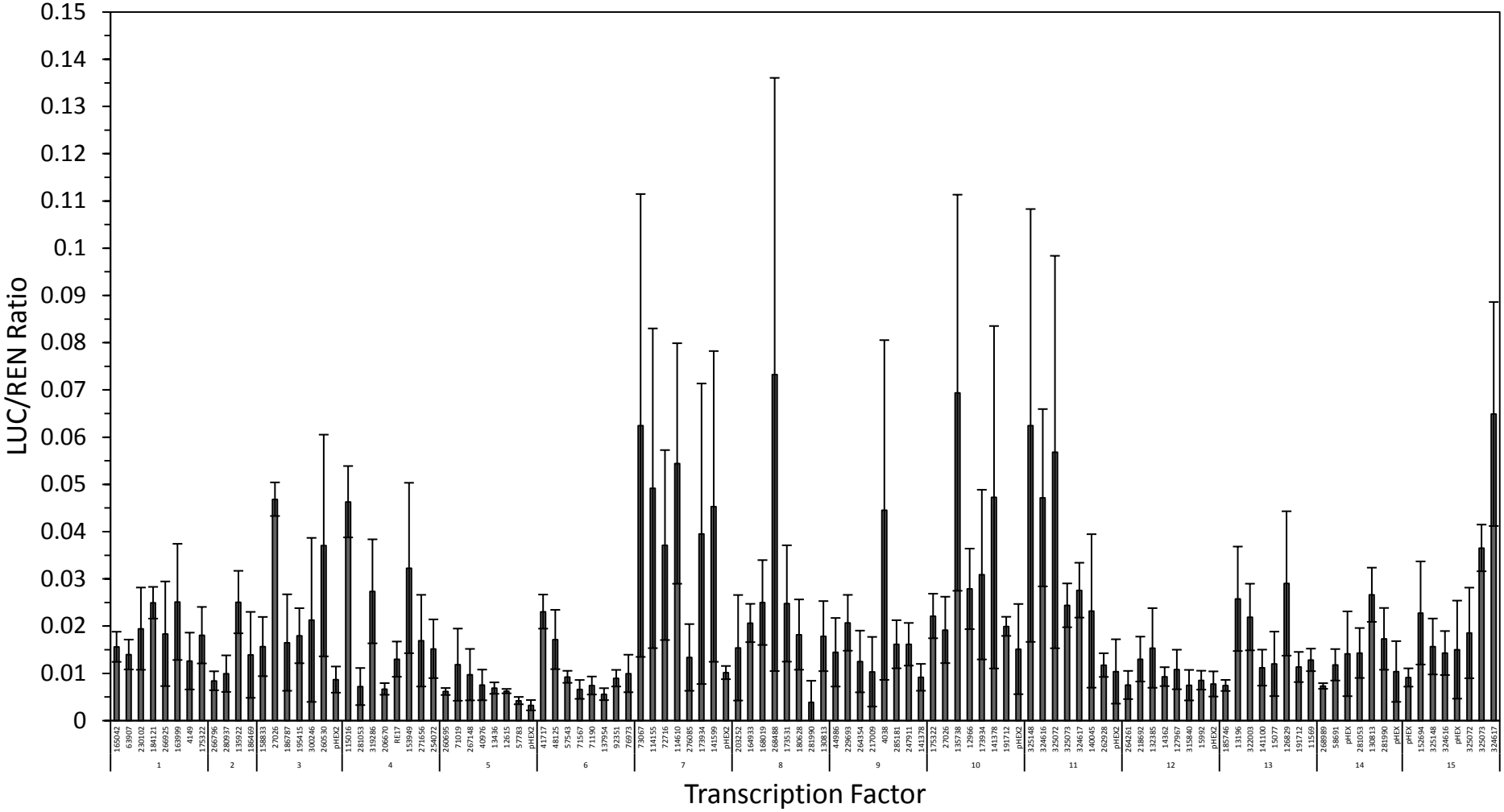

Figure 6.7. Interaction of the *PAO* promoter and selected transcription factors in transient tobacco transformation assays. Luminescence measurements are expressed as a ratio of luciferase to renilla (LUC/REN ratio) for the *PAO* promoter and selected transcription factors. The transcription factors are described by their EST number from the Plant & Food Research EST collection (see Table 6.2), and grouped by the plate on which they were assayed with the relevant *pHEX2* control sample. Error is standard error (n=4).

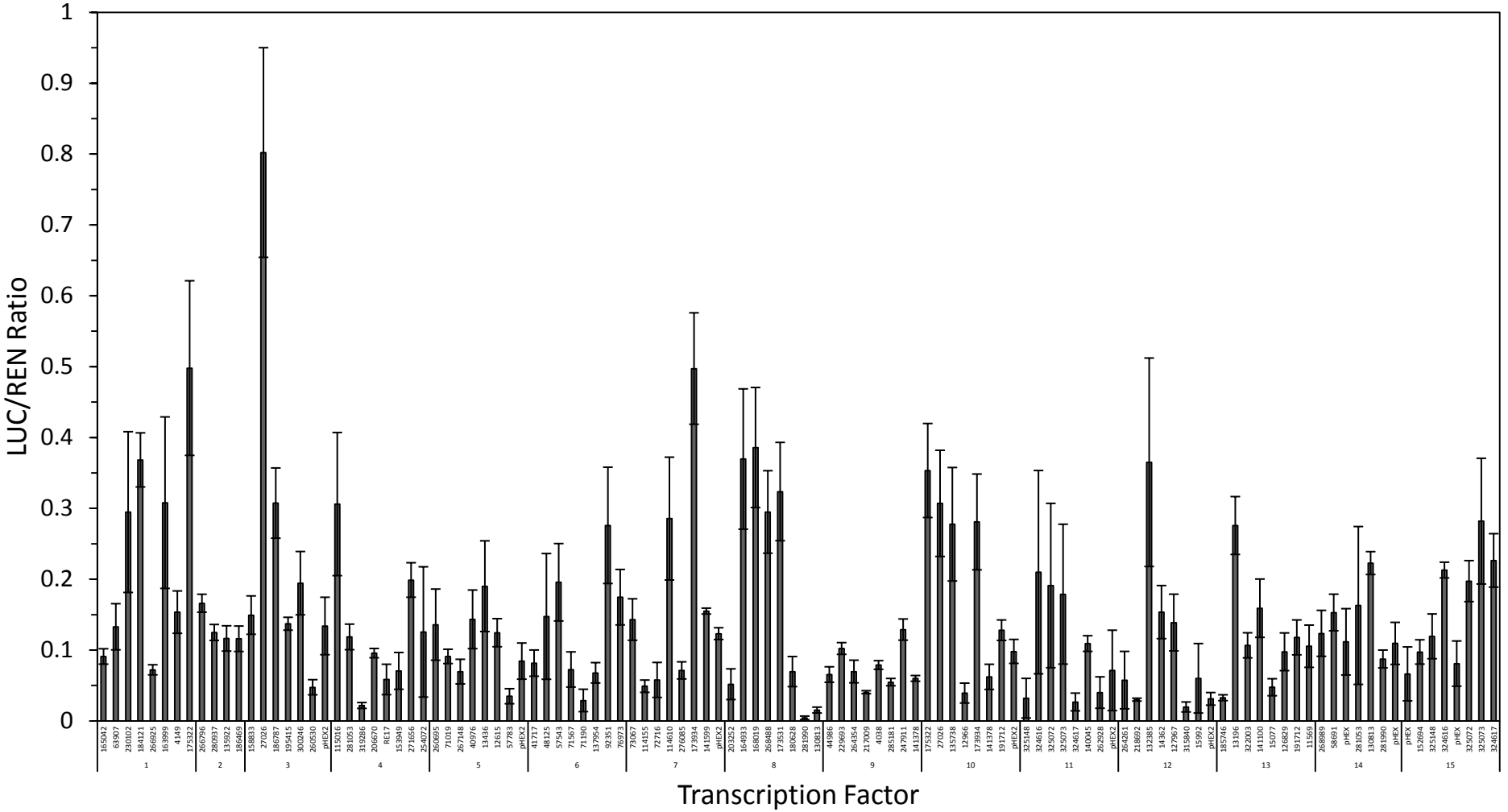

Figure 6.8. Interaction of the *SGR* promoter and selected transcription factors in transient tobacco transformation assays. Luminescence measurements are expressed as a ratio of luciferase to renilla (LUC/REN ratio) for the *SGR* promoter and selected transcription factors. The transcription factors are described by their EST number from the Plant & Food Research EST collection (see Table 6.2), and grouped by the plate on which they were assayed with the relevant *pHEX2* control sample. Error is standard error (n=4).

The interaction of the COLs with the *RBCS*, *PAO* and *SGR* promoters is shown in Figure 6.9. There was a large activation of the *SGR* promoter with *AeCOL5* (27026) on plate 3. When this was repeated on plate 10 with a *pHEX* control, the ratio was not as high, but still showed activation of the promoter. *AaCOL1* (175322), *MdCOL11* (230102), *MdCOL9* (184121) and *MdCOL7* (163999) also activated the *SGR* promoter. In contrast, there was very little interaction between any of these TFs and the *RBCS* or *PAO* promoters.

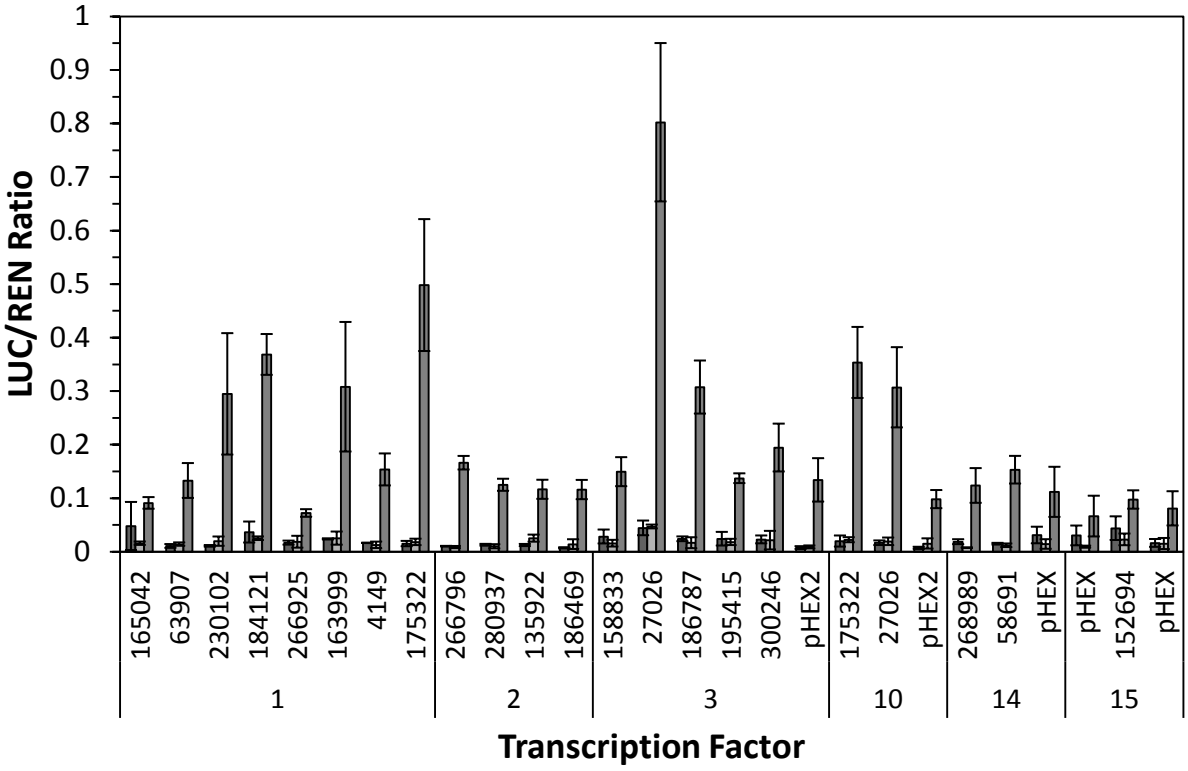

Figure 6.9. Interaction of the *RBCS*, *PAO*, and *SGR* promoters and selected *COL* transcription factors in transient tobacco transformation assays. Luminescence measurements are expressed as a ratio of luciferase to renilla (LUC/REN ratio) for *RBCS* (dark grey bars), *PAO* (light grey bars) and *SGR* (mid grey bars) promoters and selected transcription factors. The transcription factors are described by their EST number from the Plant & Food Research EST collection (see Table 6.2), and grouped by the plate on which they were assayed with the relevant *pHEX2* control sample. Error is standard error (n=4).

The interaction of selected MYBs with the *RBCS*, *PAO* and *SGR* promoters is shown in Figure 6.10. Several MYBs showed a moderate interaction with the *SGR* promoter, *AdMYB8* (115016), *MdMYB4* (92351), *AdMYB14* (114610), *AaMYB19* (173934), *MdMYB47* (164933), *AeMYB14* (168019), *MdMYB88* (268488) and *MdMYB18* (173531). Like the COLs, the MYBs were only able to activate the *RBCS* or *PAO* promoters to a low level.

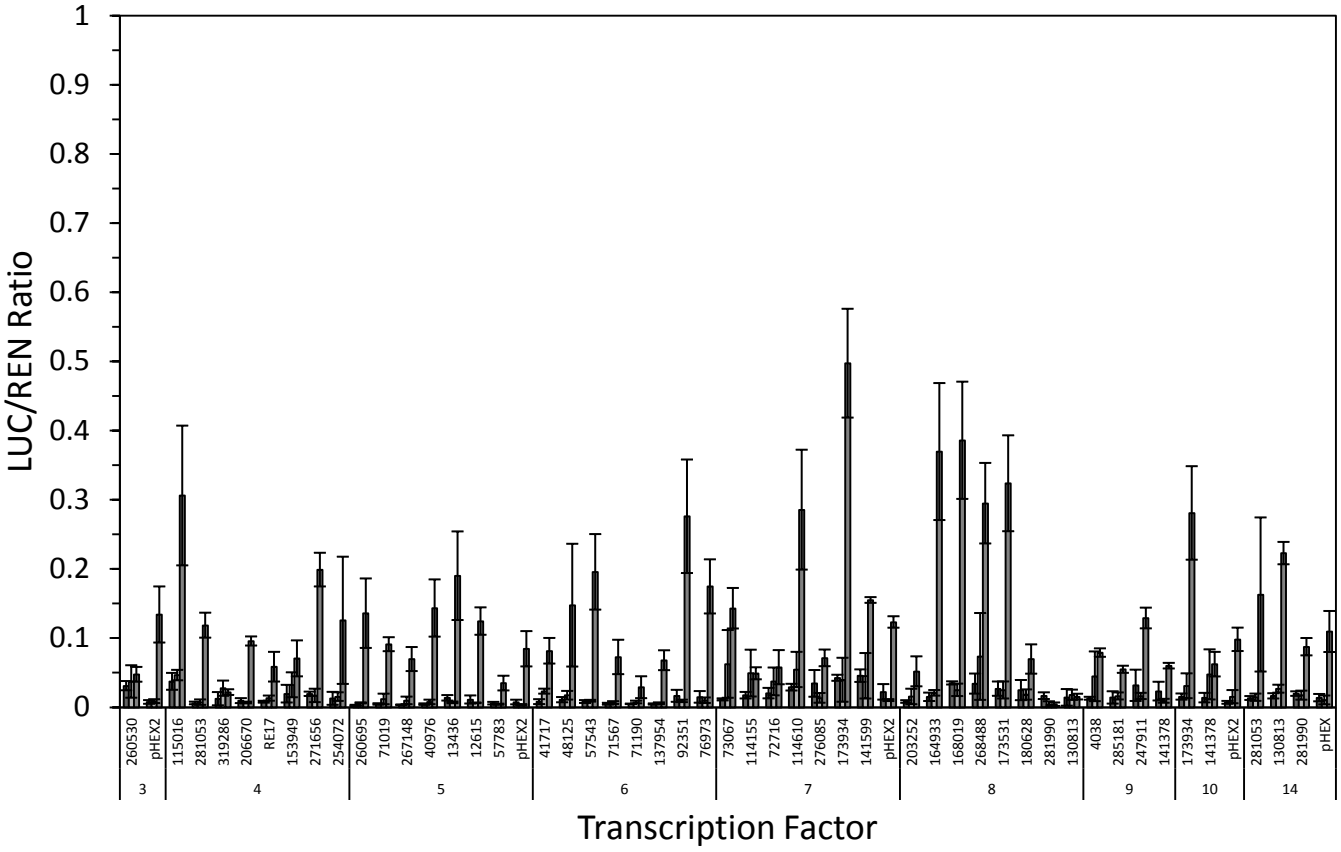

Figure 6.10. Interaction of the *RBCS*, *PAO*, and *SGR* promoters and selected *MYB* transcription factors in transient tobacco transformation assays. Luminescence measurements are expressed as a ratio of luciferase to renilla (LUC/REN ratio) for *RBCS* (dark grey bars), *PAO* (light grey bars) and *SGR* (mid grey bars) promoters and selected transcription factors. The transcription factors are described by their EST number from the Plant & Food Research EST collection (see Table 6.2), and grouped by the plate on which they were assayed with the relevant *pHEX2* control sample. Error is standard error (n=4).

The interaction of the chosen MADS transcription factors is graphed in Figure 6.11. Five MADS transcription factors, *MdMADS19* (135738), *MdMADS14* (132385), and *MADS/AGL-like* (13196) were able to activate the *SGR* promoter to a moderate degree above control levels. Like the COLs and the MYBs, the MADS were only able to activate the *RBCS* or *PAO* promoters to a low level.

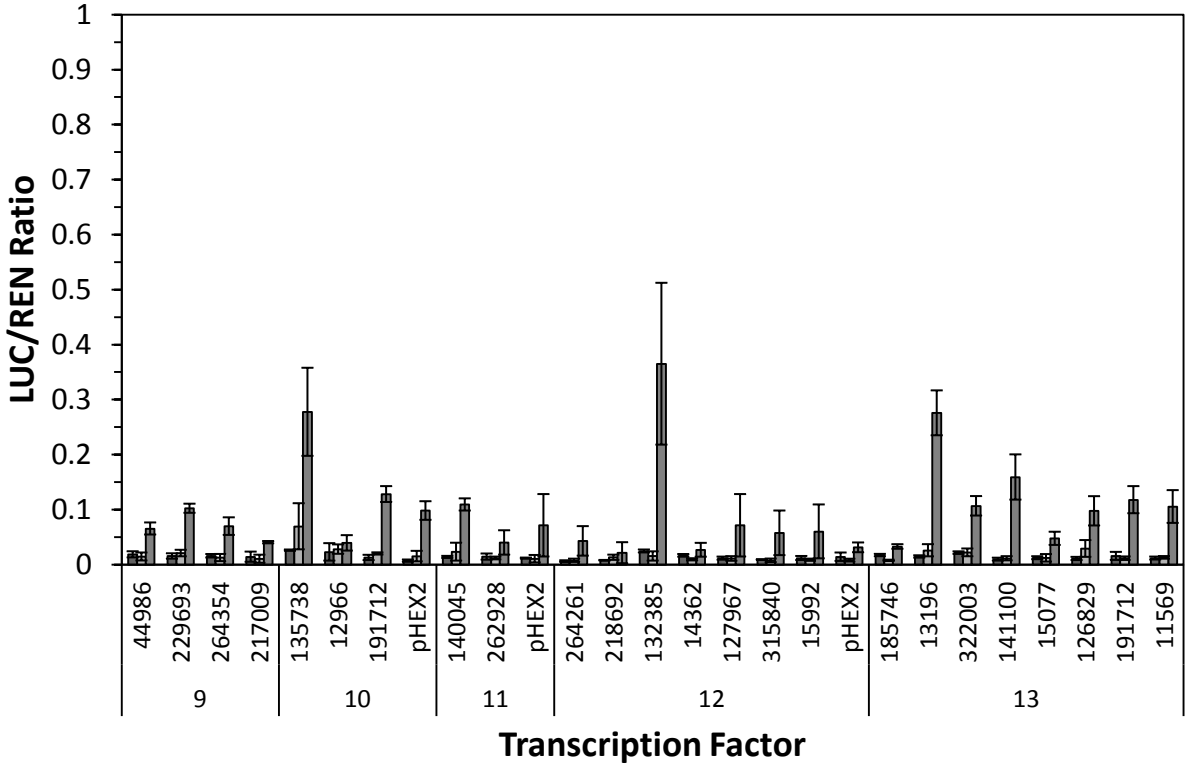

Figure 6.11. Interaction of the *RBCS*, *PAO*, and *SGR* promoters and selected *MADS* transcription factors in transient tobacco transformation assays. Luminescence measurements are expressed as a ratio of luciferase to renilla (LUC/REN ratio) for *RBCS* (dark grey bars), *PAO* (light grey bars) and *SGR* (mid grey bars) promoters and selected transcription factors. The transcription factors are described by their EST number from the Plant & Food Research EST collection (see Table 6.2), and grouped by the plate on which they were assayed with the relevant *pHEX2* control sample. Error is standard error (n=4).

The interaction of the promoters with the *ARR* genes is shown in Figure 6.12. All of the ARRs showed a slight activation of the *SGR* promoter compared to the *pHEX* control.

ARR12b showed the highest activation over both plates, and *ARR17* was able to activate the SGR promoter to a moderate level when the assay was repeated on plate 15. *ARR17* was the only transcription factor able to activate all three promoters.

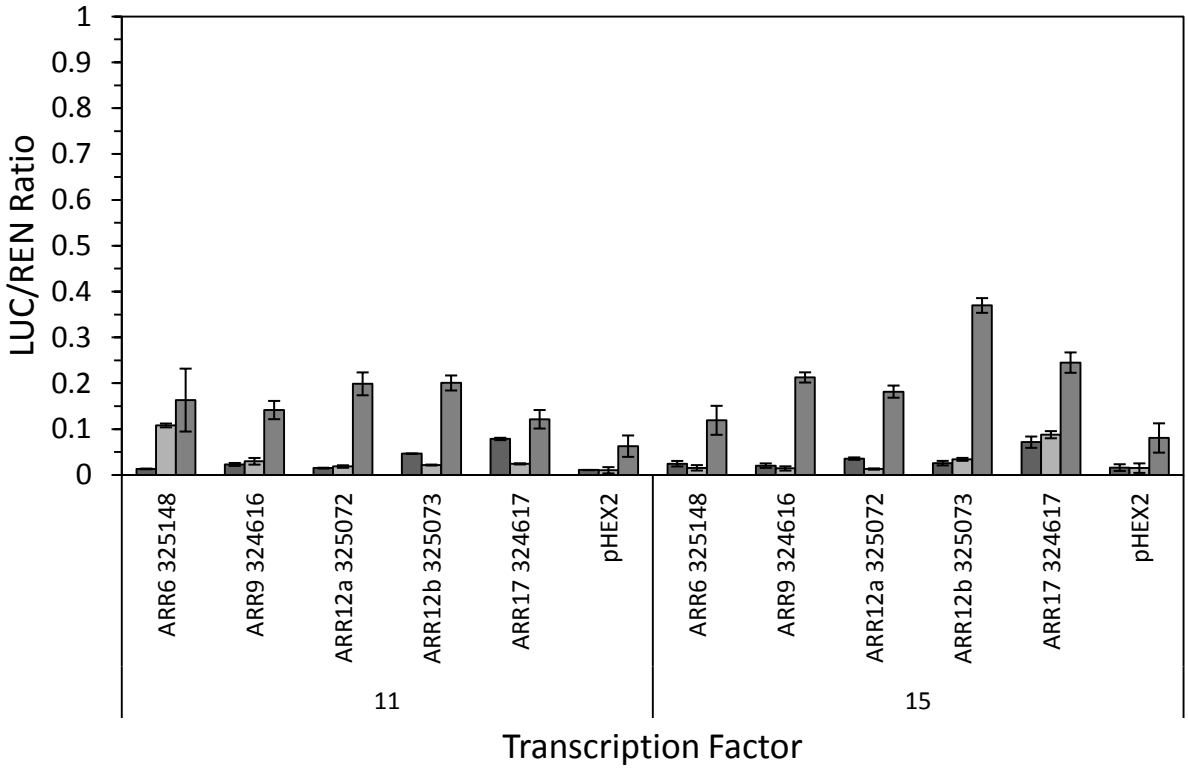

Figure 6.12. Interaction of the *RBCS*, *PAO*, and *SGR* promoters and selected *ARR* transcription factors in transient tobacco transformation assays. Luminescence measurements are expressed as a ratio of luciferase to renilla (LUC/REN ratio) for *RBCS* (dark grey bars), *PAO* (light grey bars) and *SGR* (mid grey bars) promoters and selected transcription factors. The transcription factors are described by their EST number from the Plant & Food Research EST collection (see Table 6.2), and grouped by the plate on which they were assayed with the relevant *pHEX2* control sample. Error is standard error (n=4).

Transcription factors were combined to investigate whether they had an additive effect on promoter activation. Because *ARR6* was a potential repressor due to its low activation of the promoters, it was also selected for combinatorial experiments. *ARR12b* and *ARR17* were also chosen because these TFs were able to activate the *SGR* promoter. *MdMADS19* (135738), *MADS/AGL-like* (13196), *MdMADS14* (132385) and *AaMYB19* (173934) were chosen as these TFs produced the highest level of *SGR* promoter activation. These TFs were co-infiltrated with the *SGR* promoter, in order to test the level of activation. Most TFs produced a similar level of activation when co-infiltrated, compared with the TF alone, with the exception of *ARR6* which had a lower level of activation with *MADS/AGL-like* (13196), *ARR12b* which had a higher level of activation with *MdMADS14* (132385) and *AaMYB19* (173934), and *ARR17* which had a higher level of activation with *MdMADS19* (135735) and *MdMADS14* (132385).

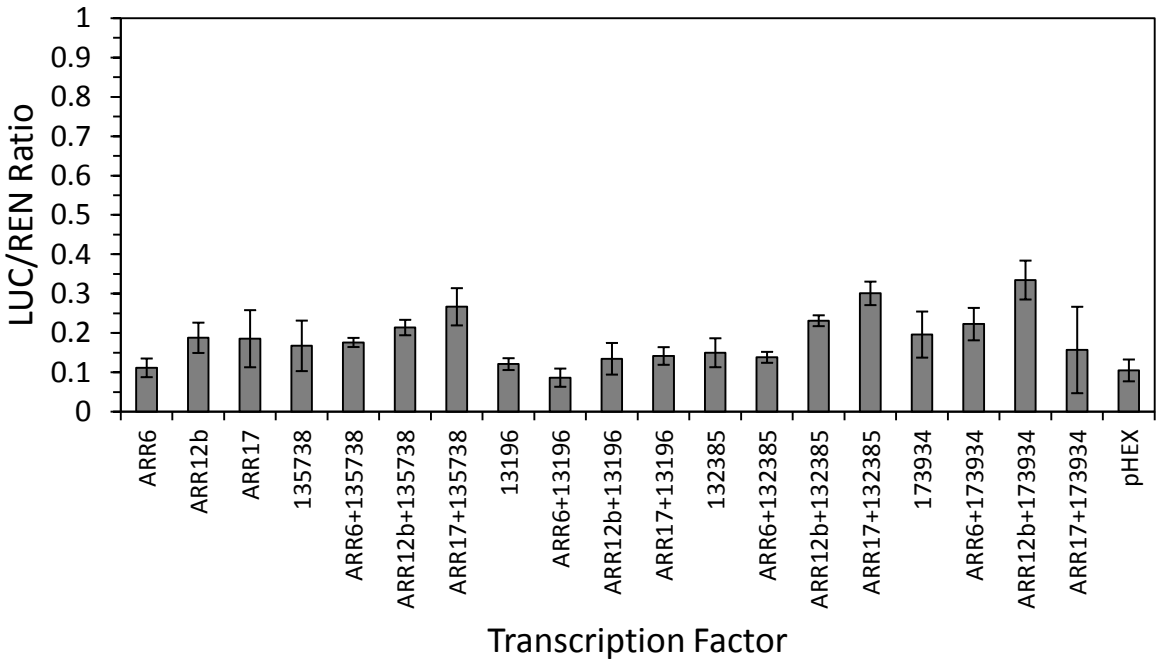

Figure 6.13. Interaction of the *SGR* promoter and selected ARR transcription factors with selected transcription factors in transient tobacco transformation assays. Luminescence measurements are expressed as a ratio of luciferase to renilla (LUC/REN ratio) for *SGR* (mid grey bars) promoter and selected transcription factors. The transcription factors are described by their EST number from the Plant & Food Research EST collection (see Table 6.2), and grouped by the plate on which they were assayed with the relevant *pHEX2* control sample. Error is standard error (n=4).

6.7 Discussion

The transcriptional control of chlorophyll de-greening was investigated using transient assays of candidate transcription factors and the promoters from the three kiwifruit genes, *RBCS*, *PAO* and *SGR*, previously shown to be differentially regulated in maturing kiwifruit. Cytokinin levels also peak during maturity in both green and yellow kiwifruit. Cytokinin is perceived *via* a phosphorelay, which leads to the activation of cytokinin response regulators, the ARRs. Nine putative *ARRs* were mined from the *Actinidia* EST database at Plant & Food Research, and their expression was measured in an *A. chinensis* and *A. deliciosa* fruit series from 2010. Expression of a number of the *ARRs* was similar in green and yellow fruit at most sampling time points. However, *ARR 6* and *9* showed higher expression in green fruit at the beginning of development. *ARR17* increased over fruit development in green fruit, with little expression in yellow fruit. *ARR12b* and *ARR13* had increased expression at maturity in green fruit. The expression of *ARRs* is important, as differential expression may contribute to having either a unique or a redundant role in cytokinin responses (Hwang and Sheen 2001).

The PLACE analysis of candidate promoters revealed a number of *cis*-element recognition sites. A number of these sites were specific to the *RBCS* promoter, suggesting that *RBCS* expression may be regulated by specific transcription factors. The PLACE analysis determined six MYB recognition sites in the *RBCS* promoter, three recognition sites in the *PAO* promoter and five recognition sites in the *SGR* promoter. One MYB transcription factor was able to activate the *RBCS* promoter in dual luciferase assays (*MdMYB91*). This MYB is most closely related to the *Arabidopsis asymmetric leaves 1* (*AS1*) gene, which is reported to control leaf polarity (Zhu *et al.* 2008). Similarly, one MYB transcription factor was able to activate the *PAO* promoter, *MdMYB88*, which is closely related to *AtMYB124*, a MYB implicated in stomatal adaptation to stress (Xie *et al.* 2010). This MYB was also able to activate the *SGR* promoter. Seven other MYB transcription factors were also able to bind the *SGR* promoter, including *AdMYB8*, which is involved in response to jasmonate during stamen development (Cheng *et al.* 2009). *MdMYB4* is similar to *AtMYB3R5* which is chloroplast localised but has not been functionally characterised to date. *MdMYB14* is closely related to *AtMYB17*, which is involved in floral meristem identity (William *et al.* 2004). *AaMYB19* is related to *AtMYB61*, which is implicated in seed coat development

(Arsovski *et al.* 2009). *AeMYB14* may be involved in hormone responses and pollen tube growth (Wang *et al.* 2008). *MdMYB18* is related to *AtMYB102* which has been implicated in response to wounding and osmotic stress (Denekamp and Smeekens 2003). The MYB transcription factors were included in transient assays as some family members, such as *AtMYB2,* have been previously implicated in plant senescence and cytokinin regulation (Guo and Gan 2011). *AtMYB2* is most closely related to *AdMYB7* and *AcMYB7*. These transcription factors only showed a slight activation of the *SGR* promoter compared with the *pHEX2* control. This result is in agreement with previous research where knockout of the *AtMYB2* did not affect the progression of leaf senescence, suggesting other factors that may function redundantly with *AtMYB2* in regulating leaf senescence.

Only one MADS recognition site was identified in the *PAO* and *SGR* promoters using the PLACE analysis. No MADS recognition sites were identified in the PLACE analysis of the *RBCS* promoter, and none of the MADS TFs included in the study were able to activate this promoter. One MADS TF, *MdMADS19,* was able to activate the *PAO* promoter. The *Arabidopsis* homologue of this TF has been implicated in fertilisation and seed development (Brambilla *et al.* 2007). This TF was also able to activate the *SGR* promoter. Three other MADS TFs were able to activate the *SGR* promoter, *MdMADS14* is related to an *Arabidopsis* gene involved in ovule and fruit development (Flanagan *et al.* 1996), a *MADS*/*AGL*-like gene involved in floral meristems and carpel and stamen identity (Chen *et al.* 1999), and *SBP-like*, involved in shoot development (DeCook *et al.* 2006).

There were no COL recognition sites identified in the PLACE analysis. However, the *RBCS* promoter was activated by two COL transcription factors, *MdCOL8* and *MdCOL1*. The *Arabidopsis* homologues of these genes have been implicated in control of circadian rhythm and flowering time (*AtCOL1*) (Ledger *et al.* 2001), and regulation of chloroplast transcription (*AtCOL4*) (Hu *et al.* 2003), respectively. The *PAO* promoter was not activated by any of the COL TFs included in the study. There were five COL genes able to activate the *SGR* promoter. These were *MdCOL11*, which is similar to *AtLZF1*, a gene that is involved in light responses (Chang *et al.* 2008), *MdCOL9,* similar to *AtCOL9*, which is involved in floral promotion (Veley and Michaels 2008), *MdCOL7*, related to an *Arabidopsis* COL gene involved in salt tolerance which co-localises with proteins involved in light signalling (Nagaoka and Takano 2003), *AaCOL1*, is closely related to *AtCOL4,* which is involved in circadian signalling (Li *et al.* 2011), and *AeCOL5*, related to an

Arabidopsis COL gene which may be involved in the regulation of flowering (Wenkel *et al.* 2006). Taken together, these transient assay results suggest that *RBCS* promoter is regulated by a wide range of TFs in a number of plant processes.

Some TFs need to be members of a transcriptional complex in order to produce a high level of promoter activations. For example, the petunia AN2 MYB interacts with the bHLH TFs AN1 and JAF13 (Mol *et al.* 1998). When the TFs which activated the *SGR* promoter were combined with the most effective ARRs, a higher level of activation was seen, for example, in the co-infiltration of *ARR12b* which had a higher level of activation with *MdMADS14* and *AaMYB19*, and *ARR17* which had a higher level of activation with *MdMADS19* and *MdMADS14*. This could indicate that the presence of a co-factor with an ARR can activate promoter transcription to a high level.

Another possible method to achieve higher activation levels could be to optimise the *N. benthamiana* leaf stage used in transient infiltration assays. Two leaves were infiltrated per plant for the infiltration experiments. Although care was taken to ensure the leaves were of similar size, they were randomised for each promoter TF interaction. This led to a larger error between leaves, possibly due to differences in cytokinin levels in smaller leaves, where increased cell division or elongation is occurring, compared with larger leaves, which could mask subtle differences in activation. Transient assays with and without exogenous cytokinin could also be performed to test the effect of cytokinin on promoter activation.

All ARRs showed a degree of activation of the *SGR* promoter. *ARR17* was the only TF in the study able to activate all three candidate promoters, with the highest activation of the *SGR* promoter, suggesting an important role in regulation of chlorophyll levels. This TF was expressed in green fruit towards maturity, and was only expressed in yellow fruit at low levels. *ARR17* clusters in the Type-A response regulator clade of *Arabidopsis*, which encode transcription repressors that mediate a negative feedback loop in cytokinin signalling (Hwang and Sheen 2001). In this way, a high level of *ARR17* expression could negatively feedback to the cytokinin pathway, resulting in the cytokinin storage seen in green kiwifruit in Chapter Five, by glucosylation of active cytokinins in a feedback loop.

ARR12b was also able to activate the *SGR* promoter. This gene was highly expressed in green fruit at fruit maturity, when the fruit were beginning to de-green slightly. The Type-B ARRs bind primary response genes which initiates downstream cytokinin signalling cascades. ARRs have been shown to activate CRF genes which are closely related to the AP2/ethylene response factor genes and participate in mediating the cytokinin response (Rashotte *et al.* 2006).

The differential expression of *ARRs* could lead to differential regulation of cytokinin levels in the two fruit. This could also lead to differential regulation of the chlorophyll degradation pathway, *via* activation of the *SGR* promoter.

6.7.1 Conclusions

There are differences in *ARR* expression between green and yellow kiwifruit. Two of these ARRs, *ARR17* and *ARR12b*, showed an ability to activate the *SGR* promoter, in addition to other TFs from the COL, MYB and MADS TF families. Differences in *ARR* gene expression or a SNP or insertion/deletion in the *SGR* promoter which affects ARR activation could lead to differential regulation of cytokinin feedback and chlorophyll degradation in kiwifruit. Future work could include sequencing of these promoters in green and yellow fruit for possible SNPs, insertions or deletions.

7. DISCUSSION AND CONCLUSIONS

In this chapter the results reported in this thesis are discussed in terms of the gain of scientific understanding of the control of chlorophyll levels in plants, and the relevance of these findings towards future kiwifruit breeding and horticultural technology. Chlorophyll degradation is a key physiological process in plant development in response to the environment. Stay-green mutants provide a useful tool for the study of the chlorophyll degradation pathway, and the existence of a non-yellowing fruit from a species of kiwifruit provides an opportunity to elucidate the genetic and regulatory mechanisms governing this process to further our understanding of chlorophyll degradation, both in kiwifruit and in other plants.

Chlorophyll de-greening is a co-ordinated process and is reported to involve down-regulation of chlorophyll biosynthesis and up-regulation of chlorophyll degradation (Wagstaff *et al.* 2009). Consequently, in *A. deliciosa*, the overall relative rate of biosynthesis to degradation would be expected to be greater than in *A. chinensis*. The transcripts of genes from the chlorophyll biosynthetic pathway, chlorophyll degradation pathway, carotenoid biosynthetic pathway and the cytokinin biosynthetic pathway were detected in both green and yellow fruit tissue. Thus the colour difference between green and yellow fruit appears not to be due to the loss of transcription of a step, leading to retention of chlorophyll in green fruit. Overall, expression of the chlorophyll degradation genes was slightly elevated in yellow fruit across development compared with expression in green fruit. This suggested that the genes of the chlorophyll degradation pathway and other degradation associated proteins are well regulated. If these genes encode functional proteins, then it is likely that their differential regulation causes the green and yellow flesh phenotypes.

According to Rodoni *et al.* (1997), the PAO enzymatic step is the critical step for loss of green colour in canola (*Brassica napus*). *PAO1* was expressed in fruit of both kiwifruit cultivars, but was expressed more strongly and earlier in development in yellow fruit. This could indicate a possible regulatory point for chlorophyll degradation in the fruit flesh. However, as *PAO1* is expressed in green kiwifruit, lack of chlorophyll degradation in green fruit could be associated with altered accessibility or transport of chlorophyll

components to the chloroplast envelope, or the absence of another factor required for the reaction, and thus the regulatory point should be upstream (Akhtar *et al.* 1999).

Both *SGR1* and *SGR2* caused rapid chlorophyll degradation in *N. benthamiana* leaves upon transient infiltration. These results show that the over-expression of *SGR* alone is sufficient to drive chlorophyll degradation. The protein sequence of *A. chinensis* SGR1 is identical to the protein sequence of *A. deliciosa* SGR1, and the protein sequences of *A. chinensis* and *A. deliciosa* SGR2 were also identified. Therefore, it is likely that these genes produce functional SGR proteins in both *A. deliciosa* and *A. chinensis*. These genes are expressed in both green and yellow fruit, but a higher degree of *SGR2* expression is seen in yellow fruit. Together these results suggest that the control point for chlorophyll degradation in kiwifruit is upstream of the SGR protein; for example, endogenous hormone levels, expression of transcription factors, or a SNP in the *SGR* promoter which affects transcription factor binding.

The results of expression analysis of the same genes in DA x CK and *A. chinensis* mapping populations did not show *SGR* expression segregating with green and yellow colour. However, these results may be influenced by a number of factors including ploidy, and the subtle difference between green and yellow flesh colour in these fruit. *A. deliciosa* is hexaploid and *A. chinensis* is diploid (2n), thus the resulting DA x CK cross is tetraploid (4n). However, an *A. eriantha* (diploid) and *A. chinensis* (diploid) (EA x CK) cross, segregating for green and yellow colour, did not provide further insight into the control of chlorophyll degradation.

Overall, the gene transcripts for chlorophyll degradation steps accumulated to a higher level in yellow tissue and cytokinin biosynthetic and metabolic gene transcripts accumulated to a higher level in green tissue. *SGR*, *PPH*, *PAO1*, *IPT*, *ZOG* and *BGLU* showed relationships with significant pair-to-pair correlations. Taken together, the sum of these differences may explain the changes in colour and chlorophyll. However, other processes, for example the spatial separation of chlorophyll and the degradation machinery, or hormonal perception, may be delaying de-greening in green fruit.

As the expression of both *IPT* and *ZOG* differed significantly between *A. deliciosa* and *A. chinensis* and as previous work had shown a marked increase in endogenous cytokinins in

maturing *A. deliciosa* (Lewis *et al.* 1996b), a comprehensive analysis of the cytokinins in the fruit of these two species was performed in Neil Emery's laboratory at Trent University, Canada, using triple quadrupole LC-MS/MS analysis. The endogenous cytokinin levels were unusually high in both species but differed significantly in the profile of the *O*-glucosides. Interestingly, while the expression of *IPT*, the rate-limiting step in the cytokinin biosynthetic pathway, showed an increase towards maturity in green fruit, which was not seen in yellow fruit, both species had high levels of nucleotides, tZ and tZR. A possible reason for this could be that another *IPT* gene family member is responsible for the production of excess nucleotides and free bases in yellow kiwifruit. The unusually high levels of cytokinin nucleotides suggest that the early steps of cytokinin metabolism may be differentially regulated in kiwifruit compared with other fruit.

A key enzyme in maintaining cytokinin homeostasis is CKX. While *IPT* expression is mirrored by *CKX* expression in a number of species such as *N. tabacum* and *B. rapa* (Jones and Schreiber 1997; Motyka *et al.* 2003; Gális *et al.* 2005; O'Keefe *et al.* 2011), this did not occur in *A. deliciosa* kiwifruit, suggesting that there could be a breakdown in homoeostatic regulation. However, the differences between *IPT* and *CKX* expression are not as apparent in the DA x CK cross, indicating that *CKX* may not be a key factor in moderating the cytokinin levels in maturing fruit

However, another gene involved with cytokinin homeostasis, *ZOG*, showed substantially higher expression in *A. deliciosa* fruit, and increased towards fruit maturity. Moreover, there was a significant positive correlation between *ZOG* and green fruit flesh colour in the DA x CK population, indicating that the homeostatic mechanism of *O*-glucosylation is operational in green kiwifruit but not in yellow. If this is the case, the perceived very high tZR could be activating the glucosylation process. Yellow kiwifruit may not have such a large requirement for *O*-glucosylation because of observed lower tZR concentrations, especially at later stages compared with green fruit, or due to a lack of on-going cytokinin biosynthesis in yellow fruit.

Down-regulation of cytokinin activity, by lowering production of early pathway iPNT, is consistent with lower *IPT* gene expression in yellow fruit compared with green fruit. Both species contained a large pool of tZNT, so the critical difference might be at the adenosine kinase step, which phosphorylates tZR to tZNT (Moffatt *et al.* 2000), possibly at a greater

rate in yellow fruit. The *O*-glucosyltransferases might therefore only have had excess tZR levels in green kiwifruit. In addition, yellow fruit could have a feedback loop which down-regulates the fruit's own synthesis, leading to lower iPNT levels. This could lead to the high tZ levels observed in yellow fruit, due to the action of LOG, the enzyme responsible for the one-step conversion of cytokinin nucleotides to free bases. Conversely, green fruit could be unable to down-regulate synthesis, leading to the observed *O*-glucosylation.

The cytokinin biosynthetic and homeostatic enzymes are encoded by large gene families. In this PhD project all primers used in the expression studies were designed for the single best kiwifruit gene family member candidate for the control of chlorophyll levels, based on high transcript levels, tissue source and putative function based on *Arabidopsis* BLAST matches. However, research in maize by Vyroubalova *et al.* (2009) showed that the regulation of gene family members is not uniform, as all *CKX* genes were upregulated by cytokinin treatment except one. A further expression analysis of all kiwifruit cytokinin biosynthesis and homeostasis gene family members, now more possible with available genome sequencing, could better describe their role in kiwifruit.

As both species have high levels of potentially active cytokinin forms, the possibility exists for differences in perception. Previous cytokinin receptor research has revealed differing affinities of the three *Arabidopsis* AHK receptors for different forms of cytokinin (Higuchi *et al.* 2004; Nishimura *et al.* 2004; Riefler *et al.* 2006). However, the AHK receptors have not yet been characterised in fruit tissue. It is possible that there are fruit-specific cytokinin receptors that have different affinities for different forms of cytokinin. It is also possible that there is differential expression of these receptors or gene homeologues in hexaploid *A. deliciosa* compared with diploid *A. chinensis* fruit.

Cytokinin is signalled *via* a phosphorelay, which leads to the activation of cytokinin response regulators, the ARRs. The expression of *ARRs* is, therefore, important as differential expression may contribute to having either a unique or a redundant role in cytokinin responses (Hwang and Sheen 2001). The differential expression of *ARRs* could lead to differential regulation of cytokinin levels in the two fruit. This could also lead to differential regulation of the chlorophyll degradation pathway, *via* activation of the *SGR* promoter.

Cytokinins have been shown to stimulate chloroplast transcription in detached barley leaves (Zubo *et al.* 2008). However, the effect of cytokinin levels on the transcription of chlorophyll degradation genes, which are nuclear encoded, has not been elucidated. The transcriptional control of chlorophyll de-greening was investigated using transient assays of candidate transcription factors and three kiwifruit promoters (*RBCS*, *PAO* and *SGR*), shown to be differentially regulated in maturing kiwifruit.

All ARRs showed a degree of activation of the *SGR* promoter. *ARR17* was the only TF in the study able to activate all three candidate promoters, with the highest activation of the *SGR* promoter, suggesting a role in regulation of chlorophyll levels. This TF was expressed in green fruit towards maturity, and was only expressed in yellow fruit at low levels. *ARR17* clusters in the Type-A response regulator clade of *Arabidopsis*, which encode transcription repressors that mediate a negative feedback loop in cytokinin signalling (Hwang and Sheen 2001). A high level of *ARR17* expression could result in the accumulation of the cytokinin glucosides seen in green kiwifruit, by glucosylation of active cytokinins in a feedback loop.

ARR12b was also able to activate the *SGR* promoter. This gene showed a similar expression pattern in both fruit, with a high expression in green fruit at fruit maturity, when the fruit were beginning to de-green slightly. The Type-B ARRs bind primary response genes which initiates downstream cytokinin signalling cascades. ARRs have been shown to activate cytokinin response factor (CRF) genes, which are closely related to the AP2/ethylene response factor genes and participate in mediating the cytokinin response (Rashotte *et al.* 2006). More recently, the CRFs were identified as AP2/ERF-like transcription factors induced by cytokinin from global expression analyses in *Arabidopsis* (Shi *et al.* 2012). CRFs form a branch pathway of cytokinin signalling and may regulate downstream cytokinin targets independently or in conjunction with Type-B response regulators (Rashotte *et al.* 2006; Werner and Schmülling 2009). A study of their expression and involvement in kiwifruit would be informative.

Transient activation of candidate promoters by TFs, such as ARRs, is only one indication of an interaction. Stable transformation and/or protein techniques, such as gel shift assays, are required to confirm this. TFs are involved in modulating target gene expression. There are differences in *ARR* expression between green and yellow kiwifruit. Two of these

ARRs, *ARR17* and *ARR12b*, showed an ability to activate the *SGR* promoter, in addition to other TFs from the COL, MYB and MADS TF families. Differences in *ARR* gene expression or a SNP or insertion/deletion in the *SGR* promoter which affects ARR activation could lead to differential regulation of cytokinin feedback and chlorophyll degradation in kiwifruit. Future work could include sequencing of these promoters in green and yellow fruit for possible SNPs, insertions or deletions.

Initial transcription factor screens revealed candidates for the transcriptional control of chlorophyll degradation. The increased promoter activation seen upon ARR infiltration with a cofactor could indicate that ARRs need to be members of a transcriptional complex to activate chlorophyll degradation gene expression. Pull-down or yeast II hybrid assays could reveal a binding partner for the ARRs. Gel shift/retardation assays are required to confirm that TF candidates, revealed in activation assay screens, actually bind targeted promoters.

High cytokinin levels should lead to the delay of yellowing, as cytokinin has been postulated to protect cell membranes and the photosynthetic machinery from oxidative damage during senescence in previous research (Zavaleta-Mancera *et al.* 2007). It is possible, despite its high cytokinin levels, if indeed the yellow fruit do perceive the cytokinin, that there may still not be sufficient cytokinin to delay de-greening, compared with green fruit. Similarly, other processes such as ethylene-induced ripening or signalling due to levels of hydrogen peroxide or sugars could overcome the high cytokinin levels in yellow fruit but not green fruit. Previous research in tobacco leaves showed that delay of senescence by high cytokinin levels due to the over-expression of *IPT* can be overcome by high sugar levels (Wingler *et al.* 1998). Yellow kiwifruit accumulates sugars to slightly higher levels of around 18 °Brix, compared to green kiwifruit at around 15 °Brix. It has been shown that a substantial part of leaf cytokinins are localised to chloroplasts (Benkova *et al.* 1999). Cytokinins have also been linked to chloroplasts during senescence of detached leaf segments, where protein degradation in mutant white leaves blocked for chloroplast development occurred much more rapidly and was less retarded by cytokinin than in green leaves (Kulaeva *et al.* 2002). In this case, if yellow fruit no longer have functional chloroplasts, there could be less of a response to high cytokinin levels, as cytokinin would be unable to stimulate chloroplast gene expression. Notably, the application of CPPU at 165 DAFB was found to have no effect on the colour of the fruit.

This could be due to initiation of the irreversible de-greening process prior to CPPU production. As the application of CPPU to kiwifruit has been shown to increase the greening of outer pericarp tissue in both *A. chinensis* and *A. deliciosa* when applied at early stages of fruit development (Iwahori *et al.* 1988; Patterson *et al.* 1993), further experiments could ascertain the point of 'no return' for de-greening in *A. chinensis,* but also indicate if the fruit lose sensitivity to cytokinin.

Linking these findings together, a possible model is proposed for the regulation of chlorophyll levels in *A. deliciosa* and *A. chinensis* in Figure 7.1.

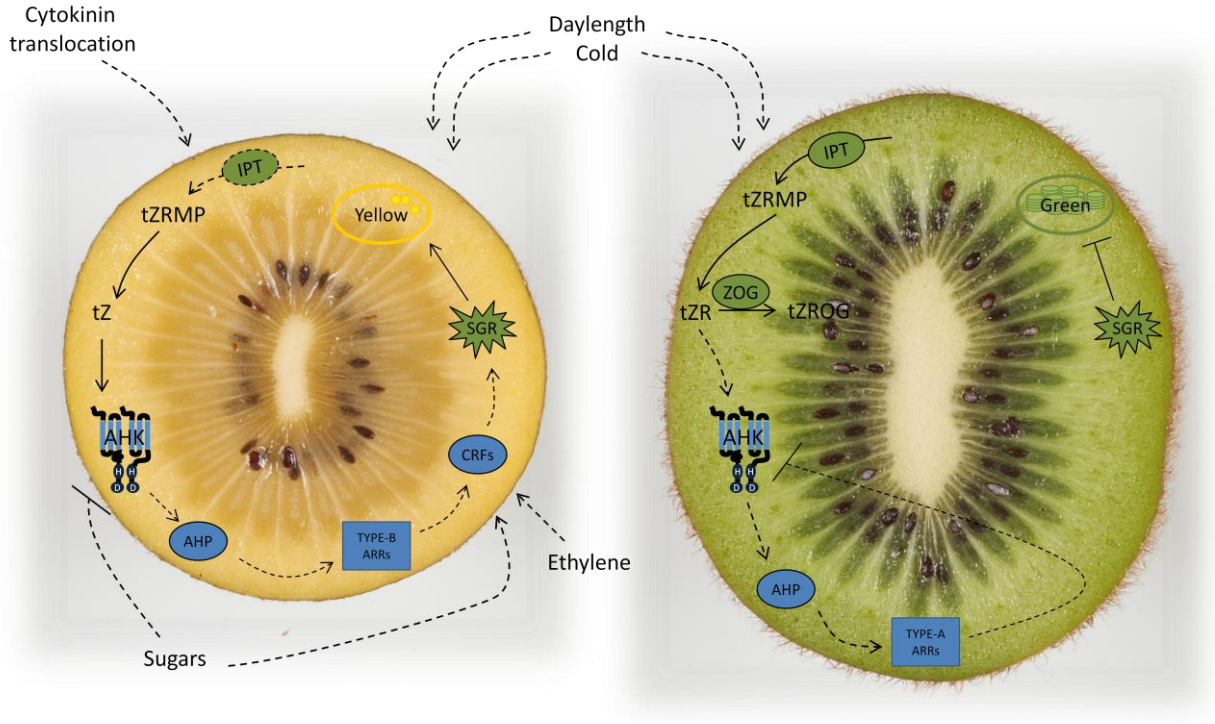

Figure 7.1. Possible model of the regulation of chlorophyll levels in *A. chinensis* and *A. deliciosa*. Possible model of the regulation of chlorophyll levels in *A. chinensis* (left) and *A. deliciosa* (right). Black arrows indicate pathways proposed from results in this study. Black dashed arrows indicate possible pathways which have not yet been investigated.

7.1 Future directions for the study of the regulation of chlorophyll levels in kiwifruit

In addition to revealing new information on the chlorophyll degradation pathway and cytokinin metabolism in kiwifruit, these studies have also revealed areas for future work.

In plants where stay-green genes have been described, for example capsicum and tomato, research has often involved genetic linkage of the phenotype to candidate genes (Akhtar *et al.* 1999; Efrati *et al.* 2005). Genetic analysis to test the linkage of candidate genes to the trait in kiwifruit is more difficult due to variation between chromosome counts of different kiwifruit species. The two species used in this study, which are the two kiwifruit species commonly grown and consumed, differ in ploidy, where *A. deliciosa* is hexaploid and *A. chinensis* is diploid. This makes an interspecific cross difficult and the resulting inheritance pattern complicated, even in the case of a single major gene influencing the phenotype. *A. eriantha* is a green-fleshed kiwifruit species which is diploid, and has been crossed with yellow *A. chinensis*. Progeny of this cross segregate for green and yellow flesh colour with the majority of progeny being green. In many other species the stay-green phenotype is a single recessive gene (Armstead *et al.* 2006; Sato *et al.* 2007). This may indicate that the stay-green kiwifruit phenotype is not inherited as a single recessive gene. However, the small and variable number of seedlings per family limits the reliability of this data, and a further study would be valuable for the study of green and yellow colour inheritance patterns in kiwifruit. Mapping some of the key candidate genes from this study, such as *SGR*, *IPT* and *ZOG*, on a genetic map and over a population segregating for colour such as this EA x CK population, could provide clues to a regulator of chlorophyll degradation which maps to the same region. If this genetic map was anchored to whole genome sequence, then genes under such a locus would be the lead candidates for controlling de-greening. The most consistent difference between green and yellow kiwifruit was high *ZOG* expression and subsequent high concentrations of *O*-glucosides in green-fleshed species, and mapping this gene could lead to the identification of a locus for green flesh colour.

A. deliciosa fruit produced two *IPT* qRT-PCR products, where one contained a 36 base pair deletion. When translated into a theoretical protein, the resulting protein contained a

deletion of 12 amino acids near the N-terminus of the protein. This deletion was not located in a conserved region of the protein, so may not interfere with its function. Despite the lack of amino acid conservation, the theoretical protein could be conformationally altered by the short N-terminus, so further experiments should be performed to determine whether the IPTΔ protein from *A. deliciosa* is a different *IPT* gene homoeologue or a different allele, and whether the resulting protein is functional. This gene variant may be ideal as a genetic marker in a segregating population.

Plant ageing, programmed cell death, senescence, ripening, post harvest deterioration and other cell death processes are inter-related (Thomas *et al.* 2003). Therefore, it is important to study chlorophyll degradation in kiwifruit in a kiwifruit system, as well as both leaf and fruit chlorophyll degradation. Kiwifruit seedlings and mature leaf patches show different dark- and cold-induced senescence responses to other known model species. As kiwifruit are a vine that must survive under a canopy, these species may have disassociated their dark-related senescence from light signals to some degree in their leaves. Cold treatment was also insufficient to drive chlorophyll degradation. This could be due to lack of a link between kiwifruit cold response and de-greening in leaves. Moreover, the genes involved with chlorophyll biosynthesis in the fruit showed fluctuations in expression over development. This included a spike in expression in many genes, which may be the result of these genes being under the control of circadian rhythm or temperature changes, as seen in the expression of *CAB* in *Arabidopsis* (Millar and Kay 1996) and *LHCB* in bean (Kaldis *et al.* 2003). This is an interesting area for future work, as it indicates that despite the fruit flesh not being exposed to light, there are still internal rhythms regulating the expression of light-responsive genes. Regular sampling throughout the day and night, or under temperature manipulation, could elucidate this regulation in an area of importance to the industry. Green fruit generally had higher expression of genes encoding biosynthetic pathway enzymes, and lower expression of genes encoding degradation pathway enzymes. If these genes encode functional proteins, then it is likely that their differential regulation causes the green and yellow flesh phenotypes. Future work on enzymatic activity would be challenging but could reveal differences in functionality between yellow and green kiwifruit.

Direct infiltration of both kiwifruit leaves and fruit with transgenes showed some promising results with the anthocyanin regulator *MYB10*. However, these methods appear

to need further development before they can be applied to the chlorophyll degradation pathway. Whole kiwifruit vine transformation was also a useful tool for studying the over-expression of *SGR*, and the first fruiting season of the transgenic plants, expected in 2013, could provide some interesting results of plants harbouring a transgene that drives fruit-specific over-expression of *SGR*.

Since the inception of this project in 2009, the kiwifruit industry faces devastation by *Pseudomonas syringae* pv. *actinidae* infection. A recent experiment has linked *SGR* over-expression with *P. syringae* infection in *Arabidopsis*, where modification of SGR expression can influence a hypersensitive response elicited by *P. syringae* pv *tomato* on *Arabidopsis* (Mur *et al.* 2010). Similarly, cytokinin has also been shown to be involved with resistance to *P. syringae* pv *tabaci* in tobacco, by inducing production of antimicrobial phytoalexins (Großkinsky *et al.* 2011). Thus *SGR* knock-out plants which do not degrade chlorophyll or modifications to cytokinin metabolism could provide insight into *P. syringae*-resistant kiwifruit plants.

7.2 Conclusions/Significance

The aim of this thesis was to elucidate the genetic mechanisms that control the changes in pigment composition that lead to flesh yellowing in kiwifruit cultivars. This is essential for developing an understanding of chlorophyll degradation in kiwifruit, and may also provide knowledge of the control of chlorophyll degradation in other plants. Furthermore, de-greening of commercial yellow cultivars is sometimes incomplete, resulting in poor perceived quality. Thus elucidation of the control of chlorophyll levels provides knowledge of this key process in kiwifruit and important leads to assist in the kiwifruit breeding program for new kiwifruit cultivars.

Candidate genes for the control of chlorophyll degradation in kiwifruit were identified and characterised using the kiwifruit germplasm resources available at Plant & Food Research. A possible link between delayed chlorophyll degradation and cytokinin accumulation in maturing *A. deliciosa* kiwifruit was also investigated. In yellow kiwifruit there was generally lower expression of genes encoding chlorophyll biosynthetic pathway enzymes, and higher expression of genes encoding degradation pathway enzymes. There are two

versions of the *SGR* gene in both species, both of which were shown to drive rapid de-greening in heterologous plant systems. The accumulation of active cytokinins in both green and yellow fruit suggests that the differences between the fruit might lie in cytokinin perception and/or signalling. This could lead to differential regulation of chlorophyll levels *via* activation of the *SGR* promoter by the ARR transcription factors, leading to a possible link between the chlorophyll degradation pathway and cytokinins. Chlorophyll degradation is involved in a large number of plant processes, and elucidation of the control of this pathway could have far-reaching benefits, from crop manipulation for the increase of yield and reduced drought response, to increased health benefits of cytokinins and chlorophyll in humans.

8. REFERENCES

Abe H., Urao T., Ito T., Seki M., Shinozaki K., Yamaguchi-Shinozaki K. (2003). *Arabidopsis AtMYC2* (bHLH) and *AtMYB2* (MYB) function as transcriptional activators in abscisic acid signaling. *The Plant Cell Online* 15(1): 63-78.

Akhtar M., Goldschmidt E., John I., Rodoni S., Matile P., Grierson D. (1999). Altered patterns of senescence and ripening in *gf*, a stay-green mutant of tomato (*Lycopersicon esculentum* Mill.). *Journal of Experimental Botany* 50(336): 1115-1122.

Allan A.C., Hellens R.P., Laing W.A. (2008). MYB transcription factors that colour our fruit. *Trends in Plant Science* 13(3): 99-102.

Alos E., Roca M., Iglesias D.J., Minguez-Mosquera M.I., Damasceno C.M.B., Thannhauser T.W., Rose J.K.C., Talon M., Cercos M. (2008). An evaluation of the basis and consequences of a stay-green mutation in the navel *negra citrus* mutant using transcriptomic and proteomic profiling and metabolite analysis. *Plant Physiology* 147(3): 1300-1315.

Ampomah-Dwamena C., McGhie T., Wibisono R., Montefiori M., Hellens R.P., Allan A.C. (2009). The kiwifruit lycopene beta-cyclase plays a significant role in carotenoid accumulation in fruit. *Journal of Experimental Botany* 60(13): 3765-3779.

Andersson I., Backlund A. (2008). Structure and function of Rubisco. *Plant Physiology and Biochemistry* 46(3): 275-291.

Antognozzi E., Battistelli A., Famiani F., Moscatello S., Stanica F., Tombesi A. (1996). Influence of CPPU on carbohydrate accumulation and metabolism in fruits of *Actinidia deliciosa* (A. Chev.). *Scientia Horticulturae* 65(1): 37-47.

Argueso C.T., Raines T., Kieber J.J. (2010). Cytokinin signaling and transcriptional networks. *Current Opinion in Plant Biology* 13(5): 533-539.

Argyros R.D., Mathews D.E., Chiang Y.H., Palmer C.M., Thibault D.M., Etheridge N., Argyros D.A., Mason M.G., Kieber J.J., Schallera G.E. (2008). Type B response regulators of *Arabidopsis* play key roles in cytokinin signaling and plant development. *Plant Cell* 20(8): 2102-2116.

Armstead I., Donnison I., Aubry S., Harper J., Hortensteiner S., James C., Mani J., Moffet M., Ougham H., Roberts L., Thomas A., Weeden N., Thomas H., King I. (2007). Cross-species identification of Mendel's *I* locus. *Science* 315(5808): 73-.

Armstead I., Donnison I., Aubry S., Harper J., Hörtensteiner S., James C., Mani J., Moffet M., Ougham H., Roberts L., Thomas A., Weeden N., Thomas H., King I. (2006). From crop to model to crop: Identifying the genetic basis of the staygreen mutation in the *Lolium*/*Festuca* forage and amenity grasses. *New Phytologist* 172(4): 592-597.

Arsovski A.A., Villota M.M., Rowland O., Subramaniam R., Western T.L. (2009). MUM ENHANCERS are important for seed coat mucilage production and mucilage secretory cell differentiation in *Arabidopsis thaliana*. *Journal of Experimental Botany* 60(9): 2601-2612.

Aubry S., Mani J., Hörtensteiner S. (2008). Stay-green protein, defective in Mendel's green cotyledon mutant, acts independent and upstream of pheophorbide *a* oxygenase in the chlorophyll catabolic pathway. *Plant Molecular Biology* 67(3): 243-256.

Balazadeh S., Riaño-Pachón D.M., Mueller-Roeber B. (2008). Transcription factors regulating leaf senescence in *Arabidopsis thaliana*. *Plant Biology* 10(s1): 63-75.

Barry C.S. (2009). The stay-green revolution: Recent progress in deciphering the mechanisms of chlorophyll degradation in higher plants. *Plant Science* 176(3): 325-333.

Barry C.S., McQuinn R.P., Chung M.-Y., Besuden A., Giovannoni J.J. (2008). Amino acid substitutions in homologs of the stay-green protein are responsible for the green-flesh and chlorophyll retainer mutations of tomato and pepper. *Plant Physiology* 147(1): 179-187.

Bartley G.E., Scolnik P.A., Beyer P. (1999). Two *Arabidopsis thaliana* carotene desaturases, phytoene desaturase and ζ-carotene desaturase, expressed in *escherichia coli*, catalyze a poly-cis pathway to yield pro-lycopene. *European Journal of Biochemistry* 259(1-2): 396-403.

Becker A., Theißen G. (2003). The major clades of MADS-box genes and their role in the development and evolution of flowering plants. *Molecular Phylogenetics and Evolution* 29(3): 464-489.

Beever D.J., Hopkirk G. (1990). Chapter five: Fruit development and fruit physiology. In: Warrington, I.J. and Weston, G.C., *Kiwifruit: Science and management*. Ray Richards Publisher and New Zealand Society for Horticultural Science, Auckland.

Ben-Arie R., Gross J., Sonego L. (1982). Changes in ripening-parameters and pigments of the chinese gooseberry (kiwi) during ripening and storage. *Scientia Horticulturae* 18(1): 65-70.

Bohner J., Bangerth F. (1988). Cell number, cell size and hormone levels in semi-isogenic mutants of *Lycopersicon pimpinellifolium* differing in fruit size. *Physiologia Plantarum* 72(2): 316-320.

Borovsky Y., Paran I. (2008). Chlorophyll breakdown during pepper fruit ripening in the chlorophyll retainer mutation is impaired at the homolog of the senescence-inducible stay-green gene. *TAG Theoretical and Applied Genetics* 117(2): 235-240.

Brambilla V., Battaglia R., Colombo M., Masiero S., Bencivenga S., Kater M.M., Colombo L. (2007). Genetic and molecular interactions between *BELL1* and MADS box factors support ovule development in *Arabidopsis*. *The Plant Cell Online* 19(8): 2544-2556.

Buchanan-Wollaston V., Ainsworth C. (1997). Leaf senescence in *Brassica napus*: Cloning of senescence related genes by subtractive hybridisation. *Plant Molecular Biology* 33(5): 821-834.

Büchert A.M., Civello P.M., Martínez G.A. (2011). Chlorophyllase versus pheophytinase as candidates for chlorophyll dephytilation during senescence of broccoli. *Journal of Plant Physiology* 168(4): 337-343.

Bustin S.A., Benes V., Garson J.A., Hellemans J., Huggett J., Kubista M., Mueller R., Nolan T., Pfaffl M.W., Shipley G.L., Vandesompele J., Wittwer C.T. (2009). The MIQE guidelines: Minimum information for publication of quantitative real-time PCR experiments. *Clinical Chemistry* 55(4): 611-622.

Cha K.W., Lee Y.J., Koh H.J., Lee B.M., Nam Y.W., Paek N.C. (2002). Isolation, characterization, and mapping of the stay green mutant in rice. *TAG Theoretical and Applied Genetics* 104(4): 526-532.

Chang C.-s.J., Li Y.-H., Chen L.-T., Chen W.-C., Hsieh W.-P., Shin J., Jane W.-N., Chou S.-J., Choi G., Hu J.-M., Somerville S., Wu S.-H. (2008). LZF1, a HY5-regulated transcriptional factor, functions in *Arabidopsis* de-etiolation. *The Plant Journal* 54(2): 205-219.

Chang S., Puryear J., Cairney J. (1993). A simple and efficient method for isolating RNA from pine trees. *Plant Molecular Biology Reporter* 11(2): 113-116.

Chen Q., Atkinson A., Otsuga D., Christensen T., Reynolds L., Drews G.N. (1999). The *Arabidopsis FILAMENTOUS FLOWER* gene is required for flower formation. *Development* 126(12): 2715-2726.

Cheng H., Song S., Xiao L., Soo H.M., Cheng Z., Xie D., Peng J. (2009). Gibberellin acts through jasmonate to control the expression of *MYB21*, *MYB24*, and *MYB57* to promote stamen filament growth in *Arabidopsis*. *PLoS Genetics* 5(3): e1000440.

Chung D.W., Pruzinska A., Hortensteiner S., Ort D.R. (2006). The role of pheophorbide *a* oxygenase expression and activity in the canola green seed problem. *Plant Physiology* 142(1): 88-97.

Crowhurst R., Gleave A., MacRae E., Ampomah-Dwamena C., Atkinson R., Beuning L., Bulley S., Chagne D., Marsh K., Matich A., Montefiori M., Newcomb R., Schaffer R., Usadel B., Allan A., Boldingh H., Bowen J., Davy M., Eckloff R., Ferguson A.R., Fraser L., Gera E., Hellens R., Janssen B., Klages K., Lo K., MacDiarmid R., Nain B., McNeilage M., Rassam M., Richardson A., Rikkerink E., Ross G., Schroder R., Snowden K., Souleyre E., Templeton M., Walton E., Wang D., Wang M., Wang Y., Wood M., Wu R., Yauk Y.-K., Laing W. (2008). Analysis of expressed sequence tags from *Actinidia*: Applications of a cross species EST database for gene discovery in the areas of flavor, health, color and ripening. *BMC Genomics* 9(1): 351.

Cunningham F.X., Gantt E. (1998). Genes and enzymes of carotenoid biosynthesis in plants. *Annual Review of Plant Physiology and Plant Molecular Biology* 49(1): 557-583.

DeCook R., Lall S., Nettleton D., Howell S.H. (2006). Genetic regulation of gene expression during shoot development in *Arabidopsis*. *Genetics* 172(2): 1155-1164.

Degenhardt J., Tobin E.M. (1996). A DNA binding activity for one of two closely defined phytochrome regulatory elements in an *LHCB* promoter is more abundant in etiolated than in green plants. *The Plant Cell Online* 8(1): 31-41.

Denekamp M., Smeekens S.C. (2003). Integration of wounding and osmotic stress signals determines the expression of the *AtMYB102* transcription factor gene. *Plant Physiology* 132(3): 1415-1423.

Dobrev P.I., Kamínek M. (2002). Fast and efficient separation of cytokinins from auxin and abscisic acid and their purification using mixed-mode solid-phase extraction. *Journal of Chromatography A* 950(1-2): 21-29.

Drummond A.J., Ashton B., Buxton S., Cheung M., Cooper A., Duran C., Field M., Heled J., Kearse M., Markowitz S., Moir R., Stones-Havas S., Sturrock S., Thierer T., Wilson A. (2011). Geneious v5.4, available from http://www.geneious.com/.

Eckhardt U., Grimm B., Hörtensteiner S. (2004). Recent advances in chlorophyll biosynthesis and breakdown in higher plants. *Plant Molecular Biology* 56(1): 1-14.

Efrati A., Eyal Y., Paran I. (2005). Molecular mapping of the *chlorophyll retainer* (*cl*) mutation in pepper (*Capsicum* spp.) and screening for candidate genes using tomato ESTs homologous to structural genes of the chlorophyll catabolism pathway. *Genome* 48: 347-351.

Emanuelsson O., Nielsen H., Heijne G.V. (1999). ChloroP, a neural network-based method for predicting chloroplast transit peptides and their cleavage sites. *Protein Science* 8(5): 978-984.

Espley R.V., Hellens R.P., Putterill J., Stevenson D.E., Kutty-Amma S., Allan A.C. (2007). Red colouration in apple fruit is due to the activity of the MYB transcription factor, mdmyb10. *The Plant Journal* 49(3): 414-427.

Ferguson A.R. (1990). Chapter one: The genus *Actinidia*. In: Warrington, I.J. and Weston, G.C., *Kiwifruit: Science and management*. Ray Richards Publisher and New Zealand Society for Horticultural Science, Auckland.

Ferguson A.R., Bollard E.G. (1990). Chapter eight: Domestication of the kiwifruit. In: Warrington, I.J. and Weston, G.C., *Kiwifruit: Science and management*. Ray Richards Publisher and New Zealand Society for Horticultural Science, Auckland.

Ferguson A.R., Huang H. (2007). Genetic resources of kiwifruit: Domestication and breeding. *Horticultural reviews*. John Wiley & Sons, Inc.

Flanagan C.A., Hu Y., Ma H. (1996). Specific expression of the *AGL1* MADS-box gene suggests regulatory functions in *Arabidopsis* gynoecium and ovule development. *The Plant Journal* 10(2): 343-353.

Folter S.d., Angenent G.C. (2006). *trans* meets *cis* in MADS science. *Trends in Plant Science* 11(5): 224-231.

Fraser L., Tsang G., Datson P., De Silva H., Harvey C., Gill G., Crowhurst R., McNeilage M. (2009). A gene-rich linkage map in the dioecious species *Actinidia chinensis* (kiwifruit) reveals putative x/y sex-determining chromosomes. *BMC Genomics* 10(1): 102.

Fusada N., Masuda T., Kuroda H., Shimada H., Ohta H., Takamiya K.-i. (2005). Identification of a novel *cis*-element exhibiting cytokinin-dependent protein binding *in vitro* in the 5′-region of NADPH-protochlorophyllide oxidoreductase gene in cucumber. *Plant Molecular Biology* 59(4): 631-645.

Gajdošová S., Spíchal L., Kamínek M., Hoyerová K., Novák O., Dobrev P.I., Galuszka P., Klíma P., Gaudinová A., Žižková E., Hanuš J., Dančák M., Trávníček B., Pešek B., Krupička M., Vaňková R., Strnad M., Motyka V. (2011). Distribution, biological activities, metabolism, and the conceivable function of *cis*-zeatin-type cytokinins in plants. *Journal of Experimental Botany* 62(8): 2827-2840.

Gális I., Bilyeu K.D., Godinho M.J.G., Jameson P.E. (2005). Expression of three *Arabidopsis* cytokinin oxidase/dehydrogenase promoter::Gus chimeric constructs in tobacco: Response to developmental and biotic factors. *Plant Growth Regulation* 45(3): 173-182.

Gan S., Amasino R.M. (1995). Inhibition of leaf senescence by autoregulated production of cytokinin. *Science* 270(5244): 1986-1988.

Gilmartin P.M., Sarokin L., Memelink J., Chua N.H. (1990). Molecular light switches for plant genes. *The Plant Cell Online* 2(5): 369-378.

Großkinsky D.K., Naseem M., Abdelmohsen U.R., Plickert N., Engelke T., Griebel T., Zeier J., Novák O., Strnad M., Pfeifhofer H., van der Graaff E., Simon U., Roitsch T. (2011). Cytokinins mediate resistance against Pseudomonas syringae in tobacco through increased antimicrobial phytoalexin synthesis independent of salicylic acid signaling. *Plant Physiology* 157(2): 815-830.

Guiamet J.J., Schwartz E., Pichersky E., Nooden L.D. (1991). Characterization of cytoplasmic and nuclear mutations affecting chlorophyll and chlorophyll-binding proteins during senescence in soybean. *Plant Physiology* 96(1): 227-231.

Guo Y., Gan S. (2011). AtMYB2 regulates whole plant senescence by inhibiting cytokinin-mediated branching at late stages of development in *Arabidopsis*. *Plant Physiology* 156(3): 1612-1619.

Haberer G., Kieber J.J. (2002). Cytokinins. New insights into a classic phytohormone. *Plant Physiology* 128(2): 354-362.

Harman J.E., McDonald B. (1989). Controlled atmosphere storage of kiwifruit. Effect on fruit quality and composition. *Scientia Horticulturae* 37(4): 303-315.

Harpaz-Saad S., Azoulay T., Arazi T., Ben-Yaakov E., Mett A., Shiboleth Y.M., Hortensteiner S., Gidoni D., Gal-On A., Goldschmidt E.E., Eyal Y. (2007). Chlorophyllase is a rate-limiting enzyme in chlorophyll catabolism and is posttranslationally regulated. *Plant Cell* 19(3): 1007-1022.

Hellens R., Allan A., Friel E., Bolitho K., Grafton K., Templeton M., Karunairetnam S., Gleave A., Laing W. (2005). Transient expression vectors for functional genomics, quantification of promoter activity and RNA silencing in plants. *Plant Methods* 1(1): 13.

Hernandez Minana F.M., Primo Millo E., Primo Millo J. (1989). Endogenous cytokinins in developing fruits of seeded and seedless citrus cultivars. *Journal of Experimental Botany* 40(10): 1127-1134.

Heyl A., Schmülling T. (2003). Cytokinin signal perception and transduction. *Current Opinion in Plant Biology* 6(5): 480-488.

Higo K., Ugawa Y., Iwamoto M., Korenaga T. (1999). Plant cis-acting regulatory DNA elements (PLACE) database: 1999. *Nucleic Acids Research* 27(1): 297-300.

Higuchi M., Pischke M.S., Mähönen A.P., Miyawaki K., Hashimoto Y., Seki M., Kobayashi M., Shinozaki K., Kato T., Tabata S., Helariutta Y., Sussman M.R., Kakimoto T. (2004). *In planta* functions of the *Arabidopsis* cytokinin receptor family. *Proceedings of the National Academy of Sciences of the United States of America* 101(23): 8821-8826.

Hinder B., Schellenberg M., Rodoni S., Ginsburg S., Vogt E., Martinoia E., Matile P., Hortensteiner S. (1996). How plants dispose of chlorophyll catabolites. Directly energized uptake of tetrapyrrolic breakdown products into isolated vacuoles. *Journal of Biological Chemistry* 271(44): 27233-27236.

Hirose N., Takei K., Kuroha T., Kamada-Nobusada T., Hayashi H., Sakakibara H. (2008). Regulation of cytokinin biosynthesis, compartmentalization and translocation. *Journal of Experimental Botany* 59(1): 75-83.

Hirschberg J. (2001). Carotenoid biosynthesis in flowering plants. *Current Opinion in Plant Biology* 4(3): 210-218.

Hopping M.E. (1990). Chapter four: Floral biology, pollination and fruit set. In: Warrington, I.J. and Weston, G.C., *Kiwifruit: Science and management*. Ray Richards Publisher and New Zealand Society for Horticultural Science, Auckland.

Hörtensteiner S. (2006). Chlorophyll degradation during senescence. *Annual Review of Plant Biology* 57: 55-77.

Hörtensteiner S. (2009). Stay-green regulates chlorophyll and chlorophyll-binding protein degradation during senescence. *Trends in Plant Science* 14(3): 155-162.

Hoyerová K., Gaudinová A., Malbeck J., Dobrev P.I., Kocábek T., Solcová B., Trávnícková A., Kamínek M. (2006). Efficiency of different methods of extraction and purification of cytokinins. *Phytochemistry* 67(11): 1151-1159.

Hu W., Wang Y., Bowers C., Ma H. (2003). Isolation, sequence analysis, and expression studies of florally expressed cDNAs in *Arabidopsis*. *Plant Molecular Biology* 53(4): 545-563.

Hwang I., Sheen J. (2001). Two-component circuitry in *Arabidopsis* cytokinin signal transduction. *Nature* 413(6854): 383-389.

Iwahori S., Tominaga S., Yamasaki T. (1988). Stimulation of fruit growth of kiwifruit, *Actinidia chinensis* Planch., by N-(2-chloro-4-pyridyl)-N'-phenylurea, a diphenylurea-derivative cytokinin. *Scientia Horticulturae* 35(1–2): 109-115.

Jacob-Wilk D., Holland D., Goldschmidt E.E., Riov J., Eyal Y. (1999). Chlorophyll breakdown by chlorophyllase: Isolation and functional expression of the *Chlase1*

gene from ethylene-treated citrus fruit and its regulation during development. *The Plant Journal* 20(6): 653-661.

Jameson P.E. (2003). Regulators of growth | cytokinins. *Encyclopedia of applied plant sciences*. Academic Press, Oxford.

Jones R.J., Schreiber B.M.N. (1997). Role and function of cytokinin oxidase in plants. *Plant Growth Regulation* 23(1): 123-134.

Kakimoto T. (2001). Identification of plant cytokinin biosynthetic enzymes as dimethylallyl diphosphate:ATP/ADP isopentenyltransferases. *Plant and Cell Physiology* 42(7): 677-685.

Kaldis A.-D., Kousidis P., Kesanopoulos K., Prombona A. (2003). Light and circadian regulation in the expression of *LHY* and *Lhcb* genes in *phaseolus vulgaris*. *Plant Molecular Biology* 52(5): 981-997.

Kamada-Nobusada T., Sakakibara H. (2009). Molecular basis for cytokinin biosynthesis. *Phytochemistry* 70(4): 444-449.

Kim H.J., Ryu H., Hong S.H., Woo H.R., Lim P.O., Lee I.C., Sheen J., Nam H.G., Hwang I. (2006). Cytokinin-mediated control of leaf longevity by AHK3 through phosphorylation of ARR2 in *Arabidopsis*. *Proceedings of the National Academy of Sciences of the United States of America* 103(3): 814-819.

Kleber-Janke T., Krupinska K. (1997). Isolation of cDNA clones for genes showing enhanced expression in barley leaves during dark-induced senescence as well as during senescence under field conditions. *Planta* 203(3): 332-340.

Kudo T., Kiba T., Sakakibara H. (2010). Metabolism and long-distance translocation of cytokinins. *Journal of Integrative Plant Biology* 52(1): 53-60.

Kulaeva O.N., Burkhanova E.A., Karavaiko N.N., Selivankina S.Y., Porfirova S.A., Maslova G.G., Zemlyachenko Y.V., Börner T. (2002). Chloroplasts affect the leaf response to cytokinin. *Journal of Plant Physiology* 159(12): 1309-1316.

Kulaeva O.N., Karavaiko N.N., Selivankina S.Y., Moshkov I.E., Novikova G.V., Zemlyachenko Y.V., Shipilova S.V., Orudgev E.M. (1996). Cytokinin signalling systems. *Plant Growth Regulation* 18(1): 29-37.

Kusaba M., Ito H., Morita R., Iida S., Sato Y., Fujimoto M., Kawasaki S., Tanaka R., Hirochika H., Nishimura M., Tanaka A. (2007). Rice NON-YELLOW COLORING1 is involved in light-harvesting complex II and grana degradation during leaf senescence. *Plant Cell* 19(4): 1362-1375.

Lam E., Chua N.H. (1989). ASF-2: A factor that binds to the cauliflower mosaic virus 35S promoter and a conserved GATA motif in *Cab* promoters. *The Plant Cell Online* 1(12): 1147-1156.

Ledger S., Strayer C., Ashton F., Kay S.A., Putterill J. (2001). Analysis of the function of two circadian-regulated *CONSTANS-like* genes. *The Plant Journal* 26(1): 15-22.

Letham D.S. (1963). Regulators of cell division in plant tissues. *New Zealand Journal of Botany* 1(3): 336-350.

Lewis D.H., Burge G.K., Hopping M.E., Jameson P.E. (1996a). Cytokinins and fruit development in the kiwifruit (*Actinidia deliciosa*). II. Effects of reduced pollination and CPPU application. *Physiologia Plantarum* 98(1): 187-195.

Lewis D.H., Burge G.K., Schmierer D.M., Jameson P.E. (1996b). Cytokinins and fruit development in the kiwifruit (*Actinidia deliciosa*). I. Changes during fruit development. *Physiologia Plantarum* 98(1): 179-186.

Li G., Siddiqui H., Teng Y., Lin R., Wan X.-y., Li J., Lau O.-S., Ouyang X., Dai M., Wan J., Devlin P.F., Deng X.W., Wang H. (2011). Coordinated transcriptional regulation underlying the circadian clock in *Arabidopsis*. *Nature Cell Biology* 13(5): 616-622.

Lu S., Li L. (2008). Carotenoid metabolism: Biosynthesis, regulation, and beyond. *Journal of Integrative Plant Biology* 50(7): 778-785.

Lüscher B., Eisenman R.N. (1990). New light on Myc and Myb. Part II. Myb. *Genes & Development* 4(12b): 2235-2241.

Manzara T., Gruissem W. (1988). Organization and expression of the genes encoding ribulose-1,5-bisphosphate carboxylase in higher plants. *Photosynthesis Research* 16(1): 117-139.

McGhie T.K., Ainge G.D. (2002). Color in fruit of the genus *Actinidia*: Carotenoid and chlorophyll compositions. *Journal of Agricultural and Food Chemistry* 50(1): 117-121.

Meskauskiene R., Nater M., Goslings D., Kessler F., op den Camp R., Apel K. (2001). Flu: A negative regulator of chlorophyll biosynthesis in *Arabidopsis thaliana*. *Proceedings of the National Academy of Sciences of the United States of America* 98(22): 12826-12831.

Millar A.J., Kay S.A. (1996). Integration of circadian and phototransduction pathways in the network controlling *CAB* gene transcription in *Arabidopsis*. *Proceedings of the National Academy of Sciences* 93(26): 15491-15496.

Miyawaki K., Tarkowski P., Matsumoto-Kitano M., Kato T., Sato S., Tarkowska D., Tabata S., Sandberg G., Kakimoto T. (2006). Roles of *Arabidopsis* ATP/ADP isopentenyltransferases and tRNA isopentenyltransferases in cytokinin biosynthesis. *Proceedings of the National Academy of Sciences* 103(44): 16598-16603.

Moffatt B.A., Wang L., Allen M.S., Stevens Y.Y., Qin W., Snider J., von Schwartzenberg K. (2000). Adenosine kinase of *Arabidopsis*. Kinetic properties and gene expression. *Plant Physiology* 124(4): 1775-1785.

Mok D.W.S., Martin R.C., Shan X., Mok M.C. (2000). Genes encoding zeatin *O*-glycosyltransferases. *Plant Growth Regulation* 32(2): 285-287.

Mok D.W.S., Mok M.C. (2001). Cytokinin metabolism and action. *Annual Review of Plant Physiology and Plant Molecular Biology* 52(1): 89-118.

Mol J., Grotewold E., Koes R. (1998). How genes paint flowers and seeds. *Trends in Plant Science* 3(6): 212-217.

Montefiori M., McGhie T.K., Costa G., Ferguson A.R. (2005). Pigments in the fruit of red-fleshed kiwifruit (*Actinidia chinensis* and *Actinidia deliciosa*). *Journal of Agricultural and Food Chemistry* 53(24): 9526-9530.

Montefiori M., McGhie T.K., Hallett I.C., Costa G. (2009). Changes in pigments and plastid ultrastructure during ripening of green-fleshed and yellow-fleshed kiwifruit. *Scientia Horticulturae* 119(4): 377-387.

Morita R., Sato Y., Masuda Y., Nishimura M., Kusaba M. (2009). Defect in non-yellow coloring 3, an α/β hydrolase-fold family protein, causes a stay-green phenotype during leaf senescence in rice. *The Plant Journal* 59(6): 940-952.

Motyka V., Vaňková R., Čapková V., Petrášek J., Kamínek M., Schmülling T. (2003). Cytokinin-induced upregulation of cytokinin oxidase activity in tobacco includes changes in enzyme glycosylation and secretion. *Physiologia Plantarum* 117(1): 11-21.

Mur L.A.J., Aubry S., Mondhe M., Kingston-Smith A., Gallagher J., Timms-Taravella E., James C., Papp I., Hörtensteiner S., Thomas H., Ougham H. (2010). Accumulation of chlorophyll catabolites photosensitizes the hypersensitive response elicited by *Pseudomonas syringae* in *Arabidopsis*. *New Phytologist* 188(1): 161-174.

Nagaoka S., Takano T. (2003). Salt tolerance-related protein STO binds to a Myb transcription factor homologue and confers salt tolerance in *Arabidopsis*. *Journal of Experimental Botany* 54(391): 2231-2237.

Nakamura M., Tsunoda T., Obokata J. (2002). Photosynthesis nuclear genes generally lack TATA-boxes: A tobacco photosystem I gene responds to light through an initiator. *The Plant Journal* 29(1): 1-10.

Nishimura C., Ohashi Y., Sato S., Kato T., Tabata S., Ueguchi C. (2004). Histidine kinase homologs that act as cytokinin receptors possess overlapping functions in the regulation of shoot and root growth in *Arabidopsis*. *The Plant Cell Online* 16(6): 1365-1377.

Novák O., Hauserová E., Amakorová P., Dolezal K., Strnad M. (2008). Cytokinin profiling in plant tissues using ultra-performance liquid chromatography-electrospray tandem mass spectrometry. *Phytochemistry* 69(11): 2214-2224.

O'Keefe D., Song J., Jameson P. (2011). Isopentenyl transferase and cytokinin oxidase/dehydrogenase gene family members are differentially expressed during pod and seed development in rapid-cycling *Brassica*. *Journal of Plant Growth Regulation* 30(1): 92-99.

Ozga J., Reinecke D. (2003). Hormonal interactions in fruit development. *Journal of Plant Growth Regulation* 22(1): 73-81.

Park S.-Y., Yu J.-W., Park J.-S., Li J., Yoo S.-C., Lee N.-Y., Lee S.-K., Jeong S.-W., Seo H.S., Koh H.-J., Jeon J.-S., Park Y.-I., Paek N.-C. (2007). The senescence-induced staygreen protein regulates chlorophyll degradation. *Plant Cell* 19(5): 1649-1664.

Patterson K.J., Mason K.A., Gould K.S. (1993). Effects of CPPU (N-(2-chloro-4-pyridyl)-N'-phenylurea) on fruit growth, maturity, and storage quality of kiwifruit. *New Zealand Journal of Crop and Horticultural Science* 21(3): 253-261.

Piechulla B., Merforth N., Rudolph B. (1998). Identification of tomato *Lhc* promoter regions necessary for circadian expression. *Plant Molecular Biology* 38(4): 655-662.

Planchais S., Perennes C., Glab N., Mironov V., Inzé D., Bergounioux C. (2002). Characterization of *cis*-acting element involved in cell cycle phase-independent activation of Arath;*CycB1*;1 transcription and identification of putative regulatory proteins. *Plant Molecular Biology* 50(1): 109-125.

Porra R.J., Thompson W.A., Kriedemann P.E. (1989). Determination of accurate extinction coefficients and simultaneous equations for assaying chlorophylls *a* and *b* extracted with four different solvents: Verification of the concentration of chlorophyll standards by atomic absorption spectroscopy. *Biochimica et Biophysica Acta (BBA) - Bioenergetics* 975(3): 384-394.

Quesnelle P.E., Emery R.J.N. (2007). *cis*-cytokinins that predominate in *Pisum sativum* during early embryogenesis will accelerate embryo growth *in vitro*. *Canadian Journal of Botany* 85(1): 91-103.

Rashotte A.M., Mason M.G., Hutchison C.E., Ferreira F.J., Schaller G.E., Kieber J.J. (2006). A subset of *Arabidopsis* AP2 transcription factors mediates cytokinin responses in concert with a two-component pathway. *Proceedings of the National Academy of Sciences* 103(29): 11081-11085.

Reid M.S., Heatherbell D.A., Pratt H.K. (1982). Seasonal patterns in chemical composition of the fruit of *Actinidia chinensis. Journal of the American Society for Horticultural Science* 107: 316-319.

Reyes J.C., Muro-Pastor M.I., Florencio F.J. (2004). The GATA family of transcription factors in *Arabidopsis* and rice. *Plant Physiology* 134(4): 1718-1732.

Richmond A.E., Lang A. (1957). Effect of kinetin on protein content and survival of detached *Xanthium* leaves. *Science* 125(3249): 650-a-651.

Riefler M., Novak O., Strnad M., Schmülling T. (2006). *Arabidopsis* cytokinin receptor mutants reveal functions in shoot growth, leaf senescence, seed size, germination, root development, and cytokinin metabolism. *The Plant Cell Online* 18(1): 40-54.

Rivero R.M., Kojima M., Gepstein A., Sakakibara H., Mittler R., Gepstein S., Blumwald E. (2007). Delayed leaf senescence induces extreme drought tolerance in a flowering plant. *Proceedings of the National Academy of Sciences* 104(49): 19631-19636.

Robson P.R.H., Donnison I.S., Wang K., Frame B., Pegg S.E., Thomas A., Thomas H. (2004). Leaf senescence is delayed in maize expressing the *Agrobacterium IPT* gene under the control of a novel maize senescence-enhanced promoter. *Plant Biotechnology Journal* 2(2): 101-112.

Rodoni S., Muhlecker W., Anderl M., Krautler B., Moser D., Thomas H., Matile P., Hortensteiner S. (1997). Chlorophyll breakdown in senescent chloroplasts (cleavage of pheophorbide *a* in two enzymic steps). *Plant Physiology* 115(2): 669-676.

Ross E.J.H., Stone J.M., Elowsky C.G., Arredondo-Peter R., Klucas R.V., Sarath G. (2004). Activation of the *Oryza sativa* non-symbiotic haemoglobin-2 promoter by the cytokinin-regulated transcription factor, ARR1. *Journal of Experimental Botany* 55(403): 1721-1731.

Rubio-Somoza I., Martinez M., Abraham Z., Diaz I., Carbonero P. (2006). Ternary complex formation between HvMYBS3 and other factors involved in transcriptional control in barley seeds. *The Plant Journal* 47(2): 269-281.

Rüdiger W. (2002). Biosynthesis of chlorophyll *b* and the chlorophyll cycle. *Photosynthesis Research* 74(2): 187-193.

Sakai H., Aoyama T., Oka A. (2000). *Arabidopsis* ARR1 and ARR2 response regulators operate as transcriptional activators. *The Plant Journal* 24(6): 703-711.

Sakakibara H. (2006). Cytokinins: Activity, biosynthesis, and translocation. *Annual Review of Plant Biology* 57(1): 431-449.

Sakamoto T., Sakakibara H., Kojima M., Yamamoto Y., Nagasaki H., Inukai Y., Sato Y., Matsuoka M. (2006). Ectopic expression of knotted1-like homeobox protein induces expression of cytokinin biosynthesis genes in rice. *Plant Physiology* 142(1): 54-62.

Santos-Rosa M., Poutaraud A., Merdinoglu D., Mestre P. (2008). Development of a transient expression system in grapevine *via* agro-infiltration. *Plant Cell Reports* 27(6): 1053-1063.

Sato Y., Morita R., Katsuma S., Nishimura M., Tanaka A., Kusaba M. (2009). Two short-chain dehydrogenase/reductases, NON-YELLOW COLORING 1 and NYC1-LIKE, are required for chlorophyll *b* and light-harvesting complex II degradation during senescence in rice. *The Plant Journal* 57(1): 120-131.

Sato Y., Morita R., Nishimura M., Yamaguchi H., Kusaba M. (2007). Mendel's green cotyledon gene encodes a positive regulator of the chlorophyll-degrading pathway. *Proceedings of the National Academy of Sciences* 104(35): 14169-14174.

Schelbert S., Aubry S., Burla B., Agne B., Kessler F., Krupinska K., Hortensteiner S. (2009). Pheophytin pheophorbide hydrolase (pheophytinase) is involved in chlorophyll breakdown during leaf senescence in *Arabidopsis*. *Plant Cell* 21(3): 767-785.

Schenk N., Schelbert S., Kanwischer M., Goldschmidt E.E., Dörmann P., Hörtensteiner S. (2007). The chlorophyllases AtCLH1 and AtCLH2 are not essential for senescence-

related chlorophyll breakdown in *Arabidopsis thaliana*. *FEBS Letters* 581(28): 5517-5525.

Schmülling T., Werner T., Riefler M., Krupková E., Bartrina y Manns I. (2003). Structure and function of cytokinin oxidase/dehydrogenase genes of maize, rice, *Arabidopsis* and other species. *Journal of Plant Research* 116(3): 241-252.

Seymour G., Poole M., Manning K., King G.J. (2008). Genetics and epigenetics of fruit development and ripening. *Current Opinion in Plant Biology* 11(1): 58-63.

Shabala S., Shabala L., Van Volkenburgh E., Newman I. (2005). Effect of divalent cations on ion fluxes and leaf photochemistry in salinized barley leaves. *Journal of Experimental Botany* 56(415): 1369-1378.

Shi X., Gupta S., Rashotte A.M. (2012). *Solanum lycopersicum cytokinin response factor* (*SlCRF*) genes: Characterization of CRF domain-containing ERF genes in tomato. *Journal of Experimental Botany* 63(2): 973-982.

Shi X., Rashotte A. (2012). Advances in upstream players of cytokinin phosphorelay: Receptors and histidine phosphotransfer proteins. *Plant Cell Reports*: 1-11.

Simpson S.D., Nakashima K., Narusaka Y., Seki M., Shinozaki K., Yamaguchi-Shinozaki K. (2003). Two different novel *cis*-acting elements of *erd1*, a *clpA* homologous *Arabidopsis* gene function in induction by dehydration stress and dark-induced senescence. *The Plant Journal* 33(2): 259-270.

Spreitzer R.J. (2003). Role of the small subunit in ribulose-1,5-bisphosphate carboxylase/oxygenase. *Archives of Biochemistry and Biophysics* 414(2): 141-149.

Suarez-Lopez P., Wheatley K., Robson F., Onouchi H., Valverde F., Coupland G. (2001). *CONSTANS* mediates between the circadian clock and the control of flowering in *Arabidopsis*. *Nature* 410(6832): 1116-1120.

Symons G., Reid J. (2003). Interactions between light and plant hormones during de-etiolation. *Journal of Plant Growth Regulation* 22(1): 3-14.

Takahashi S., Shudo K., Okamoto T., Yamada K., Isogai Y. (1978). Cytokinin activity of n-phenyl-n′-(4-pyridyl)urea derivatives. *Phytochemistry* 17(8): 1201-1207.

Takamiya K.-i., Tsuchiya T., Ohta H. (2000). Degradation pathway(s) of chlorophyll: What has gene cloning revealed? *Trends in Plant Science* 5(10): 426-431.

Takei K., Sakakibara H., Sugiyama T. (2001). Identification of genes encoding adenylate isopentenyltransferase, a cytokinin biosynthesis enzyme, in *Arabidopsis thaliana*. *Journal of Biological Chemistry* 276(28): 26405-26410.

Tamagnone L., Merida A., Parr A., Mackay S., Culianez-Macia F.A., Roberts K., Martin C. (1998). The AmMYB308 and AmMYB330 transcription factors from Antirrhinum regulate phenylpropanoid and lignin biosynthesis in transgenic tobacco. *The Plant Cell Online* 10(2): 135-154.

Tamura K., Dudley J., Nei M., Kumar S. (2007). MEGA4: Molecular evolutionary genetics analysis (MEGA) software version 4.0. *Molecular Biology and Evolution* 24(8): 1596-1599.

Tanaka A., Tanaka R. (2006). Chlorophyll metabolism. *Current Opinion in Plant Biology* 9(3): 248-255.

Tanaka Y., Sasaki N., Ohmiya A. (2008). Biosynthesis of plant pigments: Anthocyanins, betalains and carotenoids. *The Plant Journal* 54(4): 733-749.

Tang W., Perry S.E. (2003). Binding site selection for the plant MADS domain protein AGL15. *Journal of Biological Chemistry* 278(30): 28154-28159.

Teakle G.R., Manfield I.W., Graham J.F., Gilmartin P.M. (2002). *Arabidopsis thaliana* GATA factors: Organisation, expression and DNA-binding characteristics. *Plant Molecular Biology* 50(1): 43-56.

Terzaghi W.B., Cashmore A.R. (1995). Light-regulated transcription. *Annual Review of Plant Physiology and Plant Molecular Biology* 46(1): 445-474.

Thomas H., Howarth C.J. (2000). Five ways to stay green. *Journal of Experimental Botany* 51(s1): 329-337.

Thomas H., Ougham H.J., Wagstaff C., Stead A.D. (2003). Defining senescence and death. *Journal of Experimental Botany* 54(385): 1127-1132.

Thum K.E., Kim M., Morishige D.T., Eibl C., Koop H.-U., Mullet J.E. (2001). Analysis of barley chloroplast *psbD* light-responsive promoter elements in transplastomic tobacco. *Plant Molecular Biology* 47(3): 353-366.

Tjaden G., Edwards J.W., Coruzzi G.M. (1995). *cis* elements and *trans*-acting factors affecting regulation of a nonphotosynthetic light-regulated gene for chloroplast glutamine synthetase. *Plant Physiology* 108(3): 1109-1117.

To J.P.C., Kieber J.J. (2008). Cytokinin signaling: Two-components and more. *Trends in Plant Science* 13(2): 85-92.

Tottey S., Block M.A., Allen M., Westergren T., Albrieux C., Scheller H.V., Merchant S., Jensen P.E. (2003). *Arabidopsis* CHL27, located in both envelope and thylakoid membranes, is required for the synthesis of protochlorophyllide. *Proceedings of the National Academy of Sciences of the United States of America* 100(26): 16119-16124.

Tsuchiya T., Ohta H., Okawa K., Iwamatsu A., Shimada H., Masuda T., Takamiya K.-I. (1999). Cloning of chlorophyllase, the key enzyme in chlorophyll degradation: Finding of a lipase motif and the induction by methyl jasmonate. *Proceedings of the National Academy of Sciences of the United States of America* 96(26): 15362-15367.

Ujwal M.L., McCormac A.C., Goulding A., Madan Kumar A., Söll D., Terry M.J. (2002). Divergent regulation of the *HEMA* gene family encoding glutamyl-tRNA reductase in *Arabidopsis thaliana*: Expression of *HEMA2* is regulated by sugars, but is independent of light and plastid signalling. *Plant Molecular Biology* 50(1): 81-89.

Urao T., Yamaguchi-Shinozaki K., Urao S., Shinozaki K. (1993). An *Arabidopsis myb* homolog is induced by dehydration stress and its gene product binds to the conserved MYB recognition sequence. *The Plant Cell Online* 5(11): 1529-1539.

Veley K.M., Michaels S.D. (2008). Functional redundancy and new roles for genes of the autonomous floral-promotion pathway. *Plant Physiology* 147(2): 682-695.

Villain P., Mache R., Zhou D.-X. (1996). The mechanism of GT element-mediated cell type-specific transcriptional control. *Journal of Biological Chemistry* 271(51): 32593-32598.

Voinnet O., Rivas S., Mestre P., Baulcombe D. (2003). An enhanced transient expression system in plants based on suppression of gene silencing by the p19 protein of tomato bushy stunt virus. *The Plant Journal* 33(5): 949-956.

Vyroubalová S., Václavíková K., Turecková V., Novák O., Smehilová M., Hluska T., Ohnoutková L., Frébort I., Galuszka P. (2009). Characterization of new maize genes putatively involved in cytokinin metabolism and their expression during osmotic stress in relation to cytokinin levels. *Plant Physiology* 151(1): 433-447.

Wagstaff C., Yang T.J.W., Stead A.D., Buchanan-Wollaston V., Roberts J.A. (2009). A molecular and structural characterization of senescing *Arabidopsis* siliques and comparison of transcriptional profiles with senescing petals and leaves. *The Plant Journal* 57(4): 690-705.

Wang M., Wang G., Ji J., Wang J. (2009). The effect of *pds* gene silencing on chloroplast pigment composition, thylakoid membrane structure and photosynthesis efficiency in tobacco plants. *Plant Science* 177(3): 222-226.

Wang Y., Zhang W.-Z., Song L.-F., Zou J.-J., Su Z., Wu W.-H. (2008). Transcriptome analyses show changes in gene expression to accompany pollen germination and tube growth in *Arabidopsis*. *Plant Physiology* 148(3): 1201-1211.

Wang Z.Y., Kenigsbuch D., Sun L., Harel E., Ong M.S., Tobin E.M. (1997). A Myb-related transcription factor is involved in the phytochrome regulation of an *Arabidopsis Lhcb* gene. *The Plant Cell Online* 9(4): 491-507.

Warrington I.J., Weston G.C. (1990). Kiwifruit: Science and management. New Zealand Society for Horticultural Science, Palmerston North.

Wenkel S., Turck F., Singer K., Gissot L., Le Gourrierec J., Samach A., Coupland G. (2006). CONSTANS and the CCAAT box binding complex share a functionally important domain and interact to regulate flowering of *Arabidopsis*. *The Plant Cell Online* 18(11): 2971-2984.

Werner T., Schmülling T. (2009). Cytokinin action in plant development. *Current Opinion in Plant Biology* 12(5): 527-538.

William D.A., Su Y., Smith M.R., Lu M., Baldwin D.A., Wagner D. (2004). Genomic identification of direct target genes of LEAFY. *Proceedings of the National Academy of Sciences of the United States of America* 101(6): 1775-1780.

Wingler A., von Schaewen A., Leegood R.C., Lea P.J., Paul Quick W. (1998). Regulation of leaf senescence by cytokinin, sugars, and light. *Plant Physiology* 116(1): 329-335.

Wulfetange K., Saenger W., Schmülling T., Heyl A. (2011). *E. Coli*-based cell-free expression, purification and characterization of the membrane-bound ligand-binding CHASE-TM domain of the cytokinin receptor CRE1/AHK4 of *Arabidopsis thaliana*. *Molecular Biotechnology* 47(3): 211-219.

Xie Z., Li D., Wang L., Sack F.D., Grotewold E. (2010). Role of the stomatal development regulators FLP/MYB88 in abiotic stress responses. *The Plant Journal* 64(5): 731-739.

Yamasato A., Nagata N., Tanaka R., Tanaka A. (2005). The N-terminal domain of chlorophyllide *a* oxygenase confers protein instability in response to chlorophyll *b* accumulation. *Plant Cell*: tpc.105.031518.

Zavaleta-Mancera H.A., López-Delgado H., Loza-Tavera H., Mora-Herrera M., Trevilla-García C., Vargas-Suárez M., Ougham H. (2007). Cytokinin promotes catalase and ascorbate peroxidase activities and preserves the chloroplast integrity during dark-senescence. *Journal of Plant Physiology* 164(12): 1572-1582.

Żelisko A., García-Lorenzo M., Jackowski G., Jansson S., Funk C. (2005). AtFtsH6 is involved in the degradation of the light-harvesting complex II during high-light acclimation and senescence. *Proceedings of the National Academy of Sciences of the United States of America* 102(38): 13699-13704.

Zhang P., Wang W.-Q., Zhang G.-L., Kaminek M., Dobrev P., Xu J., Gruissem W. (2010). Senescence-inducible expression of isopentenyl transferase extends leaf life, increases drought stress resistance and alters cytokinin metabolism in cassava. *Journal of Integrative Plant Biology* 52(7): 653-669.

Zhou D.-X. (1999). Regulatory mechanism of plant gene transcription by GT-elements and GT-factors. *Trends in Plant Science* 4(6): 210-214.

Zhu Y., Li Z., Xu B., Li H., Wang L., Dong A., Huang H. (2008). Subcellular localizations of AS1 and AS2 suggest their common and distinct roles in plant development. *Journal of Integrative Plant Biology* 50(7): 897-905.

Zubo Y.O., Yamburenko M.V., Selivankina S.Y., Shakirova F.M., Avalbaev A.M., Kudryakova N.V., Zubkova N.K., Liere K., Kulaeva O.N., Kusnetsov V.V., Borner

T. (2008). Cytokinin stimulates chloroplast transcription in detached barley leaves. *Plant Physiology* 148(2): 1082-1093.

9. APPENDIX

9.1 Expression analysis

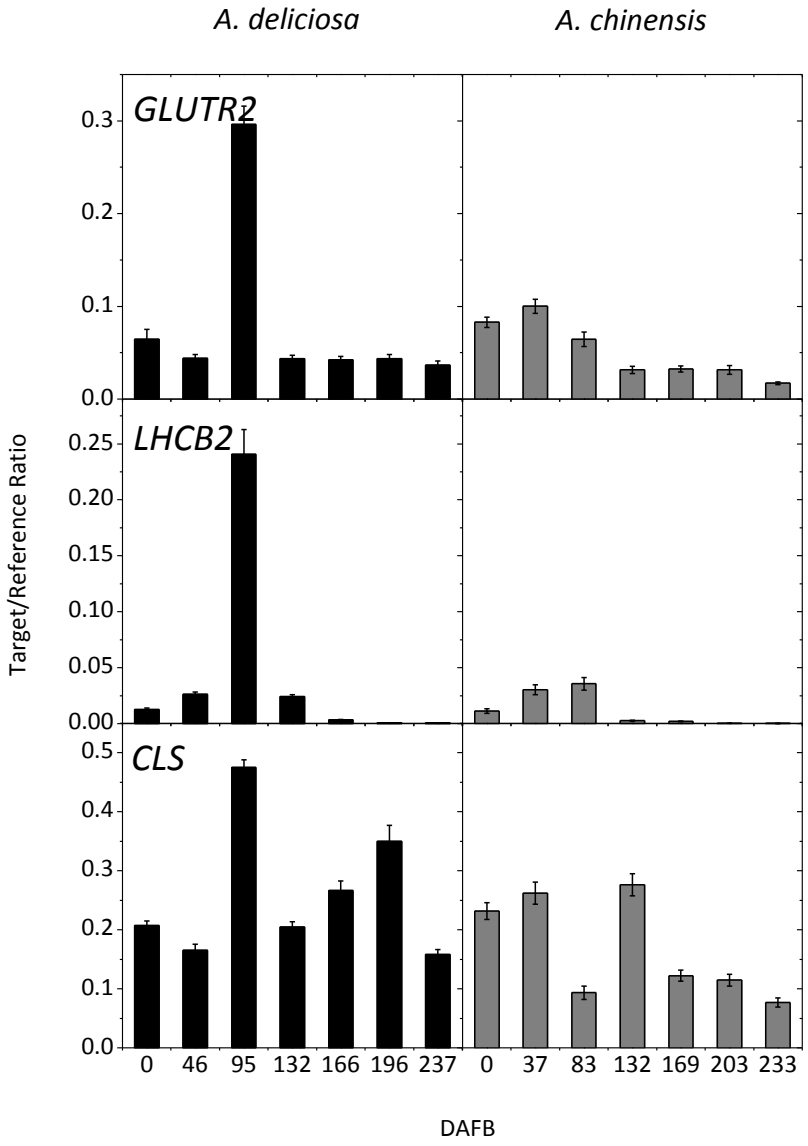

Figure 9.1. Expression of additional chlorophyll biosynthetic and photosynthesis-associated genes in *A. chinensis* and *A. deliciosa* fruit over development in 2009. Expression of chlorophyll biosynthetic pathway and photosynthesis-associated genes (see Table 3.2 for abbreviations) in *A. deliciosa* (left panels, black bars) and *A. chinensis* (right panels, grey bars) over fruit development (days after full bloom; DAFB), measured as a target/reference ratio. Error bars indicate standard error (n=4).

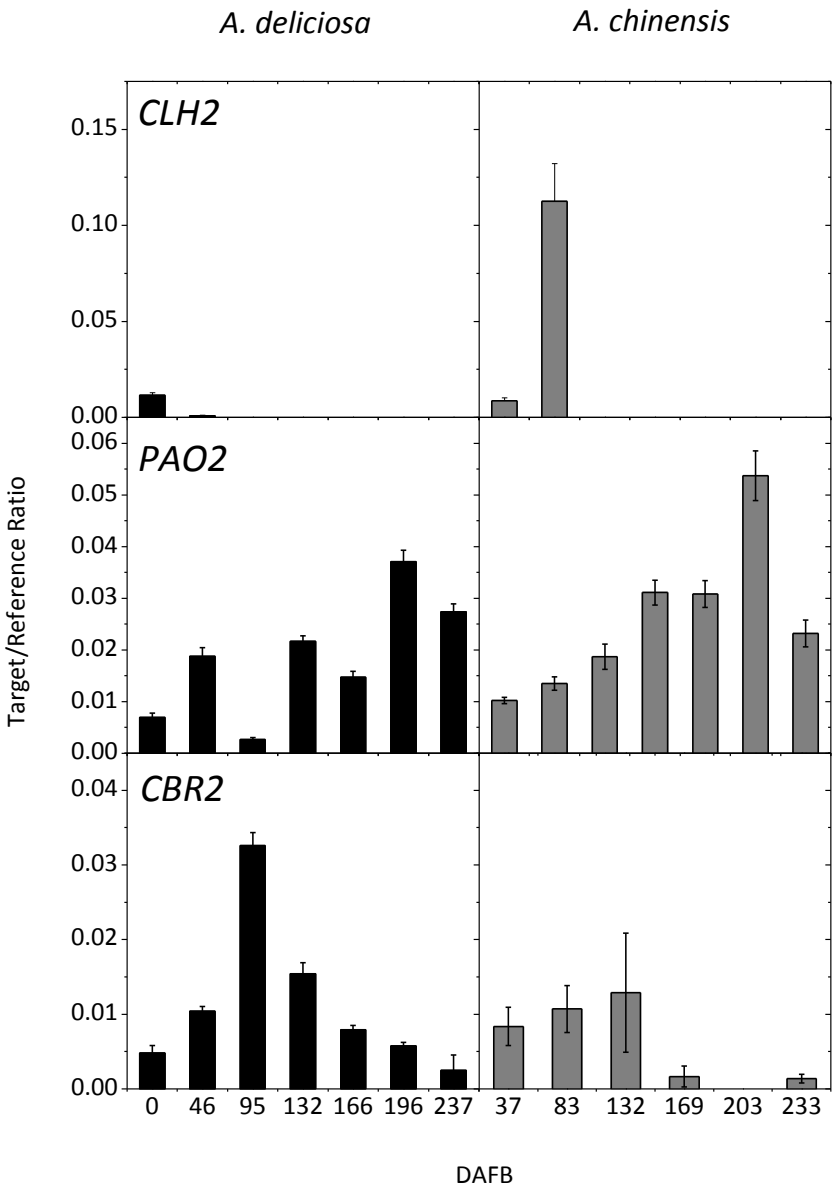

Figure 9.2. Expression of additional chlorophyll degradation genes in *A. chinensis* and *A. deliciosa* fruit over development in 2009. Expression of chlorophyll degradation pathway genes (see Table 3.2 for abbreviations) in *Actinidia deliciosa* (left panels, black bars) and *A. chinensis* (right panels, grey bars) over fruit development (days after full bloom; DAFB), measured as a target/reference ratio. Error bars indicate standard error (n=4).

9.2 Measuring cytokinin concentrations

9.2.1 Measuring cytokinin concentrations in kiwifruit using FT-ICR-LC-MS/MS

Cytokinins were extracted from kiwifruit tissue as described in Chapter Two. FT-ICR-LC-MS/MS was initially conducted on two fruit samples, *A. chinensis* at 246 DAFB and *A. deliciosa* at 203 DAFB from 2010. A representative spectrum of the *A. chinensis* sample is shown in Figure 9.3a, and a selected area of the spectrum showing the zeatin peak is shown in Figure 9.3b. These results show that zeatin can be detected in kiwifruit samples using FT-ICR-LC-MS/MS. However, the deuterated standards used were difficult to detect, even at relatively high concentrations, which made quantification difficult. Despite this, it was still possible to estimate cytokinin levels from the ratio of deuterated zeatin to endogenous zeatin. Peak areas were converted to concentration using the known concentration of deuterated zeatin standard (Figure 9.4). Initial results from the two kiwifruit samples showed that there was a higher concentration of zeatin in *A chinensis* than in *A. deliciosa*. However, these results are much higher than reported in the literature for *A. deliciosa*. Even though FT-ICR-FT-ICR mass analysers have excellent mass resolution, they are not typically used for quantitation, compared with quadrupole mass analysers.

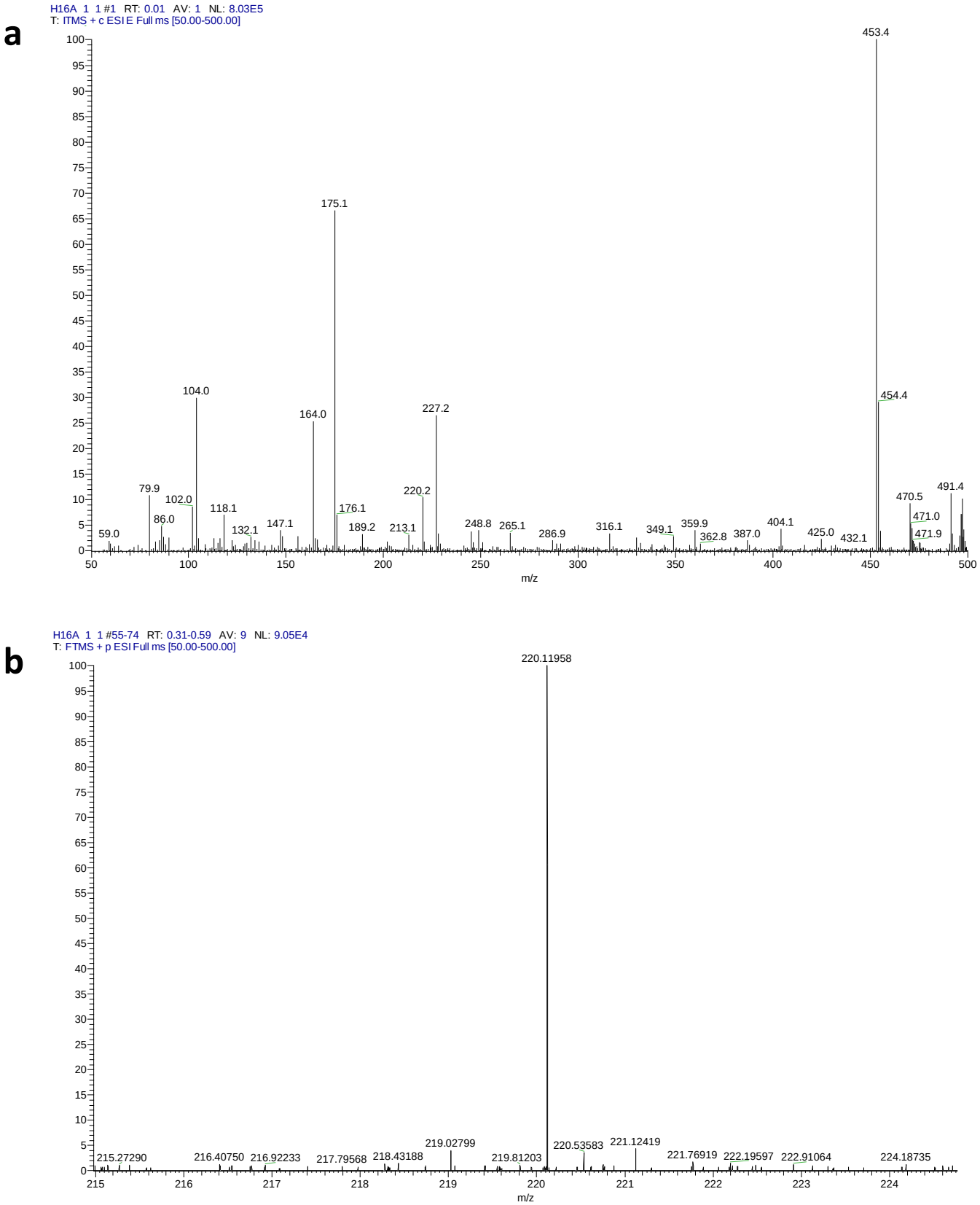

Figure 9.3. Representative FT-ICR-LC-MS/MS spectra of an *A. chinensis* sample. FT-ICR-LC-MS/MS spectrum of *A. chinensis* at 246 DAFB following cytokinin extraction (a). Selected area of the spectrum showing the peak corresponding to zeatin at a mass of 220.1958 (b).

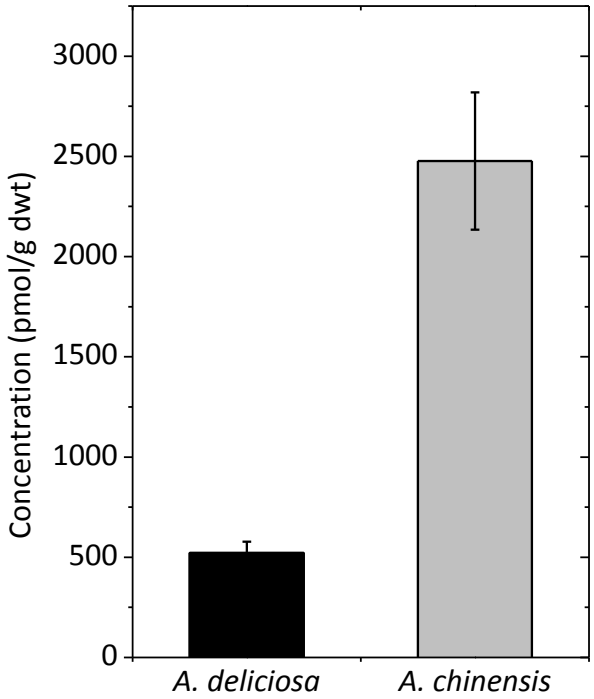

Figure 9.4. FT-ICR-LC-MS/MS concentration results of *A. deliciosa* and *A. chinensis*. The FT-ICR-LC-MS/MS results for zeatin levels in *A. deliciosa* (black bars) and *A. chinensis* (grey bars) were calculated from the relative levels of zeatin standard and deuterated cytokinin. Error bars are standard error (n=3).

Because FT-ICR-LC-MS/MS can only provide an estimate of concentration, it is not the most appropriate method for measuring cytokinin levels in kiwifruit, and triple quadrupole LC-MS/MS was used for further experiments.

9.2.2 Measuring cytokinin concentrations in kiwifruit using triple quadrupole LC-MS/MS

A triple quadrupole LC-MS/MS was available for use at Plant & Food Research, Ruakura, with the kind help of Janine Cooney. The same kiwifruit samples were analysed to measure trans-zeatin concentration, where an internal deuterated standard was used. Results from the triple quadrupole analysis showed that the zeatin standard was able to be detected at the required resolution (Figure 9.5).

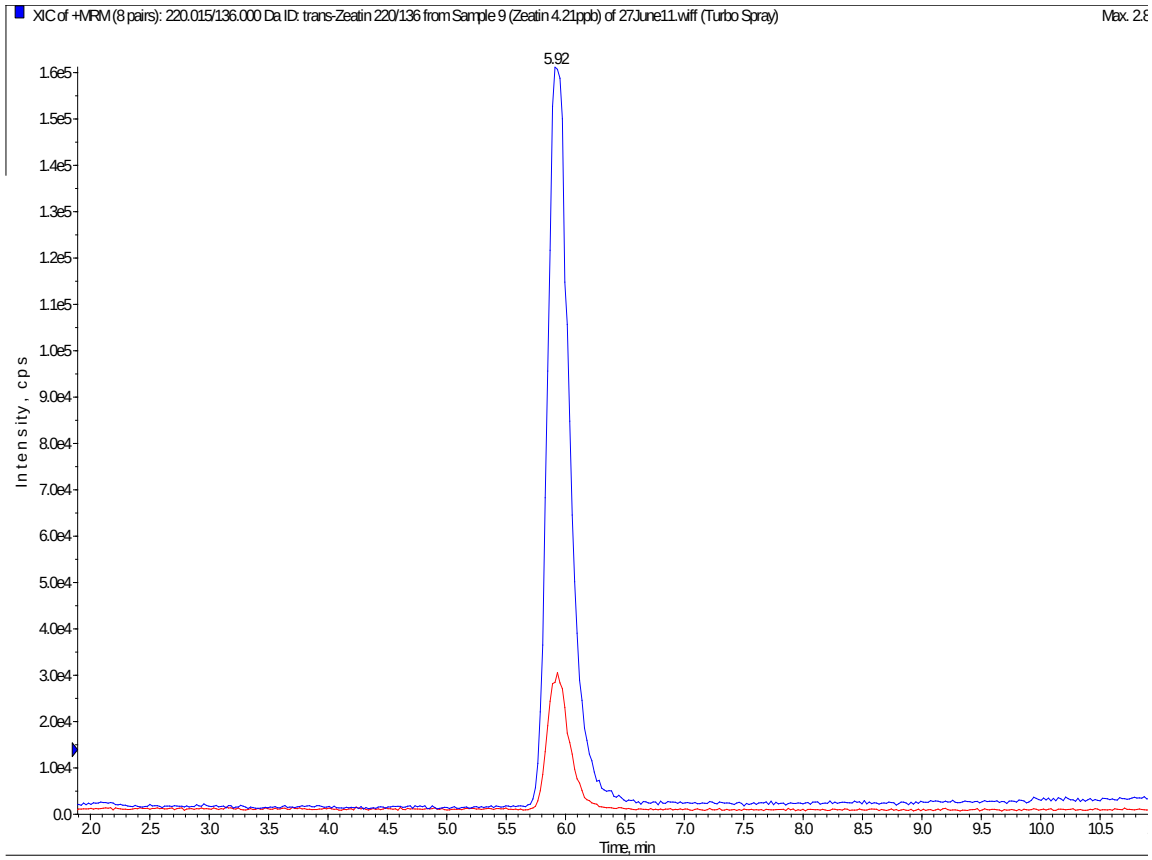

Figure 9.5. Triple quadrupole LC-MS/MS spectra of zeatin standard. Triple quadrupole LC-MS/MS spectra of trans-zeatin standard, tZ, (10µM) against the theoretical mass spectrum (red).

However, when the zeatin standard was run using deuterated zeatin as an internal standard, two deuterated zeatin peaks were observed. Thus this standard was not appropriate for further experiments. The cytokinin samples were therefore measured by triple quadrupole LC-MS/MS by Neil Emery's laboratory at Trent University, Canada, where the whole suite of cytokinin standards was available, providing a more thorough analysis of cytokinin levels.

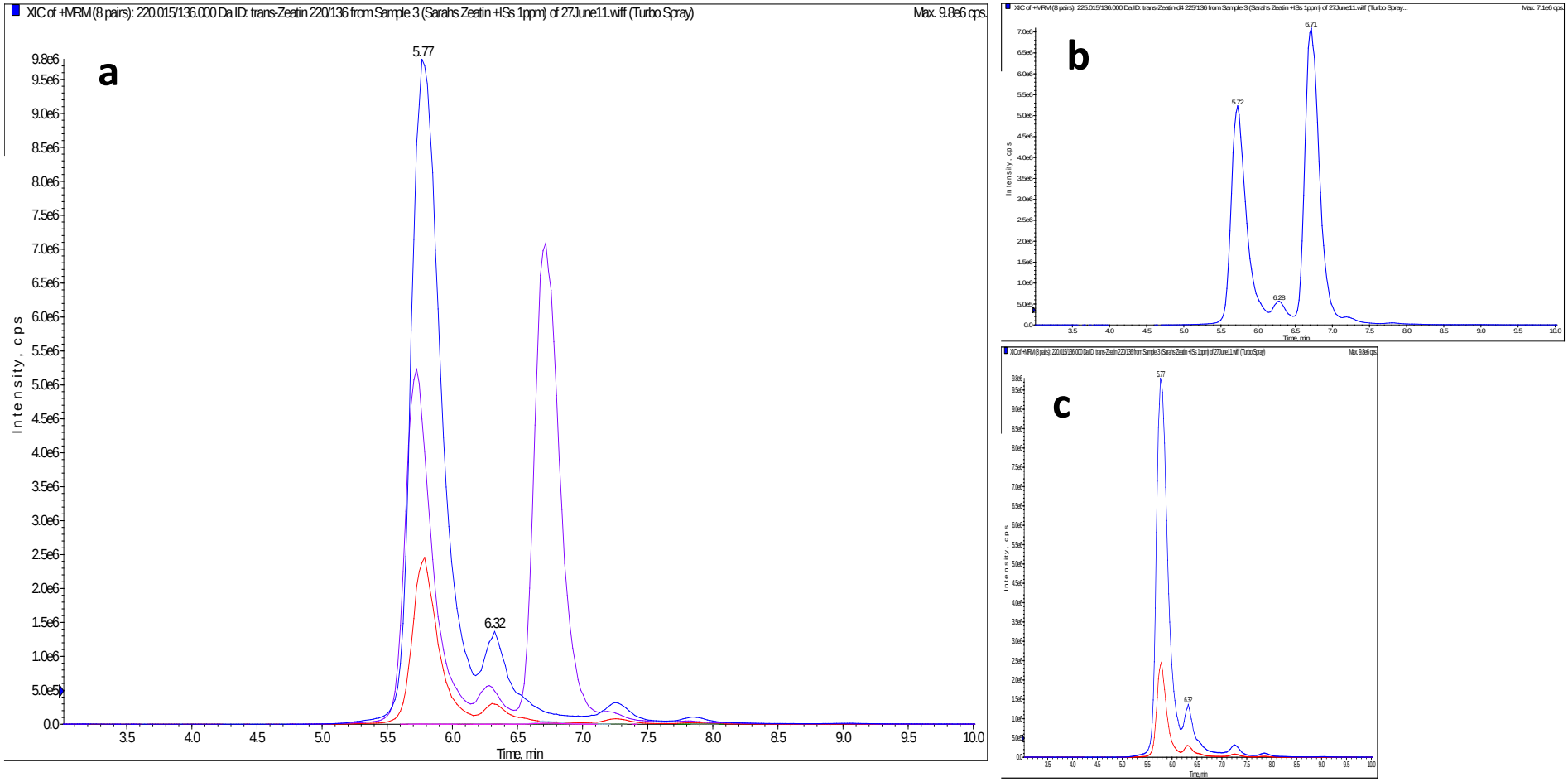

Figure 9.6. Triple quadrupole LC-MS/MS spectra of trans-zeatin standard and d_5-trans-zeatin. Triple quadrupole LC-MS/MS spectra of trans-zeatin standard, tZ, (10µM) (blue), with the deuterated trans-zeatin, d_5-tZ, (100 pmol) (purple) against the theoretical mass spectrum (red) (a). The individual spectra of d_5-tZ (b) and the tZ standard (c) are also provided.

9.2.3 Sample extraction for HPLC-MS/MS as performed by Amy Galer, Trent University

The extraction method was employed as described previously in Quesnelle and Emery (2007) with minor modifications. The biological samples were homogenised to a powder with liquid nitrogen in a mortar and pestle and freeze-dried. The samples were weighed and extracted in 1 ml cold modified Bieleski's solvent (methanol/water/formic acid: 75/20/5, v/v/v). The tissue samples were then spiked with 10 ng of labelled internal cytokinin standard mix ($^2H_7$BA, $^2H_7$[9R]cBA, $^2H_5$ZOG, $^2H_5$DHZOG, $^2H_5$[9R]ZOG, $^2H_5$[9R]DHZOG, $^2H_6$iP7G, $^2H_5$Z9G, $^2H_5$MeSZ, $^2H_6$MeSiP, $^2H_5$[9R]MeZ, $^2H_5$[9R]MeSiP, $^2H_6$[9R]iP, $^2H_5$[9R]Z, $^2H_3$[9R]DHZ, $^2H_6$iP, $^2H_3$DHZ, $^2H_6$Z, $^2H_6$iPMP, $^2H_6$ZRMP and $^2H_6$DHZRMP) (OlchemIm Ltd., Czech Republic) and 150 ng of labelled internal ABA standard ($^2H_4$ABA) (Plant Biotechnology Institute, Canada). Samples were vortexed, sonicated for one min and allowed to further passively extract overnight (approximately 12 h) at -20 ºC. After extraction, samples were centrifuged at 8,400 x *g* for 10 min and the supernatants transferred to 1.5 ml microcentrifuge tubes. Supernatants were dried using a speed vacuum concentrator at ambient temperature (UVS400, Thermo Fisher Scientific, USA).

9.2.4 Column purification and HPLC-MS/MS conditions as performed by Amy Galer, Trent University

Extraction residues were reconstituted in 1 ml of 1 M formic acid to ensure complete protonation of all cytokinins. Each extract was purified on a mixed mode, reverse-phase, cation-exchange cartridge (Oasis MCX 6cc; Waters, Canada). Cartridges were activated using 5 ml of methanol and equilibrated using 5 ml of 1 M formic acid. After equilibration, the sample was loaded and washed with 5 ml of 1 M formic acid. First, ABA was eluted using 5 ml of methanol. Nucleotide forms of cytokinin were eluted second using 5 ml of 0.35 M ammonium hydroxide. Lastly, cytokinin free base, ribosides and glucosides were eluted using 5 ml of 0.35 M ammonium hydroxide in 60% (v/v) methanol. All samples were evaporated to dryness in a speed vacuum concentrator at ambient temperature and subsequently stored at -20 °C.

Because it was not possible to measure cytokinin nucleotides directly, the nucleotides were dephosphorylated to form ribosides using 3.4 units of bacterial alkaline phosphatase (Sigma, Oakville, Ontario) in 1 ml of 0.1 M ethanolamine-HCL (pH 10.4) for 12 h at 37 °C. The resulting cytokinin ribosides were brought to dryness in a speed vacuum concentrator at ambient temperature. The dephosphorylated nucleotides were reconstituted in 1.5 ml of water for further purification on a reversed-phase C18 column (Oasis C18 3cc; Waters, Canada). Columns were activated using 3 ml of methanol and equilibrated with 6 ml of water. The samples were loaded onto the C18 cartridge and passed through the column under gravity. The sorbent was washed with 3 ml of water and analytes were eluted using 1.5 ml of methanol:water (80:20 v/v). All sample eluents were dried in a speed vacuum concentrator at ambient temperature and stored at -20 °C until analysis. Prior to mass spectrometric analysis, as described previously (Allison Hayward, PhD Thesis, University of Trent, 2011), ABA, cytokinin nucleotide, and cytokinin riboside and free bases fractions were reconstituted with 1 ml of HPLC mobile phase starting conditions (95:5 water:methanol with 0.08% (v/v) acetic acid) and transferred to glass auto-sampler vials. Samples were stored at 4 °C until analysis.

9.3 Promoter PLACE analysis

Table 9.1. Raw PLACE analysis of *RBCS*, *PAO* and *SGR* promoters.

RBCS PROMOTER

Factor or Site Name	Location	(+) or (-)	Signal Sequence
-10PEHVPSBD	703	(-)	TATTCT
-300CORE	567	(+)	TGTAAAG
-300CORE	1014	(+)	TGTAAAG
-300ELEMENT	143	(-)	TGHAAARK
ABREATCONSENSUS	837	(-)	YACGTGGC
ABRELATERD1	840	(+)	ACGTG
ABRELATERD1	623	(-)	ACGTG
ABRELATERD1	839	(-)	ACGTG
ABRERATCAL	838	(-)	MACGYGB
ACGTABREMOTIFA2OSEM	837	(-)	ACGTGKC
ACGTATERD1	624	(+)	ACGT
ACGTATERD1	663	(+)	ACGT
ACGTATERD1	840	(+)	ACGT
ACGTATERD1	624	(-)	ACGT
ACGTATERD1	663	(-)	ACGT
ACGTATERD1	840	(-)	ACGT
ANAERO1CONSENSUS	1135	(+)	AAACAAA
ANAERO1CONSENSUS	1111	(-)	AAACAAA
ARR1AT	1160	(+)	NGATT
ARR1AT	467	(+)	NGATT
ARR1AT	108	(+)	NGATT
ARR1AT	1217	(+)	NGATT
ARR1AT	98	(+)	NGATT
ARR1AT	454	(+)	NGATT
ARR1AT	687	(+)	NGATT
ARR1AT	969	(+)	NGATT
ARR1AT	1212	(+)	NGATT
ARR1AT	2	(-)	NGATT
ARR1AT	33	(-)	NGATT
ARR1AT	49	(-)	NGATT
ARR1AT	157	(-)	NGATT
ARR1AT	223	(-)	NGATT
ARR1AT	495	(-)	NGATT
ARR1AT	546	(-)	NGATT
ASF1MOTIFCAMV	1227	(+)	TGACG
ASF1MOTIFCAMV	283	(-)	TGACG
ASF1MOTIFCAMV	854	(-)	TGACG
ASF1MOTIFCAMV	938	(-)	TGACG
BIHD1OS	820	(+)	TGTCA
BIHD1OS	825	(+)	TGTCA
BIHD1OS	878	(-)	TGTCA
BIHD1OS	953	(-)	TGTCA
BIHD1OS	992	(-)	TGTCA
BOXIIPCCHS	837	(-)	ACGTGGC
CAATBOX1	1	(+)	CAAT
CAATBOX1	17	(+)	CAAT
CAATBOX1	71	(+)	CAAT
CAATBOX1	222	(+)	CAAT
CAATBOX1	376	(+)	CAAT
CAATBOX1	422	(+)	CAAT
CAATBOX1	600	(+)	CAAT
CAATBOX1	783	(+)	CAAT
CAATBOX1	956	(+)	CAAT
CAATBOX1	997	(+)	CAAT
CAATBOX1	1040	(+)	CAAT
CAATBOX1	1100	(+)	CAAT
CAATBOX1	1196	(+)	CAAT
CAATBOX1	96	(-)	CAAT
CAATBOX1	110	(-)	CAAT
CAATBOX1	130	(-)	CAAT
CAATBOX1	432	(-)	CAAT
CAATBOX1	649	(-)	CAAT
CAATBOX1	739	(-)	CAAT
CAATBOX1	876	(-)	CAAT
CAATBOX1	999	(-)	CAAT
CAATBOX1	1102	(-)	CAAT
CAATBOX1	1198	(-)	CAAT
CAATBOX1	1214	(-)	CAAT
CAATBOX1	1258	(-)	CAAT
CACGTGMOTIF	839	(+)	CACGTG
CACGTGMOTIF	839	(-)	CACGTG
CACTFTPPCA1	578	(+)	YACT
CACTFTPPCA1	714	(+)	YACT
CACTFTPPCA1	760	(+)	YACT
CACTFTPPCA1	857	(+)	YACT
CACTFTPPCA1	881	(+)	YACT
CACTFTPPCA1	941	(+)	YACT
CACTFTPPCA1	965	(+)	YACT
CACTFTPPCA1	805	(+)	YACT
CACTFTPPCA1	1108	(+)	YACT
CACTFTPPCA1	120	(-)	YACT
CACTFTPPCA1	138	(-)	YACT
CACTFTPPCA1	326	(-)	YACT
CACTFTPPCA1	357	(-)	YACT
CACTFTPPCA1	409	(-)	YACT
CACTFTPPCA1	565	(-)	YACT
CACTFTPPCA1	619	(-)	YACT
CACTFTPPCA1	655	(-)	YACT
CACTFTPPCA1	818	(-)	YACT
CACTFTPPCA1	976	(-)	YACT
CACTFTPPCA1	1005	(-)	YACT

CACTFTPPCA1	1051	(-)	YACT	EECCRCAH1	1022	(-)	GANTTNC
CACTFTPPCA1	1266	(-)	YACT	EMBP1TAEM	837	(-)	CACGTGGC
CAREOSREP1	538	(-)	CAACTC	GARE2OSREP1	662	(-)	TAACGTA
CATATGGMSAUR	922	(+)	CATATG	GATABOX	115	(+)	GATA
CATATGGMSAUR	922	(-)	CATATG	GATABOX	385	(+)	GATA
CCA1ATLHCB1	30	(+)	AAMAATCT	GATABOX	562	(+)	GATA
CCA1ATLHCB1	220	(+)	AAMAATCT	GATABOX	419	(-)	GATA
CCAATBOX1	70	(+)	CCAAT	GATABOX	481	(-)	GATA
CCAATBOX1	130	(-)	CCAAT	GATABOX	673	(-)	GATA
CCAATBOX1	1102	(-)	CCAAT	GATABOX	797	(-)	GATA
CCAATBOX1	1214	(-)	CCAAT	GT1CONSENSUS	115	(+)	GRWAAW
CCAATBOX1	1258	(-)	CCAAT	GT1CONSENSUS	124	(+)	GRWAAW
CGACGOSAMY3	861	(+)	CGACG	GT1CONSENSUS	505	(+)	GRWAAW
CPBCSPOR	181	(+)	TATTAG	GT1CONSENSUS	1033	(+)	GRWAAW
DOFCOREZM	118	(+)	AAAG	GT1CONSENSUS	1124	(+)	GRWAAW
DOFCOREZM	316	(+)	AAAG	GT1CONSENSUS	631	(-)	GRWAAW
DOFCOREZM	350	(+)	AAAG	GT1CONSENSUS	795	(-)	GRWAAW
DOFCOREZM	414	(+)	AAAG	GT1CONSENSUS	933	(-)	GRWAAW
DOFCOREZM	570	(+)	AAAG	GT1CONSENSUS	1058	(-)	GRWAAW
DOFCOREZM	653	(+)	AAAG	GT1GMSCAM4	933	(-)	GAAAAA
DOFCOREZM	682	(+)	AAAG	GT1MOTIFPSRBCS	111	(+)	KWGTGRWAAWRW
DOFCOREZM	778	(+)	AAAG	GTGANTG10	113	(+)	GTGA
DOFCOREZM	917	(+)	AAAG	GTGANTG10	139	(+)	GTGA
DOFCOREZM	1003	(+)	AAAG	GTGANTG10	248	(+)	GTGA
DOFCOREZM	1017	(+)	AAAG	GTGANTG10	476	(+)	GTGA
DOFCOREZM	1049	(+)	AAAG	GTGANTG10	543	(+)	GTGA
DOFCOREZM	1081	(+)	AAAG	GTGANTG10	842	(+)	GTGA
DOFCOREZM	1171	(+)	AAAG	GTGANTG10	1226	(+)	GTGA
DOFCOREZM	490	(-)	AAAG	GTGANTG10	464	(-)	GTGA
DOFCOREZM	636	(-)	AAAG	GTGANTG10	713	(-)	GTGA
DOFCOREZM	699	(-)	AAAG	GTGANTG10	856	(-)	GTGA
DOFCOREZM	716	(-)	AAAG	GTGANTG10	940	(-)	GTGA
DOFCOREZM	793	(-)	AAAG	HDZIP2ATATHB2	394	(-)	TAATMATTA
DOFCOREZM	849	(-)	AAAG	IBOXCORE	115	(+)	GATAA
DOFCOREZM	909	(-)	AAAG	IBOXCORE	796	(-)	GATAA
DOFCOREZM	932	(-)	AAAG	INRNTPSADB	436	(+)	YTCANTYY
DOFCOREZM	1110	(-)	AAAG	INRNTPSADB	712	(+)	YTCANTYY
DOFCOREZM	1155	(-)	AAAG	INRNTPSADB	524	(-)	YTCANTYY
DPBFCOREDCDC3	964	(+)	ACACNNG	INRNTPSADB	1119	(-)	YTCANTYY
EBOXBNNAPA	355	(+)	CANNTG	INTRONLOWER	363	(+)	TGCAGG
EBOXBNNAPA	839	(+)	CANNTG	IRO2OS	838	(-)	CACGTGG
EBOXBNNAPA	922	(+)	CANNTG	LTRE1HVBLT49	313	(+)	CCGAAA
EBOXBNNAPA	965	(+)	CANNTG	MARTBOX	425	(+)	TTWTWTTWTT
EBOXBNNAPA	997	(+)	CANNTG	MARTBOX	728	(+)	TTWTWTTWTT
EBOXBNNAPA	1100	(+)	CANNTG	MYB1AT	1104	(-)	WAACCA
EBOXBNNAPA	1196	(+)	CANNTG	MYB2CONSENSUSAT	896	(+)	YAACKG
EBOXBNNAPA	355	(-)	CANNTG	MYB2CONSENSUSAT	1221	(+)	YAACKG
EBOXBNNAPA	839	(-)	CANNTG	MYBCORE	237	(+)	CNGTTR
EBOXBNNAPA	922	(-)	CANNTG	MYBCORE	896	(-)	CNGTTR
EBOXBNNAPA	965	(-)	CANNTG	MYBCORE	980	(-)	CNGTTR
EBOXBNNAPA	997	(-)	CANNTG	MYBCORE	1221	(-)	CNGTTR
EBOXBNNAPA	1100	(-)	CANNTG	MYBCOREATCYCB1	897	(+)	AACGG
EBOXBNNAPA	1196	(-)	CANNTG	MYBCOREATCYCB1	1222	(+)	AACGG
EECCRCAH1	529	(+)	GANTTNC	MYBCOREATCYCB1	272	(-)	AACGG

MYBPLANT	201	(+)	MACCWAMC	RHERPATEXPA7	622	(+)	KCACGW
MYBPZM	769	(-)	CCWACC	RHERPATEXPA7	464	(+)	KCACGW
MYBPZM	1246	(-)	CCWACC	RHERPATEXPA7	840	(-)	KCACGW
MYCCONSENSUSAT	355	(+)	CANNTG	ROOTMOTIFTAPOX1	958	(+)	ATATT
MYCCONSENSUSAT	839	(+)	CANNTG	ROOTMOTIFTAPOX1	86	(-)	ATATT
MYCCONSENSUSAT	922	(+)	CANNTG	ROOTMOTIFTAPOX1	479	(-)	ATATT
MYCCONSENSUSAT	965	(+)	CANNTG	ROOTMOTIFTAPOX1	591	(-)	ATATT
MYCCONSENSUSAT	997	(+)	CANNTG	ROOTMOTIFTAPOX1	957	(-)	ATATT
MYCCONSENSUSAT	1100	(+)	CANNTG	RYREPEATBNNAPA	361	(+)	CATGCA
MYCCONSENSUSAT	1196	(+)	CANNTG	RYREPEATBNNAPA	359	(-)	CATGCA
MYCCONSENSUSAT	355	(-)	CANNTG	RYREPEATBNNAPA	1268	(-)	CATGCA
MYCCONSENSUSAT	839	(-)	CANNTG	RYREPEATLEGUMINBOX	358	(-)	CATGCAY
MYCCONSENSUSAT	922	(-)	CANNTG	RYREPEATLEGUMINBOX	1267	(-)	CATGCAY
MYCCONSENSUSAT	965	(-)	CANNTG	S1FBOXSORPS1L21	721	(-)	ATGGTA
MYCCONSENSUSAT	997	(-)	CANNTG	SEF1MOTIF	587	(-)	ATATTTAWW
MYCCONSENSUSAT	1100	(-)	CANNTG	SEF3MOTIFGM	343	(-)	AACCCA
MYCCONSENSUSAT	1196	(-)	CANNTG	SEF4MOTIFGM7S	732	(+)	RTTTTTR
NODCON2GM	36	(+)	CTCTT	SEF4MOTIFGM7S	29	(-)	RTTTTTR
NODCON2GM	930	(+)	CTCTT	SITEIIATCYTC	309	(+)	TGGGCY
NTBBF1ARROLB	698	(+)	ACTTTA	SORLIP1AT	837	(+)	GCCAC
NTBBF1ARROLB	117	(-)	ACTTTA	SORLIP1AT	24	(-)	GCCAC
NTBBF1ARROLB	349	(-)	ACTTTA	SORLIP2AT	310	(+)	GGGCC
NTBBF1ARROLB	1170	(-)	ACTTTA	SURECOREATSULTR11	196	(-)	GAGAC
OSE2ROOTNODULE	36	(+)	CTCTT	TAAAGSTKST1	117	(+)	TAAAG
OSE2ROOTNODULE	930	(+)	CTCTT	TAAAGSTKST1	349	(+)	TAAAG
PALBOXPPC	1240	(-)	YTYYMMCMAMCMMC	TAAAGSTKST1	413	(+)	TAAAG
POLASIG1	514	(+)	AATAAA	TAAAGSTKST1	569	(+)	TAAAG
POLASIG1	693	(+)	AATAAA	TAAAGSTKST1	916	(+)	TAAAG
POLASIG1	705	(+)	AATAAA	TAAAGSTKST1	1016	(+)	TAAAG
POLASIG1	426	(-)	AATAAA	TAAAGSTKST1	1170	(+)	TAAAG
POLASIG1	603	(-)	AATAAA	TAAAGSTKST1	699	(-)	TAAAG
POLASIG1	729	(-)	AATAAA	TAAAGSTKST1	1155	(-)	TAAAG
POLASIG2	642	(-)	AATTAAA	TATABOX2	153	(+)	TATAAAT
POLASIG2	735	(-)	AATTAAA	TATABOX2	587	(+)	TATAAAT
POLASIG2	810	(-)	AATTAAA	TATABOX2	887	(-)	TATAAAT
POLASIG3	396	(-)	AATAAT	TATABOX4	585	(+)	TATATAA
POLASIG3	429	(-)	AATAAT	TATABOX4	442	(-)	TATATAA
POLASIG3	646	(-)	AATAAT	TATABOX5	604	(+)	TTATTT
POLLEN1LELAT52	680	(+)	AGAAA	TATABOX5	730	(+)	TTATTT
POLLEN1LELAT52	1079	(+)	AGAAA	TATAPVTRNALEU	441	(+)	TTTATATA
POLLEN1LELAT52	1083	(+)	AGAAA	TATAPVTRNALEU	585	(-)	TTTATATA
POLLEN1LELAT52	487	(-)	AGAAA	TBOXATGAPB	1109	(+)	ACTTTG
POLLEN1LELAT52	717	(-)	AGAAA	TBOXATGAPB	1048	(-)	ACTTTG
PREATPRODH	536	(-)	ACTCAT	TRANSINITMONOCOTS	299	(-)	RMNAUGGC
PREATPRODH	1263	(-)	ACTCAT	WBOXATNPR1	877	(+)	TTGAC
PYRIMIDINEBOXOSRAMY1A	635	(+)	CCTTTT	WBOXATNPR1	987	(+)	TTGAC
PYRIMIDINEBOXOSRAMY1A	792	(+)	CCTTTT	WBOXATNPR1	284	(-)	TTGAC
QELEMENTZMZM13	926	(-)	AGGTCA	WBOXATNPR1	353	(-)	TTGAC
RAV1AAT	219	(+)	CAACA	WBOXATNPR1	781	(-)	TTGAC
RAV1AAT	43	(-)	CAACA	WBOXHVISO1	843	(+)	TGACT
RBCSCONSENSUS	2	(+)	AATCCAA	WBOXHVISO1	869	(+)	TGACT
RBCSCONSENSUS	1215	(-)	AATCCAA	WBOXHVISO1	988	(+)	TGACT
REALPHALGLHCB21	201	(+)	AACCAA	WBOXHVISO1	352	(-)	TGACT
REALPHALGLHCB21	1103	(-)	AACCAA	WBOXHVISO1	462	(-)	TGACT

WBOXHVISO1	780	(-)	TGACT
WBOXNTERF3	56	(+)	TGACY
WBOXNTERF3	249	(+)	TGACY
WBOXNTERF3	843	(+)	TGACY
WBOXNTERF3	869	(+)	TGACY
WBOXNTERF3	926	(+)	TGACY
WBOXNTERF3	988	(+)	TGACY
WBOXNTERF3	1043	(+)	TGACY
WBOXNTERF3	352	(-)	TGACY
WBOXNTERF3	462	(-)	TGACY
WBOXNTERF3	780	(-)	TGACY
WRKY71OS	56	(+)	TGAC
WRKY71OS	249	(+)	TGAC
WRKY71OS	843	(+)	TGAC
WRKY71OS	869	(+)	TGAC
WRKY71OS	878	(+)	TGAC
WRKY71OS	926	(+)	TGAC
WRKY71OS	953	(+)	TGAC
WRKY71OS	988	(+)	TGAC
WRKY71OS	992	(+)	TGAC
WRKY71OS	1043	(+)	TGAC
WRKY71OS	1227	(+)	TGAC
WRKY71OS	284	(-)	TGAC
WRKY71OS	353	(-)	TGAC
WRKY71OS	463	(-)	TGAC
WRKY71OS	781	(-)	TGAC
WRKY71OS	821	(-)	TGAC
WRKY71OS	826	(-)	TGAC
WRKY71OS	855	(-)	TGAC
WRKY71OS	939	(-)	TGAC

PAO PROMOTER

Factor or Site Name	Location	(+) or (-)	Signal Sequence
-10PEHVPSBD	843	(+)	TATTCT
-10PEHVPSBD	392	(-)	TATTCT
-300CORE	892	(-)	TGTAAAG
-300ELEMENT	891	(-)	TGHAAARK
2SSEEDPROTBANAPA	524	(-)	CAAACAC
ABRELATERD1	916	(+)	ACGTG
ABRERATCAL	545	(+)	MACGYGB
ABRERATCAL	915	(+)	MACGYGB
ABRERATCAL	546	(-)	MACGYGB
ACGTABREMOTIFA2OSEM	916	(+)	ACGTGKC
ACGTATERD1	238	(+)	ACGT
ACGTATERD1	326	(+)	ACGT
ACGTATERD1	916	(+)	ACGT
ACGTATERD1	238	(-)	ACGT
ACGTATERD1	326	(-)	ACGT
ACGTATERD1	916	(-)	ACGT
ACGTTBOX	325	(+)	AACGTT
ACGTTBOX	325	(-)	AACGTT
AGCBOXNPGLB	104	(-)	AGCCGCC
AMYBOX1	206	(-)	TAACARA
AMYBOX2	386	(-)	TATCCAT
ANAERO1CONSENSUS	852	(-)	AAACAAA
ARR1AT	941	(+)	NGATT
ARR1AT	1188	(+)	NGATT
ARR1AT	406	(-)	NGATT
ARR1AT	428	(-)	NGATT
ARR1AT	510	(-)	NGATT
ARR1AT	565	(-)	NGATT
ARR1AT	604	(-)	NGATT
ARR1AT	628	(-)	NGATT
ARR1AT	675	(-)	NGATT
ARR1AT	972	(-)	NGATT
ARR1AT	1139	(-)	NGATT
ARR1AT	1199	(-)	NGATT
ARR1AT	1211	(-)	NGATT
BIHD1OS	402	(+)	TGTCA
BIHD1OS	618	(+)	TGTCA
BOXIINTPATPB	390	(+)	ATAGAA
BOXIINTPATPB	376	(-)	ATAGAA
BOXIINTPATPB	845	(-)	ATAGAA
BOXIIPCCHS	916	(+)	ACGTGGC
BP5OSWX	914	(+)	CAACGTG
CAATBOX1	339	(+)	CAAT
CAATBOX1	348	(+)	CAAT
CAATBOX1	405	(+)	CAAT
CAATBOX1	627	(+)	CAAT
CAATBOX1	633	(+)	CAAT
CAATBOX1	946	(+)	CAAT
CAATBOX1	971	(+)	CAAT
CAATBOX1	1007	(+)	CAAT
CAATBOX1	1138	(+)	CAAT
CAATBOX1	1214	(+)	CAAT
CAATBOX1	212	(-)	CAAT
CAATBOX1	303	(-)	CAAT
CAATBOX1	477	(-)	CAAT
CAATBOX1	980	(-)	CAAT
CAATBOX1	1171	(-)	CAAT
CACTFTPPCA1	21	(+)	YACT
CACTFTPPCA1	126	(+)	YACT
CACTFTPPCA1	669	(+)	YACT
CACTFTPPCA1	897	(+)	YACT
CACTFTPPCA1	1053	(+)	YACT
CACTFTPPCA1	254	(+)	YACT
CACTFTPPCA1	278	(+)	YACT
CACTFTPPCA1	367	(+)	YACT
CACTFTPPCA1	416	(+)	YACT
CACTFTPPCA1	653	(+)	YACT
CACTFTPPCA1	1025	(+)	YACT
CACTFTPPCA1	1118	(+)	YACT
CACTFTPPCA1	1178	(+)	YACT
CACTFTPPCA1	37	(-)	YACT
CACTFTPPCA1	296	(-)	YACT
CACTFTPPCA1	335	(-)	YACT

CACTFTPPCA1	436	(-)	YACT	EBOXBNNAPA	519	(-)	CANNTG
CACTFTPPCA1	761	(-)	YACT	EBOXBNNAPA	1193	(-)	CANNTG
CACTFTPPCA1	1111	(-)	YACT	EECCRCAH1	1169	(+)	GANTTNC
CACTFTPPCA1	1186	(-)	YACT	EECCRCAH1	79	(-)	GANTTNC
CANBNNAPA	524	(-)	CNAACAC	EECCRCAH1	880	(-)	GANTTNC
CANBNNAPA	951	(-)	CNAACAC	GAGA8HVBKN3	1121	(-)	GAGAGAGAGAGAGAGA
CARGCW8GAT	583	(+)	CWWWWWWWWG	GAGA8HVBKN3	1123	(-)	GAGAGAGAGAGAGAGA
CARGCW8GAT	583	(-)	CWWWWWWWWG	GAGAGMGSA1	1121	(-)	GAGAGAGAGAGAGAGAGA
CBFHV	28	(+)	RYCGAC	GAREAT	206	(-)	TAACAAR
CCA1ATLHCB1	601	(+)	AAMAATCT	GATABOX	117	(+)	GATA
CCAATBOX1	1006	(+)	CCAAT	GATABOX	389	(+)	GATA
CCAATBOX1	477	(-)	CCAAT	GATABOX	452	(+)	GATA
CGACGOSAMY3	906	(-)	CGACG	GATABOX	561	(+)	GATA
CGCGBOXAT	546	(+)	VCGCGB	GATABOX	119	(-)	GATA
CGCGBOXAT	546	(-)	VCGCGB	GATABOX	219	(-)	GATA
CIACADIANLELHC	166	(+)	CAANNNNATC	GATABOX	763	(-)	GATA
CIACADIANLELHC	1193	(+)	CAANNNNATC	GATABOX	818	(-)	GATA
CPBCSPOR	757	(+)	TATTAG	GATABOX	859	(-)	GATA
CPBCSPOR	806	(+)	TATTAG	GATABOX	997	(-)	GATA
CTRMCAMV35S	1121	(+)	TCTCTCTCT	GCCCORE	101	(-)	GCCGCC
CTRMCAMV35S	1123	(+)	TCTCTCTCT	GCCCORE	104	(-)	GCCGCC
CTRMCAMV35S	1125	(+)	TCTCTCTCT	GT1CONSENSUS	452	(+)	GRWAAW
CTRMCAMV35S	1127	(+)	TCTCTCTCT	GT1CONSENSUS	561	(+)	GRWAAW
CTRMCAMV35S	1129	(+)	TCTCTCTCT	GT1CONSENSUS	811	(+)	GRWAAW
CURECORECR	236	(+)	GTAC	GT1CONSENSUS	965	(+)	GRWAAW
CURECORECR	277	(+)	GTAC	GT1CONSENSUS	816	(-)	GRWAAW
CURECORECR	236	(-)	GTAC	GT1CONSENSUS	136	(-)	GRWAAW
CURECORECR	277	(-)	GTAC	GT1CONSENSUS	731	(-)	GRWAAW
DOFCOREZM	245	(+)	AAAG	GT1CONSENSUS	857	(-)	GRWAAW
DOFCOREZM	834	(+)	AAAG	GT1GMSCAM4	811	(+)	GAAAAA
DOFCOREZM	925	(+)	AAAG	GT1GMSCAM4	965	(+)	GAAAAA
DOFCOREZM	1001	(+)	AAAG	GT1GMSCAM4	136	(-)	GAAAAA
DOFCOREZM	1109	(+)	AAAG	GT1GMSCAM4	731	(-)	GAAAAA
DOFCOREZM	1143	(+)	AAAG	GTGANTG10	38	(+)	GTGA
DOFCOREZM	75	(-)	AAAG	GTGANTG10	159	(+)	GTGA
DOFCOREZM	109	(-)	AAAG	GTGANTG10	259	(+)	GTGA
DOFCOREZM	128	(-)	AAAG	GTGANTG10	937	(+)	GTGA
DOFCOREZM	144	(-)	AAAG	GTGANTG10	1187	(+)	GTGA
DOFCOREZM	177	(-)	AAAG	GTGANTG10	20	(-)	GTGA
DOFCOREZM	198	(-)	AAAG	GTGANTG10	630	(-)	GTGA
DOFCOREZM	205	(-)	AAAG	GTGANTG10	1014	(-)	GTGA
DOFCOREZM	655	(-)	AAAG	GTGANTG10	1052	(-)	GTGA
DOFCOREZM	736	(-)	AAAG	GTGANTG10	1159	(-)	GTGA
DOFCOREZM	892	(-)	AAAG	IBOXCORE	452	(+)	GATAA
DOFCOREZM	1049	(-)	AAAG	IBOXCORE	561	(+)	GATAA
DPBFCOREDCDC3	519	(-)	ACACNNG	IBOXCORE	817	(-)	GATAA
DRE2COREZMRAB17	28	(+)	ACCGAC	IBOXCORE	858	(-)	GATAA
DRECRTCOREAT	28	(+)	RCCGAC	INRNTPSADB	639	(+)	YTCANTYY
EBOXBNNAPA	156	(+)	CANNTG	LTRECOREATCOR15	29	(+)	CCGAC
EBOXBNNAPA	230	(+)	CANNTG	LTRECOREATCOR15	122	(+)	CCGAC
EBOXBNNAPA	519	(+)	CANNTG	MYB1AT	661	(+)	WAACCA
EBOXBNNAPA	1193	(+)	CANNTG	MYB1AT	1056	(-)	WAACCA
EBOXBNNAPA	156	(-)	CANNTG	MYB2CONSENSUSAT	1193	(+)	YAACKG
EBOXBNNAPA	230	(-)	CANNTG	MYBCORE	447	(+)	CNGTTR

MYBCORE	1193	(-)	CNGTTR
MYBGAHV	206	(-)	TAACAAA
MYBST1	388	(+)	GGATA
MYBST1	119	(-)	GGATA
MYBST1	818	(-)	GGATA
MYBST1	859	(-)	GGATA
MYCATERD1	519	(+)	CATGTG
MYCATRD22	519	(-)	CACATG
MYCCONSENSUSAT	156	(+)	CANNTG
MYCCONSENSUSAT	230	(+)	CANNTG
MYCCONSENSUSAT	519	(+)	CANNTG
MYCCONSENSUSAT	1193	(+)	CANNTG
MYCCONSENSUSAT	156	(-)	CANNTG
MYCCONSENSUSAT	230	(-)	CANNTG
MYCCONSENSUSAT	519	(-)	CANNTG
MYCCONSENSUSAT	1193	(-)	CANNTG
NAPINMOTIFBN	797	(+)	TACACAT
NODCON2GM	73	(+)	CTCTT
NODCON2GM	175	(+)	CTCTT
NODCON2GM	332	(-)	CTCTT
OSE2ROOTNODULE	73	(+)	CTCTT
OSE2ROOTNODULE	175	(+)	CTCTT
OSE2ROOTNODULE	332	(-)	CTCTT
P1BS	312	(+)	GNATATNC
P1BS	312	(-)	GNATATNC
POLASIG1	773	(+)	AATAAA
POLASIG1	831	(+)	AATAAA
POLASIG1	300	(-)	AATAAA
POLASIG1	804	(-)	AATAAA
POLASIG2	785	(+)	AATTAAA
POLASIG3	532	(-)	AATAAT
POLASIG3	610	(-)	AATAAT
POLASIG3	1009	(-)	AATAAT
POLLEN1LELAT52	810	(+)	AGAAA
POLLEN1LELAT52	964	(+)	AGAAA
POLLEN1LELAT52	138	(-)	AGAAA
POLLEN1LELAT52	643	(-)	AGAAA
POLLEN1LELAT52	703	(-)	AGAAA
POLLEN1LELAT52	733	(-)	AGAAA
PRECONSCRHSP70A	90	(+)	SCGAYNRNNNNNNNN NNNNNNNHD
PRECONSCRHSP70A	426	(-)	SCGAYNRNNNNNNNN NNNNNNNHD
RAV1AAT	6	(+)	CAACA
RAV1AAT	59	(-)	CAACA
RAV1AAT	305	(-)	CAACA
RAV1AAT	952	(-)	CAACA
RAV1AAT	982	(-)	CAACA
RAV1BAT	156	(-)	CACCTG
REBETALGLHCB21	119	(-)	CGGATA
RHERPATEXPA7	430	(-)	KCACGW
RHERPATEXPA7	595	(-)	KCACGW
ROOTMOTIFTAPOX1	728	(+)	ATATT
ROOTMOTIFTAPOX1	749	(+)	ATATT
ROOTMOTIFTAPOX1	756	(+)	ATATT
ROOTMOTIFTAPOX1	842	(+)	ATATT
ROOTMOTIFTAPOX1	313	(-)	ATATT
ROOTMOTIFTAPOX1	725	(-)	ATATT
ROOTMOTIFTAPOX1	748	(-)	ATATT
ROOTMOTIFTAPOX1	755	(-)	ATATT
ROOTMOTIFTAPOX1	777	(-)	ATATT
RYREPEATBNNAPA	383	(-)	CATGCA
RYREPEATLEGUMINBOX	382	(-)	CATGCAY
SEF1MOTIF	749	(+)	ATATTTAWW
SEF1MOTIF	773	(-)	ATATTTAWW
SEF4MOTIFGM7S	849	(+)	RTTTTTR
SEF4MOTIFGM7S	600	(-)	RTTTTTR
SEF4MOTIFGM7S	711	(-)	RTTTTTR
SEF4MOTIFGM7S	454	(-)	RTTTTTR
SEF4MOTIFGM7S	552	(-)	RTTTTTR
SEF4MOTIFGM7S	744	(-)	RTTTTTR
SEF4MOTIFGM7S	788	(-)	RTTTTTR
SORLIP1AT	918	(-)	GCCAC
SREATMSD	817	(+)	TTATCC
SREATMSD	858	(+)	TTATCC
SURECOREATSULTR11	353	(-)	GAGAC
SURECOREATSULTR11	910	(-)	GAGAC
SV40COREENHAN	971	(-)	GTGGWWHG
T/GBOXATPIN2	915	(+)	AACGTG
TAAAGSTKST1	244	(+)	TAAAG
TAAAGSTKST1	833	(+)	TAAAG
TAAAGSTKST1	177	(-)	TAAAG
TAAAGSTKST1	892	(-)	TAAAG
TATABOX2	48	(+)	TATAAAT
TATABOX2	585	(+)	TATAAAT
TATABOX2	781	(+)	TATAAAT
TATABOX3	722	(-)	TATTAAT
TATABOX4	779	(+)	TATATAA
TATABOX5	270	(+)	TTATTT
TATABOX5	533	(+)	TTATTT
TATABOX5	772	(-)	TTATTT
TATABOX5	830	(-)	TTATTT
TATABOXOSPAL	750	(+)	TATTTAA
TATAPVTRNALEU	779	(-)	TTTATATA
TATCCAOSAMY	387	(-)	TATCCA
TATCCAYMOTIFOSRAMY3D	386	(-)	TATCCAY
TBOXATGAPB	127	(+)	ACTTTG
TBOXATGAPB	204	(+)	ACTTTG
TBOXATGAPB	1000	(-)	ACTTTG
TBOXATGAPB	1108	(-)	ACTTTG
WBBOXPCWRKY1	359	(-)	TTTGACY
WBOXATNPR1	360	(-)	TTGAC
WBOXATNPR1	403	(-)	TTGAC
WBOXATNPR1	619	(-)	TTGAC
WBOXHVISO1	227	(-)	TGACT
WBOXHVISO1	359	(-)	TGACT
WBOXNTERF3	227	(-)	TGACY
WBOXNTERF3	359	(-)	TGACY
WBOXNTERF3	411	(-)	TGACY
WBOXNTERF3	481	(-)	TGACY

WRKY71OS	228	(-)	TGAC
WRKY71OS	360	(-)	TGAC
WRKY71OS	403	(-)	TGAC
WRKY71OS	412	(-)	TGAC
WRKY71OS	482	(-)	TGAC
WRKY71OS	619	(-)	TGAC

SGR PROMOTER

Factor or Site Name	Location	(+) or (-)	Signal Sequence
-300ELEMENT	706	(-)	TGHAAARK
ABRERATCAL	11	(+)	MACGYGB
ABRERATCAL	12	(-)	MACGYGB
ACGTATERD1	746	(+)	ACGT
ACGTATERD1	746	(-)	ACGT
ACGTTBOX	745	(+)	AACGTT
ACGTTBOX	745	(-)	AACGTT
AMYBOX1	533	(-)	TAACARA
ANAERO1CONSENSUS	995	(+)	AAACAAA
ANAERO3CONSENSUS	789	(+)	TCATCAC
ARR1AT	242	(+)	NGATT
ARR1AT	552	(+)	NGATT
ARR1AT	1008	(+)	NGATT
ARR1AT	486	(+)	NGATT
ARR1AT	425	(-)	NGATT
ARR1AT	600	(-)	NGATT
ARR1AT	893	(-)	NGATT
ARR1AT	936	(-)	NGATT
ASF1MOTIFCAMV	406	(-)	TGACG
ASF1MOTIFCAMV	787	(-)	TGACG
BIHD1OS	96	(-)	TGTCA
BOXIINTPATPB	119	(+)	ATAGAA
BS1EGCCR	161	(+)	AGCGGG
CAATBOX1	99	(+)	CAAT
CAATBOX1	354	(+)	CAAT
CAATBOX1	414	(+)	CAAT
CAATBOX1	424	(+)	CAAT
CAATBOX1	434	(+)	CAAT
CAATBOX1	505	(+)	CAAT
CAATBOX1	728	(+)	CAAT
CAATBOX1	736	(+)	CAAT
CAATBOX1	892	(+)	CAAT
CAATBOX1	926	(+)	CAAT
CAATBOX1	67	(-)	CAAT
CAATBOX1	356	(-)	CAAT
CAATBOX1	488	(-)	CAAT
CAATBOX1	803	(-)	CAAT
CAATBOX1	1010	(-)	CAAT
CAATBOX2	1008	(-)	GGCCAATCT
CACTFTPPCA1	149	(+)	YACT
CACTFTPPCA1	752	(+)	YACT
CACTFTPPCA1	839	(+)	YACT
CACTFTPPCA1	1	(+)	YACT
CACTFTPPCA1	293	(+)	YACT
CACTFTPPCA1	388	(+)	YACT
CACTFTPPCA1	575	(+)	YACT
CACTFTPPCA1	774	(+)	YACT
CACTFTPPCA1	46	(-)	YACT
CACTFTPPCA1	454	(-)	YACT
CACTFTPPCA1	516	(-)	YACT
CACTFTPPCA1	539	(-)	YACT
CACTFTPPCA1	781	(-)	YACT
CACTFTPPCA1	810	(-)	YACT
CACTFTPPCA1	877	(-)	YACT
CARGCW8GAT	967	(+)	CWWWWWWWG
CARGCW8GAT	967	(-)	CWWWWWWWG
CBFHV	19	(+)	RYCGAC
CBFHV	19	(-)	RYCGAC
CCA1ATLHCB1	597	(+)	AAMAATCT
CCA1ATLHCB1	242	(-)	AAMAATCT
CCA1ATLHCB1	552	(-)	AAMAATCT
CCAATBOX1	423	(+)	CCAAT
CCAATBOX1	891	(+)	CCAAT
CCAATBOX1	925	(+)	CCAAT
CCAATBOX1	356	(-)	CCAAT
CCAATBOX1	1010	(-)	CCAAT
CGACGOSAMY3	21	(+)	CGACG
CGACGOSAMY3	495	(-)	CGACG
CGCGBOXAT	12	(+)	VCGCGB
CGCGBOXAT	12	(-)	VCGCGB
CIACADIANLELHC	482	(-)	CAANNNNATC
CRTDREHVCBF2	19	(+)	GTCGAC
CRTDREHVCBF2	19	(-)	GTCGAC
CTRMCAMV35S	842	(+)	TCTCTCTCT
CTRMCAMV35S	844	(+)	TCTCTCTCT
CTRMCAMV35S	846	(+)	TCTCTCTCT
CTRMCAMV35S	848	(+)	TCTCTCTCT
CTRMCAMV35S	850	(+)	TCTCTCTCT
CTRMCAMV35S	852	(+)	TCTCTCTCT
CTRMCAMV35S	956	(+)	TCTCTCTCT
CTRMCAMV35S	958	(+)	TCTCTCTCT
CURECORECR	333	(+)	GTAC
CURECORECR	333	(-)	GTAC
DOFCOREZM	79	(+)	AAAG
DOFCOREZM	144	(+)	AAAG
DOFCOREZM	514	(+)	AAAG
DOFCOREZM	545	(+)	AAAG
DOFCOREZM	639	(+)	AAAG
DOFCOREZM	650	(+)	AAAG
DOFCOREZM	686	(+)	AAAG
DOFCOREZM	762	(+)	AAAG
DOFCOREZM	900	(+)	AAAG
DOFCOREZM	920	(+)	AAAG
DOFCOREZM	941	(+)	AAAG
DOFCOREZM	999	(+)	AAAG
DOFCOREZM	572	(-)	AAAG
DOFCOREZM	577	(-)	AAAG

DOFCOREZM	754	(-)	AAAG	MYCATRD22	712	(+)	CACATG
DOFCOREZM	776	(-)	AAAG	MYCATRD22	376	(-)	CACATG
DPBFCOREDCDC3	148	(+)	ACACNNG	MYCCONSENSUSAT	272	(+)	CANNTG
E2FAT	236	(-)	TYTCCCGCC	MYCCONSENSUSAT	354	(+)	CANNTG
EBOXBNNAPA	272	(+)	CANNTG	MYCCONSENSUSAT	374	(+)	CANNTG
EBOXBNNAPA	354	(+)	CANNTG	MYCCONSENSUSAT	376	(+)	CANNTG
EBOXBNNAPA	374	(+)	CANNTG	MYCCONSENSUSAT	712	(+)	CANNTG
EBOXBNNAPA	376	(+)	CANNTG	MYCCONSENSUSAT	808	(+)	CANNTG
EBOXBNNAPA	712	(+)	CANNTG	MYCCONSENSUSAT	272	(-)	CANNTG
EBOXBNNAPA	808	(+)	CANNTG	MYCCONSENSUSAT	354	(-)	CANNTG
EBOXBNNAPA	272	(-)	CANNTG	MYCCONSENSUSAT	374	(-)	CANNTG
EBOXBNNAPA	354	(-)	CANNTG	MYCCONSENSUSAT	376	(-)	CANNTG
EBOXBNNAPA	374	(-)	CANNTG	MYCCONSENSUSAT	712	(-)	CANNTG
EBOXBNNAPA	376	(-)	CANNTG	MYCCONSENSUSAT	808	(-)	CANNTG
EBOXBNNAPA	712	(-)	CANNTG	NODCON1GM	686	(+)	AAAGAT
EBOXBNNAPA	808	(-)	CANNTG	NODCON2GM	428	(+)	CTCTT
EECCRCAH1	433	(-)	GANTTNC	NODCON2GM	80	(-)	CTCTT
EECCRCAH1	933	(-)	GANTTNC	NTBBF1ARROLB	571	(+)	ACTTTA
EECCRCAH1	940	(-)	GANTTNC	NTBBF1ARROLB	576	(+)	ACTTTA
EECCRCAH1	951	(-)	GANTTNC	NTBBF1ARROLB	775	(+)	ACTTTA
ELRECOREPCRP1	756	(+)	TTGACC	OSE1ROOTNODULE	686	(+)	AAAGAT
GAGA8HVBKN3	842	(-)	GAGAGAGAGAGAGAGA	OSE2ROOTNODULE	428	(+)	CTCTT
GAGA8HVBKN3	844	(-)	GAGAGAGAGAGAGAGA	OSE2ROOTNODULE	80	(-)	CTCTT
GAGAGMGSA1	842	(-)	GAGAGAGAGAGAGAGAGA	POLASIG2	591	(+)	AATTAAA
GAREAT	533	(-)	TAACAAR	POLASIG2	558	(-)	AATTAAA
GATABOX	88	(+)	GATA	POLASIG2	607	(-)	AATTAAA
GATABOX	689	(+)	GATA	POLASIG3	71	(+)	AATAAT
GATABOX	37	(-)	GATA	POLLEN1LELAT52	121	(+)	AGAAA
GT1CONSENSUS	707	(-)	GRWAAW	POLLEN1LELAT52	128	(+)	AGAAA
GT1GMSCAM4	707	(-)	GAAAAA	POLLEN1LELAT52	950	(+)	AGAAA
GTGANTG10	864	(+)	GTGA	POLLEN1LELAT52	993	(+)	AGAAA
GTGANTG10	882	(+)	GTGA	POLLEN1LELAT52	417	(-)	AGAAA
GTGANTG10	711	(-)	GTGA	POLLEN2LELAT52	438	(+)	TCCACCATA
GTGANTG10	792	(-)	GTGA	RAV1AAT	946	(+)	CAACA
GTGANTG10	904	(-)	GTGA	RAV1AAT	860	(-)	CAACA
HEXAMERATH4	21	(-)	CCGTCG	RAV1AAT	886	(-)	CAACA
IBOXCORE	36	(-)	GATAA	REALPHALGLHCB21	681	(+)	AACCAA
INRNTPSADB	965	(+)	YTCANTYY	ROOTMOTIFTAPOX1	58	(+)	ATATT
INRNTPSADB	324	(-)	YTCANTYY	ROOTMOTIFTAPOX1	65	(+)	ATATT
INRNTPSADB	486	(-)	YTCANTYY	ROOTMOTIFTAPOX1	57	(-)	ATATT
LECPLEACS2	111	(+)	TAAAATAT	ROOTMOTIFTAPOX1	64	(-)	ATATT
MARTBOX	520	(+)	TTWTWTTWTT	ROOTMOTIFTAPOX1	114	(-)	ATATT
MYB1AT	680	(+)	WAACCA	SEF1MOTIF	58	(+)	ATATTTAWW
MYBCORE	33	(+)	CNGTTR	SEF1MOTIF	53	(-)	ATATTTAWW
MYBCORE	654	(+)	CNGTTR	SEF3MOTIFGM	835	(+)	AACCCA
MYBCORE	859	(+)	CNGTTR	SEF3MOTIFGM	358	(-)	AACCCA
MYBCORE	946	(-)	CNGTTR	SEF4MOTIFGM7S	244	(+)	RTTTTTR
MYBCORE	783	(-)	CNGTTR	SITEIIATCYTC	348	(+)	TGGGCY
MYBGAHV	533	(-)	TAACAAA	SITEIIATCYTC	922	(-)	TGGGCY
MYBPZM	833	(+)	CCWACC	SITEIIATCYTC	176	(-)	TGGGCY
MYCATERD1	376	(+)	CATGTG	SORLIP1AT	372	(+)	GCCAC
MYCATERD1	374	(-)	CATGTG	SORLIP1AT	724	(-)	GCCAC
MYCATERD1	712	(-)	CATGTG	SORLIP2AT	175	(+)	GGGCC
MYCATRD22	374	(+)	CACATG	SORLIP2AT	194	(+)	GGGCC

SORLIP2AT	229	(+)	GGGCC	WBOXHVISO1	269	(-)	TGACT
SORLIP2AT	25	(-)	GGGCC	WBOXHVISO1	547	(-)	TGACT
SORLIP2AT	176	(-)	GGGCC	WBOXHVISO1	641	(-)	TGACT
SP8BFIBSP8BIB	43	(-)	TACTATT	WBOXHVISO1	902	(-)	TGACT
SURECOREATSULTR11	137	(-)	GAGAC	WBOXHVISO1	943	(-)	TGACT
TAAAGSTKST1	572	(-)	TAAAG	WBOXNTCHN48	269	(-)	CTGACY
TAAAGSTKST1	577	(-)	TAAAG	WBOXNTERF3	344	(+)	TGACY
TAAAGSTKST1	776	(-)	TAAAG	WBOXNTERF3	569	(+)	TGACY
TATABOX2	90	(+)	TATAAAT	WBOXNTERF3	757	(+)	TGACY
TATABOX2	626	(+)	TATAAAT	WBOXNTERF3	269	(-)	TGACY
TATABOXOSPAL	59	(+)	TATTTAA	WBOXNTERF3	547	(-)	TGACY
TATABOXOSPAL	54	(-)	TATTTAA	WBOXNTERF3	641	(-)	TGACY
TBOXATGAPB	753	(+)	ACTTTG	WBOXNTERF3	902	(-)	TGACY
TBOXATGAPB	899	(-)	ACTTTG	WBOXNTERF3	943	(-)	TGACY
WBBOXPCWRKY1	342	(+)	TTTGACY	WRKY71OS	96	(+)	TGAC
WBBOXPCWRKY1	567	(+)	TTTGACY	WRKY71OS	344	(+)	TGAC
WBBOXPCWRKY1	755	(+)	TTTGACY	WRKY71OS	569	(+)	TGAC
WBOXATNPR1	343	(+)	TTGAC	WRKY71OS	757	(+)	TGAC
WBOXATNPR1	568	(+)	TTGAC	WRKY71OS	270	(-)	TGAC
WBOXATNPR1	756	(+)	TTGAC	WRKY71OS	407	(-)	TGAC
WBOXATNPR1	407	(-)	TTGAC	WRKY71OS	548	(-)	TGAC
WBOXATNPR1	548	(-)	TTGAC	WRKY71OS	642	(-)	TGAC
WBOXATNPR1	642	(-)	TTGAC	WRKY71OS	788	(-)	TGAC
WBOXATNPR1	944	(-)	TTGAC	WRKY71OS	903	(-)	TGAC
WBOXHVISO1	344	(+)	TGACT	WRKY71OS	944	(-)	TGAC
WBOXHVISO1	569	(+)	TGACT				